EARLY AMYLOID PATHOLOGY

identical twins
two of a kind?

Elles Konijnenberg

EARLY AMYLOID PATHOLOGY
identical twins, two of a kind?

Elles Konijnenberg

VRIJE UNIVERSITEIT

EARLY AMYLOID PATHOLOGY
identical twins, two of a kind?

ACADEMISCH PROEFSCHRIFT

ter verkrijging van de graad van Doctor aan
de Vrije Universiteit Amsterdam,
op gezag van de rector magnificus
prof. dr. V. Subramaniam,
in het openbaar te verdedigen
ten overstaan van de promotiecommissie
van de Faculteit der Geneeskunde
op 25 juni 2019 om 11:45 uur
in de aula van de universiteit,
De Boelelaan 1105

door
Elles Konijnenberg
geboren te Warnsveld

voor opa Dieren

Table of contents

CHAPTER

1

Introduction

I. GENERAL BACKGROUND

Alzheimer's disease (AD) is the most common cause of dementia worldwide, with an increasing prevalence expected to reach 75 million people by 2030 [1]. Abnormal deposition of amyloid-β in the brain into plaques is hypothesized to be the first event in AD and starts years before cognitive impairment occurs [2-5]. This is presumed to be followed by the formation of intracellular neurofibrillary tangles consisting of hyperphosphorylated tau [6]. Eventually these two processes are thought to lead to neuronal injury, cell loss and eventually cognitive impairment (Figure 1)[7]. However, the exact disease mechanisms from amyloid aggregation to neuronal injury and consecutive cognitive decline in AD are subject of intense debate and research.

To date, trials in AD patients with mild to moderate cognitive symptoms have not been successful, probably because brain damage in these disease stages is already extensive. For example, beta-secretase-1 (BACE1) inhibitors, which reduce the production of amyloid, and amyloid antibodies such as solanezumab, have not been effective in late-stage AD [8]. As a result, current research is shifting towards secondary prevention in the cognitively healthy elderly population with amyloid pathology. Treating these subjects might prevent further amyloid accumulation, subsequent neuronal injury and cognitive decline [9]. Although BACE1 inhibitors are currently being tested in this population [10], it has not been established yet in which disease stage increased amyloid production is present. To determine the best treatment targets in early AD it is therefore key to unravel early pathophysiological changes and risk factors for AD.

Aim of this thesis is to investigate the early pathophysiology of AD using a cognitively normal monozygotic twin sample and cerebrospinal fluid proteomic analysis in AD patients.

II. PRECLINICAL AD

The earliest stage of AD, when subjects with normal cognition have amyloid pathology, is referred to as preclinical AD [11]. The prevalence of preclinical AD increases between 20% at age 60 to 40% at age 90 [4]. There are several challenges with the definition of preclinical AD, relating to diagnostic procedures and pathophysiology behind early amyloid pathology, which we will address in this thesis.

Assessment of amyloid pathology

Biomarkers give us the opportunity to measure amyloid pathology *in vivo* using positron emission tomography (PET) or cerebrospinal fluid (CSF) analysis. Amyloid aggregation in the brain is reflected with increased PET amyloid tracer binding [12, 13] and decreased levels of CSF amyloid-b 1-42 [14]. Although both measures are usually in good agreement, in about
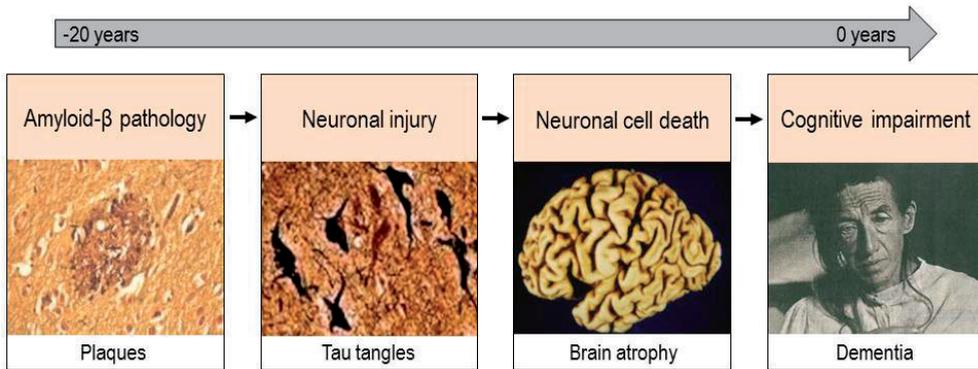
Figure 1. Hypothetical model for development of Alzheimer's disease before dementia onset
From left to right, time to onset from -20 to 0 years, amyloid aggregation into plaques in the brain, neuronal injury caused by intracellular tau-tangles, followed by neuronal cell death leading to brain atrophy, resulting in clinical AD-type dementia with impaired cognition and interference in activities of daily living.

15% of the subjects, results are conflicting [15]. For inclusion in trials, reliable identification of amyloid pathology in vivo is of utmost importance in this preclinical AD population.

Amyloid-beta is produced through amyloidogenic processing of the amyloid precursor protein (APP) that is initiated through cleavage by beta secretase-1 (BACE1) and followed by cleavage by gamma secretase [16]. This results in several amyloid-beta isoforms in CSF including amyloid beta 1-42, 1-40, and 1-38, of which amyloid-beta 1-42 is the most prone for aggregation [17]. Recent studies in subjects with normal cognition and mild cognitive impairment show significant heterogeneity in CSF amyloid-beta 1-42 values, differing per center and assay used [18]. It has therefore been suggested that amyloid-beta 1-42 in CSF might partly reflect amyloid production. Following this, it has been proposed to use the CSF amyloid beta 1-42/1-40 ratio, including correction for amyloid beta metabolism, which might be more specific for detecting actual amyloid beta pathology in CSF [18, 19].

For amyloid-PET imaging, it is current practice to identify amyloid pathology by visual interpretation of summed late images of semi-quantitative standardized uptake value ratio (SUVr) PET images by a nuclear physician. Previous studies have shown a high inter-reader agreement for the visual assessment of SUVr images and a high imaging-pathology correlation in clinical populations and end-of-life subjects [20-22]. However, visually rating SUVr images might lead to overestimation of amyloid burden compared to rating of quantitative non-displaceable binding potential values (BP_{ND}) [23], which also takes clearance and cerebral blood flow into account. As such, quantitative BP_{ND} images may be more reliable even for visual interpretation, particularly in subjects with early stage amyloid deposition, as amyloid-PET scans in the lowest ranges may include more noise. For [18F]-amyloid-tracers it has not yet been examined whether visual rating can best be performed on SUVr or BP_{nd} images to assess amyloid pathology.

CSF and PET biomarkers for amyloid pathology show the largest disagreement in cognitively normal subjects [15, 24, 25], possibly due to the early stage subjects are in, where amyloid aggregation has started, but it is not visible in amyloid plaques on PET yet, and it is unclear which biomarker can define preclinical AD best. It has been suggested that amyloid changes can be detected earlier in CSF than by PET but this requires further investigation [26].

Memory performance in preclinical AD

Previous studies showed that amyloid pathology in cognitively normal individuals may be associated with low normal memory performance and cognitive complaints. However, findings have been conflicting, possibly due to variability in memory tests, cognitive complaints definitions and amyloid measures used [27-29]. So far, it is not clear whether the relation between amyloid pathology and cognitive performance has a common underlying biology.

III. PATHOPHYSIOLOGY OF AMYLOID AGGREGATION

Genetics

Previous studies using AD-type dementia as an outcome estimated the maximum contribution of genetic factors to be around 80% [30], suggesting a major genetic role in the development of AD. This is further supported by the increasing twin similarity for clinical AD with longer follow up duration (i.e. both twins will develop AD-type dementia, but one of them has a protective factor, non-shared within a pair, leading to a later age of onset for this twin). However, there is also support for a substantial effect of environmental influences, reflected by the variation in age of onset in monozygotic twins concordant (i.e. both twins of a pair are affected) for AD type dementia (Figure 2) [31]. Little is known about the genetic mechanisms behind amyloid production and pathology in cognitively normal elderly [32, 33].

The Apolipoprotein-E (APOE) ε4 allele is the major genetic risk factor for AD [34]. While its exact mechanisms are unknown, it lowers the age of onset of amyloid accumulation [4]. About 25-40% of patients with AD-type dementia do not have an APOE ε4 allele [35], for these subjects the pathophysiological mechanisms involved in AD are less clear [36]. In previous studies, the apoE4 protein isoform has been associated with impaired amyloid clearance and transport, synaptogenesis, glucose and cholesterol metabolism in the brain [37, 38]. Earlier studies report APOE ε4 dependent protein levels in CSF for two other proteins associated with AD-type dementia, BACE1 [39] and chitinase-3-like protein-1 (YKL40) [40], and so it is plausible that APOE ε4 genotype may influence other protein markers in CSF as well. Investigating CSF protein expression might give insight into pathophysiological mechanisms involved in AD, and whether these differ according to APOE ε4 genotype.

Genome Wide Association Studies have shown that neuro-inflammation seems to play a major role in the development and severity of sporadic AD [41]. GWAS have identified AD risk
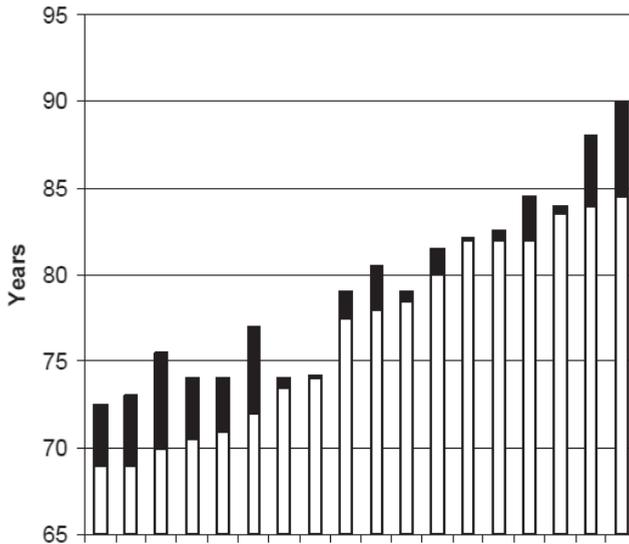
Figure 2. Difference in age of onset of AD-type dementia in 18 monozygotic twin pairs concordant for AD-type dementia (adapted from Gatz et al. 2005)
Each bar represents one monozygotic twin pair, both twins have developed AD-type dementia. The age of onset in the first twin is shown with a white bar, the age of onset in the co-twin is indicate by the additional black bar on top of the white bar. Length of the black bar represents within-pair difference for age of onset of AD-type dementia.

genes, that are associated with inflammation, such as TREM2, CR1, CD33, and INPP5D [42-46]. Inflammation has been associated with AD pathophysiology including amyloid aggregation in the brain [47]. Mouse and human AD brain tissue show altered pro-inflammatory gene expression in vitro, which is linked to amyloid plaque associated microglia [48]. Examining inflammatory proteins in CSF might give in vivo insight into the role of inflammation in AD.

Finally, about 1% of AD-type dementia cases are caused by an autosomal dominant mutation in amyloid production genes amyloid precursor protein (APP), presenilin1 (PSEN1), or presenilin2 (PSEN2). These mutations lead to a drastic increase in the production of amyloid proteins, which is followed by amyloid aggregation into plaques [49]. It is not yet known whether overproduction of amyloid also plays a role in sporadic AD [50], this might be clarified by examining the relation between amyloid production and aggregation markers in cognitively normal elderly.

Environment

Previous studies have identified a number of environmental risk factors for amyloid pathology, such as level of education, medical history, and lifestyle factors such as smoking, alcohol use, and dietary exposures [4, 51-53]. As environmental factors might be modifiable, evidence to show that protection against AD is feasible has been lacking. Furthermore, the influence of environmental factors on AD biomarkers remains to be determined.
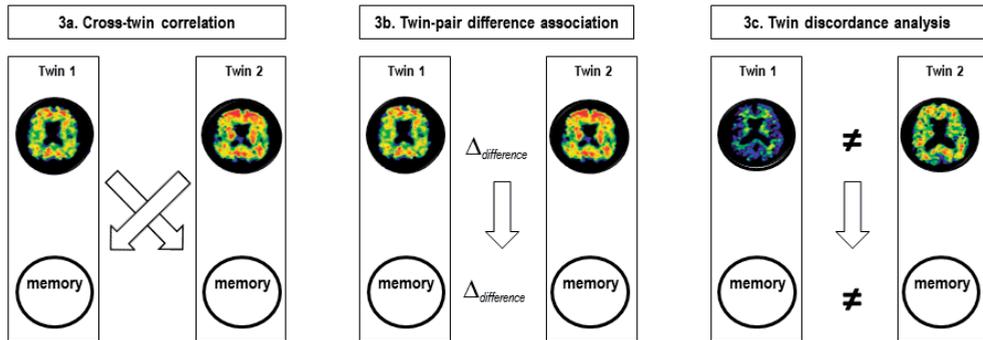
Figure 3. Twins methodology for assessment of genetic and environmental influences
3a. cross-twin correlation, to estimate whether an association between amyloid and memory has a shared underlying biology, 3b. twin-pair difference and 3c. discordance analysis, to test whether amyloid (continuous and dichotomous respectively) is associated with memory even when correcting for all confounders, as twins share 100% of their genes and early life environmental influences.

IV. METHODOLOGY

Twin studies in AD

Monozygotic twins are genetically identical, thus similarities within a twin-pair can be explained by genes and/or shared environment, where differences must be due to unique environmental factors. Hereby it is important that unique environmental influences (i.e., non-shared between the twins in a pair) might be modifiable, and therefore can reveal possible novel anti-AD targets. Studying monozygotic twins enables exploring the nature of an observed relation between two traits: 1) the cross-twin cross-trait design, studying if marker 1 in one twin can predict marker 2 in its co-twin, gives the opportunity to study the contribution of shared familial factors (genes and common environment) to the relation (Figure 3a) [54], 2) the monozygotic twin differences approach gives the possibility to study the relation while excluding confounding caused by genetic factors (the twins are genetically identical) (Figure 3b) [55], and 3) the twin discordance approach can also clarify involvement of environmental factors, by exploring whether twins discordant for one marker also differ for other AD markers (Figure 3c).

CSF proteomics in AD

A better understanding of biological processes disrupted in subjects with amyloid pathology is crucial for the development of AD treatment. The first CSF proteomic studies have identified novel markers associated with Alzheimer's disease-type dementia when comparing patients with cognitively normal controls, including NrCAM, YKL-40, FABPH, VGF, APOE, complement-3, chromogranin-A, carnosinase-I [56-58]. However, since these studies did not take amyloid pathology into account, it remains uncertain which of the previously reported markers are specific for amyloid pathology.
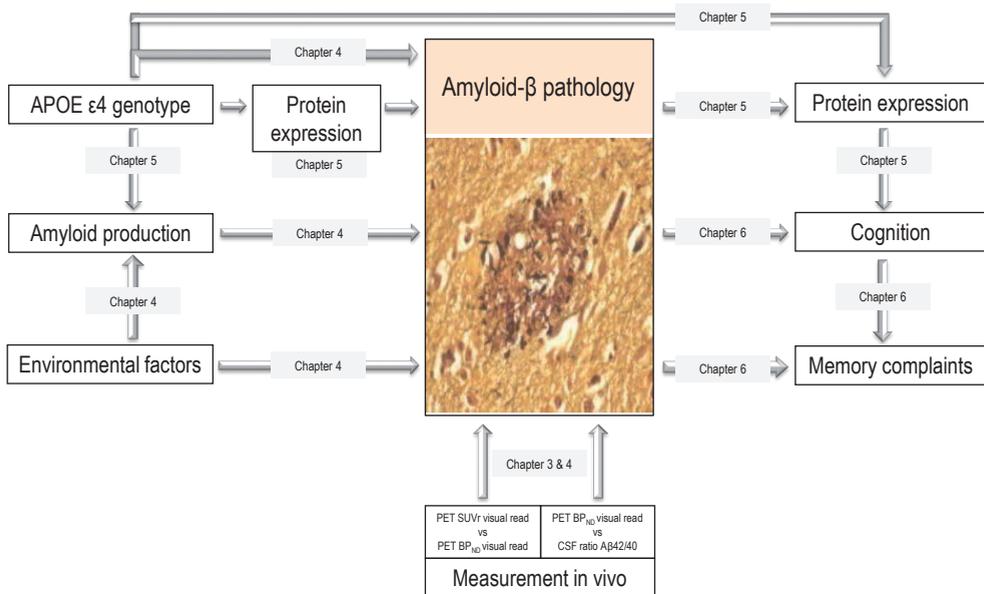
Figure 4. Pathophysiological model for amyloid pathology
Summary of research questions on early amyloid pathology investigated in this thesis.

V. GENERAL AIM

This thesis focuses on exploring the mechanisms underlying early amyloid accumulation in the brain of cognitively normal elderly, by investigating the relation of amyloid production with amyloid aggregation, the influence of APOE on AD pathophysiology, and the relation between amyloid aggregation and memory performance. We investigated the following research questions (Figure 4):

I. Diagnosis of preclinical AD:
 – - What is the most accurate method to visually rate [^{18}F]flutemetamol amyloid-PET images, dynamic BP_{ND} or static SUV?
 – - Are CSF and PET measures for amyloid aggregation comparable in cognitively normal subjects?

II. Pathophysiology:
 – - Does amyloid production influence amyloid aggregation in very early AD?
 – - Can we identify APOE-dependent molecular pathways associated with amyloid aggregation?
 – - Is amyloid aggregation related to memory performance in preclinical AD?

THESIS OUTLINE

In the first chapters of this thesis we describe our sample of cognitively normal monozygotic twins (chapter 2), and identify the optimal image analysis method for most accurate rating of visual amyloid-PET images in cognitively normal subjects (chapter 3). In the next part of this thesis we will investigate the early pathophysiology of AD. We aim to assess the underlying mechanisms for the association between amyloid production and aggregation using a monozygotic twins design (chapter 4). In patients with AD across the disease spectrum, we aim to identify molecular pathways associated with amyloid aggregation using cerebrospinal fluid proteomics, and to study potential modifying effects of APOE ε4 genotype (chapter 5). Finally, we investigate the relation between amyloid pathology, memory performance and cognitive complaints in cognitively normal elderly twins (chapter 6). We conclude this thesis by a summary and general discussion of the results from these studies (chapter 7).

REFERENCES

1. International, W.H.O.a.A.s.D., *Dementia: a public health priority [Internet]*. 2012, WHO Press.
2. Bateman, R.J., et al., *Clinical and biomarker changes in dominantly inherited Alzheimer's disease.* N Engl J Med, 2012. **367**(9): p. 795-804.
3. Villemagne, V.L., et al., *Amyloid beta deposition, neurodegeneration, and cognitive decline in sporadic Alzheimer's disease: a prospective cohort study*, in *Lancet neurology*. 2013. p. 357-367.
4. Jansen, W.J., et al., *Prevalence of cerebral amyloid pathology in persons without dementia: a meta-analysis*, in *JAMA : the journal of the American Medical Association*. 2015. p. 1924-1938.
5. Jellinger, K.A. and J. Attems, *Prevalence of dementia disorders in the oldest-old: an autopsy study.* Acta Neuropathol, 2010. **119**(4): p. 421-33.
6. Braak, H. and E. Braak, *Diagnostic criteria for neuropathologic assessment of Alzheimer's disease.* Neurobiol Aging, 1997. **18**(4 Suppl): p. S85-8.
7. Selkoe, D.J. and J. Hardy, *The amyloid hypothesis of Alzheimer's disease at 25 years.* EMBO Mol Med, 2016. **8**(6): p. 595-608.
8. Hardy, J. and B. De Strooper, *Alzheimer's disease: where next for anti-amyloid therapies?* Brain, 2017. **140**(4): p. 853-855.
9. Sperling, R.A., et al., *The A4 study: stopping AD before symptoms begin?* Sci Transl Med, 2014. **6**(228): p. 228fs13.
10. Timmers, M., et al., *BACE1 Dynamics Upon Inhibition with a BACE Inhibitor and Correlation to Downstream Alzheimer's Disease Markers in Elderly Healthy Participants.* J Alzheimers Dis, 2017. **56**(4): p. 1437-1449.
11. Dubois, B., et al., *Research criteria for the diagnosis of Alzheimer's disease: revising the NINCDS-ADRDA criteria*, in *Lancet neurology*. 2007. p. 734-746.
12. Nelissen, N., et al., *Phase 1 study of the Pittsburgh compound B derivative 18F-flutemetamol in healthy volunteers and patients with probable Alzheimer disease.*, in *Journal of nuclear medicine : official publication, Society of Nuclear Medicine*. 2009, Society of Nuclear Medicine. p. 1251-1259.
13. Klunk, W.E., et al., *Imaging brain amyloid in Alzheimer's disease with Pittsburgh Compound-B.* Ann Neurol, 2004. **55**(3): p. 306-19.
14. Molinuevo, J.L., et al., *The clinical use of cerebrospinal fluid biomarker testing for Alzheimer's disease diagnosis: a consensus paper from the Alzheimer's Biomarkers Standardization Initiative*, in *Alzheimer's & dementia : the journal of the Alzheimer's Association*. 2014. p. 808-817.
15. Landau, S.M., et al., *Comparing PET imaging and CSF measurements of Ass*, in *Annals of neurology*. 2013.
16. Vassar, R., et al., *Beta-secretase cleavage of Alzheimer's amyloid precursor protein by the transmembrane aspartic protease BACE.* Science, 1999. **286**(5440): p. 735-41.
17. Sanchez, L., et al., *Abeta40 and Abeta42 amyloid fibrils exhibit distinct molecular recycling properties.* J Am Chem Soc, 2011. **133**(17): p. 6505-8.
18. Janelidze, S., et al., *Concordance Between Different Amyloid Immunoassays and Visual Amyloid Positron Emission Tomographic Assessment.* JAMA Neurol, 2017. **74**(12): p. 1492-1501.
19. Lewczuk, P., et al., *Cerebrospinal Fluid Abeta42/40 Corresponds Better than Abeta42 to Amyloid PET in Alzheimer's Disease.* J Alzheimers Dis, 2017. **55**(2): p. 813-822.
20. Buckley, C.J., et al., *Validation of an electronic image reader training programme for interpretation of [18F]flutemetamol beta-amyloid PET brain images.* Nucl Med Commun, 2017. **38**(3): p. 234-241.
21. Thurfjell, L., et al., *Automated quantification of 18F-flutemetamol PET activity for categorizing scans as negative or positive for brain amyloid: concordance with visual image reads.* J Nucl Med, 2014. **55**(10): p. 1623-8.
22. Salloway, S., et al., *Performance of [(18)F]flutemetamol amyloid imaging against the neuritic plaque component of CERAD and the current (2012) NIA-AA recommendations for the neuropathologic diagnosis of Alzheimer's disease.* Alzheimers Dement (Amst), 2017. **9**: p. 25-34.

23. van Berckel, B.N., et al., *Longitudinal amyloid imaging using 11C-PiB: methodologic considerations.* J Nucl Med, 2013. **54**(9): p. 1570-6.

24. Zwan, M., et al., *Concordance between cerebrospinal fluid biomarkers and [11C]PIB PET in a memory clinic cohort.*, in *Journal of Alzheimer's disease : JAD.* 2014, IOS Press. p. 801-807.

25. Mattsson, N., et al., *Independent information from cerebrospinal fluid amyloid-beta and florbetapir imaging in Alzheimer's disease.* Brain, 2015. **138**(Pt 3): p. 772-83.

26. Palmqvist, S., et al., *Cerebrospinal fluid analysis detects cerebral amyloid-beta accumulation earlier than positron emission tomography.* Brain, 2016. **139**(Pt 4): p. 1226-36.

27. Perrotin, A., et al., *Subjective cognition and amyloid deposition imaging: a Pittsburgh Compound B positron emission tomography study in normal elderly individuals.* Arch Neurol, 2012. **69**(2): p. 223-9.

28. Jansen, W.J., et al., *Association of Cerebral Amyloid-beta Aggregation With Cognitive Functioning in Persons Without Dementia.* JAMA Psychiatry, 2017.

29. Chetelat, G., et al., *Relationship between atrophy and beta-amyloid deposition in Alzheimer disease.* Ann Neurol, 2010. **67**(3): p. 317-24.

30. Gatz, M., et al., *Role of genes and environments for explaining Alzheimer disease.* Arch Gen Psychiatry, 2006. **63**(2): p. 168-74.

31. Gatz, M., et al., *Complete ascertainment of dementia in the Swedish Twin Registry: the HARMONY study.* Neurobiol Aging, 2005. **26**(4): p. 439-47.

32. Hinrichs, A.L., et al., *Cortical binding of pittsburgh compound B, an endophenotype for genetic studies of Alzheimer's disease.* Biol Psychiatry, 2010. **67**(6): p. 581-3.

33. Johansson, V., et al., *Cerebrospinal fluid microglia and neurodegenerative markers in twins concordant and discordant for psychotic disorders.* Eur Arch Psychiatry Clin Neurosci, 2016.

34. Corder, E.H., et al., *Gene dose of apolipoprotein E type 4 allele and the risk of Alzheimer's disease in late onset families.* Science, 1993. **261**(5123): p. 921-3.

35. Ward, A., et al., *Prevalence of apolipoprotein E4 genotype and homozygotes (APOE e4/4) among patients diagnosed with Alzheimer's disease: a systematic review and meta-analysis.* Neuroepidemiology, 2012. **38**(1): p. 1-17.

36. Jun, G., et al., *A novel Alzheimer disease locus located near the gene encoding tau protein.* Mol Psychiatry, 2016. **21**(1): p. 108-17.

37. Rohn, T.T., *Proteolytic cleavage of apolipoprotein E4 as the keystone for the heightened risk associated with Alzheimer's disease.* Int J Mol Sci, 2013. **14**(7): p. 14908-22.

38. Lee, L.C., M.Q.L. Goh, and E.H. Koo, *Transcriptional regulation of APP by apoE: To boldly go where no isoform has gone before: ApoE, APP transcription and AD: Hypothesised mechanisms and existing knowledge gaps.* Bioessays, 2017. **39**(9).

39. Ewers, M., et al., *Increased CSF-BACE 1 activity is associated with ApoE-epsilon 4 genotype in subjects with mild cognitive impairment and Alzheimer's disease.* Brain, 2008. **131**(Pt 5): p. 1252-8.

40. Gispert, J.D., et al., *The APOE epsilon4 genotype modulates CSF YKL-40 levels and their structural brain correlates in the continuum of Alzheimer's disease but not those of sTREM2.* Alzheimers Dement (Amst), 2017. **6**: p. 50-59.

41. Villegas-Llerena, C., et al., *Microglial genes regulating neuroinflammation in the progression of Alzheimer's disease.* Curr Opin Neurobiol, 2016. **36**: p. 74-81.

42. Lambert, J.C., et al., *Meta-analysis of 74,046 individuals identifies 11 new susceptibility loci for Alzheimer's disease*, in *Nature genetics.* 2013.

43. Seshadri, S., et al., *Genome-wide analysis of genetic loci associated with Alzheimer disease.* JAMA, 2010. **303**(18): p. 1832-40.

44. Hollingworth, P., et al., *Common variants at ABCA7, MS4A6A/MS4A4E, EPHA1, CD33 and CD2AP are associated with Alzheimer's disease.* Nat Genet, 2011. **43**(5): p. 429-35.

45. Sims, R., et al., *Rare coding variants in PLCG2, ABI3, and TREM2 implicate microglial-mediated innate immunity in Alzheimer's disease.* Nat Genet, 2017. **49**(9): p. 1373-1384.

46. Zhou, X., et al., *Identification of genetic risk factors in the Chinese population implicates a role of immune system in Alzheimer's disease pathogenesis.* Proc Natl Acad Sci U S A, 2018. **115**(8): p. 1697-1706.
47. Hoozemans, J.J., et al., *Neuroinflammation and regeneration in the early stages of Alzheimer's disease pathology.* Int J Dev Neurosci, 2006. **24**(2-3): p. 157-65.
48. Yin, Z., et al., *Immune hyperreactivity of Abeta plaque-associated microglia in Alzheimer's disease.* Neurobiol Aging, 2017. **55**: p. 115-122.
49. Morris, J.C., et al., *Developing an international network for Alzheimer research: The Dominantly Inherited Alzheimer Network.* Clin Investig (Lond), 2012. **2**(10): p. 975-984.
50. Zuroff, L., et al., *Clearance of cerebral Abeta in Alzheimer's disease: reassessing the role of microglia and monocytes.* Cell Mol Life Sci, 2017. **74**(12): p. 2167-2201.
51. Wirth, M., et al., *Gene-Environment Interactions: Lifetime Cognitive Activity, APOE Genotype, and Beta-Amyloid Burden.* Journal of Neuroscience, 2014. **34**(25): p. 8612-8617.
52. Xu, W., et al., *Meta-analysis of modifiable risk factors for Alzheimer's disease.* J Neurol Neurosurg Psychiatry, 2015. **86**(12): p. 1299-306.
53. Livingston, G., et al., *Dementia prevention, intervention, and care.* Lancet, 2017. **390**(10113): p. 2673-2734.
54. De Moor, M.H., et al., *Testing causality in the association between regular exercise and symptoms of anxiety and depression.* Arch Gen Psychiatry, 2008. **65**(8): p. 897-905.
55. Vitaro F, B.M., Arseneault L, *The discordant MZ-twin method: One step closer to the holy grail of causality.* International Journal of Behavioral Development, 2009. **33**(4): p. 376–382.
56. Spellman, D.S., et al., *Development and evaluation of a multiplexed mass spectrometry based assay for measuring candidate peptide biomarkers in Alzheimer's Disease Neuroimaging Initiative (ADNI) CSF*, in *Prot. Clin. Appl.* 2015. p. 715-731.
57. Perrin, R.J., et al., *Identification and validation of novel cerebrospinal fluid biomarkers for staging early Alzheimer's disease.* PLoS One, 2011. **6**(1): p. e16032.
58. Llano, D.A., et al., *A multivariate predictive modeling approach reveals a novel CSF peptide signature for both Alzheimer's Disease state classification and for predicting future disease progression.* PLoS One, 2017. **12**(8): p. e0182098.

PART

1

Cohort outline and PET rating methodology

CHAPTER

2

The EMIF-AD PreclinAD study: Study Design and Baseline Cohort Overview

Konijnenberg E, Carter SF, Ten Kate M, Den Braber A, Tomassen J, Nguyen HT, Yaqub MM, Demuru M, Teunissen CE, Serne E, Hillebrand AH, Moll A, Barkhof F, Lammertsma AA, Hinz R, Pendleton N, Amadi C, Boomsma DI, Scheltens P, Van Berckel BNM, Herholz K, Visser PJ

ABSTRACT

Background: Amyloid pathology is the pathological hallmark in Alzheimer's Disease (AD) and can precede clinical dementia by decades. So far it remains unclear how amyloid pathology leads to cognitive impairment and dementia. To design AD prevention trials it is key to include cognitively normal subjects at high risk for amyloid pathology and to find predictors of cognitive decline in these subjects. These goals can be accomplished by targeting twins, with additional benefits to identify genetic and environmental pathways for amyloid pathology, other AD biomarkers and cognitive decline.

Methods: From December 2014 to October 2017 we enrolled cognitively normal partici- pants aged 60 years and older from the ongoing Manchester and Newcastle Age and Cognitive Performance Research Cohort and the Netherlands Twins Register. In Manchester we included single individuals and in Amsterdam monozygotic twin pairs. At baseline, participants completed neuropsychological tests and questionnaires, and underwent physical examination, blood sampling, ultrasound of the carotid arteries, structural and resting state functional brain magnetic resonance imaging and dynamic amyloid positron emission tomography (PET) scanning with [^{18}F]flutemetamol. In addition, the twin cohort underwent lumbar puncture for cerebrospinal fluid collection, buccal cell collection, magnetoencephalography, optical coherence tomography, and retinal imaging.

Results: We included 285 participants, who were on average 74.8 ± 9.7 years old, 64% female. Fifty-eight participants (22%) had an abnormal amyloid PET scan.

Conclusions: A rich baseline dataset of cognitively normal elderly has been established to estimate risk factors and biomarkers for amyloid pathology and future cognitive decline.

BACKGROUND

Alzheimer's disease (AD) is the most common cause of dementia and is characterized by amyloid plaques and neurofibrillary tangles with subsequently progressive neuronal loss and eventually death [1]. Aggregation of amyloid is supposed to be the first event in AD and starts years before cognitive impairment occurs [2-4]. Post mortem pathological and biomarker studies have demonstrated that 20-40% of cognitively normal elderly possess abnormal amyloid levels in their brain [4-9]. These subjects are considered to be in the preclinical stage of AD [10, 11]. This presymptomatic window provides a unique opportunity for secondary prevention studies, as subjects have limited brain damage and no symptoms yet. Understanding the pathophysiological mechanisms underlying amyloid pathology in this preclinical stage of AD might also be critical to identify possible drug targets for the development of effective treatments.

There are, however, several research challenges for the development of prevention strategies in the preclinical AD stage. First, amyloid markers are needed for the diagnosis of preclinical AD. There is an urgent need for readily applicable screening markers, such as blood or imaging markers, to identify cognitively normal subjects at increased risk for amyloid pathology so that more expensive or invasive tests such as positron emission tomography (PET) scan or cerebrospinal fluid (CSF) via lumbar puncture can be performed in more selected populations. A number of markers have already been identified for this purpose but these need to be validated in preclinical/prodromal stages of the disease [12-15]. Secondly, there is still an incomplete understanding of what drives the development of amyloid pathology in cognitively normal subjects. Previous studies have identified a limited number of risk factors for amyloid pathology, such as Apolipoprotein E (APOE) genotype, age, and level of education [4, 16-18]. These established risk factors, however, can only explain part of the risk for amyloid pathology. Third, amyloid pathology has been associated with an increased risk for cognitive decline, but the rate of decline varies greatly [19]. A few possible prognostic factors in preclinical AD have been identified but they await replication [20, 21]. Fourth, current normative data for biomarkers and cognitive markers may be suboptimal as many cognitively normal subjects already have amyloid pathology. Finally, CSF and PET biomarkers for amyloid pathology do not match in about 15% of cases [22-24], in particular in cognitively normal subjects. It has been suggested that amyloid changes can be detected earlier in CSF than by PET but this requires further investigation [25].

In this paper, we describe the study design of the multisite PreclinAD study, which aims to address these clinical research challenges. Within this study, cognitively normal elderly are recruited from the Manchester and Newcastle Age and Cognitive Performance Research Cohort (ACPRC) in Manchester [26] and the Netherlands Twin Register (NTR) in Amsterdam [27]. From the NTR we recruited monozygotic (MZ) twins. When a relation is observed between two markers, studying MZ twins enables exploring the nature of the observed relation: 1) the MZ twin differences approach gives the possibility to study the
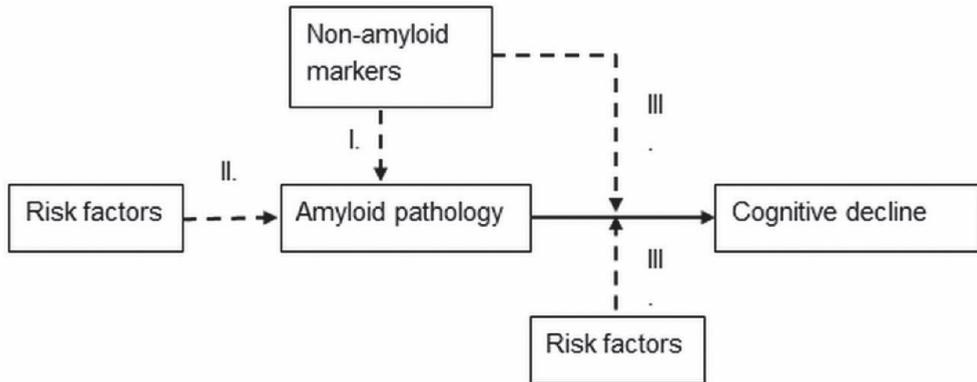
Figure 1. Hypothetical model amyloid pathology
Hypothetical model for evaluating risk factors for amyloid pathology, for cognitive decline in subjects with amyloid pathology and other markers that might be involved in early AD pathology. I: markers for amyloid pathology in cognitively healthy elderly, II: risk factors for amyloid pathology, III: prognostic markers for cognitive decline in cognitively normal subjects with amyloid pathology.

relation excluding confounding by genetic factors (the twins are genetically identical) and 2) the cross-twin cross-trait design, studying if marker 1 in one twin can predict marker 2 in its co-twin, gives the opportunity to study the contribution of shared familial factors (genes and common environment) to the relation. Previous studies using AD-type dementia as an outcome estimated the amount of variance explained by genetic factors to be around 80% [28], suggesting a major genetic role in the development of AD. However, there is a lack of studies estimating the contribution of genetic and environmental influences on AD biomarkers in non-demented individuals and the role of environmental risk and protective factors for AD remains unclear [18].

The PreclinAD study aimed to (i) validate existing and discover new markers for amyloid pathology in cognitively normal elderly, (ii) identify risk factors for amyloid pathology, (iii) identify prognostic markers for cognitive decline in cognitively normal subjects with amyloid pathology (Figure 2) and (iv) determine the contribution of genetic and environmental influences on these markers.

METHODS

Project

The European Information Framework for AD (EMIF-AD)
The study is part of the Innovative Medicine Initiative EMIF-AD project, which aims to facilitate the development of treatment for AD in non-demented subjects (http://www.emif.

eu/) by discovering and validating diagnostic markers, prognostic markers and risk factors for AD in non-demented subjects using existing data resources where possible.

Sample selection

We included 81 cognitively normal participants from the ACPRC. The ACPRC originally comprised over 6000 adults from the North of England, United Kingdom, who have undergone detailed batteries of cognitive function biannually until 2003 [26]. In 1999 and 2000 active members of this cohort were invited and consented to providing a deoxyribonucleic acid (DNA) sample in the Dyne-Steel DNA Archive for study of Cognitive Genetics in later life. In 2003 a subsample of 500 Manchester volunteers underwent detailed physical examination and provided samples of saliva, serum, and plasma. Over time, the cohort has reduced in size through attrition largely by mortality to a number of approximately 660 volunteers. Since 2003 study participants have been assessed biannually with a smaller battery of tests and rating scales in order to diagnose pathological cognitive impairment and emotional problems. The current study coincides with the fourth wave of follow-up investigations. In Amsterdam, monozygotic twins were recruited from the NTR [29]. The NTR started recruiting adolescent and adult twins and their relatives in 1987 and has included over 200.000 participants by 2012 [27]. Twins who gave consent for the NTR also allow researchers to approach them for participation in scientific studies. From 1991 onwards participants completed extensive questionnaires every two or three years and DNA was collected in the NTR-Biobank project [30]. Smaller subgroups of participants underwent biomarker collection such as lab tests, electroencephalogram or magnetic resonance imaging (MRI) [31-33]. The current study is a new NTR sub study.

Ethical considerations

The National Research Ethics Service Committee North West - Greater Manchester South performed ethical approval of the study in Manchester. The Medical Ethics Review Committee of the VU University Medical Center performed approval of the study in Amsterdam. Research was performed according to the principles of the Declaration of Helsinki and in accordance with the Medical Research Involving Human Subjects Act and codes on 'good use' of clinical data and biological samples as developed by the Dutch Federation of Medical Scientific Societies. All participants gave written informed consent.

Inclusion criteria

Inclusion criteria for the PreclinAD cohort were age 60 years and older, a delayed recall score above -1.5 SD of demographically adjusted normative data on the Consortium to Establish a Registry for Alzheimer's Disease 10 word list [34, 35], a Telephone Interview for Cognitive Status-modified score of 23 or higher [36], a 15-item Geriatric Depression Scale score <11 [37], and a Clinical Dementia Rating score of 0 [38] (Supplementary Table 1).

Exclusion criteria

To avoid possible interference with normal cognition, subjects with the following medical conditions, at present or in the past, were excluded: diagnosis of mild cognitive impairment (MCI), probable AD or other neurodegenerative disorders such as Huntington disease, cortical basal degeneration, multiple system atrophy, Creutzfeldt-Jakob disease, primary progressive aphasia or Parkinson's disease, stroke resulting in physical impairment, epilepsy with current use of antiepileptic drugs, brain infection (e.g. herpes simplex encephalitis), brain tumor, severe head trauma with loss of consciousness longer than five minutes, cancer with terminal life expectancy, untreated vitamin B12 deficiency, diabetes mellitus, thyroid disease, schizophrenia, bipolar disorders, or recurrent psychotic disorders. Furthermore, a history of recreational drug use, alcohol consumption >35 units per week (1 unit = 10ml or 8g of pure alcohol), use of high dose benzodiazepine, lithium carbonate, antipsychotics (including atypical agents), high dose antidepressants, or Parkinson's disease medication were exclusion criteria. Finally, subjects who were not able to attend the hospital due to physical morbidity or illness or who had a contraindication for MRI (e.g. metal implants, pacemaker etc.) were excluded (Supplementary Table 1).

Data collection

Neuropsychological testing battery and questionnaires

During a 4-hour screening research facility visit (Manchester) or home visit (Amsterdam), participants underwent extensive neuropsychological testing and questionnaires. A complete overview of the neuropsychological testing battery and questionnaires is provided in Supplementary Tables 2 and 3, respectively. In short, we assessed memory function with the Rey auditory verbal learning task [39], visual association task [40], face name associative memory exam [41], Rey complex figure recall [42], CANTAB paired associate learning [43], and digit span [44]. We also tested verbal fluency, naming [45], visuo-constructional skills and executive functions [42, 46, 47] (see Supplementary Table 2). Using questionnaires we assessed social and physical activities [48-50], sleep quality [51, 52], activities of daily living [53, 54], memory complaints [55], and psychiatric symptoms [56] (see Supplementary Table 3).

Physical examination

Data on waist circumference, hip circumference, body mass index, resting blood pressure, heart rate, and grip strength of dominant hand were collected for all participants (Table 1). In Manchester an ankle/brachial pressure index and a four-minute walking test were also performed. In Amsterdam, a trained physician performed exploratory neurological examination. In addition, a Bio-electrical Impedance Analysis, repeated resting blood pressure measurement, and lead 1 of an electrocardiogram (measured by holding a Diagnostick [57] for one minute) and a color photograph of the face of each participant was taken. See Table 1 and Supplementary Table 4 for all biomarker data availability.

Table 1. Sample characteristics

Demographic	n	Combined sample n=285 mean (SD) or n (%)	n	Amsterdam site n=204 mean (SD) or n (%)	n	Manchester site n=81 mean (SD) or n (%)
Age (years)	285	75.0 (9.7) (range 60-95)	204	70.8 (7.8) (range 60-94)	81	85.7 (4.3)*** (range 79-95)
Gender (% female)	285	182 (64)	204	119 (58)	81	63 (78)**
Education (years)	278	14.8 (4.2)	204	14.9 (4.5)	74	14.2 (3.0)
NART	285	41.9 (6.0)	204	41.2 (6.4)	81	43.7 (4.3)***
MMSE	281	28.9 (1.2)	204	28.9 (1.2)	77	28.7 (1.3)
TICS-m	282	28.3 (3.2)	204	28.3 (3.0)	78	28.5 (3.7)
CERAD 10 word recall	285	22.8 (3.3)	204	22.0 (3.0)	81	24.8 (3.3)***
GDS	282	1.0 (1.5)	204	0.7 (1.2)	78	1.9 (1.7)***
CDR total	284	0 (0.1)	204	0	80	0.03 (0.1)*
CDR sum of boxes	284	0.03 (0.1)	204	0	80	0.1 (0.3)**
APOE ε4 carrier	282	85 (30)	202	66 (33)	80	19 (24)
APOE4 genotype	282		202		80	
ε2ε2		2 (1)		2 (1)		-
ε2ε3		24 (9)		12 (6)		12 (15)
ε2ε4		9 (3)		6 (3)		3 (4)
ε3ε3		171 (61)		122 (60)		49 (61)
ε3ε4		69 (25)		54 (27)		15 (19)
ε4ε4		7 (3)		6 (3)		1 (1)
Family history dementia	273	106 (39)	203	92 (45)	70	14 (20)***
Diabetes type II	-	-	204	13 (6)	-	-
Current smoker	281	23 (8)	203	21 (10)	78	2 (3)
Alcohol use present	282	224 (79)	204	158 (77)	78	66 (85)
Blood pressure (mmHg)	281	152 (21)/80 (12)	202	155 (21)/83 (11)	79	143 (19)/70 (10)***
Pulse rate (beats/minute)	279	66 (11)	202	65 (11)	77	69 (10)**
Height (m)	283	1.66 (0.10)	204	1.69 (0.09)	79	1.60 (0.08)***
Weight (kg)	283	73.1 (14.0)	204	75.7 (13.6)	79	66.6 (13.0)***
Body Mass Index	283	26.3 (4.0)	204	26.4 (3.8)	79	26.1 (4.3)
Waist circumference (cm)	282	93.4 (13.6)	203	94.7 (12.0)	79	89.9 (16.6)**
Hip Circumference (cm)	234	101.9 (11.4)	155	102.6 (9.8)	79	100.5 (14.0)
Grip strength (kg)	283	28.5 (11.3)	204	30.9 (10.9)	79	22.2 (9.8)***
CSF Aβ1-42 pg/mL	-	-	126	889 (314)	-	-
CSF Aβ1-40 pg/mL	-	-	126	9592 (2844)	-	-
Ratio CSF Aβ1-42/1-40	-	-	126	0.10 (0.03)	-	-
CSF total-tau pg/mL	-	-	126	412 (143)	-	-
CSF p-tau 181 pg/mL	-	-	126	76 (44)	-	-
Visual read PET abnormal	272	58 (22)	196	32 (16)	76	26 (34)**
Fazekas score	279	1.3 (0.9)	199	1.2 (0.8)	80	1.7 (0.8)***
Medial Temporal lobe Atrophy score (average left and right)	277	0.7 (0.7)	197	0.6 (0.7)	80	0.9 (0.6)*
Parietal Atrophy (average left and right)	279	1.1 (0.7)	199	1.1. (0.7)	80	1.2 (0.6)*

Group differences as assessed with t-test or chi^2-test: *** p<0.001; ** p<0.01; * p<0.05 Abbreviations: NART: National Adult Reading Test, MMSE: Mini Mental State Examination, TICS-m: Modified Telephone Interview for Cognitive Status, CERAD: Consortium to Establish A Registry for Alzheimer's Disease, GDS: Geriatric Depression Scale; CDR: Clinical Dementia Rating; APOE: Apolipoprotein E; CSF: cerebrospinal fluid; Aβ: amyloid beta; p-tau: phosphorylated tau; PET: positron emission tomography

Blood collection

For all participants 50 mL blood was collected in the morning, after two hours of fasting, including EDTA blood for DNA isolation, plasma, and buffy coat, clotted blood for serum, and Paxgene tubes for RNA isolation. Immediate plasma analysis was performed for complete blood count, haemoglobin A1C, 2-hours fasting glucose, liver enzymes, lipid spectrum, C-reactive protein, erythrocyte sedimentation rate, thyroid stimulating hormone, and vitamin B12. EDTA tubes with anticoagulated whole blood were centrifuged at 1300-2000 g for ten minutes and plasma and remaining buffy coat were, like whole blood for collecting serum, aliquoted according to the standardized operating procedures of the BIOMARKAPD project [58] in aliquots of 0.25-0.5 mL and stored locally until analysis. All samples were stored at -80 °C within two hours. Two 2.5 mL Paxgene tubes were stored at room temperature for a minimum of two and a maximum of 72 hours, before they were frozen at -20 °C until RNA isolation. EDTA whole blood tube for DNA analysis was stored at -20 °C until isolation.

DNA and RNA collection

Extraction of DNA and RNA from peripheral blood samples was performed at both sites. In addition, at the Amsterdam site buccal cells were collected for zygosity, genome-wide association studies, and epigenetics [59]. Amsterdam participants were genotyped on the Affymetrix Axiom array and the Affymetrix 6 array [60], these were first cross chip imputed following the protocols as described by Fedko and colleagues [61] and then imputed to HRC with the Michigan Imputation server [62]. The APOE genotypes were assessed using isoforms in Manchester as described by Ghebranious et al [63]. In Amsterdam APOE genotype was assessed using imputed dosages of the SNP rs429358 (APOE ε4, imputation quality = 0.956) and rs7412 (APOE ε2, imputation quality = 0.729) [64].

Ultrasound carotid artery

In Manchester a duplex ultrasound scan of the left and right carotid artery was performed to collect data on velocity, vessel thickness, stenosis and plaques rated according to the North American Symptomatic Carotid Endarterectomy Trial guidelines [65]. In Amsterdam a duplex ultrasound scan of the right carotid artery was performed to assess intima media thickness and distension using ArtLab software [66-68].

Magnetic Resonance Imaging (MRI)

Acquisition protocol

In Manchester, brain scans were performed at the Wellcome Trust Manchester Clinical Research Facility (Central Manchester University Hospital NHS Foundation Trust). All MRI investigations were performed on a 3T Philips Achieva scanner using a 32 channel head

coil. Participants underwent an MRI protocol that included a 3D-T1, 3D fluid-attenuated inversion recovery (FLAIR), pseudo continuous arterial spin labeling (ASL), and quantitative magnetization transfer scans. In Amsterdam, brain scans were also obtained using a 3T Philips Achieva scanner equipped with an 8-channel head coil. The MRI protocol included structural 3D-T1, FLAIR, ASL, susceptibility weighted imaging (SWI), diffusion tensor imaging (DTI), and 6 minutes of resting state functional MRI (rs-fMRI), MRI settings are presented in Supplementary Table 5.

Visual assessment

All MRI scans were reviewed for incidental findings by an experienced neuroradiologist, and visually rated by a single experienced rater (MtK) who was blinded to demographic information and twin pairing at moment of rating. White matter hyperintensities were visually assessed on the FLAIR images using the four point Fazekas scale (none, punctuate, early confluent, confluent) [69]. Lacunes were defined as deep lesions from 3 to 15 mm with CSF like signal on T1-weighted and FLAIR images. Microbleeds were assessed on SWI images and defined as rounded hypo intense homogeneous foci of up to 10 mm in the brain parenchyma. Medial temporal lobe atrophy was assessed on coronal reconstructions of the T1-weighted images using a 5-point visual rating scale [70]. Global cortical atrophy was rated on transversal FLAIR images using a four point scale [71]. Posterior cortical atrophy was assessed using a 4-point visual rating scale [72].

Amyloid positron emission tomography (PET)

[^{18}F]flutemetamol

In both centers [^{18}F]flutemetamol was used as fibrillar amyloid radiotracer. [^{18}F]flutemetamol is a ^{11}C-Pittsburgh compound B (PiB) derivative radiolabeled with ^{18}F and has structural similarity to PiB, which is a frequently used compound for in vivo detection of amyloid plaques [73]. In Manchester, the tracer [^{18}F]flutemetamol, a specific fibrillar amyloid radiotracer, was produced at the Wolfson Molecular Imaging Centre (WMIC)'s Good Manufacturing Practice radiochemistry facility using General Electric Healthcare's (GEHC) FASTlab and cassettes. For Amsterdam, the same tracer was produced at the Cyclotron Research Center of the University of Liège (Liège, Belgium). GEHC was responsible for production and transportation of [^{18}F] flutemetamol. Prior [^{18}F]flutemetamol studies showed good brain uptake and radiation dosimetry similar to other radiopharmaceuticals in clinical use, test-retest variability for image quantitation differentiation between healthy participants and patients with AD, and the ability to detect brain amyloid [73].

Acquisition protocol

At both sites all participants were scanned dynamically from 0 to 30 minutes and then again from 90 to 110 minutes after intravenous injection of 185 MBq (± 10%) [^{18}F]flutemetamol.

The initial scan (0-30 minutes) was shortened or omitted if it was not accepted or tolerated by the participant. The second time window (90-110 minutes) is the recommended interval for assessment of amyloid biomarker abnormality. In Manchester all PET scans were performed on a High-Resolution Research Tomograph brain scanner (HRRT; Siemens/CTI, Knoxville, TN) at the WMIC of the University of Manchester. Two 7 minute transmission scans using a ^{137}Cs point source were acquired for subsequent attenuation and scatter correction; one prior to the first emission scan and another following the second emission scan [74, 75]. In Amsterdam all PET scans were performed using a Philips Ingenuity Time-of-Flight PET-MRI scanner at the department of Radiology & Nuclear Medicine of the VU University Medical Center. Immediately prior to each part of the PET scan a dedicated MR sequence (atMR) was performed for attenuation correction of the PET image [76]. For both sites, the first dynamic emission scan was reconstructed into 18 frames with progressive increase in frame length (6x5, 3x10, 4x60, 2x150, 2x300, 1x600 s). The second part of the scan consisted of 4 x 5-minute frames. During scanning, the head was immobilized to reduce movement artefacts and, using laser beams.

Visual assessment

All [18F]flutemetamol amyloid PET scans were checked for movement and frames were summed to obtain a static image (90-110 minutes). PET images were visually read as abnormal or normal by an experienced reader (SFC in Manchester and BvB in Amsterdam), blinded to clinical and demographic data, according to GEHC guidelines described in the summary of product characteristics [77].

CSF collection (Amsterdam site only)

Up to 20 mL CSF was obtained by lumbar puncture in Sarstedt polypropylene syringes using a Spinocan 25 Gauge needle in one of the intervertebral spaces between L3 and S1. One mL was immediately processed for leukocyte count, erythrocyte count, glucose, and total protein. The remaining CSF was mixed and centrifuged at 1300-2000g at 4 °C for ten minutes. Supernatants were stored in aliquots of 0.25-0.5 mL and frozen within two hours at -80 °C and stored for future biomarker discovery studies [78]. Levels of amyloid β1-40 and β1-42 were analyzed using kits from ADx Neurosciences/Euroimmun according to manufacturer instructions. All samples were measured in kits from the same lot.

Magneto-encephalography (MEG, Amsterdam site only)

MEG measurements were recorded using a 306-channel, whole-head MEG system (ElektaNeuromag Oy, Helsinki, Finland) in a magnetically shielded room (Vacuumschmelze GmbH, Hanau, Germany). Participants were instructed to lay on a bed with their eyes closed but to stay awake and reduce eye movements in order to minimize artifacts. Participants were scanned five minutes with eyes closed, two minutes with eyes open and another five minutes

with eyes closed. On MEG we used source-reconstructed time series (https://doi.org/10.1016/j.neuroimage.2011.11.005) to extract both frequency spectrum properties (relative band power and peak frequency) and functional connectivity between regions, as well as network topology using modern network theory (synchronization likelihood, modularity, path length, phase lag index) [79, 80]. These analysis techniques were applied using BrainWave software (http://home.kpn.nl/stam7883/brainwave.html)[81] and in-house MATLAB scripts (MATLAB Release 2012a, The MathWorks, Inc., Natick, Massachusetts, United States).

Ophthalmological markers (Amsterdam site only)

Exploratory eye examination
An exploratory eye examination including measurement of best corrected visual acuity, refractive error, and intra-ocular pressure (non-contact tonometry) was performed. In a subsample (n=50) slit lamp examination by a trained physician was performed as well.

Ocular Coherence Tomography (OCT)
OCT was performed using the Heidelberg Spectralis. With OCT we measured retinal nerve fiber layer tissue, total macular thickness, and the thickness of macular individual retinal layers using the built-in segmentation software from the Spectralis [82], which might correlate with cerebral amyloid pathology [83]. With the same device a fundus auto fluorescence was performed to try to detect degenerative retinal abnormalities possibly related to amyloid pathology [83, 84].

Retinal imaging
Using a non-mydriatic camera (Topcon) two digital images (mostly 50º, and some 30º) per eye were taken of the retina one centered to the macula and the other to the optic nerve head, after pupil dilation with tropicamide. On the digitalized fundoscopy image we measured retinal vascular parameters using the Singapore I vessel Assessment software [85].

Data management
Data were stored in the online database CASTOR (https://castoredc.com/) with restricted access. Each site provided clinical information and sample information to the database according to a predefined case report form. Blood and CSF samples, PET and MRI scans and MEG data are stored locally until centralized analysis.

Follow-up visit
A follow-up visit including neuropsychological testing, questionnaires at both sites, and physical examination, blood sampling, buccal cell collection, and lumbar puncture in a subset will be performed after 21 months ± 3 months. Follow-up started in February 2017 and

is still ongoing. So far 241 were invited and of those 221 (92%) participated in the follow-up. For the twin pairs an additional follow-up visit after 4 years is planned, starting January 2019. This follow-up includes, amyloid-PET, tau-PET, MRI, lumbar puncture, neuropsychological testing, questionnaires, physical examination, blood sampling and buccal cell collection.

Statistical Approaches

Group analysis

The main outcome measure will be the presence of amyloid pathology as a dichotomous and continuous outcome measure. We aim to identify for each diagnostic modality the best set of predictors for amyloid pathology using step forward selection. The best predictors for each modality will be combined in a single risk score, based on the beta of these predictors in the regression model. Analysis will be performed using multivariate multilevel Generalized Estimating Equations analysis with correction for age, gender, education, and twin status (Amsterdam only) [86]. In addition, as there are differences between the cohorts, we will correct for cohort in the analysis and test interactions of predictor variables with cohort to check whether pooling the data may introduce a bias.

RESULTS

Inclusion

Manchester

From the ACPRC in total 321 subjects were invited by letter to participate in the PreclinAD study. From this selection 81 subjects were included for participation (see Fgure 2a).

Amsterdam

In total 517 twins from the NTR were invited by letter. Of these, 100 complete pairs (99 MZ, 1 dizygotic, as confirmed with DNA analysis) and four singletons, of which the co-twin did not meet the inclusion criteria due to cognitive impairment of other neurological conditions, were included (see Figure 2b). This also included one twin who appeared to be demented at baseline hospital visit, even though this subject passed the inclusion criteria at first and one subject from a monozygotic triplet, which we included due to the unique opportunity to analyze a genetically identical triplet, but this subject did not meet the inclusion criteria due to MCI. All participants, except for one twin pair, have European descent. When analyzing genetic data this twin pair will be excluded from analysis.
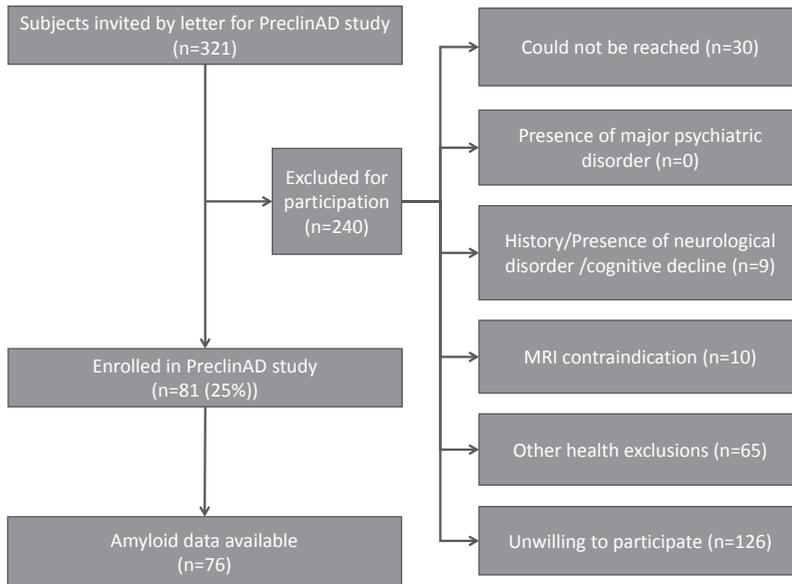
Figure 2a. Inclusion flow chart participants Manchester
Invited subjects were selected from a sample of 660 subjects that were part of the Manchester and Newcastle Age and Cognitive Performance Research Cohort (ACPRC, Manchester) at time of recruitment.
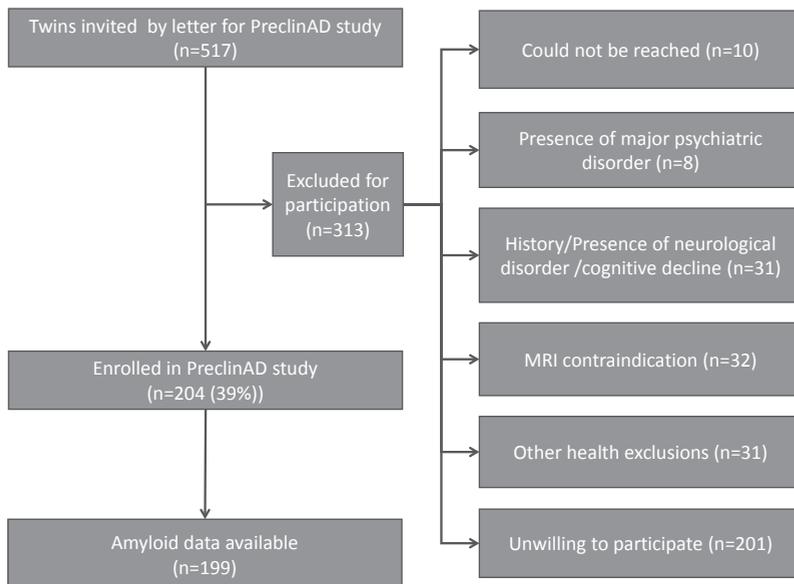
Figure 2b. Inclusion flow chart participants Amsterdam
Invited twins were selected from a sample of 678 monozygotic twins that were actively registered at the Netherlands Twin Register (Amsterdam) at time of recruitment

Percentage of subjects with abnormal PET by agegroup

Figure 3. Amyloid abnormality on PET scan per age group (n=58, 22%)
Abnormal PET scan was visually read on summed static PET images, 12% of subjects aged 60-70 years had an abnormal PET, 16% of the subjects between 70-80 years and 36% of the subjects 80 years and older.

Demographics and biomarkers

Participants were on average 74.8 years old, 64% female and 30% APOE ε4 carrier, for further baseline characteristics see Table 1. Participants tested in Manchester were older compared to Amsterdam participants (85.7 vs 70.8 years, p<0.001) and m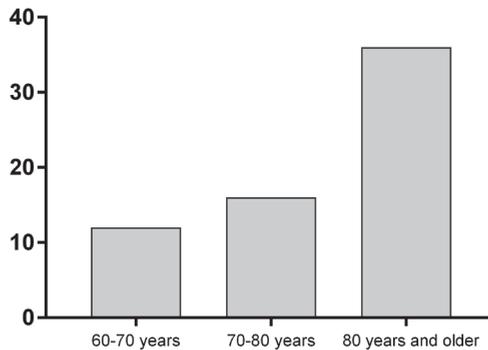ore often female (78 vs 58%, p<0.01). Manchester participants also had a higher intelligence score according to the Adult Reading Task (43.7 vs 41.2, p<0.001), less often a family member with dementia (20 vs 45%, p<0.001), lower blood pressure, (143/70 vs 155/83 mmHg, p<0.001) and higher white matter lesion load according to the Fazekas score (1.7 vs 1.2, p<0.001, Table 1).

Amyloid data were available for 275 participants (Manchester n=76, Amsterdam n=199). In Amsterdam, 123 participants had both CSF and PET available, 73 PET only and 3 CSF only. For ten participants we were unable to assess amyloid status: six participants were not able to attend the hospital after inclusion, one did not undergo PET due to meningioma's on MRI, two participants suffered from claustrophobia during the hospital visit and one had a panic attack before injection of the PET-tracer. Dynamic PET scans were present in 261 participants: four participants failed their dynamic scan due to logistic problems, in seven participants quality control of the images failed.

Amyloid pathology

Of the 272 participants with a static PET amyloid measure available, 58 (21%) had an abnormal PET scan as visually read on summed static PET image. An abnormal PET was less common in Amsterdam (16%) than in Manchester (34%) (p<0.001). The prevalence of abnormal amyloid PET scans was higher in older age groups (Figure 3).

DISCUSSION

The PreclinAD study is a prospective cohort study of 285 cognitively normal elderly individuals with extensive phenotyping for amyloid pathology, neurodegeneration markers, cognition, and life style factors.

We noted some differences in baseline characteristics between the Manchester and Amsterdam sites. This could mainly be explained by the higher age in the Manchester sub study. The prevalence of amyloid pathology increased with age, although the prevalence was somewhat lower than would be expected based on a large subject-level meta-analysis, in particular in the age range below 80 [4]. This might be explained by the relatively healthy sample of participants, due to the strict in- and exclusion criteria.

The Amsterdam sub study is the first to assess a wide range of AD markers in a large sample of cognitively normal monozygotic twin pairs above age 60. The uniqueness of studying a cohort of twin pairs sharing 100% of their genetic material enables us to further explore the nature of the relation between AD markers. If MZ twin pairs are highly similar for AD markers, this suggests involvement of shared genetic and/or shared environmental factors, whereas within-pair differences indicates the involvement of unique environmental factors [87]. The strength of the MZ twin within-pair difference model further enable us to identify environmental risk factors (e.g. smoking, alcohol use, diet, sleep, physical activity, cognitive activity and education) that, either directly or indirectly through epigenetic mechanisms, explain observed differences in AD markers within pairs. This may provide clues for novel preventive and therapeutic strategies. However, it also has the disadvantage that, because MZ twins are genetically identical, we have to correct for twin dependency in all analysis, which may reduce statistical power [86]. Further, we did not include dizygotic twins in the current study, because this optimizes power for twin difference analysis, thereby strengthening the search for environmental risk factors influencing AD development. However this has the disadvantage that the relative contribution of shared genetic and shared environmental factors to within-pair correlations cannot be estimated. Still previous studies in elderly twins, however, suggested that the contribution of shared environment at older age is highly limited, possibly because subjects are already living apart for a longer period of time [88, 89].

A strength of our study, compared to other studies on preclinical AD, is that participants have been recruited from cohorts that have been ongoing for up to 20 years, which provides the possibility to test biomarkers, cognition and life style collected in the past as predictors for AD biomarkers. Our study design also has several limitations. First, although acquisition protocols were harmonized across sites, they were not always identical (e.g. use of HRRT vs PET-MR). For this reason, site will be used as a covariate in all analyses. Some of the biomarkers were only acquired at the Amsterdam site, which will reduce the statistical power for the analysis of these markers.

CONCLUSIONS

We collected a large European cognitively normal sample with an extensive panel of AD biomarkers available at baseline, with clinical follow-up planned after two years, to identify healthy elderly at risk for amyloid pathology and future cognitive decline. Results from this study will improve understanding of the pathophysiology of AD and thereby help to adapt design of secondary prevention trials.

REFERENCES

1. Braak H, Braak E: Diagnostic criteria for neuropathologic assessment of Alzheimer's disease. *Neurobiol Aging* 1997, 18(4 Suppl):S85-88.
2. Bateman RJ, Xiong C, Benzinger TL, Fagan AM, Goate A, Fox NC, Marcus DS, Cairns NJ, Xie X, Blazey TM *et al*: Clinical and biomarker changes in dominantly inherited Alzheimer's disease. *N Engl J Med* 2012, 367(9):795-804.
3. Villemagne VL, Burnham S, Bourgeat P, Brown B, Ellis KA, Salvado O, Szoeke C, Macaulay SL, Martins R, Maruff P *et al*: Amyloid beta deposition, neurodegeneration, and cognitive decline in sporadic Alzheimer's disease: a prospective cohort study. In: *Lancet neurology*. vol. 12; 2013: 357-367.
4. Jansen WJ, Ossenkoppele R, Knol DL, Tijms BM, Scheltens P, Verhey FR, Visser PJ, Amyloid Biomarker Study G, Aalten P, Aarsland D *et al*: Prevalence of cerebral amyloid pathology in persons without dementia: a meta-analysis. In: *JAMA : the journal of the American Medical Association*. vol. 313; 2015: 1924-1938.
5. Price JL, Morris JC: Tangles and plaques in nondemented aging and "preclinical" Alzheimer's disease. In: *Annals of neurology*. vol. 45; 1999: 358-368.
6. Mintun MA, Larossa GN, Sheline YI, Dence CS, Lee SY, Mach RH, Klunk WE, Mathis CA, DeKosky ST, Morris JC: [11C]PIB in a nondemented population: potential antecedent marker of Alzheimer disease. In: *Neurology*. vol. 67; 2006: 446-452.
7. Aizenstein HJ, Nebes RD, Saxton JA, Price JC, Mathis CA, Tsopelas ND, Ziolko SK, James JA, Snitz BE, Houck PR *et al*: Frequent amyloid deposition without significant cognitive impairment among the elderly. In: *Archives of neurology*. vol. 65; 2008: 1509-1517.
8. Rowe CC, Ellis KA, Rimajova M, Bourgeat P, Pike KE, Jones G, Fripp J, Tochon-Danguy H, Morandeau L, O'Keefe G *et al*: Amyloid imaging results from the Australian Imaging, Biomarkers and Lifestyle (AIBL) study of aging. In: *Neurobiology of aging*. vol. 31; 2010: 1275-1283.
9. Chételat GLJRVNPAdLSVEFVR: Amyloid imaging in cognitively normal individuals, at-risk populations and preclinical Alzheimer's disease. In: *NeuroImage: Clinical*. vol. 2; 2013: 356-365.
10. Dubois B, Feldman HH, Jacova C, Hampel H, Molinuevo JL, Blennow K, DeKosky ST, Gauthier S, Selkoe D, Bateman R *et al*: Advancing research diagnostic criteria for Alzheimer's disease: the IWG-2 criteria. In: *Lancet neurology*. vol. 13, 2014/05/23 edn; 2014: 614-629.
11. McKhann GM, Knopman DS, Chertkow H, Hyman BT, Jack CRJ, Kawas CH, Klunk WE, Koroshetz WJ, Manly JJ, Mayeux R *et al*: The diagnosis of dementia due to Alzheimer's disease: recommendations from the National Institute on Aging-Alzheimer's Association workgroups on diagnostic guidelines for Alzheimer's disease. In: *Alzheimer's & dementia : the journal of the Alzheimer's Association*. vol. 7, 2011/04/26 edn; 2011: 263-269.
12. Dickerson BC, Wolk DA: MRI cortical thickness biomarker predicts AD-like CSF and cognitive decline in normal adults. In: *Neurology*. vol. 78, 2011/12/23 edn; 2011: 84-90.
13. Lunnon K, Sattlecker M, Furney SJ, Coppola G, Simmons A, Proitsi P, Lupton MK, Lourdusamy A, Johnston C, Soininen H *et al*: A blood gene expression marker of early Alzheimer's disease. In: *Journal of Alzheimer's disease : JAD*. vol. 33; 2013: 737-753.
14. Hye A, Riddoch-Contreras J, Baird AL, Ashton NJ, Bazenet C, Leung R, Westman E, Simmons A, Dobson R, Sattlecker M *et al*: Plasma proteins predict conversion to dementia from prodromal disease. *Alzheimers Dement* 2014, 10(6):799-807 e792.
15. Fjell AM, Walhovd KB, Fennema-Notestine C, McEvoy LK, Hagler DJ, Holland D, Blennow K, Brewer JB, Dale AM: Brain atrophy in healthy aging is related to CSF levels of Abeta1-42. In: *Cerebral cortex*. vol. 20, 2010/01/07 edn; 2010: 2069-2079.

16. Corder EH, Saunders AM, Strittmatter WJ, Schmechel DE, Gaskell PC, Small GW, Roses AD, Haines JL, Pericak-Vance MA: Gene dose of apolipoprotein E type 4 allele and the risk of Alzheimer's disease in late onset families. *Science* 1993, 261(5123):921-923.

17. Jack CRJ, Wiste HJ, Weigand SD, Knopman DS, Vemuri P, Mielke MM, Lowe V, Senjem ML, Gunter JL, Machulda MM *et al*: Age, Sex, and APOE epsilon4 Effects on Memory, Brain Structure, and beta-Amyloid Across the Adult Life Span. In: *JAMA neurology*. vol. 72; 2015: 511-519.

18. Wirth M, Villeneuve S, La Joie R, Marks SM, Jagust WJ: Gene-Environment Interactions: Lifetime Cognitive Activity, APOE Genotype, and Beta-Amyloid Burden. *Journal of Neuroscience* 2014, 34(25):8612-8617.

19. Vos SJ, Xiong C, Visser PJ, Jasielec MS, Hassenstab J, Grant EA, Cairns NJ, Morris JC, Holtzman DM, Fagan AM: Preclinical Alzheimer's disease and its outcome: a longitudinal cohort study. In: *Lancet neurology*. vol. 12; 2013: 957-965.

20. Buckley RF, Hanseeuw B, Schultz AP, Vannini P, Aghjayan SL, Properzi MJ, Jackson JD, Mormino EC, Rentz DM, Sperling RA *et al*: Region-Specific Association of Subjective Cognitive Decline With Tauopathy Independent of Global beta-Amyloid Burden. *JAMA Neurol* 2017.

21. Lim YY, Maruff P, Pietrzak RH, Ellis KA, Darby D, Ames D, Harrington K, Martins RN, Masters CL, Szoeke C *et al*: Abeta and cognitive change: examining the preclinical and prodromal stages of Alzheimer's disease. *Alzheimers Dement* 2014, 10(6):743-751 e741.

22. Landau SM, Lu M, Joshi AD, Pontecorvo M, Mintun MA, Trojanowski JQ, Shaw LM, Jagust WJ, Alzheimer's Disease Neuroimaging I: Comparing PET imaging and CSF measurements of Ass. In: *Annals of neurology*. 2013.

23. Zwan M, van Harten A, Ossenkoppele R, Bouwman F, Teunissen C, Adriaanse S, Lammertsma A, Scheltens P, van Berckel B, van der Flier W: Concordance between cerebrospinal fluid biomarkers and [11C]PIB PET in a memory clinic cohort. In: *Journal of Alzheimer's disease : JAD*. vol. 41: IOS Press; 2014: 801-807.

24. Mattsson N, Insel PS, Donohue M, Landau S, Jagust WJ, Shaw LM, Trojanowski JQ, Zetterberg H, Blennow K, Weiner MW *et al*: Independent information from cerebrospinal fluid amyloid-beta and florbetapir imaging in Alzheimer's disease. *Brain* 2015, 138(Pt 3):772-783.

25. Palmqvist S, Mattsson N, Hansson O, Alzheimer's Disease Neuroimaging I: Cerebrospinal fluid analysis detects cerebral amyloid-beta accumulation earlier than positron emission tomography. *Brain* 2016, 139(Pt 4):1226-1236.

26. Rabbitt PMAea: The University of Manchester longitudinal study of cognition in normal healthy old age, 1983 through 2003. In: *Aging Neuropsychol C*. vol. 11; 2004: 245-279.

27. Willemsen G, Vink JM, Abdellaoui A, den Braber A, van Beek JH, Draisma HH, van Dongen J, van 't Ent D, Geels LM, van Lien R *et al*: The Adult Netherlands Twin Register: twenty-five years of survey and biological data collection. *Twin Res Hum Genet* 2013, 16(1):271-281.

28. Gatz M, Reynolds CA, Fratiglioni L, Johansson B, Mortimer JA, Berg S, Fiske A, Pedersen NL: Role of genes and environments for explaining Alzheimer disease. *Arch Gen Psychiatry* 2006, 63(2):168-174.

29. Boomsma DI, de Geus EJ, Vink JM, Stubbe JH, Distel MA, Hottenga JJ, Posthuma D, van Beijsterveldt TC, Hudziak JJ, Bartels M *et al*: Netherlands Twin Register: from twins to twin families. *Twin Res Hum Genet* 2006, 9(6):849-857.

30. Willemsen G, de Geus EJ, Bartels M, van Beijsterveldt CE, Brooks AI, Estourgie-van Burk GF, Fugman DA, Hoekstra C, Hottenga JJ, Kluft K *et al*: The Netherlands Twin Register biobank: a resource for genetic epidemiological studies. *Twin Res Hum Genet* 2010, 13(3):231-245.

31. van Beijsterveldt CE, van Baal GC, Molenaar PC, Boomsma DI, de Geus EJ: Stability of genetic and environmental influences on P300 amplitude: a longitudinal study in adolescent twins. *Behav Genet* 2001, 31(6):533-543.

32. Posthuma D, Meulenbelt I, de Craen AJ, de Geus EJ, Slagboom PE, Boomsma DI, Westendorp RG: Human cytokine response to ex vivo amyloid-beta stimulation is mediated by genetic factors. *Twin Res Hum Genet* 2005, 8(2):132-137.

33. den Braber A, van 't Ent D, Cath DC, Veltman DJ, Boomsma DI, de Geus EJ: Brain activation during response interference in twins discordant or concordant for obsessive compulsive symptoms. *Twin Res Hum Genet* 2012, 15(3):372-383.

34. Morris JC, Heyman A, Mohs RC, Hughes JP, van Belle G, Fillenbaum G, Mellits ED, Clark C: The Consortium to Establish a Registry for Alzheimer's Disease (CERAD). Part I. Clinical and neuropsychological assessment of Alzheimer's disease. In: *Neurology*. vol. 39; 1989: 1159-1165.

35. Aebi C: Validierung der neuropsychologischen Testbatterie CERAD-NP: eine Multi-Center Studie [Validation of the CERAD neuropsychological assessment battery: A multi centre study]. . In. Basel Switzerland.: University of Basel Switzerland.; 2002.

36. de Jager CA, Budge MM, Clarke R: Utility of TICS-M for the assessment of cognitive function in older adults. In: *International journal of geriatric psychiatry*. vol. 18; 2003: 318-324.

37. Yesavage JA, Brink TL, Rose TL, Lum O, Huang V, Adey M, Leirer VO: Development and validation of a geriatric depression screening scale: a preliminary report. In: *Journal of psychiatric research*. vol. 17; 1982: 37-49.

38. Morris JC: The Clinical Dementia Rating (CDR): current version and scoring rules. In: *Neurology*. vol. 43; 1993: 2412-2414.

39. Rey A: L'examen clinique en psychologie. In: *Presses Universitaires de France*. 1964.

40. Lindeboom J, Schmand B, Tulner L, Walstra G, Jonker C: Visual association test to detect early dementia of the Alzheimer type. In: *Journal of neurology, neurosurgery, and psychiatry*. vol. 73; 2002: 126-133.

41. Rentz DM, Amariglio RE, Becker JA, Frey M, Olson LE, Frishe K, Carmasin J, Maye JE, Johnson KA, Sperling RA: Face-name associative memory performance is related to amyloid burden in normal elderly. In: *Neuropsychologia*. vol. 49; 2011: 2776-2783.

42. Meyers JE, Bayless JD, Meyers KR: Rey complex figure: memory error patterns and functional abilities. In: *Applied neuropsychology*. vol. 3; 1996: 89-92.

43. Robbins TW, James M, Owen AM, Sahakian BJ, McInnes L, Rabbitt P: Cambridge Neuropsychological Test Automated Battery (CANTAB): a factor analytic study of a large sample of normal elderly volunteers. In: *Dementia*. vol. 5; 1994: 266-281.

44. Wechsler D. In: *The Psychological Corporation, San Antonio, TX*. 1997.

45. McKenna P, Warrington EK: Testing for nominal dysphasia. In: *Journal of neurology, neurosurgery, and psychiatry*. vol. 43; 1980: 781-788.

46. Tombaugh TN: Trail Making Test A and B: normative data stratified by age and education. In: *Archives of clinical neuropsychology : the official journal of the National Academy of Neuropsychologists*. vol. 19; 2004: 203-214.

47. Wechsler D: Wechsler Adult Intelligence Scale - Revised manual. In: *The Psychological Corporation*. 1981.

48. Jakobsson U: Using the 12-item Short Form health survey (SF-12) to measure quality of life among older people. In: *Aging clinical and experimental research*. vol. 19; 2007: 457-464.

49. Landau SM, Marks SM, Mormino EC, Rabinovici GD, Oh H, O'Neil JP, Wilson RS, Jagust WJ: Association of lifetime cognitive engagement and low beta-amyloid deposition. In: *Archives of neurology*. vol. 69; 2012: 623-629.

50. Washburn RA, Smith KW, Jette AM, Janney CA: The Physical Activity Scale for the Elderly (PASE): development and evaluation. In: *Journal of clinical epidemiology*. vol. 46, 1993/02/01 edn; 1993: 153-162.

51. Boeve BF, Molano JR, Ferman TJ, Smith GE, Lin SC, Bieniek K, Haidar W, Tippmann-Peikert M, Knopman DS, Graff-Radford NR *et al*: Validation of the Mayo Sleep Questionnaire to screen for

REM sleep behavior disorder in an aging and dementia cohort. In: *Sleep medicine.* vol. 12; 2011: 445-453.

52. Netzer NC, Stoohs RA, Netzer CM, Clark K, Strohl KP: Using the Berlin Questionnaire to identify patients at risk for the sleep apnea syndrome. In: *Annals of internal medicine.* vol. 131; 1999: 485-491.

53. Sikkes SA, Knol DL, Pijnenburg YA, de Lange-de Klerk ES, Uitdehaag BM, Scheltens P: Validation of the Amsterdam IADL Questionnaire(c), a new tool to measure instrumental activities of daily living in dementia. In: *Neuroepidemiology.* vol. 41; 2013: 35-41.

54. Pfeffer RI, Kurosaki TT, Harrah CHJ, Chance JM, Filos S: Measurement of functional activities in older adults in the community. In: *Journal of gerontology.* vol. 37; 1982: 323-329.

55. Saykin AJ, Wishart HA, Rabin LA, Santulli RB, Flashman LA, West JD, McHugh TL, Mamourian AC: Older adults with cognitive complaints show brain atrophy similar to that of amnestic MCI. In: *Neurology.* vol. 67, 2006/09/13 edn; 2006: 834-842.

56. Kaufer DI, Cummings JL, Ketchel P, Smith V, MacMillan A, Shelley T, Lopez OL, DeKosky ST: Validation of the NPI-Q, a brief clinical form of the Neuropsychiatric Inventory. In: *The Journal of neuropsychiatry and clinical neurosciences.* vol. 12; 2000: 233-239.

57. Kaasenbrood F, Hollander M, Rutten FH, Gerhards LJ, Hoes AW, Tieleman RG: Yield of screening for atrial fibrillation in primary care with a hand-held, single-lead electrocardiogram device during influenza vaccination. In: *Europace.* The Oxford University Press; 2016: euv426.

58. Teunissen CE, Tumani H, Engelborghs S, Mollenhauer B: Biobanking of CSF: international standardization to optimize biomarker development. *Clin Biochem* 2014, 47(4-5):288-292.

59. Meulenbelt I, Droog S, Trommelen GJ, Boomsma DI, Slagboom PE: High-yield noninvasive human genomic DNA isolation method for genetic studies in geographically dispersed families and populations. *Am J Hum Genet* 1995, 57(5):1252-1254.

60. Ehli EA, Abdellaoui A, Fedko IO, Grieser C, Nohzadeh-Malakshah S, Willemsen G, de Geus EJ, Boomsma DI, Davies GE, Hottenga JJ: A method to customize population-specific arrays for genome-wide association testing. *Eur J Hum Genet* 2017, 25(2):267-270.

61. Fedko IO, Hottenga JJ, Medina-Gomez C, Pappa I, van Beijsterveldt CE, Ehli EA, Davies GE, Rivadeneira F, Tiemeier H, Swertz MA *et al*: Estimation of Genetic Relationships Between Individuals Across Cohorts and Platforms: Application to Childhood Height. *Behav Genet* 2015, 45(5):514-528.

62. Das S, Forer L, Schonherr S, Sidore C, Locke AE, Kwong A, Vrieze SI, Chew EY, Levy S, McGue M *et al*: Next-generation genotype imputation service and methods. *Nat Genet* 2016, 48(10):1284-1287.

63. Ghebranious N, Ivacic L, Mallum J, Dokken C: Detection of ApoE E2, E3 and E4 alleles using MALDI-TOF mass spectrometry and the homogeneous mass-extend technology. *Nucleic Acids Res* 2005, 33(17):e149.

64. van der Lee SJ, Wolters FJ, Ikram MK, Hofman A, Ikram MA, Amin N, van Duijn CM: The effect of APOE and other common genetic variants on the onset of Alzheimer's disease and dementia: a community-based cohort study. *The Lancet Neurology* 2018, 17(5):434-444.

65. Moneta GL, Edwards JM, Chitwood RW, Taylor LMJ, Lee RW, Cummings CA, Porter JM: Correlation of North American Symptomatic Carotid Endarterectomy Trial (NASCET) angiographic definition of 70% to 99% internal carotid artery stenosis with duplex scanning. In: *Journal of vascular surgery.* vol. 17; 1993: 152-157- discussion 157-159.

66. Cardenas VA, Reed B, Chao LL, Chui H, Sanossian N, Decarli CC, Mack W, Kramer J, Hodis HN, Yan M *et al*: Associations Among Vascular Risk Factors, Carotid Atherosclerosis, and Cortical Volume and Thickness in Older Adults. In: *Stroke; a journal of cerebral circulation.* vol. 43; 2012: 2865-2870.

67. Wendell CR, Waldstein SR, Ferrucci L, O'Brien RJ, Strait JB, Zonderman AB: Carotid Atherosclerosis and Prospective Risk of Dementia. In: *Stroke; a journal of cerebral circulation.* vol. 43; 2012: 3319-3324.

68. van Sloten MD TT, PhD MTS, van den Hurk PhD K, PhD JMD, MD GNP, MD RMAHP, MD CDASP: Local Stiffness of the Carotid and Femoral Artery Is Associated With Incident Cardiovascular Events and All-Cause Mortality. In: *Journal of the American College of Cardiology*. vol. 63: Elsevier Inc; 2014: 1739-1747.

69. Fazekas F, Chawluk JB, Alavi A, Hurtig HI, Zimmerman RA: MR signal abnormalities at 1.5 T in Alzheimer's dementia and normal aging. In: *AJR American journal of roentgenology*. vol. 149; 1987: 351-356.

70. Scheltens P, Launer LJ, Barkhof F, Weinstein HC, van Gool WA: Visual assessment of medial temporal lobe atrophy on magnetic resonance imaging: interobserver reliability. In: *Journal of neurology*. vol. 242; 1995: 557-560.

71. Pasquier F, Leys D, Weerts JG, Mounier-Vehier F, Barkhof F, Scheltens P: Inter- and intraobserver reproducibility of cerebral atrophy assessment on MRI scans with hemispheric infarcts. In: *European neurology*. vol. 36; 1996: 268-272.

72. Koedam ELGE, Lehmann M, van der Flier WM, Scheltens P, Pijnenburg YAL, Fox N, Barkhof F, Wattjes MP: Visual assessment of posterior atrophy development of a MRI rating scale. In: *European radiology*. vol. 21: Springer-Verlag; 2011: 2618-2625.

73. Curtis C, Gamez JE, Singh U, Sadowsky CH, Villena T, Sabbagh MN, Beach TG, Duara R, Fleisher AS, Frey KA *et al*: Phase 3 trial of flutemetamol labeled with radioactive fluorine 18 imaging and neuritic plaque density. *JAMA Neurol* 2015, 72(3):287-294.

74. Sibomana M. , al e: Simultaneous measurement of transmission and emission contamination using a collimated 137Cs point source for the HRRT. In: *IEEE MIC Record: 2004; Roma*; 2004.

75. Sibomana M. , al e: New attenuation correction for the HRRT using transmission scatter and total variation regularization. In: *IEEE MIC Record: 2009; Orlando*; 2009.

76. Hu Z ON, Renisch S et al: MR-based attenuation correction for a whole-body sequential PET/MR system. In: *IEEE nuclear science symposium conference*. vol. Record 3508–3512; 2009.

77. Healthcare G: EPAR Product information - Summary of product characteristics.

78. del Campo M, Mollenhauer B, Bertolotto A, Engelborghs S, Hampel H, Simonsen AH, Kapaki E, Kruse N, Le Bastard N, Lehmann S *et al*: Recommendations to standardize preanalytical confounding factors in Alzheimer's and Parkinson's disease cerebrospinal fluid biomarkers: an update. *Biomark Med* 2012, 6(4):419-430.

79. Stam CJ: Use of magnetoencephalography (MEG) to study functional brain networks in neurodegenerative disorders. In: *Journal of the neurological sciences*. vol. 289; 2010: 128-134.

80. de Haan W, van der Flier WM, Koene T, Smits LL, Scheltens P, Stam CJ: Disrupted modular brain dynamics reflect cognitive dysfunction in Alzheimer's disease. In: *NeuroImage*. vol. 59; 2012: 3085-3093.

81. Demuru M, Gouw AA, Hillebrand A, Stam CJ, van Dijk BW, Scheltens P, Tijms BM, Konijnenberg E, Ten Kate M, den Braber A *et al*: Functional and effective whole brain connectivity using magnetoencephalography to identify monozygotic twin pairs. *Sci Rep* 2017, 7(1):9685.

82. Mayer MA, Hornegger J, Mardin CY, Tornow RP: Retinal Nerve Fiber Layer Segmentation on FD-OCT Scans of Normal Subjects and Glaucoma Patients. In: *Biomedical optics express*. vol. 1; 2010: 1358-1383.

83. Koronyo Y, Salumbides BC, Black KL, Koronyo-Hamaoui M: Alzheimer's disease in the retina: imaging retinal abeta plaques for early diagnosis and therapy assessment. In: *Neurodegenerative diseases*. vol. 10, 2012/02/22 edn; 2012: 285-293.

84. Nandakumar N, Buzney S, Weiter JJ: Lipofuscin and the principles of fundus autofluorescence: a review. In: *Seminars in ophthalmology*. vol. 27, 2012/11/21 edn; 2012: 197-201.

85. Frost S, Kanagasingam Y, Sohrabi H, Vignarajan J, Bourgeat P, Salvado O, Villemagne V, Rowe CC, Macaulay SL, Szoeke C *et al*: Retinal vascular biomarkers for early detection and monitoring of Alzheimer's disease. In: *Translational psychiatry*. vol. 3; 2013: e233.

86. Minica CC, Dolan CV, Kampert MM, Boomsma DI, Vink JM: Sandwich corrected standard errors in family-based genome-wide association studies. In: *European journal of human genetics : EJHG*. 2014/06/12 edn; 2014.

87.   Vitaro F BM, Arseneault L: The discordant MZ-twin method: One step closer to the holy grail of causality. *International Journal of Behavioral Development* 2009, 33(4):376–382.
88.   Blokland GA, de Zubicaray GI, McMahon KL, Wright MJ: Genetic and environmental influences on neuroimaging phenotypes: a meta-analytical perspective on twin imaging studies. *Twin Res Hum Genet* 2012, 15(3):351-371.
89.   Fennema-Notestine C, McEvoy LK, Notestine R, Panizzon MS, Yau WW, Franz CE, Lyons MJ, Eyler LT, Neale MC, Xian H *et al*: White matter disease in midlife is heritable, related to hypertension, and shares some genetic influence with systolic blood pressure. *Neuroimage Clin* 2016, 12:737-745.

SUPPLEMENTARY DATA

Supplementary Table 1. Inclusion and exclusion criteria

Inclusion criteria – Age ≥60 years – TICS-m [36] >22 – CERAD 10 word list immediate and delayed recall [39] > -1.5 SD of age adjusted normative data – GDS-15 [37] <11 – CDR [38] 0	
Exclusion criteria – Clinical diagnosis of MCI or probable AD at baseline – Severe head trauma with loss of consciousness – Brain tumor (past, present) – Schizophrenia, bipolar disorders or recurrent psychotic disorders – Stroke resulting in cognitive impairment – Neurodegenerative diseases such as Parkinson's disease and Huntington's disease – Epilepsy, currently using anti-epileptic drugs – Brain infections (acute or a sequel of infection) – Cancer with terminal life expectancy – Known vitamin B12 deficiency without treatment – Uncontrolled diabetes mellitus	– Known thyroid disease without treatment – History of recreational drug use – Alcohol consumption >35 units per week – hysical morbidity or illness which will not permit attendance at visit sessions – ontraindication for MRI (e.g. metal implants, pacemaker etc.) – Medications that may impair cognition, at the discretion of the investigator, e.g.: • High dose benzodiazepine • Lithium carbonate • Antipsychotics including atypical agents • High dose antidepressants • Parkinson's disease medicines

TICS-m: Modified Telephone Interview for Cognitive Status; CERAD: Consortium to Establish A Registry for Alzheimer's Disease; GDS-15: 15-item Geriatric Depression Scale; CDR: Clinical Dementia Rating Scale; MCI: Mild cognitive impairment; AD: Alzheimer's disease; MRI: Magnetic resonance imaging

Supplementary Table 2. Neuropsychological tests baseline

Neuropsychological Test	Range	Participants completed	Mean (SD) Amsterdam	Participants completed	Mean (SD) Manchester
RAVLT					
- Immediate recall	0-75	197	42 (9.2)	77	49 (8.9)
- Delayed recall 20 minutes	0-15	196	8.4 (2.9)	77	10.7 (3.3)
- Learning	0-15	197	6.1 (2.0)	77	7.6 (2.1)
- Recognition	0-30	196	28.3 (2.1)	NA	-
WAIS-III digit span		204		77	
- Forward Score	0-14		8.6 (1.9)		10.2 (2.2)
- Forward Score	0-8		5.8 (1.1)		6.7 (1.3)
- Backwards Score	0-14		5.9 (1.6)		6.9 (1.9)
- Backwards Span	0-8		4.4 (1.0)		4.9 (1.1)
FNAME		182		79	
- Total names	0-48		19.6 (10.1)		18.8 (11.2)
- Total occupation	0-48		32.8 (9.0)		30.0 (10.0)
- Total names and occupation	0-96		52.4 (17.6)		49.4 (20.2)
Rey Complex Figure Test					
- Copy	0-36	204	33.5 (3.4)	77	34.3 (3.0)
- Delayed copy 3min	0-36	204	18.3 (5.5)	NA	-
- Delayed copy 20min	0-36	202	18.2 (5.4)	77	14.9 (6.2)
Verbal Fluency					
- In English testing the letters F, A, and S, in Dutch the letters D, A and T		204	37.6 (10.4)	77	49.6 (12.3)
- Category fluency animal 1 minute		204	22.0 (7.1)	76	18.8 (4.6)
- Category fluency animal 2 minutes		204	34.6 (9.3)	NA	-
- Category fluency fruits		NA	-	77	13.5 (3.9)
- Category fluency birds		NA	-	77	14.4 (4.7)
- Category fluency household items		NA	-	77	19.9 (4.9)
- Category fluency tools		NA	-	77	10.4 (3.2)
- Category fluency vehicles		NA	-	77	12.0 (3.1)
TMT A & B					
- TMT A	seconds	204	43.3 (21.3)	77	42.4 (16.0)
- TMT A errors		204	0.2 (0.4)	NA	-
- TMT B	seconds	203	107.3 (63.7)	77	88.9 (36.0)
- TMT B errors		203	0.6 (1.1)	NA	-
Graded naming	0-30	203	18.2 (3.7)	77	24.7 (3.5)
CANTAB					
- RVP-A		178	8411 (1742)	72	8585 (638)
- RVP Median response latency		178	912 (1253)	72	560 (142)

Supplementary Table 2. Continuation

Neuropsychological Test	Range	Participants completed	Mean (SD) Amsterdam	Participants completed	Mean (SD) Manchester
- PAL Total errors adjusted		203	28.8 (16.3)	75	33.9 (17.7)
- RTI Simple median RT		203	299 (61)	75	310 (50)
- RTI Five choices median RT		203	333 (48)	75	358 (47)
- RTI SD five choices RT		203	61 (36)	75	67 (23)
- SWM Between errors		200	21 (9.4)	74	22 (7.8)
- SWM Strategy		200	18 (2.5)	74	18 (2.8)
WAIS-R DSST	0-93	201	45.1 (12.1)	NA	-
Savage alphabet coding task (LLS)		NA		81	
- Trial 1 Correct			-		42 (11)
- Trial 2 Correct			-		46 (11)
- Trial 3 Correct			-		48 (11)
- Trial 4 Correct			-		49 (11)
- 2 minute recall			-		4 (3)
VAT		204		NA	
- A 2 trials	0-12		12 (0.8)		-
- B 2 trials	0-12		11 (1.3)		-
- Naming	0-12		12 (0.2)		-
One minute reading task	1-145	204	89 (16)	NA	-
Klepel B	1-145	204	82 (21)	NA	-
Heim intelligence test (AH4)		NA		81	
- Number attempted part 1			-		40 (10)
- Answers correct part 1			-		33 (10)
- Number attempted part 2			-		40 (10)
- Answers correct part 2			-		32 (9)
Memory circle test		NA		81	
- Correct name, correct segment	0-24		-		3.8 (2.1)
- Correct name, wrong segment	0-12		-		5.5 (1.6)
WAIS vocabulary test	0-74	NA	-	81	58 (11)
ACE TOTAL	100	NA	-	77	92 (5)

RAVLT: Rey auditory verbal learning test, TMT: Trail Making Test, VAT: Visual Association Test, WAIS: Wechsler Adult Intelligence Scale, DSST: Digit Symbol Substitution Task, CANTAB: Cambridge Neuropsychological Test Automated Battery, RVP: Rapid Visual information Processing, PAL: Paired Associate Learning, RTI: Reaction Time, SWM: Spatial-working Memory, F-NAME: Face-name associative memory exam

Supplementary Table 3. Questionnaires baseline

Questionnaires	Range	Participants completed	Mean (SD) Amsterdam	Participants completed	Mean (SD) Manchester
CDR - memory	0-3	204	0	80	0.03 (0.11)
PASE (self-reported)	7-60	204	27.9 (5.3)	77	23.8 (5.1)
CCI (self-reported)	20-100	204	23 (3.5)	74	36.1 (13.1)
CCI (informant-reported)	20-100	204	22 (3.7)	62	31.6 (9.6)
FAQ (informant-reported)	0-30	204	0.2 (0.7)	76	1.2 (2.6)
AD8 (informant-reported)	0-8	203	0 (0.2)	77	0.6 (1.0)
Berlin Sleep questionnaire (self-reported)	high/low	204	49/155	NA	-
Cognitive abilities questionnaire (self-reported) Manchester version	1-48	NA	-	65	21 (3.9)
Cognitive abilities questionnaire (self-reported) Amsterdam version	26-164	204	90 (17.4)	NA	-
NPI-q (informant-reported)	0-96	204	1 (3.1)	NA	-
Amsterdam iADL (informant-reported, t-score)	0-100	199	69.4 (4.4)	NA	-

CDR: Clinical Dementia Rating Scale; PASE: Physical Activity Scale for the Elderly; CCI: Cognitive Complaints Index; FAQ: Functional Activities Questionnaire; AD8: Ascertain Dementia 8; NPI-q: Neuropsychiatric Inventory Questionnaire; iADL: instrumental Activities of Daily Living

Supplementary Table 4. Biomarkers baseline

Biomarker		Amsterdam participants completed	Manchester participants completed
Physical measures			
- Bioelectrical Impedance Analysis [86]	Muscle, fat and weight analysis	144	NA
- Neurological examination		197	NA
- Lead 1 electrocardiogram	Assessed with Diagnostick [57]	169	NA
- Color photograph face		197	NA
- Ophthalmological examination	Slit lamp	50	NA
	Eye pressure	131	
	Refraction	123	
Fluid specimens			
- Blood	50 mL clotted blood and plasma	204	76
- Cerebrospinal Fluid	maximum of 20 mL	126	NA
- Buccal cells		194	NA
Imaging			
- [18F]flutemetamol PET imaging		PET-MRI scanner	HRRT scanner
• Dynamic 0-30 minutes		195	74
• Dynamic 90-110 minutes		197	76
- Magnetic Resonance Imaging		3T Philips Achieva	3T Philips Achieva
		8 coil	32 coil
• 3DT1		198	81
• 3D Fluid-attenuated inversion recovery		199	81
• pseudo continuous Arterial Spin Labeling		197	80
• Susceptibility Weighted Imaging		198	NA
• Diffusion Tensor Imaging		197	NA
• Resting state functional MRI		191	NA
• quantitative Magnetization Transfer		NA	80
- Ultrasound carotid arteries		right	bilateral
• Intima Media Thickness		155	60
• Distension		127	NA
• Stiffness		NA	64
• Velocity		NA	65
• Stenosis present?		NA	64
- Magneto Encephalography		187	NA
- Ocular Coherence Tomography		187	NA
- Fundus image		165	NA

Supplementary Table 5. MRI settings

MRI sequence	Settings
3DT1	Sagittal turbo field echo sequence (1.00 mm x 1.00 mm x 1.00 mm voxels, TR = 7.9 ms, TE = 4.5 ms, FA = 8 degrees)
3D Fluid-attenuated inversion recovery	3D sagittal fat-saturated sequence (1.12 mm x 1.12 mm x 1.12 mm voxels, TR = 4800 ms, TE = 279 ms, inversion time = 1650 ms)
pseudo continuous Arterial Spin Labeling	Perfusion images (3.0 mm x 3.0 mm x 6.0 mm voxels, labeling time = 1650 ms, post label delay = 2025 ms , TR = 4560 ms, TE = 14 ms, acquisition time = 4 minutes)
Susceptibility Weighted Imaging	A 3D transversal scan (0.8 mm x 0.8 mm x 1.20 mm voxels, TR = 19 ms, TE=27 ms, FA = 8 degrees)
Diffusion Tensor Imaging	Spin EPI scan (32 directions, b value = 1000, 2.00 mm x 2.00 mm x 2.00 mm voxels, TR = 7517 ms, TE = 92 ms, FA = 90 degrees)
Resting state functional MRI	Fast field echo EPI sequence (3.30 mm x 3.30 mm x 3.00 mm voxels, TR = 1800 ms, TE = 35 ms, FA = 80 degrees)
quantitative Magnetization Transfer	3D fast field echo acquisition with a 112x112x60 matrix (2.0 mm x 2.0 mm x 2.0 mm voxels, TR = 38.15ms TE = 1.39 ms), 8 acquisitions of differing offset frequency and flip angle

TR: repetition time; TE: echo time; FA: flip angle; EPI: echo planar imaging

CHAPTER

3

Assessing Amyloid Pathology in Cognitively Normal Subjects using [18F]Flutemetamol PET: Comparing Visual Reads and Quantitative Methods

*Collij LE, ***Konijnenberg E**, Reimand J, Ten Kate M, Den Braber A, Lopes Alves I, Zwan M, Yaqub M, Van Assema DME, Wink AM, Lammertsma AA, Scheltens P, Visser PJ, Barkhof F, Van Berckel BNM
*Authors contributed equally

ABSTRACT

Objective: Determine the optimal approach for assessing amyloid pathology in a cognitively normal elderly population.

Methods: Dynamic [¹⁸F]flutemetamol PET scans acquired using a coffee-break protocol (0-30 and 90-110 min. scan) from 190 cognitively normal elderly (mean age 70.4 years, 60% female) were included. Parametric images were generated from standard uptake value ratio (SUVr) and non-displaceable binding potential (BP_{ND}) methods, with cerebellar grey matter as a reference region and were visually assessed by three trained readers. Inter-reader agreement was calculated using Kappa statistics and (semi-)quantitative values were obtained. Global cut-offs were calculated for both SUVr and BP_{ND} using a ROC analysis and the Youden Index. Visual assessment was related to (semi-)quantitative classifications.

Results: Inter-reader agreement in visual assessment was moderate for SUVr ($\kappa = 0.57$) and good for BP_{ND} images ($\kappa = 0.77$). There was discordance between readers for 35 cases (18%) using SUVr and for 15 cases (8%) using BP_{ND}, with 9 overlapping cases. For the total cohort, the mean ($\pm$SD) SUVr and BP_{ND} values were 1.33 ($\pm$ 0.21) and 0.16 ($\pm$ 0.12), respectively. Most of the 35 cases (91%) where SUVr image assessment was discordant between readers, were classified as negative based on (semi-)quantitative measurements.

Conclusion: The use of parametric BP_{ND} images for visual assessment of [¹⁸F]flutemetamol in a population with low amyloid burden improves inter-reader agreement. Implementing semi-quantification in addition to visual assessment of SUVr images can reduce false-positive classification in this population.

INTRODUCTION

Alzheimer's disease (AD) is the most common cause of dementia, accounting for 60-80% of cases above 65 years of age [1]. Its pathological hallmark is the accumulation of the amyloid-β (Aβ) peptide, thought to start years before cognitive impairment [2]. In fact, abnormal Aβ levels are seen in 20-40% of cognitively normal subjects between the ages of 60 and 90 years [3]. These subjects are considered to be in the preclinical stage of AD [4, 5], which provides a unique opportunity for secondary prevention studies and is gaining increasing research focus [6]. To this end, reliable identification of amyloid pathology *in vivo* using Positron Emission Tomography (PET) is of the utmost importance in this population.

The identification of amyloid burden by means of visual interpretation of summed late images or of semi-quantitative standardized uptake value ratio (SUVr) images is currently suggested to be sufficient. Previous studies have shown a high inter-reader agreement for the visual assessment of SUVr images and a high imaging-pathology correlation in clinical populations and end-of-life subjects [7-9]. It has been shown, however, that SUVr overestimates amyloid burden compared with quantitative non-displaceable binding potential values (BP$_{ND}$) [10]. As such, quantitative BP$_{ND}$ images may be more reliable also for visual interpretation. In a memory clinic population, Zwan and colleagues showed that visual assessment of parametric BP$_{ND}$ ^{11}C-PiB images resulted in a higher inter-reader agreement than the frequently used SUV and SUVr images [11]. To date, it remains to be determined whether these findings translate to the increasingly available ^{18}F-labelled Aβ targeting tracers, such as [^{18}F]flutemetamol, and, more importantly, to the challenging population of cognitively normal elderly participants who have generally a minimal amyloid load.

The purpose of this study was to compare two parametric imaging methods (SUVr vs. BP$_{ND}$) to determine the optimal approach for assessment of early amyloid pathology. To this end, we investigated the agreement in visual assessment of SUVr and BP$_{ND}$ images between three readers and its relationship to (semi-)quantitative measures.

MATERIALS AND METHODS

Project

The data used in this study originate from the Innovative Medicine Initiative European Information Framework for AD (EMIF-AD) project (http://www.emif.eu/). The overall aim of the EMIF-AD project is to discover and validate diagnostic markers, prognostic markers and risk factors for AD in non-demented subjects.

Subjects

A total of 199 subjects from the PreclinAD cohort were included at the VU University Medical Center. Inclusion criteria were age ≥ 60 years and normal cognition according to a delayed recall score of > -1.5 standard deviation (SD) of demographically adjusted normative data on the Consortium to Establish a Registry for Alzheimer's Disease (CERAD) 10 word list [12], a Telephone Interview for Cognitive Status modified (TICS-m) score of 23 or higher [13], a 15-item Geriatric Depression Scale (GDS) score of <11 [14], and a Clinical Dementia Rating (CDR) scale of 0 [15]. Exclusion criteria were any physical, neurological or psychiatric condition that interfere with normal cognition. PET-acquisition failed in 3 subjects and 6 BP_{ND} images had missing visual assessment, resulting in a visual assessment for both SUVr and BP_{ND} images of 190 subjects in the present study. PET quantification failed in 5 subjects, thus a total of 185 subjects were used for the quantitative analysis. Written informed consent was obtained from all subjects and the study was approved by the Medical Ethics Review Committee of the VU University Medical Center.

Positron Emission Tomography

PET scans were obtained using a Philips Ingenuity TF PET-MRI camera (Philips Healthcare, Cleveland, USA). Thirty minutes scans were acquired immediately following a manual injection of [¹⁸F]flutemetamol (191 ± 20 MBq) [16]. After an interval of 60 minutes, in which the patient was taken from the scanner bed, a second scan of 20 minutes was acquired, starting 90 minutes after injection [17]. Immediately prior to each part of the PET scan, a T1-weighted gradient echo pulse MRI scan was acquired for attenuation correction (AC) of the PET data. The first emission scan was reconstructed into 18 frames of increasing length (6x5, 3x10, 4x60, 2x150, 2x300, 1x600 s.) using the standard LOR-RAMLA reconstruction algorithm for the brain. The second scan was reconstructed with the same algorithm into 4 frames of 300 seconds each. Fist, Vinci Software 2.56 (Max Planck Institute for Neurological Research, Cologne, Germany) was used to combine the two PET scans into a single multi-frame image. Next, each individual's T1 was co-registered to the dynamic PET using the generic multimodality setting of Vinci with a linear rigid-body schema and normalized mutual information as the similarity measure. Parametric BP_{ND} images were generated from the entire image set using the receptor parametric mapping (RPM) implementation in PPET [18-20]. SUVr images were generated based on the 90- to 110-minutes scan interval. Next, T1-based VOIs using the Hammers atlas implemented in PVElab software were projected onto the PET images to extract regional values [21]. Cerebellar grey matter was used as reference tissue for both analyses [22]. Finally, global values were computed based on the average of frontal (volume-weighted average of superior, middle, and inferior frontal gyrus), parietal (volume weighted average of posterior cingulate, superior parietal gyrus, postcentral gyrus, and inferolateral remainder of parietal lobe), and temporal (volume-weighted average of parahippocampal gyrus, hippocampus, medial temporal lobe, superior, middle, and inferior temporal gyrus) regions [23, 24].

Magnetic Resonance Imaging

Whole-brain scans were obtained using a 3T Philips Achieva scanner (Philips Healthcare, Cleveland, USA) of the PET-MRI system described above equipped with an 8-channel head coil. Isotropic structural 3D T1-weighted images were acquired using a sagittal turbo field echo (TFE) sequence with the following settings: 1.00 x 1.00 x 1.00 mm^3 voxels, repetition time (TR) = 7.9 ms, echo time (TE) = 4.5 ms, flip angle (FA) = 8º. A 3D sagittal fat-saturated fluid-attenuated inversion recovery (FLAIR) sequence was acquired using the following settings: 1.12 x 1.12 x 1.12 mm^3 voxels, TR = 4800 ms, TE=279 ms, inversion time = 1650 ms. The structural 3D-T1 and 3D FLAIR images were used for assessment of global cortical atrophy (GCA) [25], average medial temporal atrophy (MTA) [26], and Fazekas score for white matter hyperintensities (WMH) [27, 28].

Visual Assessment of PET Images

Three trained readers, blinded to clinical information, first assessed all SUVr images and subsequently all BP$_{ND}$ images, in a randomized order. Images deemed dubious by the reader were reassessed at a separate occasion. Images were scaled to 90% of the pons signal using rainbow colour scaling and transverse, sagittal, and coronal views were displayed using the software package Vinci 2.56. Images were rated as either *positive* (binding in one or more cortical brain region or striatum unilaterally) or *negative* (predominantly white matter uptake) according to criteria defined by the manufacturer (GE Healthcare). PET images were assessed together with a T1-weighted MR scan to limit the influence of atrophy on the visual assessment.

The level of experience in visual assessment of [^{18}F]flutemetamol images differed among readers; a nuclear medicine physician with considerable experience, a nuclear medicine physician trainee with basic experience, and a radiologist in training with 6 months of experience in nuclear medicine. All readers completed the [^{18}F]flutemetamol reader training provided by GE Healthcare.

Statistical Analyses

Baseline demographics were assessed using simple descriptive statistical analyses. Kappa statistics were used to asses inter-reader agreement among the three readers, intra-reader agreement between the two methods and agreement between visual read and (semi-)quantitative classifications. Agreement was considered poor if κ was less than 0.20, satisfactory if κ was 0.21–0.40, moderate if κ was 0.41– 0.60, good if κ was 0.61–0.80, and excellent if κ was more than 0.80. Differences in MRI measurements between PET- and PET+ cases were assessed using a Mann-Whitney *U* analysis. The correlation between (semi-)quantitative SUVr and BP$_{ND}$ measurements was assessed using Spearman's rho. Cut-off values were calculated for both SUVr and BP$_{ND}$ using a ROC analysis and the Youden Index. Possible overestimation of amyloid burden using semi-quantitative SUVr was

investigated by calculating the difference between SUVr -1 and BP_{ND} values. Differences in global overestimation between PET- and PET+ cases were assessed using a Mann-Whitney U analysis. Regional differences in binding and overestimation were assessed using a Wilcoxon paired test. Amyloid status resulting from quantitative assessment was considered as the "true" amyloid status for all analysis, in the absence of post-mortem confirmation.

RESULTS

Baseline demographics are provided in Table 1.

Table 1. Demographics, MRI Measurements and (Semi-)Quantitative PET Values

Total Cohort N = 190		
Demographics		
Gender	113 women (59.5%)	
Age	70.4 ± 7.56 y	
MMSE	29 ± 1.13	
Years of education	15.15 ± 4.42 y	
Brain measures		
GCA[*]	0.79 ± 0.72	
Average MTA[†]	0.65 ± 0.72	
Fazekas[‡]	1.18 ± 0.82	
	0 = 35; 1=101; 2 = 40; 3 = 14	
Quantitative Cohort _N_ = 185		
Quantitative Measures		
SUVr	1.33 ± 0.21, range = 0.79 – 2.13	
BP_{ND}	0.16 ± 0.12, range = 0.20 - 0.66	
Concordant Cohort _N_ = 149		
Brain measures	**PET- (_N_ = 130)**	**PET+ (_N_ = 19)**
GCA[*]	0.74 ± 0.67	0.89 ± 0.81
Average MTA[†]	0.57 ± 0.64	0.82 ± 0.75
Fazekas[‡]	1.18 ± 0.83	1.26 ± 0.87
Quantitative Measures		
SUVr	1.25 ± 0.09	1.83 ± 0.16[§]
	range = 1.08 – 1.63	range = 1.54 – 2.13
BP_{ND}	0.12 ± 0 .05	0.43 ± 0.12[§]
	range = 0.02 - 0.27	range = 0.27 - 0.66

Results are displayed as mean ± SD
[*]Global Cortical Atrophy score (0-3)
[†]Medial Temporal Atrophy score (0-4)
[‡]White matter hyperintensity score (0-3)
[§] $p < 0.01$

Visual Reads

Inter-reader agreement in visual assessment was moderate for SUVr images (κ = 0.57) and good for BP_{ND} images (κ = 0.77). There was discordance between readers for 35 cases (18%) using SUVr and for 15 cases (8%) using BP_{ND}, with 9 overlapping cases. Figure 1 shows examples of agreement and disagreement in visual interpretation of [¹⁸F]flutemetamol images. On average, the rating was positive in 35 (18%) of the SUVr images and in 26 (14%) of the BP_{ND} images. The reader with the least experience classified 55 (29%) SUVr images as positive compared to 21 (11%) and 29 (15%) by the intermediate and most experienced reader, respectively.

Intra-reader agreement (i.e. within reader, between SUVr and BP_{ND}) differed among readers, with moderate agreement (κ = 0.52) between methods seen in the reader with least experience, excellent agreement (κ = 0.97) seen in the reader with moderate experience, and good agreement in the reader with most experience (κ = 0.76).

When applying 'majority rules' (i.e. 2 out of 3 readers agreed on a scan being either positive or negative), positivity was assigned to 27 (14%) cases based on SUVr and to 25 (13%) cases based on the BP_{ND}, with 22 overlapping cases. Thus, 8 cases showed inter-method discordance; i.e. 5 cases were rated positive on SUVr, but negative on BP_{ND} and 3 cases were rated positive on BP_{ND} and negative on SUVr. The remaining 160 cases were classified as negative on both images (Figure 2A).

Visual Reads Related to Quantitative Measures

For the total cohort, mean (± SD) global SUVr and BP_{ND} values were 1.33 (± 0.21) and 0.16 (± 0.12), respectively. There was a good agreement between both measures (ICC = 0.89, *p* < 0.01). Inter-reader concordant positive cases had significantly higher SUVr and BP_{ND} values than concordant negative cases (*p* < 0.01) (Table 1). Based on the visual read concordant cohort alone (*N* = 149), the cut-off value for positivity using SUVr was calculated to be 1.52 (AUC = 0.98, sensitivity = 95%, specificity = 98%) and for BP_{ND} 0.26 (AUC = 1.00, sensitivity = 100%, specificity = 98%) using a ROC analysis (Supplemental Figure 1). After applying both cut-offs to the dataset, the agreement between the SUVr majority visual read and semi-quantitative negative/positive classification was good (κ = 0.78), with 16 cases (9%) discordant between the two classification methods. The agreement analysis was also done with a literature based cut-off value (1.56) [8, 29] resulting in a kappa increase of 0.01. For BP_{ND}, the agreement between majority visual read and quantitative negative/positive classification was excellent (κ = 0.93), with 3 cases (2%) discordant between the two classification methods. The majority of the 35 cases (91%) where SUVr image assessment was discordant between readers, were classified as negative using either cut-off value (Figure 2B). In addition, in the 8 cases with discordant inter-method visual read, there was full agreement between visual and quantitative measurements when using BP_{ND}, which was not the case with SUVr (Figure 2A).
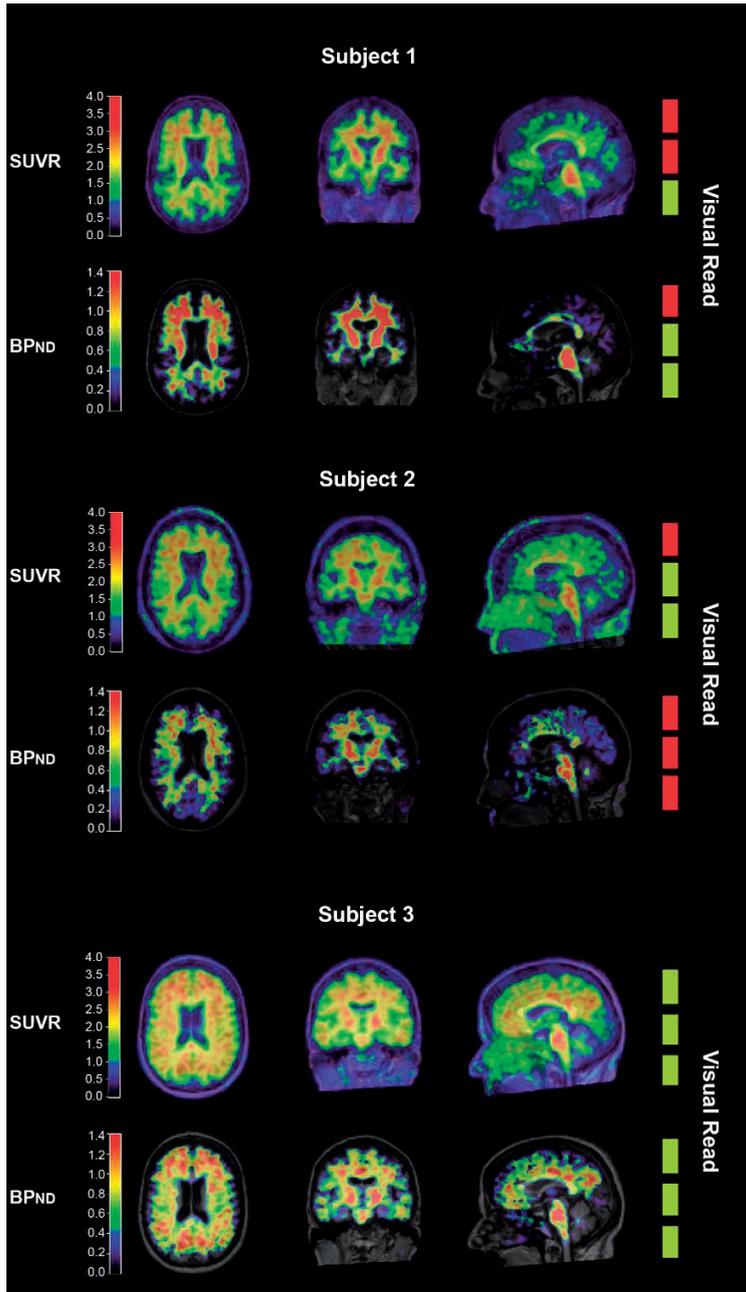
Figure 1. Examples of SUVr (top) and BPND (bottom) [¹⁸F]flutemetamol images of three different subjects
From left to right are shown axial, coronal, and sagittal views. The three boxes on the right represent the amyloid classification by the three readers (red = negative, green = positive). **Subject 1:** Example of a difficult case, represented by discordant visual reads on both SUVr and BP$_{ND}$ image. **Subject 2:** Example of a possible overestimation of amyloid pathology when only assessing the SUVr image. **Subject 3:** Example of a clear positive case.
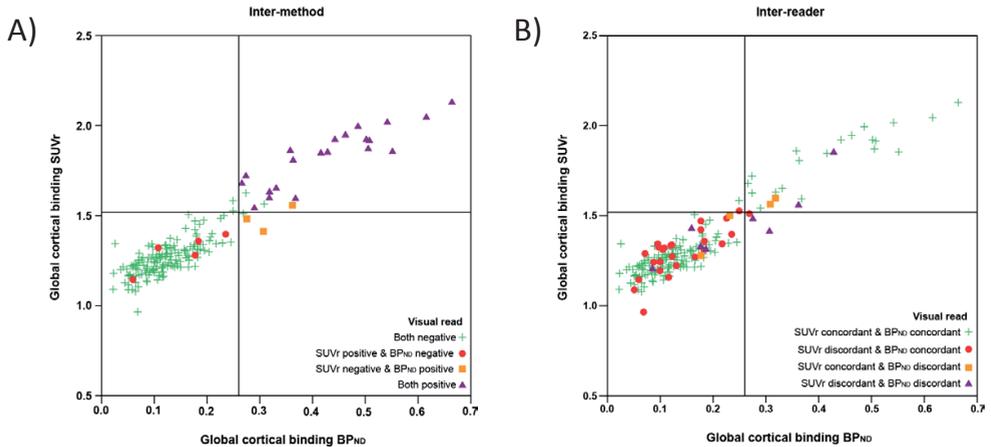
Figure 2. Scatterplot of quantitative measures compared to visual read

On X-axis the global cortical binding derived from BP_{ND}. On Y-axis the global cortical binding derived from SUVr. Reference lines denote the cut-off (1.52 for SUVr and .26 for BP_{ND}). Different colours demonstrate discordance/concordance between SUVr and BP_{ND} visual read.

A) Based on majority rules visual read. For all inter-method discordant cases (red circles and orange squares) the BP_{ND} visual read was in accordance with the quantitative value, while SUVr was not.

B) Most SUVr inter-reader discordant cases (red circles) are below the cut-off for both SUVr and BP_{ND}.

SUVr ≠ BP_{ND} Quantification

We investigated the relationship between the two quantitative measures with regard to majority visual read to assess any violations of the equilibrium assumptions (i.e. SUVr − 1 = BP_{ND}) in this population. For all cases except one, global SUVr − 1 values overestimated the corresponding global BP_{ND} values. Participants with a positive read ($M = 0.37 \pm 0.11$) had a significantly higher overestimation compared to participants with a negative read ($M = 0.14 \pm 0.07$; $p < 0.01$). This relationship was also observed on a regional level, with the frontal lobe displaying the highest mean binding and the largest mean SUVr overestimation, compared to the parietal ($p < 0.01$) and temporal ($p < 0.01$) lobes. In turn, the parietal lobe did not show a significantly higher mean binding ($p = 0.1$), but did show a significantly larger overestimation ($p < 0.01$) compared to the temporal lobe (Supplemental Figure 2 and Table 1). The SUVr overestimation seems to have a limited influence on the visual read of the high binding group (i.e. $BP_{ND} > 0.26$), considering no cases were visually assessed as positive on SUVr and negative on BP_{ND} and only 2 SUVr images (7%) had a discordant read. For the low binding group (i.e. $BP_{ND} \le 0.26$), the SUVr overestimation might have influenced the visual read, considering that 26 cases (16%) had a SUVr discordant visual read. However, no obvious pattern was discernible (Figure 3).
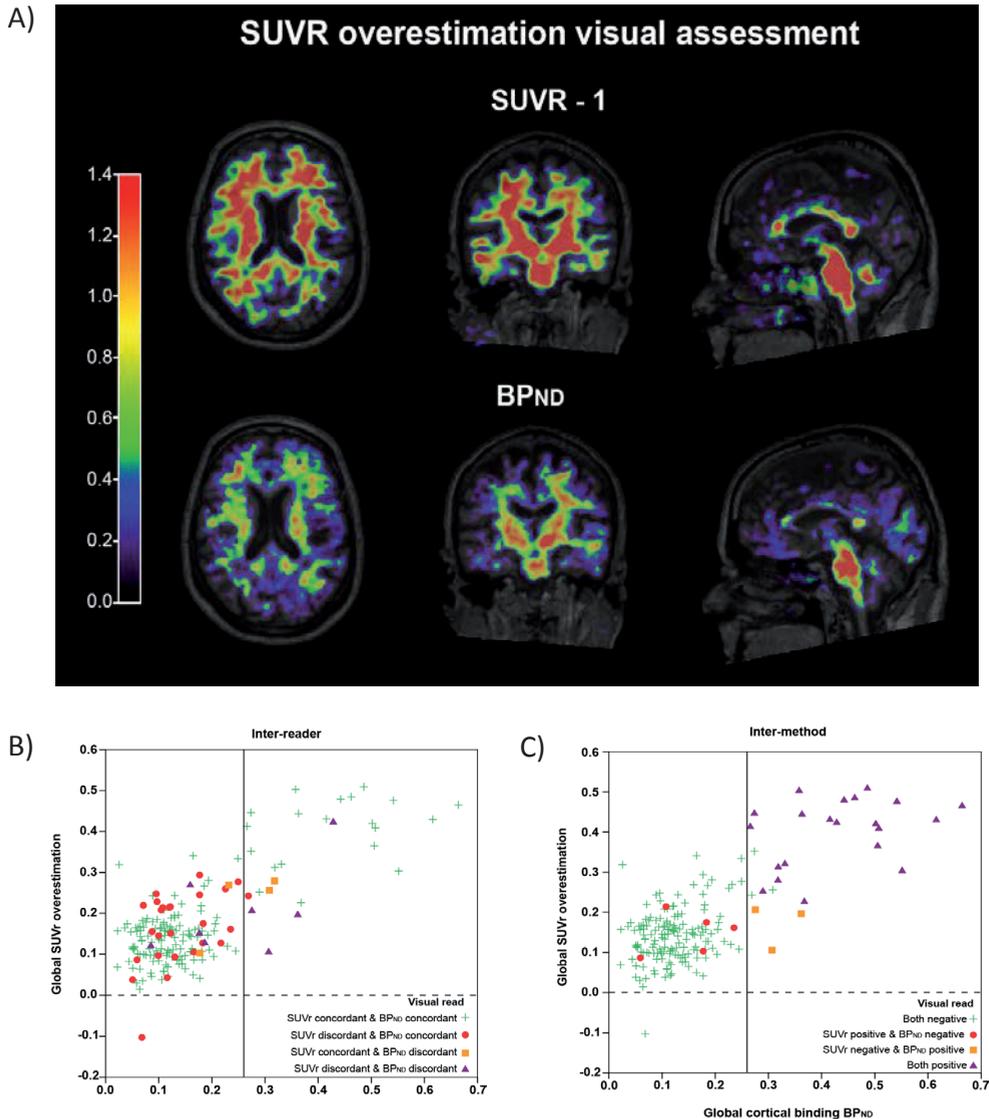
Figure 3. Illustration of binding overestimation when using semi-quantitative PET acquisition
(**A**) From left to right are shown axial, coronal, and sagittal views. (**Top**) A SUVr image with a subtraction of 1, showing clearly higher binding values than the BP_{ND} image (**bottom**), while in theory this should be the same image.
(**B/C**) Diagrams showing the difference between SUVr-1 and BP_{ND} for each subject with regard to visual read. The overestimation of SUVr is higher with increasing cortical binding.

DISCUSSION

In a cognitively normal elderly population with low amyloid burden we show a considerable improvement in inter-reader agreement of [¹⁸F]flutemetamol visual assessment when using BP_{ND} rather than standard SUVr images. Misclassifications can be reduced using semi-quantitative SUVr measures and avoided using fully quantitative BP_{ND} measures.

Our results are in line with ¹¹C-PiB findings of Zwan et al., where a comparable improve-ment in inter-reader agreement using BP_{ND} images was observed [11]. This suggests that the underlying reason for discrepant inter-reader agreements tracer-independent and likely related to the distinctive metrics being used (SUVr and BP_{ND}). SUVr is commonly used as a proxy for BP_{ND}, under the assumption that a secular equilibrium is reached during scanning. However, these equilibrium conditions are rarely met in practice. As such, while parametric BP_{ND} images reflect density of available receptors (amyloid plaques), SUVr images are affected by a non-displaceable (free and non-specific) signal and may be affected by changes in regional flow and wash-out effects [28, 30]. As a result, SUVr can overestimate specific binding [10], and influence visual assessments (Figure 3). Furthermore, our and existing data show that this overestimation is not constant, but instead increases with higher tracer binding [10, 28].

The inter-reader agreement for the SUVr images and the concordance between semi-quantitative and corresponding visual read classifications in our study, is lower than previously reported [7-9]. However, previous results were based on a clinical population and/or end-of-life subjects with higher incidence of moderate to severe amyloid burden, which highlights the challenge of assessing amyloid pathology in a population with low amyloid burden. The challenge could be due to the non-specific white matter uptake seen with [¹⁸F]flutemetamol, which together with the overestimation resulting from static scanning may translate into a tendency to visually assign regions as positive [31]. In our study, the frontal regions were most often perceived as difficult to assess, leading to most doubt for final classification. Although the [¹⁸F]flutemetamol reader training focuses on disentangling the white matter pattern from the cortical signal, assessment in this population seems additionally challenging, especially for less experienced readers. Indeed, the positive assigning tendency was the strongest for the reader with the least experience, who also showed the lowest *intra*-reader agreement between methods. This stresses the need for experienced readers to make early assessments and/or updating the reading guidelines, with focus on a cognitively normal elderly population.

Our results may have consequences for drug-intervention studies focused on early populations, since using the visual assessment of SUVr images either as an inclusion criteria could result in false-positive inclusion due to the observed overestimation of cortical amyloid burden [32, 33]. Also, studies indicate that cerebral blood flow can change with age and disease progression [34, 35]. Therefore, using BP_{ND} images in clinical trials could avoid

false-positive classification in visual assessment [28] and ensure that measured changes are due to the treatment instead of a measurement error or blood flow confounders.

An important factor in considering dynamic PET acquisition is participant burden. In this cohort, 95% of participants indicated they had no objections to undergoing a second dynamic PET scan. The coffee-break protocol used in this study may have facilitated this response and suggests the feasibility of longitudinal dynamic acquisition in cognitively normal elderly.

In a clinical setting, however, amyloid burden will more likely be moderate to severe and dynamic acquisition more challenging. In addition, the clinical utility of SUV or SUVr visual reads for the diagnosis of AD-type dementia in a clinical setting has been extensively shown [36]. Thus, in this context, visual assessment of SUVr images may indeed be sufficient. Nevertheless, the present results illustrate that semi-quantification using SUVr can help reduce false-positive classification, especially in a challenging population. Thus, the clinical preference for visual assessment could be revised in light of more available automatic (semi-)quantification methods, such as the one already provided for [¹⁸F]flutemetamol PET scans [8].

In this study, the standard manufacturer guidelines were used for reading both SUVr and BP_{ND} images. Nonetheless, an interesting finding was the improvement in inter-reader agreement when using BP_{ND} images despite the lack of official guidelines and the limited experience of readers in assessing such images. However, it might still be of interest to formally assess whether the current guidelines are optimal for assessing BP_{ND} images. In addition, optimizing visual assessment of SUVr images by updating the current guidelines and providing training specifically focused on early accumulation, may also result in improved classification certainty, comparable to the observed using dynamically derived measures. Studies have suggested that specifically medial frontal, anterior/posterior/isthmus cingulate cortex, and the precuneus are early accumulating regions [37, 38]. These regions can be visually assessed using the sagittal view of the PET image. Thus, the importance of this plane may be of most interest for updating guidelines.

A limitation of this study is the lack of a gold standard, as no post-mortem data were available, hampering the understanding of the findings in relation to underlying neuropathology. Furthermore, although the frequency of amyloid positivity in this cohort is comparable with previous reports [39], the low incidence may have induced reader bias with regards to searching for amyloid positivity. Lastly, both quantification and visual assessment of the PET images in this study were accompanied by a structural MRI, which might not always be available.

CONCLUSION

The use of parametric BP_{ND} images for visual assessment of [¹⁸F]flutemetamol in a population with low amyloid burden improves inter-reader agreement. Implementing semi-quantification in addition to visual assessment of SUVr images can reduce false-positive classification in this population.

REFERENCES

1. Alzheimer's, A., *2016 Alzheimer's disease facts and figures.* Alzheimers Dement, 2016. 12(4): p. 459-509.
2. Jansen, W.J., et al., *Prevalence of cerebral amyloid pathology in persons without dementia: a meta-analysis.* JAMA, 2015. 313(19): p. 1924-38.
3. Jansen, W.J., et al., *Prevalence of cerebral amyloid pathology in persons without dementia: a meta-analysis*, in *JAMA : the journal of the American Medical Association.* 2015. p. 1924-1938.
4. Dubois, B., et al., *Research criteria for the diagnosis of Alzheimer's disease: revising the NINCDS-ADRDA criteria*, in *Lancet neurology.* 2007. p. 734-746.
5. Sperling, R.A., et al., *Toward defining the preclinical stages of Alzheimer's disease: recommendations from the National Institute on Aging-Alzheimer's Association workgroups on diagnostic guidelines for Alzheimer's disease*, in *Alzheimer's & dementia : the journal of the Alzheimer's Association.* 2011. p. 280-292.
6. Sperling, R.A., et al., *The A4 study: stopping AD before symptoms begin?* Sci Transl Med, 2014. 6(228): p. 228fs13.
7. Buckley, C.J., et al., *Validation of an electronic image reader training programme for interpretation of [18F]flutemetamol beta-amyloid PET brain images.* Nucl Med Commun, 2017. 38(3): p. 234-241.
8. Thurfjell, L., et al., *Automated quantification of 18F-flutemetamol PET activity for categorizing scans as negative or positive for brain amyloid: concordance with visual image reads.* J Nucl Med, 2014. 55(10): p. 1623-8.
9. Salloway, S., et al., *Performance of [(18)F]flutemetamol amyloid imaging against the neuritic plaque component of CERAD and the current (2012) NIA-AA recommendations for the neuropathologic diagnosis of Alzheimer's disease.* Alzheimers Dement (Amst), 2017. 9: p. 25-34.
10. van Berckel, B.N., et al., *Longitudinal amyloid imaging using 11C-PiB: methodologic considerations.* J Nucl Med, 2013. 54(9): p. 1570-6.
11. Zwan, M.D., et al., *Comparison of simplified parametric methods for visual interpretation of 11C-Pittsburgh compound-B PET images.* J Nucl Med, 2014. 55(8): p. 1305-7.
12. Morris, J.C., et al., *The Consortium to Establish a Registry for Alzheimer's Disease (CERAD). Part I. Clinical and neuropsychological assessment of Alzheimer's disease*, in *Neurology.* 1989. p. 1159-1165.
13. de Jager, C.A., M.M. Budge, and R. Clarke, *Utility of TICS-M for the assessment of cognitive function in older adults*, in *International journal of geriatric psychiatry.* 2003. p. 318-324.
14. Yesavage, J.A., et al., *Development and validation of a geriatric depression screening scale: a preliminary report*, in *Journal of psychiatric research.* 1982. p. 37-49.
15. Morris, J.C., *The Clinical Dementia Rating (CDR): current version and scoring rules*, in *Neurology.* 1993. p. 2412-2414.
16. Nelissen, N., et al., *Phase 1 study of the Pittsburgh compound B derivative 18F-flutemetamol in healthy volunteers and patients with probable Alzheimer disease.*, in *Journal of nuclear medicine : official publication, Society of Nuclear Medicine.* 2009, Society of Nuclear Medicine. p. 1251-1259.
17. Heeman F, Y.M., Heurling K, Lopes Alves I, Gispert JD, Foley C, Lammertsma AA, *P20: Optimized coffee-break protocol for quantitative [18F]flutemetamol studies.* Human Amyloid Imaging Conference, 2018: p. 83.
18. Gunn, R.N., et al., *Parametric imaging of ligand-receptor binding in PET using a simplified reference region model*, in *NeuroImage.* 1997. p. 279-287.
19. Wu, Y. and R.E. Carson, *Noise reduction in the simplified reference tissue model for neuroreceptor functional imaging*, in *Journal of cerebral blood flow and metabolism : official journal of the International Society of Cerebral Blood Flow and Metabolism.* 2002. p. 1440-1452.
20. Boellaard, R., et al., *PPET: a software tool for kinetic and parametric analyses of dynamic PET studies.* NeuroImage, 2006. 31: p. T62.

21. Svarer, C., et al., *MR-based automatic delineation of volumes of interest in human brain PET images using probability maps.* Neuroimage, 2005. 24(4): p. 969-79.

22. Hammers, A., et al., *Three-dimensional maximum probability atlas of the human brain, with particular reference to the temporal lobe.* Hum Brain Mapp, 2003. 19(4): p. 224-47.

23. Tolboom, N., et al., *Detection of Alzheimer pathology in vivo using both 11C-PIB and 18F-FDDNP PET.* J Nucl Med, 2009. 50(2): p. 191-7.

24. Guo, T., et al., *Rate of β-amyloid accumulation varies with baseline amyloid burden: Implications for anti-amyloid drug trials.* Alzheimer's & Dementia, 2018.

25. Koedam, E.L., et al., *Visual assessment of posterior atrophy development of a MRI rating scale.* Eur Radiol, 2011. 21(12): p. 2618-25.

26. Scheltens, P., et al., *Atrophy of Medial Temporal Lobes on Mri in Probable Alzheimers-Disease and Normal Aging - Diagnostic-Value and Neuropsychological Correlates.* Journal of Neurology Neurosurgery and Psychiatry, 1992. 55(10): p. 967-972.

27. Fazekas, F., et al., *Mr Signal Abnormalities at 1.5-T in Alzheimers Dementia and Normal Aging.* American Journal of Neuroradiology, 1987. 8(3): p. 421-426.

28. Lammertsma, A.A., *Forward to the Past: The Case for Quantitative PET Imaging.* J Nucl Med, 2017. 58(7): p. 1019-1024.

29. Vandenberghe, R., et al., *18F-flutemetamol amyloid imaging in Alzheimer disease and mild cognitive impairment: a phase 2 trial.* Ann Neurol, 2010. 68(3): p. 319-29.

30. Carson, R.E., et al., *Comparison of bolus and infusion methods for receptor quantitation: application to [18F]cyclofoxy and positron emission tomography.* J Cereb Blood Flow Metab, 1993. 13(1): p. 24-42.

31. Mountz, J.M., et al., *Comparison of qualitative and quantitative imaging characteristics of [11C]PiB and [18F]flutemetamol in normal control and Alzheimer's subjects.* Neuroimage Clin, 2015. 9: p. 592-8.

32. Salloway, S., et al., *Two phase 3 trials of bapineuzumab in mild-to-moderate Alzheimer's disease.* N Engl J Med, 2014. 370(4): p. 322-33.

33. Doody, R.S., et al., *Phase 3 trials of solanezumab for mild-to-moderate Alzheimer's disease.* N Engl J Med, 2014. 370(4): p. 311-21.

34. Zhang, N., M.L. Gordon, and T.E. Goldberg, *Cerebral blood flow measured by arterial spin labeling MRI at resting state in normal aging and Alzheimer's disease.* Neurosci Biobehav Rev, 2017. 72: p. 168-175.

35. Sierra-Marcos, A., *Regional Cerebral Blood Flow in Mild Cognitive Impairment and Alzheimer's Disease Measured with Arterial Spin Labeling Magnetic Resonance Imaging.* Int J Alzheimers Dis, 2017. 2017: p. 5479597.

36. Morris, E., et al., *Diagnostic accuracy of (18)F amyloid PET tracers for the diagnosis of Alzheimer's disease: a systematic review and meta-analysis.* Eur J Nucl Med Mol Imaging, 2016. 43(2): p. 374-85.

37. Grothe, M.J., et al., *In vivo staging of regional amyloid deposition.* Neurology, 2017. 89(20): p. 2031-2038.

38. Palmqvist, S., et al., *Earliest accumulation of beta-amyloid occurs within the default-mode network and concurrently affects brain connectivity.* Nat Commun, 2017. 8(1): p. 1214.

39. Jansen, W., et al., *The prevalence of amyloid pathology in healthy individuals and individuals with mild cognitive impairment: A meta-analysis of amyloid-PET studies.* Alzheimer's & Dementia: The Journal of the Alzheimer's Association, 2013. 9(4): p. P533.

PART

2

Pathophysiology of early amyloid aggregation

4

Amyloid production and aggregation in preclinical Alzheimer's disease – a monozygotic twin study

Konijnenberg E, Den Braber A, Tijms, BM, Ten Kate M, Tomassen J, Yaqub MM, Mulder SD, Nivard MG, Vanderstichele H, Lammertsma AA, Teunissen CE, Van Berckel BNM, Boomsma DI, Scheltens P, Visser PJ

SUMMARY PARAGRAPH

One of the earliest events in Alzheimer's disease (AD) is aggregation of amyloid beta (Aβ). The production of Aβ is initiated when the amyloid precursor protein is cleaved by beta secretase-1 (BACE1)[1]. Increased Aβ production has been associated with the pathogenesis of autosomal dominant variants of AD, but the role of Aβ production in sporadic AD is less clear[2]. We investigated the relationship between Aβ production and aggregation in 96 monozygotic twin-pairs with normal cognition aged 60-94 years. Across the total sample, higher cerebrospinal fluid (CSF) concentrations of BACE1 were associated with more aggregation as measured with the CSF $Aβ_{42/40}$ ratio. Fourteen twin-pairs were discordant for amyloid aggregation on amyloid positron emission tomography (PET) scanning. Both the amyloid positive and amyloid negative twin of these pairs showed higher BACE1 levels than twins from pairs who were concordant amyloid negative. Monozygotic twin-pair correlations were high for BACE1 but moderately strong for Aβ aggregation markers, indicating that, in addition to genetic factors, unique environmental factors have a substantial effect on Aβ aggregation. These results provide evidence for a role of Aβ production in very early sporadic AD and stress the importance of identifying environmental risk factors for AD prevention strategies.

AD is the most common cause of dementia and treatments are still lacking. Clinical trials with anti-amyloid antibodies or BACE1 inhibitors have demonstrated that it is possible to remove amyloid plaques from the brain or decrease amyloid production [3, 4]. However, clinical benefits have been minimal or absent [5, 6], possibly because trials were performed in individuals with symptomatic AD, when irreversible neurodegeneration is already extensive. Understanding the pathophysiology of AD in cognitively normal subjects will be crucial for the development of primary and secondary prevention strategies. Aggregation of Aβ starts up to 20 years before the onset of dementia [7, 8], and this provides a window of opportunity for starting treatment before significant neurodegeneration has occurred.

In sporadic AD, Aβ aggregation is supposed to result from decreased clearance of Aβ [2, 9]. However, there is increasing evidence that also increased Aβ production plays a role in the pathogenesis. Brain tissue of individuals with AD-dementia showed increased expression and concentrations of BACE1, the rate-limiting enzyme in Aβ production [10, 11]. In cognitively normal individuals, CSF activity and concentration of BACE1 increased with age [12, 13], and higher CSF BACE1 levels were associated with higher CSF concentrations of Aβ 1-40 (Aβ40) and Aβ 1-38 (Aβ38) [13], non-pathogenic products of amyloid production which are indicative of total CSF Aβ peptide production [14-16]. We found that in cognitively normal individuals with normal brain amyloid, increased CSF BACE1 activity and higher CSF Aβ40 and Aβ38 levels predicted decline in CSF Aβ42, which is the Aβ peptide that is highly prone for aggregation and of which CSF levels decrease in AD [17].

We used a monozygotic twin approach to further investigate the relation between Aβ production and aggregation in cognitively normal individuals. Being genetically identical, monozygotic twins offer a unique opportunity to assess the effects of unique environmental factors on Aβ production and aggregation, because any difference within a twin-pair must result from differences in unique environmental exposures. In addition, twin discordance analysis can provide insight into the contribution of unique environmental factors on the observed relation between traits, while cross-twin cross-trait (CTCT) analysis provide the opportunity to investigate whether the observed correlation between traits is driven by shared genetic or environmental factors [18, 19].

We studied 96 cognitively normal monozygotic twin-pairs (70.1 ± 7.3 age, 57% female, 33% Apolipoprotein E (APOE) ε4 carrier, the major genetic risk factor for AD [20]). For 94 pairs an amyloid-PET scan was available for both twins, for 54 pairs CSF measures were available for both twins, and for 53 pairs PET and CSF measures were available for both twins (Table 1).

Table 1. Sample characteristics

	Total sample	PET visual read normal	PET visual read abnormal
N[§]	199	168	28
Singletons[^]	7	5	1
Age in years, mean (SD)	70.5 (7.6)	69.8 (7.3)	75.4 (7.6)**
Female gender, n (%)	114 (57)	97 (58)	17 (61)
Years of education, mean (SD)	11.5 (2.6)	11.5 (2.6)	11.3 (3.0)
MMSE, mean (SD)	29.0 (1.1)	29.1 (1.1)	28.6 (1.5)
APOE ε4 carrier[#], n (%)	65 (33)	50 (30)	14 (50)*
CSF, n (%)	126 (63)	105 (63)	18 (64)
- BACE-1, mean (SD), pg/mL	2370 (747)	2306 (696)	2744 (960)
- Amyloid β 1-40, mean (SD), pg/mL	9592 (2844)	9289 (2700)	11409 (3114)
- Amyloid β 1-38, mean (SD), pg/mL	2424 (737)	2370 (715)	2805 (797)
- Ratio amyloid β 1-42/1-40, mean (SD), pg/mL	0.10 (0.03)	0.10 (0.02)	0.05 (0.02)**
Dynamic PET, n (%)	188 (94)	163 (97)	25 (89)
- Global cortical amyloid deposition, mean (SD), BP_{ND}	0.16 (0.12)	0.12 (0.06)	0.43 (0.13)**
- Concordance status visual read amyloid positivity[§], n (%)			
§ Concordant negative pairs	- 74 (79)		
§ Concordant positive pairs	- 6 (6)		
§ Discordant pairs	- 14 (15)		

[§]PET data missing in 3 subjects; [^]In one pair PET was missing for one subject, the other twin had a normal scan and is counted as singleton for PET analysis; [§]94 twin pairs with both PET visual read available; [#]APOE status missing in 2 subjects; PET visual read was based on BP_{ND} image. Abbreviations: MZ: monozygotic; MMSE: mini mental state examination; APOE: apolipoprotein E; CSF: cerebrospinal fluid; Aβ: amyloid beta; BACE: beta secretase; PET: positron emission tomography; BP_{ND}: non-displaceable binding potential

*p<0.05 **p<0.01 different from normal PET group, for amyloid measures corrected for age, gender, and APOE ε4.

As proxy measures for Aβ production we used concentrations of BACE1, Aβ40, and Aβ38. We measured Aβ aggregation by the CSF $Aβ_{42/40}$ ratio [15] and by the non-displaceable binding potential (BP_{ND}) on a [¹⁸F]flutemetamol amyloid PET scan [21, 22] as these measures, while correlated [23], may explain different aspects of Aβ aggregation [24].

Twenty-seven individuals (14%) had an abnormal visual read of the amyloid-PET scan. These subjects were older and were more often APOE ε4 allele carriers than individuals with a normal PET scan (Table 1). Across all subjects, higher levels of BACE1 and Aβ38 were associated with a lower CSF $Aβ_{42/40}$ ratio, but not with amyloid-PET BP_{ND} (Table 2). Cross-twin cross-trait (CTCT) analyses showed that levels of amyloid production markers in one twin predicted the levels of amyloid aggregation of their co-twin. For example, a higher BACE1 or Aβ38 concentration in one twin correlated with a lower $Aβ_{42/40}$ ratio in the co-twin (r=-0.18- -0.24, p=0.02-0.07, Supplementary Table 1). This means that the correlation between production and aggregation markers is in part driven by shared genetic or environmental factors. Seventy-four pairs (79% of the 94 complete PET imaging pairs) were concordant

normal for the amyloid-PET visual read (i.e., both twins from a pair had a normal amyloid PET scan), 14 pairs (15%) were discordant, and 6 pairs (6%) were concordant abnormal (Figure 1, Supplementary Table 2). Discordant twins with a normal amyloid-PET visual read showed evidence of early amyloid aggregation as they had a higher BP_{ND} compared to twins who were concordant normal (p<0.05, Figure 1e). Both the amyloid negative and the amyloid positive twins from discordant twin-pairs had higher BACE1 concentrations than twins from concordant normal pairs (Figure 1f). Within-pair differences in aggregation markers were not associated with the within-pair differences in production markers (Supplementary Table 3). This suggests that increased BACE1 levels are a very early feature of sporadic AD and that the relation between increased BACE1 levels and aggregation is partly driven by unique environmental factors.

Table 2. Association between amyloid production and aggregation markers in total sample

Production marker	Aggregation marker	Model 1		Model 2	
		β (SE)	p-value	β (SE)	p-value
CSF BACE-1	CSF ratio Amyloid-β 1-42/1-40	-0.25 (0.10)	0.02	-0.23 (0.09)	0.008
CSF Amyloid-β 1-38	CSF ratio Amyloid-β 1-42/1-40	-0.35 (0.09)	0.0003	-0.27 (0.10)	0.005
CSF BACE-1	PET global [^{18}F]flutemetamol binding	0.13 (0.09)	0.12	0.09 (0.09)	0.31
CSF Amyloid-β 1-38	PET global [^{18}F]flutemetamol binding	0.17 (0.08)	0.03	0.09 (0.08)	0.23
CSF Amyloid-β 1-40	PET global [^{18}F]flutemetamol binding	0.09 (0.09)	0.34	0.02 (0.09)	0.85

Generalized estimating equations are shown unadjusted (Model 1) & covariate adjusted for age, APOE ε4 and gender (Model 2). All models include random effect for twin status. Standardized beta's are shown, calculated with z transformed variables. Amyloid aggregation is reflected by higher PET BP_{ND} and lower CSF amyloid-β 1-42/1-40 ratio.

Monozygotic twin-pair correlations (i.e., group-wise correlation for a trait across the twins of a pair) were high for Aβ production markers (0.79-0.86), and considerably lower for Aβ aggregation markers (0.52-0.54; Figure 2, Supplementary Table 4). None of the markers were correlated in randomly paired unrelated individuals (r=0.05-0.3, p=0.15-0.90) and twin correlations remained similar when correcting for age, gender and APOE ε4 allele (Supplementary Table 4). These results indicate that the variance in Aβ aggregation explained by unique environmental factors (0.46-0.48) is more than twice as high than the variance explained by unique environmental factors for Aβ production (0.14-0.21). The twin-pair correlation for aggregation markers is in line with estimates reported by smaller studies in cognitively normal subjects [25, 26], but lower compared to estimates for twin-pair correlation for AD-type dementia (up to 79%) [27]. Further longitudinal research is needed to investigate if the twin similarity of Aβ aggregation markers will increase with disease progression [27].
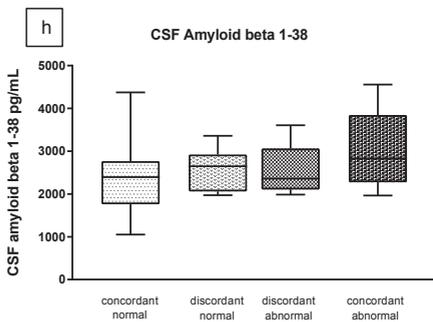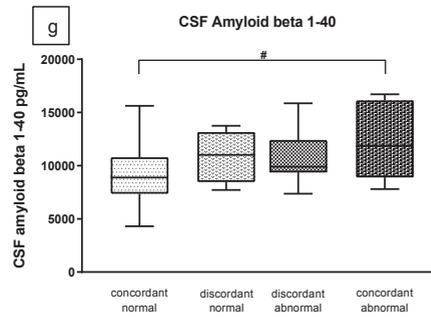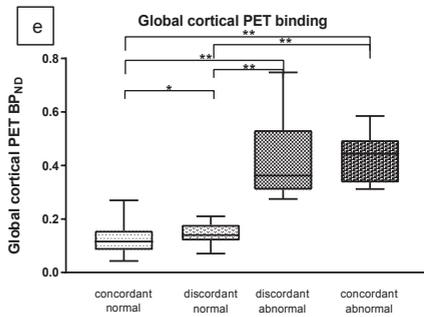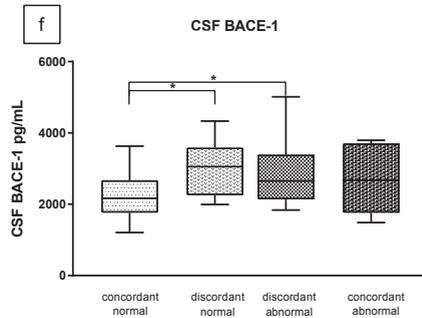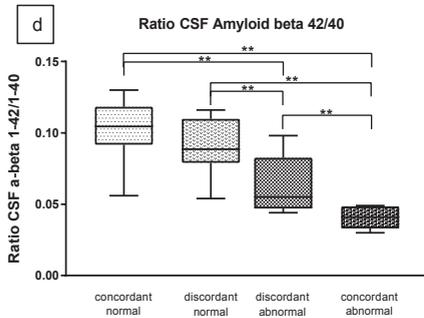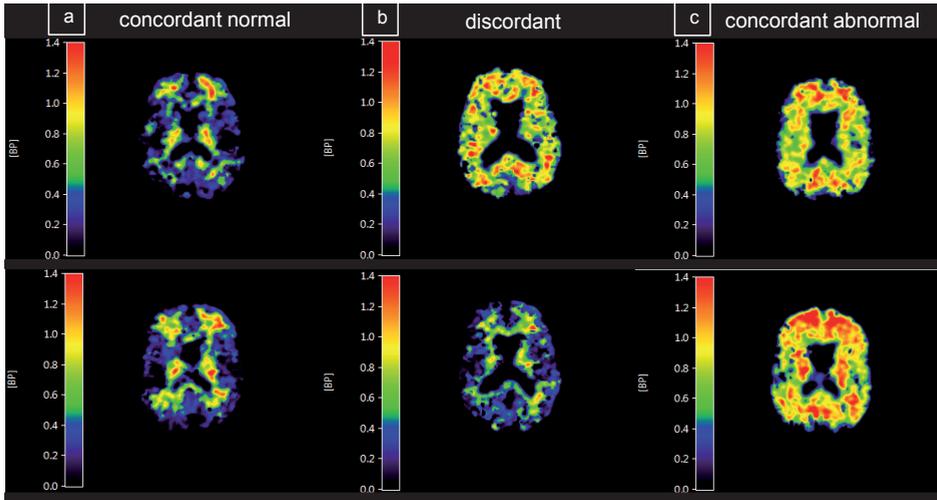
◀ **Figure 1. Patterns of amyloid production and aggregation markers for twin discordance**
[18F]flutemetamol PET images from a concordant twin pair (a) with a normal scan, a discordant pair (b) and a concordant pair with an abnormal scan (c). Boxplots show amyloid β 1-42/1-40 ratio (d); global cortical PET binding (e); BACE-1 (f); amyloid-β 1-40 (g); and amyloid-β 1-38 (h) for twins who have both a normal amyloid-PET scan (concordant normal, n=148 of which 93 have CSF markers), twins from a discordant pair with a normal amyloid-PET (discordant normal, n=14 of which 8 have CSF markers), twins from a discordant pair with abnormal amyloid-PET (discordant abnormal, n=14 of which 9 have CSF markers), and twin pairs who both have an abnormal amyloid-PET scan (concordant abnormal, n=12, of which 9 have CSF markers). All analyses for group comparisons were corrected for age, APOE ε4 and gender. *p<0.05; **p<0.01.
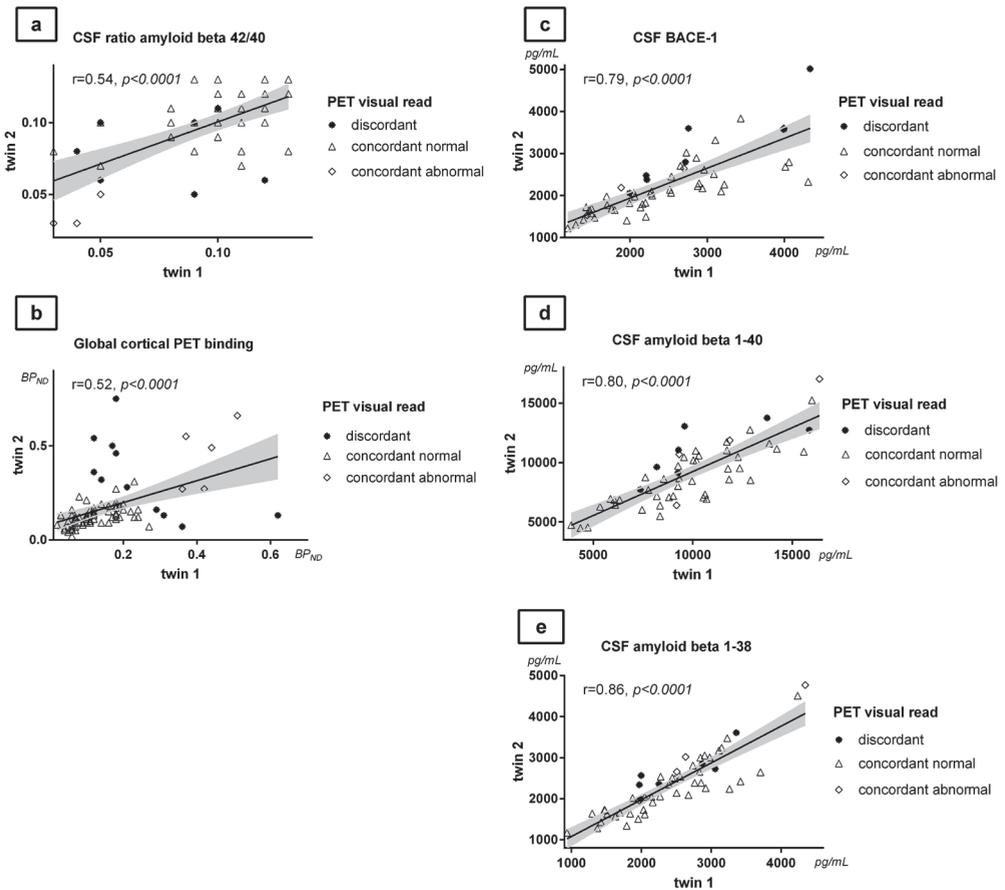
Figure 2. Monozygotic twin-pair correlations
Partial correlation values for association of amyloid markers between one twin and its co-twin, corrected for gender, age and APOE status. Each dot represents one twin pair. Left panel shows amyloid aggregation markers (a) CSF amyloid-β 1-42/1-40 ratio; (b) global cortical PET binding (BP$_{ND}$); right panel production markers (c) CSF BACE-1; (d) CSF amyloid-β 1-40; (e) CSF amyloid-β 1-38.

Finally, we examined the relation between the two Aβ aggregation markers and between the three Aβ production markers in order to confirm that the different markers for each category reflect the same biological process. The correlation between PET-BP$_{ND}$ and the CSF Aβ$_{42/40}$ ratio across the total sample was moderately strong (β=-0.57 (SE=0.09), p<0.0001; Supplementary Table 5), in line with previous studies in cognitively normal individuals [28]. The CTCT correlation and within-pair difference analyses (Supplementary Table 6 and 7, Supplementary Figure 1) were statistically significant, which supports the view that PET and CSF Aβ aggregation markers indeed reflect the same biological process. Aβ production markers correlated strongly with each other (r=0.45-0.82, p<0.0001) in the total sample and the statistically significant CTCT and twin difference analysis indicated that these markers also have the same underlying biology (Supplementary Table 5, 6, and 7, Supplementary Figure 1).

In summary, our findings suggest a role of increased Aβ production in the very early pathophysiology of sporadic AD and provides support for the notion that BACE1 inhibition may be of therapeutic value in the preclinical stage of sporadic AD [29], or perhaps when subjects still have a normal amyloid-PET scan. Identification of genes and mechanisms associated with increased Aβ production in cognitively normal individuals may provide novel clues for strategies to reduce Aβ aggregation.

The moderately high monozygotic twin-pair correlation of Aβ aggregation measures indicates that unique environmental factors substantially influence the onset and/or the rate of aggregation. Population studies have provided ample evidence for the role of environmental factors on dementia risk [30] and our study suggests such factors may play a role in amyloid aggregation as well.

Data availability statement
The data that support the findings of this study are available from the corresponding author after signing a material transfer agreement.

Author contributions
EK, MtK, AdB, and JT collected data. EK, MtK and MMY performed image analysis and SDM and CET CSF analysis. EK, AdB and MGN performed statistical analysis. EK and AdB drafted the manuscript. BT, MtK, JT, MMY, SDM, MGN, HV, AAL, CET, BNMvB, DIB, PHS, and PJV edited the manuscript for critical content. PJV conceived the study, designed the protocol, and provided overall study supervision. All authors read and approved the final version of the manuscript.

Competing interests
The authors declare the following competing interests: HV is employee of ADx Neuroscience, which provided the ELISA's used in this study. The other authors do not have a competing interest.

REFERENCES

1. Vassar, R., et al., *Beta-secretase cleavage of Alzheimer's amyloid precursor protein by the transmembrane aspartic protease BACE.* Science, 1999. **286**(5440): p. 735-41.
2. Selkoe, D.J. and J. Hardy, *The amyloid hypothesis of Alzheimer's disease at 25 years.* EMBO Mol Med, 2016. **8**(6): p. 595-608.
3. Sevigny, J., et al., *The antibody aducanumab reduces Abeta plaques in Alzheimer's disease.* Nature, 2016. **537**(7618): p. 50-6.
4. Kennedy, M.E., et al., *The BACE1 inhibitor verubecestat (MK-8931) reduces CNS beta-amyloid in animal models and in Alzheimer's disease patients.* Sci Transl Med, 2016. **8**(363): p. 363ra150.
5. Doody, R.S., et al., *Phase 3 trials of solanezumab for mild-to-moderate Alzheimer's disease.* N Engl J Med, 2014. **370**(4): p. 311-21.
6. Salloway, S., R. Sperling, and H.R. Brashear, *Phase 3 trials of solanezumab and bapineuzumab for Alzheimer's disease.* N Engl J Med, 2014. **370**(15): p. 1460.
7. Jansen, W.J., et al., *Prevalence of cerebral amyloid pathology in persons without dementia: a meta-analysis*, in *JAMA : the journal of the American Medical Association.* 2015. p. 1924-1938.
8. Gordon, B.A., et al., *Spatial patterns of neuroimaging biomarker change in individuals from families with autosomal dominant Alzheimer's disease: a longitudinal study.* Lancet Neurol, 2018. **17**(3): p. 241-250.
9. Mawuenyega, K.G., et al., *Decreased clearance of CNS beta-amyloid in Alzheimer's disease.* Science, 2010. **330**(6012): p. 1774.
10. Fukumoto, H., et al., *Beta-secretase protein and activity are increased in the neocortex in Alzheimer disease.* Arch Neurol, 2002. **59**(9): p. 1381-9.
11. Holsinger, R.M., et al., *Increased expression of the amyloid precursor beta-secretase in Alzheimer's disease.* Ann Neurol, 2002. **51**(6): p. 783-6.
12. Miners, J.S., et al., *Changes with age in the activities of beta-secretase and the Abeta-degrading enzymes neprilysin, insulin-degrading enzyme and angiotensin-converting enzyme.* Brain Pathol, 2010. **20**(4): p. 794-802.
13. Timmers, M., et al., *BACE1 Dynamics Upon Inhibition with a BACE Inhibitor and Correlation to Downstream Alzheimer's Disease Markers in Elderly Healthy Participants.* J Alzheimers Dis, 2017. **56**(4): p. 1437-1449.
14. Portelius, E., et al., *Determination of beta-amyloid peptide signatures in cerebrospinal fluid using immunoprecipitation-mass spectrometry.* J Proteome Res, 2006. **5**(4): p. 1010-6.
15. Lewczuk, P., et al., *Cerebrospinal Fluid Abeta42/40 Corresponds Better than Abeta42 to Amyloid PET in Alzheimer's Disease.* J Alzheimers Dis, 2017. **55**(2): p. 813-822.
16. Janelidze, S., et al., *Concordance Between Different Amyloid Immunoassays and Visual Amyloid Positron Emission Tomographic Assessment.* JAMA Neurol, 2017. **74**(12): p. 1492-1501.
17. Tijms, B.M., et al., *Pre-amyloid stage of Alzheimer's disease in cognitively normal individuals* Annals of Clinical and Translational Neurology 2018. **in press**.
18. De Moor, M.H., et al., *Testing causality in the association between regular exercise and symptoms of anxiety and depression.* Arch Gen Psychiatry, 2008. **65**(8): p. 897-905.
19. F, V., B. M, and A. L, *The discordant MZ-twin method:One step closer to the holy grail of causality.* International Journal of Behavioral Development, 2009. **33**(4): p. 376-382.
20. Corder, E.H., et al., *Gene dose of apolipoprotein E type 4 allele and the risk of Alzheimer's disease in late onset families.* Science, 1993. **261**(5123): p. 921-3.
21. Klunk, W.E., et al., *Imaging brain amyloid in Alzheimer's disease with Pittsburgh Compound-B.* Ann Neurol, 2004. **55**(3): p. 306-19.
22. Nelissen, N., et al., *Phase 1 study of the Pittsburgh compound B derivative 18F-flutemetamol in healthy volunteers and patients with probable Alzheimer disease.*, in *Journal of nuclear medicine : official publication, Society of Nuclear Medicine.* 2009, Society of Nuclear Medicine. p. 1251-1259.

23. Zwan, M.D., et al., *Use of amyloid-PET to determine cutpoints for CSF markers: A multicenter study.*, in *Neurology.* 2016, Lippincott Williams & Wilkins. p. 50-58.

24. Mattsson, N., et al., *Independent information from cerebrospinal fluid amyloid-beta and florbetapir imaging in Alzheimer's disease.* Brain, 2015. **138**(Pt 3): p. 772-83.

25. Hinrichs, A.L., et al., *Cortical binding of pittsburgh compound B, an endophenotype for genetic studies of Alzheimer's disease.* Biol Psychiatry, 2010. **67**(6): p. 581-3.

26. Johansson, V., et al., *Cerebrospinal fluid microglia and neurodegenerative markers in twins concordant and discordant for psychotic disorders.* Eur Arch Psychiatry Clin Neurosci, 2016.

27. Gatz, M., et al., *Role of genes and environments for explaining Alzheimer disease.* Arch Gen Psychiatry, 2006. **63**(2): p. 168-74.

28. Zwan, M., et al., *Concordance between cerebrospinal fluid biomarkers and [11C]PIB PET in a memory clinic cohort.* Journal of Alzheimer's disease : JAD, 2014. **41**(3): p. 801-807.

29. Lopez Lopez C., e.a., *The Alzheimer's Prevention Initiative Generation Program: Evaluating CNP520 Efficacy in the Prevention of Alzheimer's Disease.* The journal of prevention of Alzheimer's disease 2017. **4**(4): p. 242-246.

30. Livingston, G., et al., *Dementia prevention, intervention, and care.* Lancet, 2017. **390**(10113): p. 2673-2734.

31. Rabbitt, P.M.A.e.a., *The University of Manchester longitudinal study of cognition in normal healthy old age, 1983 through 2003.*, in *Aging Neuropsychol C.* 2004. p. 245-279.

32. Boomsma, D.I., et al., *Netherlands Twin Register: from twins to twin families.* Twin Res Hum Genet, 2006. **9**(6): p. 849-57.

33. Morris, J.C., et al., *The Consortium to Establish a Registry for Alzheimer's Disease (CERAD). Part I. Clinical and neuropsychological assessment of Alzheimer's disease*, in *Neurology.* 1989. p. 1159-1165.

34. de Jager, C.A., M.M. Budge, and R. Clarke, *Utility of TICS-M for the assessment of cognitive function in older adults*, in *International journal of geriatric psychiatry.* 2003. p. 318-324.

35. Yesavage, J.A., et al., *Development and validation of a geriatric depression screening scale: a preliminary report*, in *Journal of psychiatric research.* 1982. p. 37-49.

36. Morris, J.C., *The Clinical Dementia Rating (CDR): current version and scoring rules*, in *Neurology.* 1993. p. 2412-2414.

37. E, K., et al., *The EMIF-AD PreclinAD study: Study Design and Baseline Cohort Overview.* Alzheimer's Research and Therapy, 2018(in press).

38. Boomsma, D.I., et al., *An Extended Twin-Pedigree Study of Neuroticism in the Netherlands Twin Register.* Behav Genet, 2018. **48**(1): p. 1-11.

39. Willemsen, G., et al., *The Netherlands Twin Register biobank: a resource for genetic epidemiological studies.* Twin Res Hum Genet, 2010. **13**(3): p. 231-45.

40. del Campo, M., et al., *Recommendations to standardize preanalytical confounding factors in Alzheimer's and Parkinson's disease cerebrospinal fluid biomarkers: an update.* Biomark Med, 2012. **6**(4): p. 419-30.

41. De Vos, A., et al., *C-terminal neurogranin is increased in cerebrospinal fluid but unchanged in plasma in Alzheimer's disease.* Alzheimers Dement, 2015. **11**(12): p. 1461-9.

42. Gunn, R.N., et al., *Parametric imaging of ligand-receptor binding in PET using a simplified reference region model*, in *NeuroImage.* 1997. p. 279-287.

43. Wu, Y. and R.E. Carson, *Noise reduction in the simplified reference tissue model for neuroreceptor functional imaging*, in *Journal of cerebral blood flow and metabolism : official journal of the International Society of Cerebral Blood Flow and Metabolism.* 2002. p. 1440-1452.

44. Svarer, C., et al., *MR-based automatic delineation of volumes of interest in human brain PET images using probability maps.* Neuroimage, 2005. **24**(4): p. 969-79.

45. Hammers, A., et al., *Three-dimensional maximum probability atlas of the human brain, with particular reference to the temporal lobe.* Hum Brain Mapp, 2003. **19**(4): p. 224-47.

46. Tolboom, N., et al., *Detection of Alzheimer pathology in vivo using both 11C-PIB and 18F-FDDNP PET.* J Nucl Med, 2009. **50**(2): p. 191-7.

47. Healthcare, G., *EPAR product information - summary of product characteristics.*

48. Ehli, E.A., et al., *A method to customize population-specific arrays for genome-wide association testing.* Eur J Hum Genet, 2017. **25**(2): p. 267-270.

49. Fedko, I.O., et al., *Estimation of Genetic Relationships Between Individuals Across Cohorts and Platforms: Application to Childhood Height.* Behav Genet, 2015. **45**(5): p. 514-28.

50. Das, S., et al., *Next-generation genotype imputation service and methods.* Nat Genet, 2016. **48**(10): p. 1284-1287.

51. van der Lee, S.J., et al., *The effect of APOE and other common genetic variants on the onset of Alzheimer's disease and dementia: a community-based cohort study.* The Lancet Neurology, 2018. **17**(5): p. 434-444.

52. Minica, C.C., et al., *Sandwich corrected standard errors in family-based genome-wide association studies*, in *European journal of human genetics : EJHG*. 2014.

53. Boker, S., et al., *OpenMx: An Open Source Extended Structural Equation Modeling Framework.* Psychometrika, 2011. **76**(2): p. 306-317.

SUPPLEMENTARY DATA

METHODS

Subjects

This study is part of the Innovative Medicine Initiative (IMI) European Information Framework for AD (EMIF-AD) project (http://www.emif.eu/). The overall aim of EMIF-AD is to discover and validate diagnostic markers, prognostic markers, and risk factors for AD in non-demented individuals. The PreclinAD study enrolled 260 cognitively normal subjects from two on-going cohort studies: the Manchester and Newcastle aging study (MNAS) [31] and the Netherlands Twin Register (NTR), from which monozygotic twins were selected [32]. Inclusion criteria were age 60 years and older, a delayed recall score of > -1.5 SD of demographically adjusted normative data of the Consortium to Establish a Registry for Alzheimer's Disease (CERAD) 10 word list [33], a Telephone Interview for Cognitive Status modified (TICS-m) score of 23 or higher [34], a 15-item Geriatric Depression Scale (GDS) score of <11 [35], and a Clinical Dementia Rating (CDR) scale of 0 with a score on the memory sub domain of 0 [36]. Exclusion criteria were any physical, neurological or psychiatric condition that could lead to interference with normal cognition in aging. Monozygotic twins subjects were asked to collect buccal cell samples for DNA extraction to confirm zygosity. The design of the PreclinAD study has been described elsewhere [37]. For the present study we included monozygotic twins who had an amyloid measurement available (n=197).

Netherlands Twins Register

The NTR started recruiting adolescent and adult twins and their relatives in 1987, and contained over 275.000 participants in 2018 [38]. From 1991 participants completed extensive questionnaires every 2-3 years and DNA was collected with the NTR-Biobank project [39]. Twins who were recruited for the current study gave consent for researchers to approach them for participation in scientific studies.

Ethical considerations

The Medical Ethics Review Committee of the VU University Medical Center provided approval for the study. The research was performed according to the principles of the Declaration of Helsinki and in accordance with the Medical Research Involving Human Subjects Act and codes on 'good use' of clinical data and biological samples as developed by the Dutch Federation of Medical Scientific Societies. All subjects gave written informed consent. The study was registered in the EU Clinical Trials Register (EudraCT) with number 2014-000219-15.

Cerebrospinal fluid analysis

CSF samples were collected in 126 (62%) participants through a lumber puncture, performed between 10am and 2pm, after at least two hours of fasting. Maximal 20 ml CSF was collected in Sarstedt polypropylene syringes using a Spinocan 25 Gauge needle in one of the intervertebral spaces between L3 and S1. Samples were centrifuged at 1300-2000 g at 4°C for 10 minutes and supernatants were then stored in aliquots at -80°C until analysis [40]. A maximum of 2 hours was allowed between lumbar puncture and freezing. Levels of amyloid beta 1-38, 1-40, 1-42 and BACE1 were analyzed using kits from ADx Neurosciences/ Euroimmun according to manufacturer instructions [41]. All samples were measured in kits from the same lot.

[¹⁸F]flutemetamol Positron Emission Tomography

196 subjects had [^{18}F]flutemetamol PET available. PET scanning was generally performed on the same day as the lumber puncture, except for 26 subjects, due to technical issues (range 2.2 months before to 6.7 months after lumbar puncture). PET scans were acquired with a Philips Ingenuity TF PET-MRI camera (Philips Healthcare, Cleveland, USA). All subjects were dynamically scanned under standard resting conditions (eyes closed in dimmed ambient light) from 0 to 30 minutes and then again from 90 to 110 minutes after intravenous injection of 185 MBq (±10%) [^{18}F]flutemetamol [22]. After data acquisition, the first emission scan was reconstructed into 18 frames of increasing length (6x5, 3x10, 4x60, 2x150, 2x300, 1x600 sec.) using the standard LOR-RAMLA reconstruction algorithm for the brain. Using the same reconstruction algorithm, the second scan was reconstructed into 4 frames of 5 minutes each. Subsequently, data from the two scans were combined into a single image data set after co-registration using Vinci Software 2.56 (Max Planck Institute for Neurological Research, Cologne, Germany). Parametric non-displaceable binding potential (BP$_{ND}$) images were generated from the entire image set using receptor parametric mapping [42, 43]. Next, T1-based VOIs using the Hammers atlas implemented in PVElab software were projected onto the [^{18}F]flutemetamol parametric images to extract regional values [44]. Cerebellar grey matter, computed from a T1-weighted structural MRI scan that was obtained immediately prior to the PET scan, was used for attenuation correction of the PET data and used to indicate the reference tissue [45]. A whole brain BP$_{ND}$ was calculated based on the volume-weighted average of frontal (i.e., superior, middle, and inferior frontal gyrus), parietal (i.e., posterior cingulate, superior parietal gyrus, postcentral gyrus, and inferolateral remainder of parietal lobe), and temporal (i.e., parahippocampal gyrus, hippocampus, medial temporal lobe, superior, middle, and inferior temporal gyrus) cortical regions [46].

Measures of PET amyloid pathology

We classified twins as amyloid positive (abnormal) or negative (normal) by visual read of the [18F]flutemetamol scans. Rating was performed on the dynamic BP_{ND} images by three readers (nuclear physician or radiologist) trained according to GEHC guidelines [47]. We applied the 'majority rules' (i.e. when not all readers agreed, the rating of 2 readers who agreed was followed). In other analyses we used the whole brain BP_{ND}.

APOE genotyping

All subjects were genotyped on the Affymetrix Axiom array and the Affymetrix 6 array [48] these were first cross chip imputed following the protocols as described by Fedko and colleagues [49] and then imputed to HRC with the Michigan Imputation server[50]. APOE genotype was assessed using imputed dosages of the SNP rs429358 (APOE ε4, imputation quality = 0.956) and rs7412 (APOE ε2, imputation quality = 0.729) [51]. Single nucleotide polymorphisms at rs429358 and rs7412 were used to identify APOE allele variants. Participants with either 1 or 2 ε4 variants were considered APOE ε4 carriers. Carrier status was available for 197 participants.

Statistical analysis

We used Generalized Estimating Equations (GEE) to test group differences for amyloid-PET positivity, including a random effect for twin status. Analyses were performed unadjusted (model 1) and adjusted for age, gender, and APOE ε4 genotype (model 2) when applicable. Next we performed three types of twin analyses. Monozygotic twin-pair correlations (i.e. the correlations for a trait between twin 1 and twin 2 across the group) for CSF (n=54 pairs) and PET amyloid (n=94 pairs) were assessed using Pearson's correlations. The correlation coefficient is a proxy for the amount of variance of a trait explained by the combination of shared genetic and shared environmental factors. The correlation coefficient-1 indicates the percentage of the trait explained by unique environmental factors. Partial correlations were also calculated adjusting for age, gender and APOE ε4 genotype. Within-subject and cross-twin-cross-trait analysis were assessed using GEE including random effect for twin status, unadjusted (model 1) and adjusted for age, gender, and APOE ε4 genotype (model 2) [52]. PET data were log-transformed to improve normal distribution of the data. When two variables showed a significant correlation, we performed cross-twin cross-trait analysis to test whether levels of marker A in one twin could predict levels of marker B in the co-twin using OpenMx [53]. We also performed a monozygotic within-pair difference analysis [18] when there was a significant association between variables. This model allows examining whether within-pair differences in marker A can be explained by within-pair differences in marker B. Statistical analyses were performed in SPSS version 23 for Windows and R version 3.3.1, http://www.r-project.org/.

Supplementary Table 1. Cross-twin cross-trait analyses for amyloid production with aggregation markers

Production	Aggregation	Model 1 R (SE)	p-value	Model 2 R (SE)	p-value
BACE-1	Ratio CSF Amyloid-β 1-42/1-40	-0.19 (0.10)	0.06	-0.18 (0.10)	0.07
Amyloid-β 1-38	Ratio CSF Amyloid-β 1-42/1-40	-0.36 (0.09)	0.0005	-0.24 (0.10)	0.02
Amyloid-β 1-38	PET global [^{18}F]flutemetamol binding	0.23 (0.09)	0.03	0.16 (0.10)	0.14

Data are displayed as correlation coefficient (SE), comparable to standardized beta's given in GEE results. Unadjusted (Model 1), calculated for residuals adjusted for age, APOE ε4 and gender (Model 2). Correlation coefficient indicates the correlation of the production marker in one twin with the aggregation marker in its co-twin. Cross-twin cross-trait analyses are shown for variables that had a statistically significant association in the whole sample (Table 2).

Supplementary Table 2. Baseline characteristics according to amyloid-PET discordance status

	Concordant normal PET (CN, n=148, 74 pairs)	Discordant normal PET (DN, n=14)	Discordant abnormal PET (DA, n=14)	Concordant abnormal PET (CA, n=12, 6 pairs)	Group difference
Age in years, mean (SD)	69.1 (6.9)	73.6 (7.6)	73.6 (7.6)	76.1 (6.9)	CN* < DN, DA, CA
Female gender, n (%)	84 (57)	8 (57)	8 (57)	8 (67)	-
Years of education, mean (SD)	11.6 (2.5)	10.9 (3.0)	11.6 (3.1)	10.9 (3.1)	-
APOE ε4 carrier#, n (%)	40 (27)	8 (57)	8 (57)	6 (50)	CN* < DN, DA, CA
MMSE, mean (SD)	29.1 (1.0)	28.7 (1.4)	28.9 (1.3)	28.0 (1.6)	CN* > CA
CSF, n (%)	93 (63)	8 (57)	9 (64)	9 (75)	
- BACE1, mean (SD), pg/mL	2253 (665)	2585 (821)	2867 (1014)	2622 (946)	CN* < DN, DA
- Amyloid-β 1-40, mean (SD), pg/mL	9141 (2694)	10900 (2511)	10788 (2564)	12031 (3628)	-
- Amyloid-β 1-38, mean (SD), pg/mL	2349 (723)	2585 (487)	26096 (562)	3000 (975)	-
- Ratio amyloid-β 1-42/1-40, mean (SD), pg/mL	0.10 (0.02)	0.09 (0.02)	0.06 (0.02)	0.04 (0.01)	CN** > DA, CA; DN** > DA, CA; DA** > CA
Dynamic PET, n (%)	143 (97)	14 (100)	12 (86)	11 (92)	
- Global cortical amyloid deposition, mean (SD), BP$_{ND}$	0.12 (0.06)	0.15 (0.04)	0.43 (0.15)	0.43 (0.12)	CN < DN* DA**, CA**; DN** < DA, CA

Concordant status based on visual read on BP$_{ND}$ image. Comparisons for cognitive, CSF, and PET variables were corrected for age, gender and education. All models include random effect for twin status.

Abbreviations: MZ: monozygotic; MMSE: mini mental state examination; APOE: apolipoprotein E; CSF: cerebrospinal fluid; Aβ: amyloid beta; BACE: beta secretase; PET: positron emission tomography; BP$_{ND}$: non-displaceable binding potential; CN: concordant normal; DN: discordant normal; CN: discordant abnormal; DN: concordant abnormal.

*p<0.05 **p<0.01 different from normal PET group

Supplementary Table 3. Within-pair difference analyses for amyloid production with aggregation markers

Production	Aggregation	Model 1 β (SE)	p-value	Model 2 β (SE)	p-value
BACE-1	Ratio CSF Amyloid-β 1-42/1-40	-0.16 (0.14)	0.26	-0.13 (0.14)	0.34
Amyloid-β 1-38	Ratio CSF Amyloid-β 1-42/1-40	-0.07 (0.14)	0.61	-0.05 (0.14)	0.72
Amyloid-β 1-38	PET global [^{18}F]flutemetamol binding	0.08 (0.16)	0.63	0.08 (0.16)	0.64

Linear regression results are shown for the relation between the standardized difference scores (z-scores) within a twin-pair per amyloid marker (Model 1), and adjusted for age, APOE ε4 and gender (Model 2). Beta indicates the association between the within-pair difference in the production marker and the within-pair difference in the aggregation marker. Within-pair difference analyses are shown for variables that had a statistically significant association in the whole sample (see Table 2).

Supplementary Table 4. Monozygotic twin-pair correlations for amyloid production and aggregation markers

Monozygotic twin-pair correlations	Model 1 Pearson's r	p-value	Model 2 Pearson's r	p-value
BACE-1	0.794	<0.0001	0.789	<0.0001
Amyloid-β 1-38	0.881	<0.0001	0.859	<0.0001
Amyloid-β 1-40	0.811	<0.0001	0.796	<0.0001
Ratio CSF Amyloid-β 1-42/1-40	0.647	<0.0001	0.536	<0.0001
PET global [^{18}F]flutemetamol binding	0.564	<0.0001	0.523	<0.0001

Pearson's r is shown for monozygotic twin-pair correlations without covariates (Model 1), and as partial correlations with covariates (age, APOE ε4 and gender, Model 2). Correlations are shown in figure 2.

Supplementary Table 5. Correlations among amyloid production markers and among aggregation markers in total cohort

Predictor	Dependent	Model 1 β (SE)	p-value	Model 2 β (SE)	p-value
Production markers					
BACE-1	Amyloid-β 1-38	0.48 (0.08)	<0.0001	0.45 (0.07)	<0.0001
BACE-1	Amyloid-β 1-40	0.83 (0.07)	<0.0001	0.82 (0.06)	<0.0001
Amyloid-β 1-38	Amyloid-β 1-40	0.80 (0.06)	<0.0001	0.82 (0.07)	<0.0001
Aggregation markers					
Ratio CSF Amyloid-β 1-42/1-40	PET global [^{18}F] flutemetamol binding	-0.58 (0.09)	<0.0001	-0.57 (0.09)	<0.0001

Generalized estimating equations are shown unadjusted (model 1) and covariate adjusted for age, APOE ε4 and gender (model 2). All models include random effect for twin status. Standardized beta's are shown, calculated with z-scores.
Amyloid aggregation is reflected by higher values on PET and lower CSF amyloid-β 1-42/1-40 ratio.

Supplementary Table 6. Cross-twin cross-trait analyses for amyloid production markers and for aggregation markers

Production markers		Model 1 R (SE)	p-value	Model 2 R (SE)	p-value
BACE-1	CSF Amyloid-β 1-38	0.45 (0.09)	<0.0001	0.41 (0.09)	<0.0001
BACE-1	CSF Amyloid-β 1-40	0.67 (0.06)	<0.0001	0.66 (0.06)	<0.0001
Amyloid-β 1-38	CSF Amyloid-β 1-40	0.62 (0.07)	<0.0001	0.51 (0.08)	<0.0001
Aggregation markers					
Ratio Amyloid-β 1-42/1-40	PET global [18F]flutemetamol binding	-0.42 (0.08)	<0.0001	-0.33 (0.09)	0.0004

Data are displayed as correlation coefficient (SE), comparable to standardized beta's given in GEE results. Unadjusted (Model 1) and residuals adjusted for age, APOE ε4 and gender (Model 2). Correlation coefficient indicates the correlation of the production marker in one twin with the aggregation marker in the co-twin.

Supplementary Table 7. Within-pair difference analyses for amyloid production markers and for aggregation markers

Predictor	Dependent	Model 1 β (SE)	p-value	Model 2 β (SE)	p-value
Production					
BACE-1	Amyloid-β 1-38	0.57 (0.11)	<0.0001	0.57 (0.12)	<0.0001
BACE-1	Amyloid-β 1-40	0.73 (0.09)	<0.0001	0.73 (0.10)	<0.0001
Amyloid-β 1-38	Amyloid-β 1-40	0.78 (0.09)	<0.0001	0.78 (0.09)	<0.0001
Aggregation					
Ratio Amyloid-β 1-42/1-40	PET global [18F]flutemetamol binding	-0.56 (0.13)	0.0001	-0.58 (0.14)	0.0001

Linear regression results are shown for the relation between the standardized difference scores (z-scores) within a twin pair per amyloid marker (Model 1), and adjusted for age, APOE ε4 and gender (Model 2). Beta indicates the association between the within-pair difference in predictor and the within-pair difference in dependent variable.
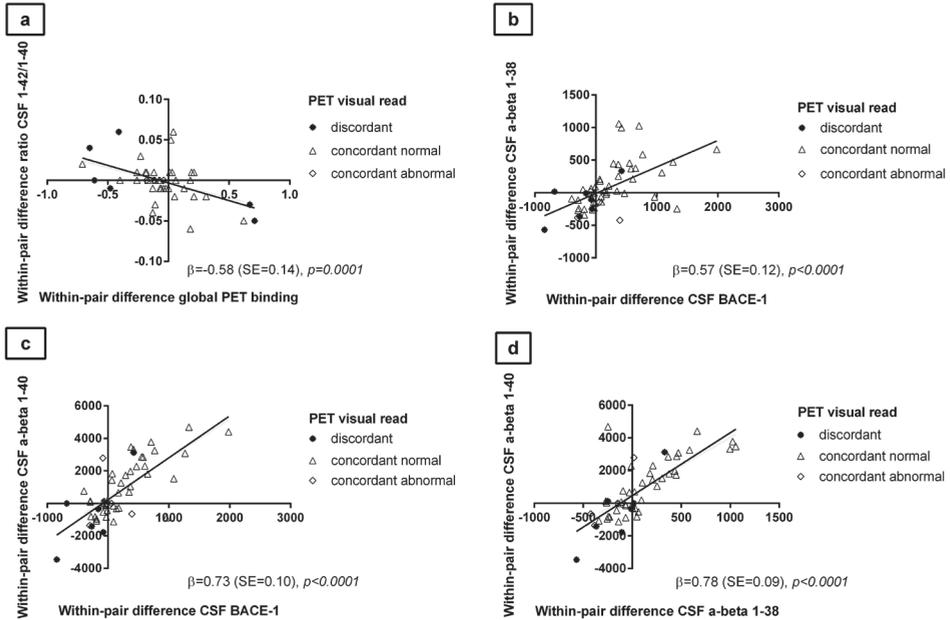
Supplementary Figure 1. Monozygotic within-pair difference associations between amyloid aggregation markers and between amyloid production markers

Within-pair differences of (a) CSF amyloid-β 1-42/1-40 ratio with global cortical PET binding (BP$_{ND}$); (b) CSF BACE-1 with CSF amyloid-β 1-38; (c) CSF BACE1 with CSF amyloid-β 1-40; (d) CSF amyloid-β 1-38 with CSF amyloid-β 1-40. Each dot represents one twin pair, twin pairs who are concordant normal on visual amyloid-PET read are shown as open triangles, twin pairs who are concordant normal on visual amyloid-PET read are shown as open diamonds. Discordant pairs on visual amyloid-PET read are shown as black asterisks. Lower CSF ratio amyloid beta 1-42/1-40 and higher global cortical PET binding indicate more amyloid aggregation.

CHAPTER

5

APOE ε4 genotype dependent cerebrospinal fluid proteomic signatures in Alzheimer's disease

Konijnenberg E, Tijms, BM, Teunissen CE, Veerhuis R, Smit AB, Scheltens P, Visser PJ for the Alzheimer's Disease Neuroimaging Initiative**

ABSTRACT

Aggregation of amyloid β into plaques in the brain is one of the earliest pathological events in Alzheimer's disease (AD). The exact pathophysiology leading to dementia is still uncertain, but the Apolipoprotein E (APOE) ε4 genotype plays a major role. We aimed to identify molecular pathways associated with amyloid β aggregation using cerebrospinal fluid (CSF) proteomics, and to study potential modifying effects of APOE ε4 genotype. We tested 243 proteins and protein fragments in CSF comparing 193 subjects with AD across the cognitive spectrum (65% APOE ε4 carriers; average age 75±7 years) against 60 controls with normal CSF amyloid β, normal cognition and no APOE ε4 allele (average age 75±6 years). One hundred twenty-nine proteins (53%) were associated with aggregated amyloid β. APOE ε4 carriers with AD showed altered concentrations of proteins involved in the complement pathway and glycolysis when cognition was normal and lower concentrations of proteins involved in synapse structure and function when cognitive impairment was moderately severe. APOE ε4 non-carriers with AD showed lower expression of proteins involved in synapse structure and function when cognition was normal, and lower concentrations of proteins that were associated with complement and other inflammatory processes when cognitive impairment was mild. These results imply that AD pathophysiology depends on APOE genotype and that treatment for AD may need to be tailored according to APOE genotype and severity of the cognitive impairment.

Amyloid β aggregation in the brain is one of the earliest pathological events in Alzheimer's Disease (AD) and is thought to start decades before the manifestation of dementia [1-3]. The presence of an Apolipoprotein-E (APOE) ε4 allele, the major risk genetic risk factor for AD [4], lowers the age of onset through an as of yet unknown mechanism. In general, it is largely unclear which biological processes eventually lead to cognitive decline once amyloid β has aggregated, as well as whether such processes are influenced by the presence of the APOE ε4 allele. A better understanding of biological processes disrupted in AD subjects is crucial for the development of precision medicine. The apoE4 protein isoform has been associated with impaired amyloid clearance and transport, synaptogenesis, glucose and cholesterol metabolism in the brain [5, 6]. However, about 25-40% of patients with AD dementia lack the APOE ε4 allele [7], and for these individuals the pathophysiological mechanisms involved in AD are less clear [8].

Unbiased proteomic analysis in cerebrospinal fluid (CSF) allows studying multiple molecular processes at the same time in patients, and it can be hypothesized that distinct patterns of protein concentrations exist in the CSF that are associated with aggregated amyloid. The first CSF proteomic studies have identified novel markers associated with AD-type dementia when comparing patients with cognitively normal controls [9-11]. Yet, not all subjects with a clinical diagnosis of AD-type dementia have aggregated amyloid [12, 13], and on average 30% of cognitively normal subjects are already in the preclinical stage of AD [3, 12, 13]. Consequently, it remains uncertain which of the previously reported markers are specific for AD pathology, i.e., aggregated amyloid. Furthermore, protein levels in CSF may depend on APOE ε4 genotype, which has been reported for beta secretase-1 [BACE1] [14] and chitinase-3-like protein-1 [YKL40] [15], both proteins associated with AD-type dementia, and so it is plausible that APOE ε4 genotype may influence other protein markers in CSF as well.

In this study, we used a CSF proteomic approach to test the hypothesis that protein signatures can be detected that show APOE ε4 genotype dependent associations with AD across the cognitive spectrum.

RESULTS

Sample characteristics by APOE ε4 genotype

We included 253 subjects from the Alzheimer's Disease Neuroimaging Initiative-1 (ADNI-1) who had available baseline proteomic CSF data (see Materials and Methods section, and Supplementary Table 1 for a list of all studied proteins). AD was defined by the presence of aggregated amyloid in CSF, as indicated by amyloid β 1-42 concentrations lower than 192 pg/ml [16]. We stratified subjects with aggregated amyloid according to APOE ε4 genotype (carriers versus non-carriers), and for cognitive stage defined as 'normal cognition' (Mini

Mental State Examination (MMSE) >27), 'mild impairment' (MMSE 24-27) and 'moderate impairment' (MMSE <24).

We compared concentrations of 243 proteins between AD subjects in each cognitive stage and a control group of APOE ε4 non-carriers with normal amyloid β and normal cognition [17], using ANCOVAs adjusted for age and gender. Compared to the control group, APOE ε4 carriers and non-carriers with aggregated amyloid β had similar average age, level of education and gender distributions (Table 1).

Figure 1 shows that proteins associated with aggregated amyloid formed distinct clusters depending on APOE genotype and cognitive stage. In total 129 (53%) proteins and protein fragments were associated with aggregated amyloid, with 27 (21%) proteins showing higher levels and the majority of proteins (102, 79%) showing lower levels in AD compared to controls. The large majority (90%) of proteins associated with aggregated amyloid showed expression differences with controls that depended on cognitive stage. Tau, another major pathological hallmark for AD, was the only protein that showed higher levels in all AD subjects across the cognitive spectrum, with higher concentrations for more severe impairment, regardless of APOE ε4 status. We further observed two patterns of protein expression levels: 1) 83 of the 129 proteins (64%) had altered levels either in ε4 carriers or non-carriers; 2) 46 of the 129 proteins (36%) had altered levels in both APOE ε4 carriers and non-carriers, but in different cognitive stages.

APOE ε4 genotype associations of proteins with aggregated amyloid β

Compared to controls, APOE ε4 carriers with normal cognition showed higher levels of nicastrin [NCSTN], which is part of the gamma secretase complex, and of a group of proteins that were associated with glycolysis (Figure 1, first column). Carriers further showed higher levels of markers known to increase with neuronal injury [18] (neurogranin [NRGN], fatty acid-binding protein, heart [FABP3], visinin-like protein-1 [VILIP1]) and YKL40, and growth factors fibroblast growth factor-4 [FGF4] and hepatocyte growth factor [HGF]. These proteins were also higher in subjects with mild and moderate cognitive impairment. Furthermore, a large group of proteins had lower levels in AD, including immune-system related complement factors (C2, C3, C5, C6, factor-B [CFB], factor-H [CFH]) and factors that interact with the complement system (plasminogen [PLG], prothrombin [F2], serum amyloid P component [APCS], and C-reactive protein [CRP]). Subjects with moderate cognitive impairment showed lower levels of proteins that were mostly associated with cell-adhesion related processes (Figure 1, fifth column), including markers functionally associated with 'transsynaptic signaling'(e.g., cadherin-13 [CDH13], neogenin [NEO1], neural cell adhesion molecule-1 [NCAM1], neuronal cell adhesion molecule [NRCAM]), 'peptide neurotrophin signaling'(chromogranin-A [CHGA], proenkephalin-B [PDYN], secretogranin-2 [SCG2], proSAAS [PCSK1]) and 'GPCR signaling'(glutamate receptor-4 [GRM4], latrophilin-1 [ADGRL1]) [19]. The top pathways enriched in KEGG for proteins associated with aggregated

Table 1. Sample description

APOE ε4	Non-carriers				Carriers			
Amyloid	Normal (Control)	Abnormal	Abnormal	Abnormal	Normal	Abnormal	Abnormal	Abnormal
MMSE	> 27	> 27	27-24	<24	>27	> 27	27-24	<24
N	60	24	34	9	8	40	63	23
(% total sample)	(23%)	(9%)	(13%)	(3%)	(3%)	(15%)	(24%)	(27%)
Age	75.30 (6.44)	76.70 (4.90)	75.37 (8.10)	78.82 (5.55)	72.1 (6.43)	74.97 (6.16)	74.53 (6.88)	73.32 (8.70)
Female N (%)	29 (48%)	10 (42%)	13 (38%)	4 (44%)	4 (50%)	12 (30%)	30 (48%)	8 (35%)
Education years	16.00 (2.76)	16.08 (3.32)	15.62 (3.23)	16.22 (3.23)	15.50 (2.00)	16.02 (3.22)	15.25 (2.83)	15.30 (2.67)
MMSE	29.15 (0.73)	29.21 (0.78)	25.59 (1.05)[c]	21.89 (1.05)[c]	29.12 (0.64)	28.73 (0.78)[b]	25.49 (1.11)[c]	21.91 (1.12)[c]
Amyloid β 1-42 pg/ml	245.53 (26.38)	150.5 (28.76)[c]	142.29 (25.06)[c]	148.78 (19.32)[c]	235.75 (22.13)	132.05 (23.19)[c]	131.94 (28.07)[c]	128.61 (23.52)[c]
T-tau pg/ml	63.41 (22.05)	88.12 (55.61)[a]	110.68 (51.83)[c]	149.44 (75.91)[c]	77.12 (19.77)	106.91 (48.96)[c]	120.98 (54.37)[c]	124.91 (51.75)[c]
P-tau pg/ml	20.56 (7.86)	31.33 (15.95)[a]	40.21 (18.04)[c]	49.33 (20.43)[c]	22 (4.41)	37.18 (14.81)[c]	39.84 (13.70)[c]	44.39 (23.78)[c]
APOE ε4 isoform	6.18 (2.18)	5.98 (3.26)	5.84 (2.68)	5.61 (4.44)	10.07 (5.80)[c]	11.92 (1.24)[c]	11.89 (1.43)[c]	11.63 (1.17)[c]

Values are mean (SD). All comparisons are made against the control group (APOE ε4 non-carriers with normal amyloid and MMSE > 27). [a] is p<.05, [b] is p <.01, [c] is p <.001.
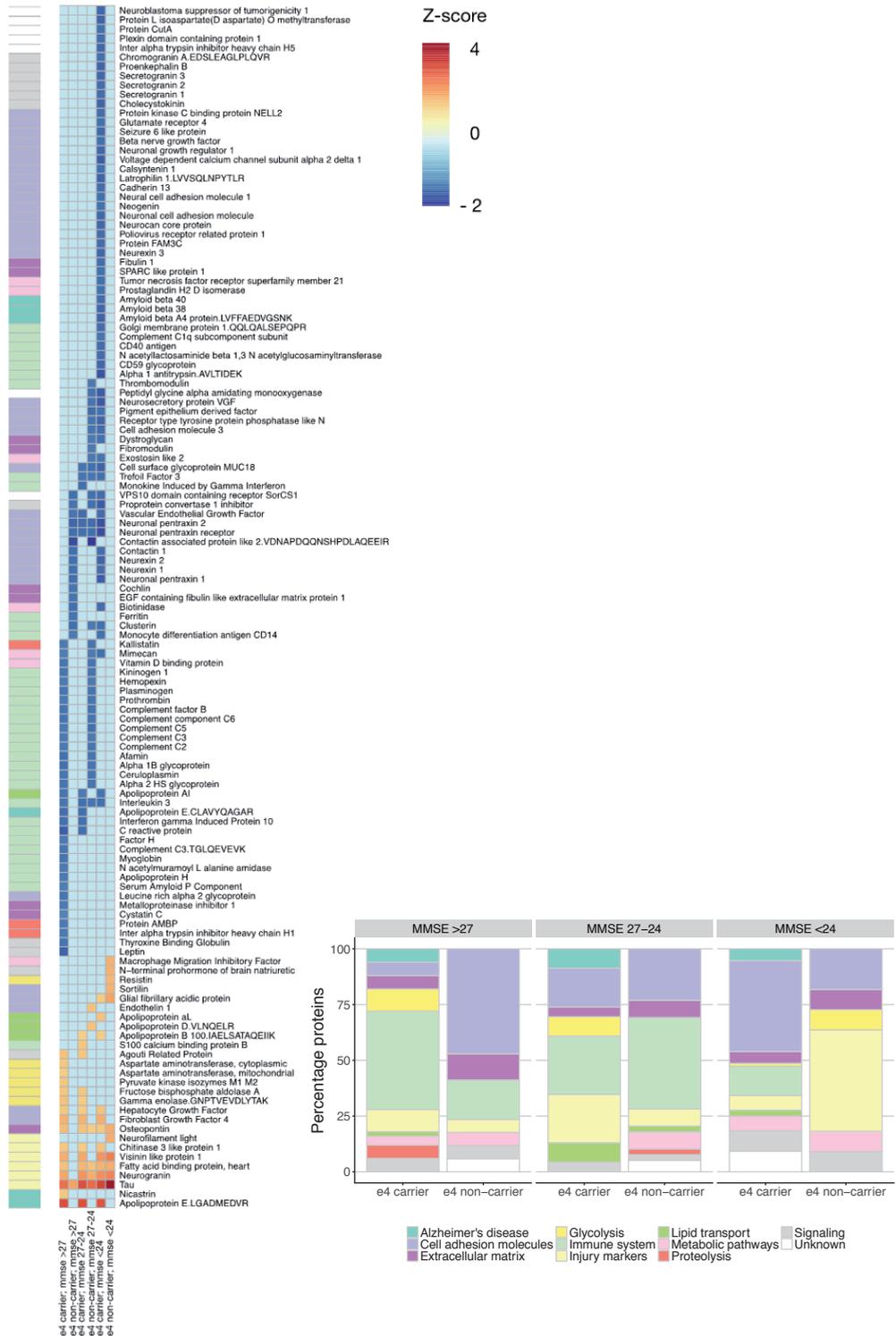
Table 2. Summary of pathways enriched in KEGG of proteins associated with aggregated amyloid according to APOE ε4 genotype

	APOE ε4 carriers			APOE ε4 non-carriers		
Cognitive stage	**Pathway enriched**	**pFDR**	**Proteins**	**Pathway enriched**	**pFDR**	**Proteins**
MMSE > 27	Complement and coagulation cascades	8.20E-12	C2, C3, C5, C6, CFB, CFH, F2, KNG1, PLG	Cell adhesion molecules	0.000165	CADM3, NRXN2, NRXN1, CNTN1, CNTNAP2
MMSE 27-24	No enrichment detected	n.a.	n.a.	Complement and coagulation cascades	8.61E-13	C2, C3, C5, C6, CFB, F2, KNG1, PLG
MMSE < 24	Cell adhesion molecules	8.44E-09	CADM3, CNTN1, CNTNAP2, NCAM1, NEGR1, NEO1, NRCAM, NRXN1, NRXN2, PVRL1	No enrichment detected	n.a.	n.a.

N.a. is not applicable, MMSE is mini-mental state examination, FDR is false discovery rate. Please note that APOE and APP were excluded from enrichment analyses.

amyloid were 'Complement and coagulation cascades' for subjects with normal cognition, no enrichment was observed in mild impairment, and for moderate cognitive impairment 'Cell adhesion molecules' (Table 2).

APOE ε4 non-carrier associations of proteins with aggregated amyloid β

APOE ε4 non-carriers with aggregated amyloid showed a different proteomic profile than APOE ε4 carriers, in type of proteins expressed and/or the cognitive stage of expression. Non-carriers with normal cognition showed lower levels of a large group of proteins associated with cell-adhesion processes compared to the control group. A subset of these proteins included synaptic markers contactin-1 [CNTN1], neurexin-1 [NRXN1] and neurexin-2 [NRXN2] that were associated with 'transsynaptic signaling' [19], and the neuronal pentraxin receptor [NPTXR]. In this stage only tau showed higher levels.

APOE ε4 non-carriers with mild impairment showed lower levels of complement related proteins, which overlapped with the complement proteins that showed lower levels in

Figure 1. Heatmap of proteins associated with amyloid pathology
Columns indicate APOE ε4 carriers and non-carriers with AD according to the severity of their cognitive impairment (MMSE >27, 27-24, or <24). Color scale indicates the Z value of proteins showing a significant difference (p<.05) with the control group.
Proteins are expressed as Z-scores using the control group as reference, and plotted when showing a significant difference (p<.05). Light blue indicates non-significance (p >.05). Right the percentage of proteins associated with one of the 11 biological process categories (please see Supplementary Table 2 for detailed description of biological processes enriched).

APOE ε4 carriers with normal cognition. Further alterations observed in non-carriers with mild impairment were higher levels of a wide range of neuronal injury markers (NRGN, FAPB3, VILIP1). APOE ε4 non-carriers with moderate cognitive impairment also had higher levels of glial fibrillary acidic protein [GFAP], neurofilament light [NFL], resistin [RETN], and macrophage migration inhibitory factor [MIF].

These proteins did not show a clear association with a shared biological pathway (Figure 1, sixth column), but might be related to inflammatory responses. In addition, sortilin [SORT1] levels were higher in these subjects. SORT1 has several functions and is involved in APP processing [20]. No proteins showed lower levels in this stage, but it should be noted that this group had a small sample size, which may have limited statistical power.

The top pathways enriched in KEGG for proteins associated with aggregated amyloid in APOE ε4 non-carriers were 'Cell adhesion molecules' for subjects with normal cognition and 'Complement and coagulation cascades' for subjects with mild impairment (Table 2).

APOE ε4 effect on amyloid processing in asymptomatic subjects with normal amyloid β

We further explored whether protein differences could be observed in APOE ε4 carriers with normal amyloid β and cognition, as these subjects are at increased genetic risk of developing amyloid pathology [4] and so for these subjects proteomic alterations may indicate very early pathological changes associated with AD. Injury markers were normal in these subjects.

Compared to the control group, nine proteins (BACE1, b-nerve growth factor [NGF], macrophage inflammatory protein-1b [CCL4], osteopontin [SPP1], AXL receptor tyrosine kinase [AXL], calsyntenin-1 [CLSTN1], monokine induced by gamma interferon [CXCL9], carbonic anhydrase-1 [CA1], interferon gamma induced protein-10 [CXCL10]) showed altered levels (Figure 2). CCL4, CXCL10, CXCL9 together showed enrichment for 'Toll-like receptor signaling pathway' (KEGG p_{fdr}= 0.00537).

DISCUSSION

Summary

In this study we show that the presence of the APOE ε4 allele was associated with distinct CSF proteomic profiles in subjects with aggregated CSF amyloid β 1-42, suggesting that specific biological processes depending on APOE genotype are involved in the development of AD. Both APOE ε4 carriers and non-carriers showed alterations of large groups of proteins involved in neuronal injury, complement and inflammatory processes, and cell adhesion processes, but in a different temporal ordering.
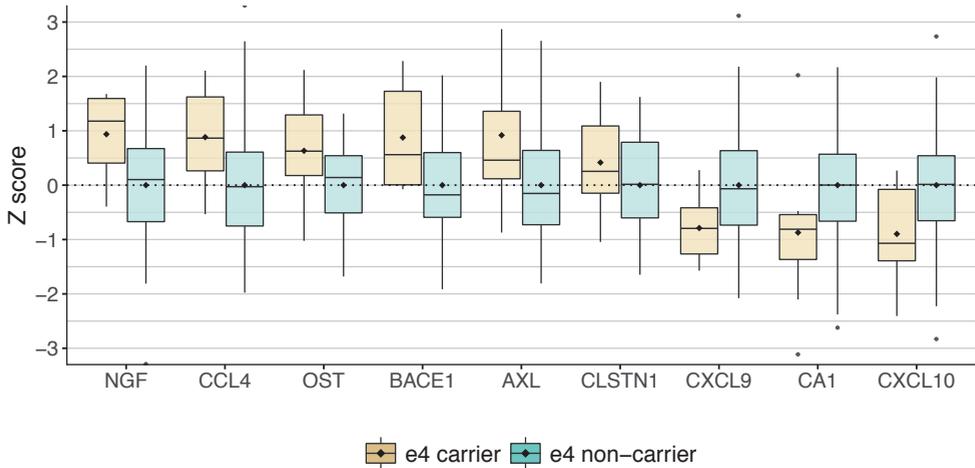
Figure 2. Proteins associated with APOE ε4 carrier status in subjects with normal amyloid
Z-scores are plotted for proteins that were different between subjects with APOE ε4 (in brown) and normal amyloid and normal cognition (MMSE >27) compared to the control group (in blue). All values are standardized according to the control group (i.e., APOE ε4 non-carriers with normal amyloid and MMSE > 27).

APOE ε4 carriers showed altered protein levels of complement related proteins in the normal cognition stage, while lower levels of proteins associated with cell adhesion and synaptic signaling were found in cognitive impairment stages. Non-carriers with aggregated amyloid showed a reversed temporal ordering of these processes with proteins involved in cell adhesion processes showing altered levels in cognitively normal subjects, which was followed by alterations in complement related proteins in cognitive impairment stages. These results suggest that subjects with AD may require specific treatment tailored to their APOE genotype and degree of cognitive impairment.

CSF proteome signatures associated with APOE ε4

APOE ε4 carriers with normal cognition showed lower levels of complement related proteins C2, C3, C5, C6, CFB, CFH, PLG, F2, APCS, and CRP. The complement system is a major part of the innate immune system, and it has been demonstrated that amyloid aggregates can activate the complement system [21, 22]. Previous studies investigating complement related protein concentrations in CSF have, however, reported divergent results with higher concentrations in AD-type dementia patients [23-25], and also lower concentrations in AD-type dementia patients [26] and in subjects with mild cognitive impairment who showed cognitive decline at follow-up [24].

Our results suggest that levels may be altered in different cognitive stages according to APOE genotype, with ε4 carriers showing more extensive complement involvement in the

cognitively normal stage, whereas non-carriers showed alterations in the mild impairment stage. Possibly this observation reflects that the apoE4 protein enhances complement activation in the presence of aggregated amyloid β [27]. Still, at this point we can only speculate as to how reduced levels of complement proteins in CSF can be interpreted. Lower protein concentrations may reflect binding of complement proteins to pathogen surfaces, possibly to tag these for phagocytosis [21], and the presence of complement proteins in amyloid plaques seems to support this explanation [21, 22, 28]. Alternatively, lower levels of complement proteins could point towards decreased production, which seems to be in line with the observation that regulators of complement activation like CFH also showed lower levels in these subjects. Furthermore, complement C1q subcomponent subunit-B [C1QB] and CD59 showed lower levels in mild and moderate cognitive impairment stage. C1QB can directly bind to amyloid β fibrils, which can lead to activation of C1 as well as C3 [22, 29]. Whereas C3 is associated with several pathways of the complement system, C1QB is specific for classical complement activation [21, 22]. The involvement of different complement proteins according to cognitive stage suggests that triggers of the complement system might exist that depend on the level of neuronal injury and/or the degree of amyloid fibril formation. Future research should further study how complement levels change longitudinally during the development of AD, and how these processes depend on APOE genotype.

Alterations of complement protein concentrations were accompanied by a range of inflammatory markers in APOE ε4 carriers, some of these showing altered levels in carriers who had still normal amyloid β levels, suggesting that inflammation processes may play a role in the development in AD before amyloid aggregation becomes manifest in CSF. Some of these markers have been associated with microglia dysfunction or response associated with neurodegeneration (AXL, SPP1, FABP3) [30, 31] and reactive astrocytes (CCL4, S100 calcium binding protein B [S100B], YKL40, GFAP) [32]. In APOE ε4 non-carriers most of these protein levels were similar to controls, except for inflammation markers SPP1, FABP3 and GFAP that were higher in more severe stages of cognitive impairment. Together, these results support the notion that inflammation plays an important role in AD [33], and we further show that the precise inflammation processes involved seem to be distinct according to APOE genotype. It is conceivable that these differences reflect apoE isoform specific interactions with astrocyte and microglia functioning [30, 31, 34, 35].

APOE ε4 carriers with normal amyloid β showed higher levels of BACE1, which is the secretase that initiates amyloidogenic processing of APP [36]. This suggests that increased APP processing might be a pre-amyloid event [37]. Cognitively normal APOE ε4 carriers also showed higher levels of proteins associated with glycolysis. High levels of proteins involved in glycolysis have previously been reported in brain pathology studies in early stage AD [38]. APOE ε4 has been associated dysfunction of mitochondria [39], and so increased levels of glycolysis may indicate compensation for mitochondrial dysfunction [39-42]. In the mild

impairment stage, APOE ε4 carriers showed lower levels of a small group of cell adhesion molecules, and substantially more cell adhesion proteins showed lower levels in the moderate impairment stage, among which proteins associated with synapse development (NPTXR, NRCAM, NEO1, NCAM1, CDH13) [19], and proteins associated with presynaptic dense core vesicles (CHGA, secretogranin-3 [SGC3], voltage-dependent calcium channel subunit alpha-2 delta-1 [CACNA2D1], PDYN, CDH13, SPARC-like protein 1[SPARCL1], alpha-1-antitrypsin [SERPINA1])[43]. These proteins are associated with peptide neurotrophin signaling. Since synapse loss correlates well with cognitive decline [44], and in more severe cognitive impairment stages these proteins showed lower levels, this might indicate impaired synaptic functioning. However, APOE ε4 non-carriers showed normal levels of the majority of these proteins despite the same stage of cognitive impairment and similar levels of neuronal injury markers.

CSF proteome signatures associated with aggregated amyloid β in APOE ε4 non-carriers

Non-carriers with aggregated amyloid and normal cognition showed lower levels of presynaptic proteins (NRX1 and NRX2), proteins involved intracellular trafficking (vacuolar protein sorting 10 [VPS10] domain-containing receptor SorCS1 [SORCS1]) and neuronal pentraxins [45], suggesting alterations in presynaptic cell structure may be an early event in AD for subjects lacking the ε4 allele. In particular SORCS1 stands out in this group, as this gene has been associated with an increased risk for AD [46], and this protein plays a key role in intracellular sorting and trafficking of proteins, including APP, neuronal pentraxins and NRX1 and NRX2 [46-48]. This leads us to propose that the lower levels we observed presently in ε4 non-carriers with still normal cognition might reflect disruption of these cellular transport mechanisms and subsequent failure of intracellular processes such as protein recycling, exocytosis or autophagocytosis.

Levels of the synaptic proteins were low in the mild impairment stage, and in that stage additional proteins associated with cell adhesion processes, like e.g., cell adhesion molecule-3 [CADM3] also showed lower levels. Another finding was that we observed higher NFL levels in non-carriers specifically. Higher levels of CSF NFL indicate axonal injury, and such higher levels have been associated with neurodegenerative processes in several neurological disorders [49].

Strengths and limitations

A potential limitation of this study is that the interpretation of higher and lower levels of proteins measured in CSF in terms of activated biological processes is not always straightforward. Still, interpretations for some proteins, such as amyloid β and tau, have been well established through associations with histopathological measurements in post-mortem research, [50], and/or with PET imaging [51]. Our results may be useful to select

proteins for further detailed studies, as these seem to be involved in AD pathology in vivo. Other diseases such as diabetes mellitus type 2 and cardiovascular disease might interact with APOE ε4 genotype [52, 53], that could potentially affect the integrity of the blood brain barrier, which may have influenced protein levels in CSF. The medical history in our sample suggests that the presence of such comorbidities did not differ between carriers and non-carriers, and so it this alternative explanation for our results is unlikely. Furthermore, we have operationalized disease severity in our sample based on the MMSE, which is a screening tool. An alternative approach would have been categorization based on syndrome diagnosis, but a drawback of that approach is that individuals with normal cognition, MCI and dementia can have the same MMSE. At this point no tools exist to accurately delineate disease severity in a non-demented population, and future research should focus on developing tools that are sensitive to cognitive impairment in predementia stages of AD. Another potential limitation is that we labeled proteins based on the top pathways found, and although this simplifies the interpretation of the results, this approach does not take into account the notion that proteins could be involved in multiple biological processes. In addition, in the present study we defined AD based on abnormal CSF amyloid levels, because (as of yet) the majority (97%) of subjects did not have pathological data available, which can be seen as a limitation of this study. Still, it has been shown previously that amyloid biomarker values correlate with histopathological measures for amyloid plaques [50]. Using biomarkers to define AD can also be regarded to be a strong aspect of our study. This way we avoided potential biases in our results that may arise when defining groups based only on clinical characteristics, as clinical features do not always accurately reflect the underlying pathology. Finally, although our results suggest that several processes associated with aggregated amyloid might be transient, further longitudinal CSF proteomic studies are required to investigate these dynamics in more detail.

CONCLUSION AND IMPLICATIONS

In conclusion, we found CSF proteomic signatures that were associated with aggregated amyloid β and were dependent on APOE ε4 genotype and cognitive stage. An implication of our results is that AD subjects may require treatments tailored to APOE genotype, and that clinical trials may need to consider APOE ε4 dependent endpoints in CSF.

MATERIALS AND METHODS

Subjects

We downloaded ADNI data in August 2017 from the ADNI database (all data is available at adni.loni.usc.edu), including subjects from over 50 sites across the United States and Canada (www.adni-info.org). As such, the investigators within the ADNI contributed to the design and implementation of ADNI and/or provided data but did not participate in analysis or writing of this report. Further details about ADNI are given in the Acknowledgments section. Study protocols were approved by the institutional review boards of all participating ADNI centers (a complete list of ADNI sites is available at http://adni.loni.usc.edu/about/centers-cores/study-sites/ and written informed consent was obtained from all participants or authorized representatives. All analyses were performed on de-identified ADNI data and methods were carried out in accordance with the approved guidelines.

For the present study, we included subjects who had baseline CSF data available for amyloid-β 1–42 and proteomics (see next section). Aggregated amyloid in CSF was defined as having CSF amyloid-ß 1-42 levels below 192 pg/ml [16]. APOE genotype was assessed with two SNPs (rs429358, rs7412) that define the epsilon 2, 3, and 4 alleles, using DNA extracted by Cogenics from a 3 mL aliquot of EDTA blood. Subjects were classified according to amyloid status (normal/abnormal) APOE ε4 genotype (carrier/non-carrier) and cognitive stage as measured with the MMSE (normal cognition: MMSE > 27; mild impairment: MMSE scores between 27-24; moderate impairment: MMSE <24).

CSF protein analysis

CSF samples were collected with lumbar puncture, and samples were stored at the ADNI core laboratory at University of Pennsylvania Medical Center on dry ice until further analysis. In total 313 proteins and protein fragments were measured: 12 with ELISA; 159 with proteomics RBM; 142 with proteomics MRM targeted mass spectroscopy (see Supplementary Table 1 for an overview of all included proteins). Information on protein assessment and quality control is described at http://adni.loni.usc.edu/data-samples/biospecimen-data/. For MRM we used the finalized 'Normalized Intensity' data [9], that was the result of a two-step normalization procedure of the raw peak area data to remove variability between samples processed on different days introduced by the depletion method: First, process related bias was removed by correcting for trends when observed, by computing the predicted average log-intensity values from smoothing spline function to the CSF sample averages. For each sample at a given transition the predicted value was subtracted from the sample average log-intensity. Second, using two regression models to model the daily sample average and the global sample average, the log-intensity values of the CSF samples after step 1 normalized were further normalized to account for the depletion day of the samples. (please see for detailed explanation of the normalization procedure the "Biomarkers Consortium CSF

ProteomicsMRM data set" in the "Data Primer" document at adni.loni.ucla.edu). All CSF protein levels were Z-transformed to the control group (normal amyloid, APOE ε4 non-carrier, MMSE > 27), such that negative values indicate lower and positive values indicate higher levels compared to the normal state. If peptides from the same protein showed a moderate to strong correlation (r > .6), we combined peptides into a composite measure by averaging their Z scores. This resulted in 243 protein measures tested.

Statistical analysis

T-test, χ^2, and Kruskal Wallis tests were used to compare subject characteristics between the AD and controls groups. We compared protein levels between subjects with AD (defined as having aggregated amyloid) and the control group, stratified for APOE ε4 genotype and cognitive stage with ANCOVAs that included age and gender as potential confounders. All statistical analyses were performed using R, version 3.2.3.

Pathway enrichment analyses

We used the online database STRING [54] to identify enriched biological processes (based on KEGG pathways and GO biological processes) for each protein that showed significant differences with the control group. In addition, we used this database to test for pathway enrichment entering all proteins associated with a particular group at the same time.

REFERENCES

1. Jack, C.R.J., et al., *Age-specific population frequencies of cerebral beta-amyloidosis and neuro-degeneration among people with normal cognitive function aged 50-89 years: a cross-sectional study*, in *Lancet neurology*. 2014. p. 997-1005.

2. Bateman, R.J., et al., *Clinical and Biomarker Changes in Dominantly Inherited Alzheimer's Disease*, in *The New England journal of medicine*. 2012.

3. Jansen, W.J., et al., *Prevalence of cerebral amyloid pathology in persons without dementia: a meta-analysis*, in *JAMA : the journal of the American Medical Association*. 2015. p. 1924-1938.

4. Corder, E.H., et al., *Gene dose of apolipoprotein E type 4 allele and the risk of Alzheimer's disease in late onset families*. Science, 1993. **261**(5123): p. 921-3.

5. Rohn, T.T., *Proteolytic cleavage of apolipoprotein E4 as the keystone for the heightened risk associated with Alzheimer's disease*. Int J Mol Sci, 2013. **14**(7): p. 14908-22.

6. Lee, L.C., M.Q.L. Goh, and E.H. Koo, *Transcriptional regulation of APP by apoE: To boldly go where no isoform has gone before: ApoE, APP transcription and AD: Hypothesised mechanisms and existing knowledge gaps*. Bioessays, 2017. **39**(9).

7. Ward, A., et al., *Prevalence of apolipoprotein E4 genotype and homozygotes (APOE e4/4) among patients diagnosed with Alzheimer's disease: a systematic review and meta-analysis*. Neuroepidemiology, 2012. **38**(1): p. 1-17.

8. Jun, G., et al., *A novel Alzheimer disease locus located near the gene encoding tau protein*. Mol Psychiatry, 2016. **21**(1): p. 108-17.

9. Spellman, D.S., et al., *Development and evaluation of a multiplexed mass spectrometry based assay for measuring candidate peptide biomarkers in Alzheimer's Disease Neuroimaging Initiative (ADNI) CSF*, in *Prot. Clin. Appl.* 2015. p. 715-731.

10. Perrin, R.J., et al., *Identification and validation of novel cerebrospinal fluid biomarkers for staging early Alzheimer's disease*. PLoS One, 2011. **6**(1): p. e16032.

11. Llano, D.A., et al., *A multivariate predictive modeling approach reveals a novel CSF peptide signature for both Alzheimer's Disease state classification and for predicting future disease progression*. PLoS One, 2017. **12**(8): p. e0182098.

12. Ossenkoppele, R., et al., *Prevalence of amyloid PET positivity in dementia syndromes: a meta-analysis.*, in *JAMA : the journal of the American Medical Association*. 2015, American Medical Association. p. 1939-1949.

13. Jellinger, K.A. and J. Attems, *Prevalence of dementia disorders in the oldest-old: an autopsy study*. Acta Neuropathol, 2010. **119**(4): p. 421-33.

14. Ewers, M., et al., *Increased CSF-BACE 1 activity is associated with ApoE-epsilon 4 genotype in subjects with mild cognitive impairment and Alzheimer's disease*. Brain, 2008. **131**(Pt 5): p. 1252-8.

15. Gispert, J.D., et al., *The APOE epsilon4 genotype modulates CSF YKL-40 levels and their structural brain correlates in the continuum of Alzheimer's disease but not those of sTREM2*. Alzheimers Dement (Amst), 2017. **6**: p. 50-59.

16. Shaw, L.M., et al., *Cerebrospinal fluid biomarker signature in Alzheimer's disease neuroimaging initiative subjects*, in *Annals of neurology*. 2009. p. 403-413.

17. Vos, S.J., et al., *Preclinical Alzheimer's disease and its outcome: a longitudinal cohort study*, in *Lancet neurology*. 2013. p. 957-965.

18. Fagan, A.M. and R.J. Perrin, *Upcoming candidate cerebrospinal fluid biomarkers of Alzheimer's disease*. Biomark Med, 2012. **6**(4): p. 455-76.

19. Ruano, D., et al., *Functional gene group analysis reveals a role of synaptic heterotrimeric G proteins in cognitive ability*, in *Am J Hum Genet*. 2010. p. 113-125.

20. Gustafsen, C., et al., *Sortilin and SorLA display distinct roles in processing and trafficking of amyloid precursor protein*. J Neurosci, 2013. **33**(1): p. 64-71.

21. Akiyama, H., et al., *Inflammation and Alzheimer's disease*. Neurobiol Aging, 2000. **21**(3): p. 383-421.

22. Veerhuis, R., *Histological and direct evidence for the role of complement in the neuroinflammation of AD.* Curr Alzheimer Res, 2011. **8**(1): p. 34-58.
23. Finehout, E.J., Z. Franck, and K.H. Lee, *Complement protein isoforms in CSF as possible biomarkers for neurodegenerative disease.* Dis Markers, 2005. **21**(2): p. 93-101.
24. Toledo, J.B., et al., *Low levels of cerebrospinal fluid complement 3 and factor H predict faster cognitive decline in mild cognitive impairment.* Alzheimers Res Ther, 2014. **6**(3): p. 36.
25. Bonham, L.W., et al., *The relationship between complement factor C3, APOE epsilon4, amyloid and tau in Alzheimer's disease.* Acta Neuropathol Commun, 2016. **4**(1): p. 65.
26. Smyth, M.D., et al., *Decreased levels of C1q in cerebrospinal fluid of living Alzheimer patients correlate with disease state.* Neurobiol Aging, 1994. **15**(5): p. 609-14.
27. McGeer, P.L., et al., *Apolipoprotein E4 (ApoE4) but not ApoE3 or ApoE2 potentiates beta-amyloid protein activation of complement in vitro.* Brain Res, 1997. **749**(1): p. 135-8.
28. Eikelenboom, P. and F.C. Stam, *Immunoglobulins and complement factors in senile plaques. An immunoperoxidase study.* Acta Neuropathol, 1982. **57**(2-3): p. 239-42.
29. Hong, S., et al., *Complement and microglia mediate early synapse loss in Alzheimer mouse models.* Science, 2016. **352**(6286): p. 712-716.
30. Keren-Shaul, H., et al., *A Unique Microglia Type Associated with Restricting Development of Alzheimer's Disease.* Cell, 2017. **169**(7): p. 1276-1290 e17.
31. Krasemann, S., et al., *The TREM2-APOE Pathway Drives the Transcriptional Phenotype of Dysfunctional Microglia in Neurodegenerative Diseases.* Immunity, 2017. **47**(3): p. 566-581 e9.
32. Orre, M., et al., *Isolation of glia from Alzheimer's mice reveals inflammation and dysfunction.* Neurobiol Aging, 2014. **35**(12): p. 2746-2760.
33. Hoozemans, J.J., et al., *Neuroinflammation and regeneration in the early stages of Alzheimer's disease pathology.* Int J Dev Neurosci, 2006. **24**(2-3): p. 157-65.
34. Cudaback, E., et al., *APOE genotype-dependent modulation of astrocyte chemokine CCL3 production.* Glia, 2015. **63**(1): p. 51-65.
35. Chung, W.S., et al., *Novel allele-dependent role for APOE in controlling the rate of synapse pruning by astrocytes.* Proc Natl Acad Sci U S A, 2016. **113**(36): p. 10186-91.
36. Vassar, R., *BACE1: the beta-secretase enzyme in Alzheimer's disease.* J Mol Neurosci, 2004. **23**(1-2): p. 105-14.
37. Tijms, B.M., et al., *Pre-amyloid stage of Alzheimer's disease in cognitively normal individuals.* Annals of Clinical and Translational Neurology, 2018. **5**(9): p. 1037-1047.
38. Hondius, D.C., et al., *Profiling the human hippocampal proteome at all pathologic stages of Alzheimer's disease.* Alzheimers & Dementia, 2016. **12**(6): p. 654-668.
39. Valla, J., et al., *Reduced posterior cingulate mitochondrial activity in expired young adult carriers of the APOE epsilon4 allele, the major late-onset Alzheimer's susceptibility gene.* J Alzheimers Dis, 2010. **22**(1): p. 307-13.
40. Perkins, M., et al., *Altered Energy Metabolism Pathways in the Posterior Cingulate in Young Adult Apolipoprotein E varepsilon4 Carriers.* J Alzheimers Dis, 2016. **53**(1): p. 95-106.
41. Nakamura, T., et al., *Apolipoprotein E4 (1-272) fragment is associated with mitochondrial proteins and affects mitochondrial function in neuronal cells.* Mol Neurodegener, 2009. **4**: p. 35.
42. Chang, S., et al., *Lipid- and receptor-binding regions of apolipoprotein E4 fragments act in concert to cause mitochondrial dysfunction and neurotoxicity.* Proc Natl Acad Sci U S A, 2005. **102**(51): p. 18694-9.
43. Wegrzyn, J.L., et al., *Proteomics of dense core secretory vesicles reveal distinct protein categories for secretion of neuroeffectors for cell-cell communication.* J Proteome Res, 2010. **9**(10): p. 5002-24.
44. Selkoe, D.J., *Alzheimer's disease is a synaptic failure.* Science, 2002. **298**(5594): p. 789-91.
45. Dean, C. and T. Dresbach, *Neuroligins and neurexins: linking cell adhesion, synapse formation and cognitive function.* Trends Neurosci, 2006. **29**(1): p. 21-9.
46. Hermey, G., *The Vps10p-domain receptor family.* Cell Mol Life Sci, 2009. **66**(16): p. 2677-89.

47. Reitz, C., et al., *SORCS1 alters amyloid precursor protein processing and variants may increase Alzheimer's disease risk.* Ann Neurol, 2011. **69**(1): p. 47-64.

48. Lane, R.F., et al., *Protein sorting motifs in the cytoplasmic tail of SorCS1 control generation of Alzheimer's amyloid-beta peptide.* J Neurosci, 2013. **33**(16): p. 7099-107.

49. Zetterberg, H., et al., *Association of Cerebrospinal Fluid Neurofilament Light Concentration With Alzheimer Disease Progression*, in *JAMA neurology.* 2016. p. 60-8.

50. Tapiola, T., et al., *Cerebrospinal fluid {beta}-amyloid 42 and tau proteins as biomarkers of Alzheimer-type pathologic changes in the brain.* Arch Neurol, 2009. **66**(3): p. 382-9.

51. Zwan, M.D., et al., *Subjective Memory Complaints in APOEε4 Carriers are Associated with High Amyloid-β Burden.*, in *Journal of Alzheimer's disease : JAD.* 2015, IOS Press. p. 1115-1122.

52. Bu, G., *Apolipoprotein E and its receptors in Alzheimer's disease: pathways, pathogenesis and therapy.* Nat Rev Neurosci, 2009. **10**(5): p. 333-44.

53. El-Lebedy, D., H.M. Raslan, and A.M. Mohammed, *Apolipoprotein E gene polymorphism and risk of type 2 diabetes and cardiovascular disease.* Cardiovasc Diabetol, 2016. **15**: p. 12.

54. Szklarczyk, D., et al., *STRING v10: protein-protein interaction networks, integrated over the tree of life.* Nucleic Acids Res, 2015. **43**(Database issue): p. D447-52.

SUPPLEMENTARY DATA

Supplementary Table 1. Average protein levels (Z-scores) for each group stratified for APOE ε4 genotype, amyloid status and MMSE category

Protein	Single protein, composite, Fragment	Non-carrier MMSE category			Carrier MMSE category			Carrier Normal amyloid β
		>27	27-24	<24	>27	27-24	<24	>27
Apolipoprotein E	LGADMEDVR	-0.09 (1.49)	-0.15 (1.23)	-0.26 (2.04) [c]	2.64 (0.57) [c]	2.62 (0.65) [c]	2.5 (0.54) [c]	1.78 (2.66) [c]
Nicastrin	composite	-0.11 (0.99)	-0.14 (1.16)	0.13 (1.29)	0.45 (1.1) [a]	0.12 (1.01)	-0.23 (0.99)	0.16 (1.22)
Tau	single	1.15 (2.58) [b]	2.19 (2.41) [c]	3.99 (3.52) [c]	2.02 (2.27) [c]	2.67 (2.52) [c]	2.85 (2.4) [c]	0.64 (0.92) [a]
Neurogranin	single	0.85 (2.75)	0.98 (1.45) [c]	1.66 (2.02) [c]	1.04 (1.36) [c]	1.38 (1.61) [c]	1.47 (1.9) [c]	0.61 (1.11)
Fatty acid-binding protein, heart	single	0.18 (0.94)	0.61 (0.85) [b]	0.9 (1.21) [a]	0.56 (0.93) [b]	0.75 (0.89) [c]	0.8 (0.74) [c]	0.34 (0.76)
Visinin-like protein 1	single	0.05 (0.93)	0.39 (1.18)	1.8 (1.16) [a]	0.9 (1.32) [b]	1.06 (1.32) [c]	1.4 (2.08) [a]	0.26 (0.9)
Chitinase-3-like protein 1	composite	-0.1 (0.94)	0.28 (0.83)	0.75 (0.76)	0.45 (0.96) [a]	0.34 (1.01) [a]	0.56 (0.86) [c]	0.08 (0.82)
Neurofilament light	single	0.09 (0.55)	0.13 (0.48)	0.95 (1.37) [a]	0.02 (0.35)	0.15 (0.5)	0.26 (0.64)	-0.28 (0.17)
Osteopontin	composite	0.15 (1.3)	0.39 (0.96) [a]	0.92 (1.37) [a]	0.67 (1) [c]	0.53 (1.03) [c]	0.5 (0.97) [a]	0.63 (1.06) [a]
Fibroblast growth factor 4	single	0.24 (0.93)	0.42 (0.96)	0.31 (0.58)	0.83 (0.64) [c]	0.86 (0.86) [c]	0.96 (0.98) [c]	0.74 (0.92)
Hepatocyte growth factor	single	0.47 (1.01)	0.44 (1.09)	0.59 (1.02)	0.46 (1.18) [a]	0.41 (1.2) [a]	0.53 (1.04) [a]	0.37 (1.45)
Gamma-enolase	GNPTVEVDLYTAK	0.42 (0.72)	0.37 (0.98)	0.61 (1.29)	0.57 (0.84) [b]	0.4 (0.89) [a]	0.31 (0.69)	0.64 (1.08)
Fructose-bisphosphate aldolase A	composite	0.05 (1.02)	0.22 (1.04)	0.63 (1.23)	0.51 (0.93) [b]	0.47 (1.07) [b]	0.29 (0.83)	0.46 (0.8)
Pyruvate kinase isozymes M1 M2	LDIDSPPITAR	0.09 (1.05)	0.2 (1.18)	0.4 (1.37)	0.48 (0.97) [a]	0.34 (1.1)	0.13 (0.88)	0.34 (0.83)
Aspartate aminotransferase, cytoplasmic	composite	0.04 (1.04)	0.11 (1.09)	0.19 (1.17)	0.48 (0.96) [a]	0.25 (1.09)	-0.09 (0.84)	0.48 (0.93)
Aspartate aminotransferase, mitochondrial	FVTVQTISGTGALR	-0.03 (1.1)	-0.05 (1.15)	0.17 (1.08)	0.42 (0.96) [a]	0.24 (1.05)	0.07 (0.87)	0.74 (1.07)
Agouti related protein	single	0.1 (1.2)	0.18 (1.06)	0.17 (1.44)	0.52 (1) [b]	0.51 (1.11) [b]	0.08 (1.12)	0.72 (1.29)
S100 calcium binding protein B	single	-0.16 (0.87)	-0.11 (1.17)	0.56 (1.16)	0.26 (0.96)	0.44 (1.14) [a]	0.37 (0.86)	0.4 (0.83)
Apolipoprotein B-100	IAELSATAQEIIK	0.44 (0.39)	0.22 (0.59)	0.03 (0.97)	0.27 (0.58)	0.3 (0.47) [a]	0.42 (0.26) [a]	0.41 (0.38)
Apolipoprotein D	VLNQELR	0.17 (0.75)	0.56 (0.54) [b]	0.41 (0.78)	0.24 (0.79)	0.23 (0.79)	0.09 (1.01)	0.13 (0.8)

Supplementary Table 1. Continuation

Protein	Single protein, composite, Fragment	Non-carrier MMSE category			Carrier MMSE category			Carrier Normal amyloid β
		>27	27-24	<24	>27	27-24	<24	>27
Apolipoprotein aL	single	0.09 (1.2)	-0.2 (1.02)	-0.26 (1.31)	0.19 (1.23)	-0.06 (1.09)	0.58 (1.23) [a]	-0.23 (1.52)
Endothelin1ET1pgmL		0.41 (1.19)	0.52 (1.19) [a]	0.2 (1.24)	0.14 (1.34)	0.22 (1.05)	-0.03 (1.28)	0.38 (1.05)
Glial fibrillary acidic protein	ALAAELNQLR	-0.25 (0.97)	0.23 (1.16)	1.16 (0.87) [b]	0.29 (1.31)	0.31 (1.28)	0.39 (1.14) [a]	-0.13 (0.9)
Sortilin	single	-0.26 (0.97)	0.05 (1.13)	0.86 (1.37) [a]	0.28 (1.05)	0.22 (1.29)	0.29 (1.11)	0.5 (1.12)
Resistin	single	0.31 (1.38)	0.27 (1.12)	0.75 (1.01) [a]	0.05 (1.31)	0.42 (1.56)	0.29 (1.42)	-0.3 (2.2)
N terminal pro hormone of brain natriuretic peptide	single	0.32 (0.96)	0.23 (1.08)	0.82 (1.11) [a]	0.07 (0.94)	0.24 (1.06)	0.24 (1.05)	0.12 (1.06)
Macrophage migration inhibitory factor	single	0.52 (0.99)	0.05 (1.13)	0.85 (0.82) [a]	0.27 (1.07)	0.33 (1)	0.35 (0.85)	-0.33 (0.61)
Leptin	single	-0.03 (0.97)	-0.29 (0.85)	-0.28 (1.04)	-0.76 (0.99) [c]	-0.16 (1.09)	0.19 (0.79)	0.07 (1.18)
Thyroxine binding globulin	single	-0.12 (0.81)	-0.23 (0.93)	-0.03 (1.2)	-0.39 (0.9) [a]	-0.14 (0.98)	0.19 (1.13)	-0.19 (0.76)
Inter-alpha-trypsin inhibitor heavy chain H1	composite	-0.24 (0.89)	-0.28 (0.81)	-0.21 (1.2)	-0.36 (0.79) [a]	-0.22 (0.79)	0 (0.87)	0.11 (1)
Protein AMBP	composite	-0.09 (1.16)	-0.17 (1.03)	0.13 (1.23)	-0.27 (0.85) [a]	-0.19 (0.88)	-0.2 (1.09)	-0.25 (0.8)
Cystatin-C	composite	0.04 (0.37)	-0.07 (0.25)	-0.12 (0.36)	-0.1 (0.23) [a]	0.02 (0.23)	-0.06 (0.3)	-0.1 (0.16)
Metalloproteinase inhibitor 1	composite	-0.09 (0.94)	-0.29 (1.1)	0.27 (1.43)	-0.29 (0.85) [a]	-0.12 (0.89)	-0.16 (1.27)	0.02 (0.59)
Leucine-rich alpha-2-glycoprotein	composite	0.08 (0.87)	-0.2 (0.89)	0.09 (1.09)	-0.37 (1.01) [a]	-0.16 (0.98)	0 (1.24)	-0.43 (1.12)
Serum amyloid P component	single	-0.01 (1.04)	-0.22 (1.07)	-0.31 (0.84)	-0.26 (0.94) [a]	-0.08 (0.9)	-0.01 (0.95)	0.01 (1)
Apolipoprotein H	single	-0.05 (1.13)	-0.25 (1.25)	-0.06 (1.04)	-0.28 (0.87) [a]	-0.2 (0.94)	-0.04 (1.11)	0.02 (0.88)
N-acetylmuramoyl-L-alanine amidase	composite	-0.16 (0.78)	-0.25 (0.83)	-0.08 (1.22)	-0.27 (0.73) [a]	-0.06 (0.68)	-0.16 (0.81)	-0.17 (0.59)
Myoglobin	single	-0.24 (0.8)	-0.33 (0.9)	-0.18 (0.82)	-0.4 (0.68) [b]	-0.24 (1.03)	-0.21 (1.16)	-0.55 (0.59)
Complement C3	TGLQEVEVK	-0.06 (1)	-0.05 (0.92)	0.5 (0.76)	-0.45 (0.89) [a]	-0.03 (0.97)	-0.33 (0.91)	-0.35 (0.82)
Factor H	single	-0.18 (1.09)	-0.13 (1.12)	0.37 (1.78)	-0.34 (0.76) [b]	-0.18 (0.88)	0.11 (1.12)	0 (0.71)
C-reactive protein	composite	-0.02 (0.95)	-0.28 (1.14)	-0.43 (0.78)	-0.85 (1.35) [c]	-0.55 (1.32) [a]	-0.46 (1.72)	-0.16 (0.82)

Protein	Type							
Interferon gamma induced protein 10	single	0.12 (1.3)	-0.2 (1.34)	-0.34 (0.95)	-0.48 (1.05) [b]	-0.48 (1.01) [a]	-0.28 (1.16)	-0.9 (0.91) [a]
Apolipoprotein E	CLAVVQAGAR	-0.41 (1.14)	-0.2 (1.29)	-0.44 (0.25)	-0.56 (0.87) [b]	-0.53 (0.97) [b]	-0.48 (1)	-0.07 (0.32)
Interleukin 3	single	-0.34 (0.86)	-0.4 (1.11) [a]	-0.27 (0.51)	-0.44 (0.88) [a]	-0.51 (1) [b]	-0.53 (0.74) [a]	-0.28 (0.74)
Apolipoprotein AI	single	-0.24 (0.89)	-0.3 (0.92)	-0.21 (1.03)	-0.42 (0.99) [a]	-0.33 (0.83) [a]	-0.45 (0.97) [a]	-0.41 (1.08)
Alpha-2-HS-glycoprotein	composite	-0.19 (0.82)	-0.4 (0.84) [a]	-0.43 (1.02)	-0.38 (0.89) [b]	-0.2 (0.78)	-0.25 (0.79)	-0.15 (1.01)
Ceruloplasmin	composite	-0.18 (0.88)	-0.39 (0.92) [a]	-0.05 (1.22)	-0.43 (0.9) [a]	-0.18 (0.83)	-0.19 (1.09)	-0.15 (0.93)
Alpha-1B-glycoprotein	composite	-0.2 (0.78)	-0.43 (0.95) [a]	-0.26 (1.24)	-0.51 (0.93) [b]	-0.19 (0.82)	-0.12 (0.96)	-0.11 (1.09)
Afamin	composite	-0.35 (0.86)	-0.37 (0.88) [a]	-0.29 (1.18)	-0.55 (0.7) [c]	-0.27 (0.83)	-0.2 (0.86)	-0.05 (0.69)
Complement C2	composite	-0.09 (0.8)	-0.45 (1.1) [b]	-0.1 (1.31)	-0.34 (0.89) [a]	-0.26 (0.92)	-0.22 (1)	-0.09 (0.77)
Complement C3	composite	-0.05 (0.99)	-0.32 (1.02) [a]	0.15 (1.27)	-0.33 (0.84) [a]	-0.23 (0.77)	0.01 (0.97)	-0.2 (0.88)
Complement C5	composite	-0.21 (0.96)	-0.54 (1.1) [b]	-0.17 (1.59)	-0.28 (0.98) [a]	-0.19 (0.87)	-0.13 (1.02)	0.05 (0.98)
Complement component C6	composite	-0.23 (1.06)	-0.42 (0.96) [a]	-0.06 (1.58)	-0.38 (0.91) [a]	-0.16 (0.95)	-0.25 (1.19)	-0.04 (1.12)
Complement factor B	composite	-0.2 (0.95)	-0.44 (0.92) [b]	-0.39 (1.19)	-0.41 (0.79) [b]	-0.22 (0.97)	-0.3 (1.17)	-0.09 (1.11)
Prothrombin	composite	-0.28 (1)	-0.41 (1) [a]	-0.05 (1.4)	-0.36 (0.86) [a]	-0.16 (0.9)	-0.28 (1.08)	0.03 (0.76)
Plasminogen	composite	-0.2 (0.85)	-0.39 (0.85) [a]	-0.15 (1.33)	-0.41 (0.83) [b]	-0.16 (0.84)	-0.28 (0.88)	0.11 (0.75)
Hemopexin	composite	-0.11 (0.83)	-0.33 (0.91) [a]	0.03 (1.38)	-0.34 (0.86) [a]	-0.1 (0.79)	-0.06 (0.88)	-0.24 (0.95)
Kininogen-1	composite	-0.23 (0.86)	-0.38 (0.9) [a]	-0.19 (1.17)	-0.44 (0.72) [b]	-0.26 (0.78)	-0.23 (0.86)	-0.05 (0.68)
Vitamin D-binding protein	composite	-0.28 (0.88)	-0.37 (0.9) [a]	-0.26 (1.22)	-0.39 (0.89) [a]	-0.18 (0.77)	-0.22 (0.87)	-0.07 (0.81)
Mimecan	composite	-0.33 (1.05)	-0.29 (1.02) [a]	-0.41 (1.32)	-0.26 (0.82) [a]	-0.28 (0.82)	-0.46 (0.84) [c]	-0.22 (0.56)
Kallistatin	composite	-0.2 (0.88)	-0.42 (0.97) [a]	-0.21 (1.39)	-0.35 (0.86) [a]	-0.15 (0.78)	-0.27 (0.94)	-0.08 (0.75)
Monocyte differentiation antigen CD14	composite	-0.36 (0.95) [a]	-0.3 (1.24)	0.11 (1.15)	-0.06 (1.24)	-0.26 (1.16)	-0.53 (0.98) [a]	-0.09 (0.71)
Clusterin	composite	-0.46 (0.85) [b]	-0.35 (1.13) [a]	0.31 (0.68)	0.02 (0.96)	-0.04 (1.03)	-0.5 (1.15) [a]	0.13 (0.62)
Ferritin	single	-0.43 (0.9) [a]	0.05 (1.22)	0.48 (1.18)	0.4 (1.2)	0.36 (1.34)	0.43 (1.27)	0.61 (1.05)
Biotinidase	composite	-0.53 (1.14) [a]	-0.35 (1.23)	-0.07 (1.12)	-0.19 (1.13)	-0.34 (1)	-0.62 (1.18) [b]	0.13 (0.75)
EGF-containing fibulin-like extracellular matrix protein 1	composite	-0.37 (0.98) [a]	-0.19 (1.04)	0 (1.13)	-0.13 (0.86)	-0.17 (0.84)	-0.34 (0.74)	-0.1 (0.65)
Cochlin	GVISNSGGPVR	-0.38 (0.93) [a]	0.05 (1.03)	0.14 (0.9)	-0.03 (0.79)	-0.15 (0.77)	-0.14 (0.77)	-0.17 (0.67)
Neuronal pentraxin-1	composite	-0.51 (0.96) [a]	-0.48 (1.3)	-0.12 (0.96)	-0.11 (0.97)	-0.38 (1.2)	-0.87 (1.13) [c]	0.25 (1.28)
Neurexin-1	composite	-0.48 (0.85) [a]	-0.29 (1.25)	-0.29 (0.92)	0 (0.91)	-0.24 (1.1)	-0.62 (0.98) [a]	0.24 (0.84)

Supplementary Table 1. Continuation

Protein	Single protein, composite, Fragment	Non-carrier MMSE category			Carrier MMSE category			Carrier Normal amyloid β
		>27	27-24	<24	>27	27-24	<24	>27
Neurexin-2	composite	-0.51 (0.91) [a]	-0.36 (1.27)	-0.2 (0.97)	-0.01 (1.02)	-0.33 (1.16)	-0.76 (0.98) [c]	0.2 (1.1)
Contactin-1	composite	-0.46 (0.79) [a]	-0.26 (1.19)	0 (0.98)	0.03 (0.96)	-0.16 (0.99)	-0.64 (0.94) [b]	0.13 (0.78)
Contactin-associated protein-like 2	VDNAPDQQNSHPD-LAQEEIR	-1.14 (3.49) [a]	-1.49 (5.18) [a]	0.31 (0.94)	0.04 (0.98)	-0.57 (3.33)	-1.14 (3.64)	-0.26 (1.04)
Neuronal pentraxin receptor	composite	-0.48 (0.95) [a]	-0.54 (1.1) [a]	-0.36 (0.97)	-0.16 (0.87)	-0.5 (1.14) [a]	-1.12 (1.16) [c]	0.37 (0.94)
Neuronal pentraxin-2	composite	-0.7 (0.89) [b]	-0.61 (1.18) [b]	-0.19 (1.04)	-0.08 (1.02)	-0.61 (1.32) [b]	-1.06 (1.25) [c]	0.41 (1.02)
Vascular endothelial growth factor	single	-0.44 (1.02) [a]	-0.32 (1.11)	-0.3 (0.95)	-0.18 (0.91)	-0.56 (1.08) [b]	-0.64 (0.94) [c]	0.17 (1.01)
ProSAAS	composite	-0.4 (0.84) [a]	-0.46 (1.33) [a]	-0.26 (1.2)	-0.2 (1.1)	-0.36 (1.14)	-0.87 (0.94) [c]	0.17 (0.84)
VPS10 domain-containing receptor SorCS1	TIAVYEEFR	-0.52 (1.1) [a]	-0.52 (1.42) [a]	0.03 (1.15)	0.02 (1.11)	-0.23 (1.15)	-0.57 (0.97) [a]	0.31 (0.94)
Monokine induced by gamma interferon	single	0.14 (1.04)	-0.3 (1.41)	0.11 (0.74)	0.12 (1.5)	-0.51 (1.36) [a]	-0.15 (1.41)	-0.79 (0.61) [a]
Trefoil factor 3	single	-0.35 (0.82)	-0.39 (1.02) [a]	-0.12 (0.76)	-0.23 (0.82)	-0.42 (0.91) [a]	-0.54 (0.98) [a]	-0.4 (0.67)
Cell surface glycoprotein MUC18	composite	-0.37 (0.99)	-0.49 (1.36) [a]	0 (0.95)	-0.18 (0.97)	-0.4 (1.12) [d]	-0.81 (0.98) [d]	0.03 (0.79)
Exostosin-like 2	VIVWNNIGEK	-0.31 (0.88)	-0.35 (1.03) [a]	-0.03 (1.3)	-0.28 (1.03)	-0.17 (0.88)	-0.42 (1.07) [a]	0.15 (0.8)
Fibromodulin	YLPFVPSR	-0.24 (0.77)	-0.36 (0.93) [a]	-0.2 (0.92)	-0.28 (0.87)	-0.19 (0.7)	-0.2 (0.89)	-0.28 (1.13)
Dystroglycan	composite	-0.3 (0.91)	-0.35 (1.11) [a]	-0.06 (1)	-0.14 (1.04)	-0.24 (0.89)	-0.53 (0.85) [a]	0.25 (0.6)
Cell adhesion molecule 3	composite	-0.27 (0.86)	-0.42 (1.02) [a]	-0.06 (0.9)	-0.14 (0.91)	-0.2 (1)	-0.63 (0.82) [c]	0.26 (0.82)
Receptor-type tyrosine-protein phosphatase-like N	composite	-0.37 (0.96)	-0.44 (1.11) [a]	-0.25 (0.96)	-0.1 (1.07)	-0.34 (1.06)	-0.77 (0.88) [c]	0.38 (0.87)
Pigment epithelium-derived factor	composite	-0.34 (0.84)	-0.57 (1.3) [b]	-0.06 (1.13)	-0.05 (0.84)	-0.25 (0.78)	-0.46 (1.09) [a]	-0.01 (0.37)
Neurosecretory protein VGF	composite	-0.28 (0.93)	-0.43 (1.12) [a]	-0.4 (1.11)	-0.22 (1.04)	-0.4 (1.16)	-0.95 (1.06) [c]	0.44 (0.81)
Peptidyl-glycine alpha-amidating monooxygenase	composite	-0.3 (0.94)	-0.43 (1.17) [a]	-0.09 (1.04)	-0.13 (1.04)	-0.36 (1.17)	-0.86 (1.02) [c]	0.36 (0.95)

Protein	Type	Peptide							
Thrombomodulin	single	AVLTIDEK	0.03 (1.22)	-0.36 (1.24) [a]	-0.29 (1.11)	-0.35 (1.45)	-0.2 (0.86)	-0.23 (1.02)	0.24 (0.84)
Alpha-1-antitrypsin			-0.68 (2.96)	-0.09 (1.83)	-0.15 (0.6)	-0.3 (1.59)	-0.09 (1.97)	-1.11 (3.55) [a]	0.39 (1.14)
CD59 glycoprotein		AGLQVYNK	-0.35 (1.14)	-0.31 (1.13)	-0.16 (0.94)	-0.12 (0.99)	-0.3 (1.12)	-0.7 (1.03) [b]	0.09 (0.91)
N-acetyllactosaminide beta-1,3-N-acetylglucosaminyltransferase	composite		-0.36 (0.93)	-0.24 (1.19)	0.18 (1)	0.03 (0.96)	-0.2 (1.1)	-0.61 (0.98) [a]	0.33 (1.2)
CD40 antigen	single		-0.08 (0.89)	-0.19 (1.03)	-0.24 (0.66)	-0.05 (1.05)	-0.37 (1.03)	-0.64 (0.86) [a]	-0.01 (0.62)
Complement C1q subcomponent subunit B	composite		-0.06 (0.98)	0.04 (1.12)	0.08 (1.03)	-0.04 (0.94)	-0.2 (0.82)	-0.41 (1.16) [a]	-0.22 (0.64)
Golgi membrane protein 1		QQLQALSEPQPR	-0.08 (0.96)	-0.24 (0.88)	0.05 (1.08)	-0.11 (0.94)	-0.02 (1.01)	-0.61 (0.73) [a]	-0.18 (0.5)
Amyloid β A4 protein		LVFFAEDVGSNK	-0.1 (0.81)	-0.32 (1.05)	-0.08 (1.06)	-0.27 (0.91)	-0.32 (1.02)	-0.78 (0.9) [c]	0.32 (0.91)
Amyloid β-38	single		-0.12 (0.92)	-0.35 (0.88)	-0.33 (1.02)	-0.23 (0.84)	-0.28 (0.87)	-0.69 (0.7) [b]	0.26 (0.87)
Amyloid β-40	single		-0.16 (0.99)	-0.29 (0.93)	-0.11 (1.05)	-0.28 (0.79)	-0.33 (0.79)	-0.63 (0.69) [a]	0.41 (0.8)
Prostaglandin-H2 D-isomerase	composite		-0.33 (1.04)	-0.2 (1.07)	0.24 (1.05)	-0.03 (1.11)	-0.25 (1.03)	-0.55 (1.03) [a]	0.32 (0.82)
Tumor necrosis factor receptor superfamily member 21		ASNLIGTYR	-0.07 (1.07)	-0.17 (0.96)	-0.1 (1.07)	0.04 (1.09)	-0.12 (1.11)	-0.55 (1.09) [a]	0.32 (1.1)
SPARC-like protein 1	composite		-0.13 (0.85)	-0.15 (0.94)	0.08 (0.93)	0 (0.87)	-0.01 (0.89)	-0.46 (0.75) [a]	0.55 (0.73)
Fibulin-1	composite		-0.24 (0.81)	-0.19 (0.88)	-0.09 (1.11)	-0.17 (0.91)	-0.19 (0.76)	-0.62 (0.88) [c]	0.07 (0.62)
Neurexin-3	composite		-0.43 (0.99)	-0.34 (1.11)	-0.09 (0.95)	0.05 (0.97)	-0.26 (1.13)	-0.68 (1) [b]	0.43 (1.13)
Protein FAM3C	composite		-0.19 (0.9)	-0.28 (0.88)	-0.15 (0.79)	-0.07 (0.84)	-0.2 (0.95)	-0.61 (0.88) [a]	0.25 (0.97)
Poliovirus receptor-related protein 1		ITQVTWQK	-0.17 (1.1)	-0.15 (1.38)	-0.18 (1.03)	0.05 (1)	-0.06 (0.99)	-0.59 (0.86) [a]	0.17 (0.93)
Neurocan core protein	composite		-0.33 (0.86)	-0.19 (1)	-0.04 (1.05)	0.05 (1.02)	-0.18 (1.09)	-0.69 (1.02) [b]	0.46 (0.84)
Neuronal cell adhesion molecule	composite		-0.22 (0.89)	-0.26 (1.02)	-0.14 (0.95)	0.05 (1.02)	-0.23 (1.03)	-0.7 (0.93) [c]	0.45 (1.02)
Neogenin		DVVASLVSTR	-0.33 (0.97)	-0.19 (1.22)	-0.02 (1.05)	0.05 (1.11)	-0.24 (1.12)	-0.54 (0.99) [a]	0.23 (0.97)
Neural cell adhesion molecule 1	composite		-0.21 (0.88)	-0.17 (1.11)	-0.08 (0.91)	-0.03 (0.93)	-0.13 (0.93)	-0.51 (0.88) [a]	0.19 (0.84)
Cadherin-13	composite		-0.09 (1.04)	-0.17 (1.19)	0.05 (1.11)	0.12 (1.11)	-0.13 (1.13)	-0.57 (1.04) [a]	0.5 (0.89)
Latrophilin-1		LVVSQLNPYTLR	-0.36 (1)	-0.21 (1.21)	-0.17 (1.03)	-0.06 (1.11)	-0.35 (1.14)	-0.76 (1.18) [c]	0.52 (1.14)
Calsyntenin-1	composite		-0.21 (0.92)	-0.14 (1.08)	0.15 (0.93)	0.05 (0.98)	-0.05 (1.07)	-0.54 (0.95) [a]	0.42 (1.01) [a]
Voltage-dependent calcium channel subunit alpha-2 delta-1	composite		-0.33 (0.85)	-0.34 (1.07)	-0.15 (0.93)	-0.01 (1.06)	-0.32 (1.04)	-0.84 (1.07) [c]	0.42 (0.76)
Neuronal growth regulator 1	composite		-0.37 (0.9)	-0.29 (1.17)	0.01 (0.94)	0 (0.96)	-0.3 (1.13)	-0.67 (0.96) [b]	0.33 (1.14)
Beta-nerve growth factor		SAPAAAIAAR	0.22 (1.17)	0.24 (1.21)	0.49 (1.13)	0.01 (1.16)	-0.51 (4.18)	-0.5 (1.36) [a]	0.94 (0.78) [a]

Supplementary Table 1. Continuation

Protein	Single protein, composite, Fragment	Non-carrier MMSE category			Carrier MMSE category			Carrier Normal amyloid β
		>27	27-24	<24	>27	27-24	<24	>27
Seizure 6-like protein	composite	-0.27 (0.88)	-0.26 (1.07)	-0.08 (0.97)	0.04 (1.07)	-0.24 (1.08)	-0.67 (0.91) [b]	0.35 (0.9)
Glutamate receptor 4	composite	-0.35 (0.94)	-0.23 (1.3)	-0.18 (0.78)	0.03 (0.91)	-0.23 (1.09)	-0.47 (0.84) [a]	0.24 (1.13)
Protein kinase C-binding protein NELL2	composite	-0.31 (0.9)	-0.25 (0.98)	0 (1.01)	0.02 (1.01)	-0.25 (1.07)	-0.59 (0.92) [a]	0.47 (0.74)
Cholecystokinin	composite	0.06 (0.92)	-0.14 (1.07)	-0.12 (1.01)	-0.01 (0.99)	-0.15 (1.11)	-0.78 (1.07) [c]	0.48 (0.64)
Secretogranin-1	composite	-0.16 (0.77)	-0.33 (0.89)	-0.32 (0.9)	-0.32 (0.71)	-0.31 (0.99)	-0.6 (0.8) [a]	-0.05 (0.73)
Secretogranin-2	composite	-0.28 (0.94)	-0.29 (1.09)	-0.13 (1.11)	-0.04 (1.05)	-0.15 (1.15)	-0.64 (0.91) [a]	0.39 (0.83)
Secretogranin-3	composite	0.01 (0.92)	-0.16 (0.85)	-0.15 (0.88)	-0.08 (0.77)	-0.13 (0.89)	-0.71 (0.85) [c]	0.37 (0.77)
Proenkephalin-B	composite	-0.35 (0.69)	-0.29 (1.14)	-0.21 (1.36)	-0.07 (0.93)	-0.34 (1.11)	-0.79 (1.07) [c]	0.31 (0.9)
Chromogranin-A	EDSLEAGLPLQVR	-0.15 (0.65)	-0.27 (1.15)	-0.53 (1.84)	-0.06 (1.05)	-0.12 (0.78)	-0.5 (0.65) [a]	0.21 (0.69)
Inter-alpha-trypsin inhibitor heavy chain H5	SYLEITPSR	-0.41 (0.84)	-0.37 (1.31)	0.12 (1.1)	-0.18 (1.24)	-0.27 (1.21)	-0.72 (1.08) [c]	-0.52 (1.16)
Plexin domain-containing protein 1	LYGPSEPHSR	-0.25 (1.13)	-0.15 (1.07)	-0.01 (1.02)	0.05 (1.1)	-0.54 (3.73)	-0.59 (0.99) [a]	0.18 (1.36)
Protein CutA	TQSSLVPALTDFVR	-0.29 (1.08)	-0.28 (1.15)	0.45 (0.86)	0.07 (0.89)	-0.26 (1.17)	-0.52 (0.77) [a]	0.58 (0.91)
Protein-L-isoaspartate(D-aspartate) O-methyltransferase	VQLVVGDGR	-0.28 (1.15)	-0.19 (1.31)	-0.53 (0.97)	0.06 (0.92)	-0.25 (1.06)	-0.79 (1.03) [c]	0.01 (1.3)
Neuroblastoma suppressor of tumorigenicity 1	LALFPDK	-0.31 (0.89)	-0.35 (1.09)	-0.05 (1.15)	-0.33 (1.12)	-0.27 (1.19)	-0.73 (1) [c]	0.4 (0.8)
Beta-secretase 1 (ELISA)	single	0.14 (0.9)	-0.04 (1.02)	0.09 (1.19)	0.34 (1.29)	-0.02 (0.93)	-0.21 (0.86)	0.99 (1.29) [a]
Beta-secretase 1 (MBM)	single	0.2 (0.88)	0.19 (0.96)	0.19 (1.23)	0.28 (0.79)	-0.11 (2.34)	-0.06 (0.68)	0.77 (0.79) [a]
AXL receptor tyrosine kinase	single	-0.2 (0.9)	-0.04 (1.21)	-0.05 (0.7)	0.2 (1.04)	-0.12 (1.11)	-0.41 (0.74)	0.92 (1.51) [a]
Macrophage inflammatory protein 1 beta	single	-0.05 (0.71)	0.08 (1.3)	-0.19 (0.69)	-0.2 (0.88)	-0.1 (0.79)	-0.04 (0.66)	0.88 (0.97) [a]
Heparin binding EGF like growth factor	single	-0.28 (1.18)	0 (1.11)	-0.16 (0.5)	0.22 (0.92)	-0.12 (1.06)	-0.28 (1.1)	0.64 (0.75) [a]

Pancreatic polypeptide	single	0.25 (0.99)	0.18 (1.03)	0.71 (1.09)	-0.18 (0.78)	0.05 (1.23)	0.36 (1.07)	-0.65 (1.19)
Neuroserpin	composite	-0.29 (0.93)	-0.29 (1.09)	0.1 (0.84)	0.04 (0.97)	-0.18 (1.03)	-0.44 (1.06)	0.54 (1.15)
Alpha synuclein	single	0.2 (1.64)	0.09 (0.84)	0.11 (0.37)	0.14 (1.02)	0.16 (0.65)	0.41 (1.25)	0.63 (2.43)
Neural cell adhesion molecule L1	composite	-0.28 (0.83)	-0.26 (1.11)	0.15 (1.04)	0.15 (1.06)	-0.04 (1.11)	-0.35 (0.94)	0.56 (1.02)
Apolipoprotein CIII	single	-0.19 (0.98)	-0.29 (0.97)	-0.04 (1.03)	-0.22 (0.81)	-0.21 (0.73)	-0.24 (0.65)	-0.03 (0.72)
Apolipoprotein D (RBM)	single	-0.19 (1.07)	-0.26 (1.03)	0.13 (0.93)	0.1 (0.96)	0.23 (1.14)	0.35 (1.23)	0.55 (0.97)
Contactin-associated protein-like 2	YSSSDWVTQYR	-0.08 (0.94)	0.08 (0.97)	0.31 (1.42)	0.2 (1.1)	0.07 (1.09)	-0.29 (0.9)	0.7 (1.13)
Thioredoxin-dependent peroxide reductase, mitochondrial	HLSVNDLPVGR	-0.53 (2)	-0.28 (1.76)	0.16 (0.41)	0 (1.34)	0.13 (1)	-0.06 (0.38)	-0.96 (2.5)
Alpha-1-antitrypsin	SVLGQLGITK	0.13 (1.31)	0.12 (0.74)	-0.04 (0.59)	-0.15 (0.84)	0.14 (1.16)	0.08 (1.07)	0.75 (1.74)
Immunoglobulin A	single	-0.05 (0.81)	-0.13 (0.92)	0.17 (0.99)	-0.07 (1.11)	-0.22 (0.88)	0.13 (1.09)	0.22 (0.84)
Calsyntenin-3	composite	-0.06 (0.82)	0.01 (0.77)	0.13 (0.76)	0.01 (0.71)	-0.05 (0.87)	-0.45 (0.72)	0.53 (1.06)
Laminin subunit beta-2	AQGIAQGAIR	-0.32 (0.99)	-0.33 (1.36)	-0.02 (1.3)	0.1 (1.05)	-0.15 (1.01)	-0.47 (1.02)	0.06 (0.66)
Cathepsin L1	VFQEPLFYEAPR	-0.35 (1.07)	-0.45 (1.32)	0.28 (0.95)	-0.11 (1.39)	-0.26 (1.32)	-0.55 (1.43)	0.31 (1.63)
Chromogranin-A (RBM)	single	-0.02 (0.83)	-0.11 (0.76)	-0.05 (0.75)	0 (0.89)	-0.11 (0.97)	-0.47 (0.92)	0.48 (0.8)
Interleukin 6 receptor	single	-0.43 (1.03)	-0.23 (1.17)	-0.2 (0.7)	0.1 (1.09)	-0.18 (1.12)	-0.48 (1)	-0.3 (0.93)
Superoxide dismutase [Cu-Zn]	HVGDLGNVTADK	0.05 (0.91)	0.1 (0.92)	-0.52 (0.92)	-0.23 (0.99)	0.13 (0.98)	-0.43 (0.83)	0.14 (0.89)
Interleukin-18-binding protein	LWEGSTSR	-0.2 (0.86)	-0.14 (1.1)	0.34 (0.94)	0.03 (1.14)	-0.09 (1)	-0.4 (0.98)	0.25 (0.7)
Beta-2-microglobulin	composite	-0.14 (0.77)	-0.04 (1.28)	0.18 (0.98)	-0.24 (1.18)	-0.19 (1.14)	-0.41 (1.12)	0.03 (0.71)
Alpha-1-antitrypsin	LSITGTYDLK	0.29 (0.5)	0.27 (0.34)	-0.44 (1.76)	0.06 (0.89)	0.08 (1.02)	0.31 (0.35)	0.35 (0.56)
Kallikrein-10	ALQLPYR	-0.26 (0.91)	0.01 (0.83)	0.6 (0.71)	-0.05 (0.74)	0 (1)	-0.34 (0.8)	-0.19 (0.9)
Extracellular superoxide dismutase [Cu-Zn]	composite	-0.01 (0.66)	0.11 (0.92)	-0.12 (0.79)	0.17 (1.05)	0.22 (0.93)	-0.25 (0.94)	0.29 (0.83)
Angiotensin converting enzyme	single	-0.26 (1.08)	-0.09 (1.15)	-0.11 (0.65)	0.05 (1.1)	-0.31 (1.15)	-0.4 (0.98)	0.51 (0.97)
Immunoglobulin superfamily member 8	composite	-0.21 (0.91)	-0.08 (0.94)	-0.03 (0.91)	-0.08 (0.92)	-0.21 (0.84)	-0.33 (0.84)	0.37 (0.96)
Spondin-1	VTLSAAPPSYFR	-0.37 (0.96)	-0.15 (1.16)	0.14 (1.23)	0.09 (1.22)	0.02 (1.06)	-0.33 (1.13)	0.14 (1.03)
Vasorin	composite	-0.14 (0.99)	-0.01 (1.21)	0.33 (1.02)	0.14 (1.01)	0.02 (1.03)	-0.33 (1.08)	0.02 (0.82)
Neural cell adhesion molecule 2	composite	-0.17 (0.84)	-0.1 (1.09)	0.29 (0.89)	-0.01 (1.06)	-0.13 (0.91)	-0.32 (0.95)	0.3 (0.84)
Leucine-rich repeat-containing protein 4B	composite	-0.32 (0.94)	-0.09 (1.23)	0.29 (0.9)	0.26 (1.01)	-0.07 (1.22)	-0.38 (1.05)	0.37 (1.48)

Supplementary Table 1. Continuation

Protein	Single protein, composite, Fragment	Non-carrier MMSE category			Carrier MMSE category			Carrier Normal amyloid β
		>27	27-24	<24	>27	27-24	<24	>27
Apolipoprotein E	composite	-0.29 (0.82)	-0.25 (1.13)	-0.07 (0.7)	0.21 (1.07)	-0.03 (1.17)	-0.29 (0.93)	0.09 (0.85)
T lymphocyte secreted protein I309	composite	0.39 (1.15)	-0.04 (0.86)	-0.19 (1.2)	0.19 (0.62)	0.19 (0.92)	0.36 (1.3)	-0.13 (0.67)
Beta-Ala-His dipeptidase	composite	-0.36 (0.77)	-0.15 (1)	0.29 (1.03)	-0.02 (0.94)	-0.31 (0.84)	-0.29 (0.92)	0.33 (0.89)
Peroxiredoxin-2	composite	0.02 (1.17)	0.05 (0.9)	-0.01 (0.54)	0.22 (1.05)	0.16 (0.82)	0.37 (1.14)	0.16 (1.64)
Ectonucleotide pyrophosphatase phosphodiesterase family member 2	composite	0.08 (0.83)	-0.02 (0.9)	0.19 (0.72)	0.15 (0.7)	0.26 (0.73)	-0.31 (1.04)	-0.22 (0.65)
SLIT and NTRK-like protein 1	SLPVDVFAGVSLSK	0.11 (0.39)	-0.12 (1.3)	-0.52 (2.49)	-0.05 (1.21)	-0.1 (1.29)	-0.37 (1.46)	0.25 (0.34)
Monocyte chemotactic protein 2	single	0 (0.86)	-0.05 (1.37)	0.24 (0.89)	-0.09 (0.82)	-0.12 (0.87)	-0.27 (0.8)	-0.03 (1.21)
Papilin	VHQSPDGTLLIYNLR	-0.2 (0.98)	-0.2 (1.45)	0.17 (1.18)	-0.13 (1.13)	0.08 (0.94)	-0.31 (1.28)	0.27 (0.84)
Cancer antigen 199	single	-0.05 (0.73)	0.03 (0.83)	-0.61 (0.69)	-0.15 (0.69)	-0.04 (0.72)	-0.28 (0.75)	0.43 (0.7)
Contactin-2	composite	-0.35 (1.1)	0.09 (1.24)	0.63 (1.18)	0.06 (1)	-0.01 (1)	-0.27 (1.22)	0.04 (1.51)
Amyloid β A4 protein	composite	-0.27 (1.08)	0.04 (1.04)	0.55 (1.33)	0.25 (0.95)	0.05 (0.95)	-0.31 (0.92)	0.48 (1.24)
Interleukin 16	single	0.08 (0.79)	-0.12 (1.27)	-0.42 (1.16)	-0.22 (0.77)	-0.2 (0.83)	-0.27 (0.68)	-0.34 (0.93)
Cortisol	single	-0.13 (1.18)	-0.02 (1.05)	0.08 (1.89)	0.1 (1.12)	0.05 (1.19)	-0.31 (0.91)	-0.39 (1.13)
Amyloid-like protein 2	composite	-0.15 (1.05)	-0.03 (1.12)	0.33 (0.92)	0.15 (0.85)	-0.01 (1.04)	-0.25 (0.72)	0.31 (0.88)
Insulin-like growth factor-binding protein 2	composite	-0.24 (0.63)	-0.1 (0.89)	0.61 (1.27)	-0.08 (0.87)	-0.13 (0.76)	-0.19 (0.99)	-0.39 (0.57)
Catalase	LFAYPDTHR	0.03 (1.14)	-0.18 (1.91)	-0.38 (0.88)	-0.42 (2.56)	-0.02 (1.07)	0.33 (1.29)	-0.14 (1.51)
Prolactin	single	0.1 (0.68)	-0.03 (0.8)	0.1 (0.93)	-0.04 (1.02)	0.26 (1.2)	0.32 (1.22)	-0.26 (0.87)
Transforming growth factor alpha	single	-0.45 (1.84)	-0.52 (1.62)	-0.31 (1.59)	0.18 (0.78)	-0.3 (1.34)	-0.41 (1.53)	0.55 (0.72)
Di-N-acetylchitobiase	ATYIQNYR	-0.12 (0.91)	-0.06 (1.05)	0.53 (1.11)	-0.06 (0.89)	0.11 (0.9)	-0.24 (1.28)	0.17 (0.7)
Myelin-oligodendrocyte glycoprotein	VVHLYR	-0.18 (1)	0.02 (0.95)	0.42 (1.06)	0.1 (1.03)	-0.07 (1.03)	-0.29 (1.05)	0.39 (0.87)

SexHormoneBindingGlobulinSH-BGnmolL	single	-0.17 (0.73)	-0.19 (0.99)	-0.49 (1.4)	-0.15 (0.88)	-0.2 (0.76)	-0.25 (0.66)	-0.73 (1)
Superoxide dismutase [Cu-Zn]	composite	0 (0.95)	-0.03 (0.85)	0.17 (0.96)	0.21 (0.91)	0.09 (1.02)	-0.28 (0.79)	0.44 (0.92)
Alpha2MacroglobulinA2Macro-mgmL	single	-0.19 (1.1)	-0.14 (1.13)	0.64 (1.67)	-0.18 (0.98)	-0.13 (1.18)	-0.27 (1.06)	0.15 (0.73)
ChemokineCC4HCC4ngmL	single	0.04 (0.72)	-0.11 (0.97)	-0.21 (0.54)	-0.07 (0.59)	-0.17 (0.76)	-0.13 (0.62)	-0.09 (0.57)
Polyubiquitin-B	composite	-0.14 (0.95)	0.04 (0.96)	0.04 (1.3)	0.01 (0.96)	0.08 (0.93)	-0.24 (0.92)	0.17 (0.76)
Kallikrein-6	composite	-0.06 (0.89)	0.08 (0.81)	0.24 (0.76)	0.06 (0.88)	-0.04 (0.82)	-0.23 (0.97)	0.49 (0.87)
Angiopoietin2ANG2ngmL	single	-0.11 (1.04)	0.1 (1.25)	0.28 (0.67)	-0.02 (1.08)	-0.05 (1.11)	-0.15 (0.73)	0.08 (0.95)
Intercellular adhesion Molecule 1	single	-0.36 (0.93)	-0.32 (1.1)	-0.33 (1.03)	-0.21 (0.85)	-0.22 (0.87)	-0.14 (0.95)	-0.48 (1.08)
Brain acid soluble protein 1	ETPAATEAPSSTPK	-0.19 (1.3)	0.05 (0.82)	-0.39 (1.56)	0.16 (0.33)	0.23 (0.38)	0.24 (0.39)	-0.03 (0.24)
Transthyretin	composite	-0.1 (0.69)	0.15 (0.83)	0.6 (0.63)	0.02 (0.59)	0.21 (0.65)	-0.2 (0.75)	-0.26 (0.74)
Complement C4-A	composite	-0.18 (0.96)	-0.3 (1.11)	-0.06 (0.85)	-0.09 (0.89)	-0.17 (0.96)	-0.22 (0.99)	-0.3 (1.08)
MatrixMetalloproteinase2MMP-2ngmL	single	0.34 (1.02)	0.13 (1.35)	-0.61 (1.4)	-0.28 (0.95)	-0.18 (1.21)	-0.26 (1.05)	0.46 (0.7)
MatrixMetalloproteinase3MMP-3ngmL	single	-0.23 (1.28)	-0.03 (1.19)	0.52 (0.94)	-0.04 (1.12)	0.02 (1.05)	0.28 (0.88)	0.59 (0.88)
MonocyteChemotacticProtein-1MCP1pgmL	single	-0.19 (0.87)	0.02 (1.2)	-0.3 (0.92)	0.02 (0.91)	-0.21 (0.98)	0.21 (1.01)	0.05 (0.79)
Contactin-associated protein-like 2	HELQHPIIAR	-0.25 (1.05)	-0.15 (1.2)	0.22 (1.2)	0.31 (1.02)	0.05 (1.19)	-0.24 (1.02)	0.31 (1.26)
LectinLikeOxidizedLDLReceptor-1LOXngmL	single	-0.13 (0.76)	0.08 (0.95)	0.41 (1.09)	0.23 (0.92)	0.09 (1.11)	-0.23 (0.69)	0.36 (0.67)
PregnancyAssociatedPlasmaProteinAPmlUmL	single	-0.22 (1.22)	0.02 (1.67)	0.15 (1.02)	0.32 (0.9)	-0.01 (1.21)	-0.13 (0.99)	0.02 (0.88)
Soluble Amyloid β A4 protein (s-APP β)	single	-0.11 (0.94)	-0.15 (1.06)	0.21 (1.21)	0.05 (0.84)	0.08 (1.26)	-0.19 (0.98)	0.73 (1.13)
Hemoglobin subunit beta	composite	0 (0.98)	0.03 (0.9)	-0.12 (0.72)	0.01 (1.03)	0.08 (0.98)	0.18 (1.2)	-0.45 (1.28)
Peroxiredoxin-1	composite	-0.12 (1.18)	-0.1 (1.04)	0.44 (1.14)	0.25 (1.05)	0.18 (1.01)	0.18 (0.8)	0.52 (1.2)
Complement component C8 beta chain	composite	-0.15 (0.65)	-0.13 (0.53)	-0.04 (0.98)	-0.14 (0.59)	0.03 (0.57)	-0.05 (0.65)	0.02 (0.59)
Latent-transforming growth factor beta-binding protein 2	EQDAPVAGLQPVER	0.43 (1.19)	-0.24 (1.06)	0.41 (1.48)	-0.27 (1.11)	-0.22 (1.02)	-0.23 (0.85)	-0.61 (0.6)

Supplementary Table 1. Continuation

Protein	Single protein, composite, Fragment	Non-carrier MMSE category			Carrier MMSE category			Carrier Normal amyloid β
		>27	27-24	<24	>27	27-24	<24	>27
Glutamate receptor 4	EYPGSETPPK	-0.05 (0.79)	-0.04 (0.75)	-0.02 (1.11)	0.17 (0.81)	-0.03 (0.98)	-0.24 (1.17)	0.01 (0.41)
Kallikrein-11	LPHTLR	-0.12 (1.31)	0 (1.06)	0.03 (1.5)	0.15 (0.9)	0.34 (1.07)	-0.12 (0.96)	-0.23 (0.82)
Apolipoprotein B-100	TGISPLALIK	0.21 (0.41)	0.02 (0.68)	0.29 (0.74)	0.22 (0.44)	0.26 (0.42)	0.2 (0.88)	0.19 (0.37)
Placenta growth factor	single	-0.22 (0.95)	-0.13 (0.79)	-0.01 (0.7)	-0.01 (0.68)	-0.14 (0.76)	-0.07 (0.77)	-0.06 (1.03)
Follicle stimulating hormone	single	-0.16 (0.97)	-0.12 (0.84)	0.28 (1.35)	-0.19 (1.03)	-0.11 (0.94)	-0.02 (0.88)	0.2 (0.94)
Hemoglobin subunit alpha	composite	0.05 (1.1)	0.07 (0.98)	-0.08 (0.75)	-0.04 (1.14)	0.03 (1.03)	0.14 (1.25)	-0.21 (1.34)
Vascular cell adhesion molecule 1	single	-0.24 (0.94)	0.06 (1.46)	0.47 (1.19)	-0.09 (1.14)	-0.11 (1.13)	-0.1 (1.04)	0.13 (0.8)
Fas ligand	single	0.31 (1.36)	0.37 (2.06)	-0.13 (1.15)	-0.02 (1.36)	-0.03 (1.2)	-0.1 (0.9)	-0.21 (1.38)
Gamma-enolase	LGAEVYHTLK	0.3 (0.58)	-0.21 (2.67)	0.5 (0.83)	0.29 (0.88)	0.27 (0.93)	0.14 (0.58)	-1.62 (5.63)
Fibrinogen	single	0 (1.22)	0.1 (1.04)	0.26 (0.98)	0.22 (0.87)	0.19 (1.19)	0.17 (1.04)	0.2 (1.15)
Transforming growth factor beta-1	LLAPSDSPEWLSFD-VTGVVR	0.29 (0.91)	-1.26 (7.44)	0.04 (0.71)	0.05 (0.87)	0.32 (1.16)	-0.03 (0.83)	0.67 (1.48)
Tissue factor	single	-0.1 (0.92)	0 (1.12)	0.17 (0.72)	0.39 (0.95)	-0.05 (1.08)	-0.09 (0.72)	0.43 (0.97)
Melanotransferrin	ADTDGGLIFR	-0.42 (0.84)	-0.14 (0.7)	0.12 (0.44)	-0.27 (1.15)	-0.2 (0.9)	-0.17 (0.9)	-0.25 (1.3)
Apolipoprotein B-100	SVSLPSLDPASAK	0.01 (1.09)	-0.01 (0.9)	0.16 (0.52)	0.1 (0.37)	0.2 (0.34)	0.1 (1.1)	0.31 (0.57)
Plasminogen activator inhibitor 1	single	0.13 (0.89)	-0.01 (1.09)	0.84 (1.33)	-0.01 (1)	0 (0.9)	0.09 (1.16)	0.53 (1.28)
Interleukin 25	single	0.24 (1.08)	0.19 (0.99)	-0.29 (0.78)	-0.12 (0.85)	0.09 (0.92)	-0.09 (0.89)	0.24 (0.88)
Stem cell factor	single	0.08 (0.7)	-0.06 (0.95)	-0.28 (0.97)	-0.2 (0.89)	-0.13 (0.85)	0.1 (0.66)	0.3 (0.85)
Neutrophil gelatinase associated lipocal	single	0.06 (1.27)	-0.02 (1.25)	0.42 (1.28)	-0.03 (1)	-0.1 (0.97)	0 (0.94)	-0.48 (1.34)
Complement C3	VPVAVQGEDT-VQSLTQGDGVAK composite	-0.6 (2)	-0.41 (1.44)	-0.37 (1.83)	-0.42 (1.53)	-0.27 (1.29)	-0.12 (1.15)	-0.02 (0.2)
Peroxiredoxin-6	composite	0.05 (1.04)	-0.01 (0.94)	0.05 (0.7)	0.14 (0.87)	0.1 (0.65)	0.08 (0.75)	0.21 (1.13)
Sialate O-acetylesterase	ELSNTAAYQSVR	-0.16 (0.86)	-0.2 (0.92)	0.23 (0.81)	0.18 (0.85)	0.07 (0.94)	0.02 (0.67)	-0.04 (0.98)

Protein	Type							
Macrophage colony stimulating factor 1	single	-0.11 (0.82)	0.15 (1.14)	-0.19 (0.66)	0.09 (0.99)	-0.21 (1.1)	-0.04 (0.72)	0.25 (1.06)
Isoprostaan	single	0.12 (0.94)	0.11 (0.88)	0.36 (0.97)	-0.15 (0.9)	-0.16 (0.82)	-0.06 (1.13)	0.18 (0.74)
Tumor necrosis factor receptor 2	single	-0.06 (0.78)	0 (0.83)	0.35 (1.05)	0.08 (0.94)	0.08 (0.98)	0.05 (0.87)	0.14 (0.78)
Prostatic acid phosphatase	single	0.05 (0.82)	0.18 (0.88)	0.22 (0.82)	0.09 (0.69)	-0.11 (0.72)	0.1 (0.71)	-0.12 (0.72)
von Willebrand factor	single	0.13 (0.84)	-0.15 (1.1)	0.08 (0.95)	-0.15 (0.85)	-0.18 (0.94)	-0.04 (0.91)	0.54 (1.04)
Alpha-1-antichymotrypsin	composite	-0.19 (1.05)	-0.26 (1.02)	0.24 (1.3)	-0.24 (1.06)	-0.01 (1.05)	0.02 (1.21)	-0.24 (1.06)
T cell specific protein RANTES	single	0.05 (0.97)	-0.24 (0.63)	-0.23 (0.41)	-0.16 (0.82)	-0.02 (0.88)	-0.01 (0.86)	0.32 (1.47)
Secretogranin-1	HLEEPGETQNAFLNER	0.11 (0.21)	0.08 (0.24)	0.06 (0.38)	0.14 (0.22)	0.11 (0.3)	0.06 (0.17)	0.14 (0.28)
Cathepsin D	composite	-0.25 (0.83)	-0.13 (0.7)	0.22 (0.91)	-0.01 (0.8)	-0.12 (1.24)	-0.05 (1.06)	-0.23 (1.26)
Carbonic anhydrase 1	composite	0.08 (0.78)	-0.17 (1.25)	-0.3 (1.22)	-0.05 (1.09)	0.16 (0.68)	0.04 (1.41)	-0.87 (1.48)[a]
TNF related apoptosis inducing ligand	single	0 (0.9)	0.19 (1.24)	-0.01 (0.87)	0.11 (0.82)	-0.06 (1.06)	-0.04 (0.79)	0.17 (1.47)
Golgi membrane protein 1	DQLVIPDGQEE-EQEAAGEGR	-0.02 (0.61)	-0.01 (1.01)	0.32 (0.7)	-0.78 (3.22)	-0.12 (2.05)	-0.1 (0.82)	-0.5 (0.99)
Latrophilin-1	SGETVINTANYH-DTSPYR	0.09 (0.28)	-0.23 (1.29)	0.22 (0.35)	0.03 (0.86)	-0.03 (0.96)	0.05 (0.38)	0.16 (0.26)
Serum glutamic oxaloacetic trans-aminase	single	0.14 (0.66)	-0.06 (0.81)	0.07 (0.79)	0.03 (1.14)	0.05 (0.89)	0.01 (0.84)	0.17 (1.07)
Complement C3	LSINTHPSQKPLSITVR	0.43 (0.18)	0.14 (0.79)	0.17 (0.92)	0.18 (0.71)	0.13 (0.88)	0.05 (0.92)	0.51 (0.2)
Alpha-1-antitrypsin (RBM)	single	-0.16 (1.22)	-0.18 (1.34)	-0.63 (0.75)	-0.21 (0.87)	-0.19 (1.05)	0.03 (1.27)	-0.39 (1.54)
Adiponectin	single	0.01 (1.01)	-0.19 (0.87)	0.63 (1.56)	-0.22 (0.95)	0.01 (0.87)	0.05 (0.76)	-0.38 (1.03)
Interleukin 8	single	-0.05 (1.02)	0.2 (1.89)	0.24 (1.26)	-0.13 (0.88)	-0.27 (0.93)	0.03 (0.89)	-0.21 (0.56)
Calcitonin	single	-0.23 (0.97)	0.1 (1.03)	0.48 (0.72)	0.07 (1.07)	0.06 (1.01)	0.03 (1.05)	-0.26 (0.46)

All values are mean (SD). All comparisons are made against the reference group (APOE ε4 non-carriers with normal amyloid and MMSE > 27) and were adjusted for gender and age. [a] is $p < .05$, [b] is $p < .01$, [c] is $p_{FDR} < .05$.

Supplementary Table 2. Top enriched KEGG pathways and GO biological processes, genetic functional annotation and cell production type for proteins associated with aggregated amyloid

Protein	Figure annotation	Gene functional annotation	Cell production type	Top KEGG/GO pathway	p FDR
Apolipoprotein E _ LGADMEDVR	Alzheimer's disease	Cell metabolism	Astrocyte	05010: Alzheimer's disease	0.00762
Nicastrin	Alzheimer's disease	Peptide neurotrophin signaling	n.r.	05010 Alzheimer's disease	1.55e-08
Tau	Injury markers	Structural plasticity	Neuronal	04012: ErbB signaling pathway	1.31e-12
Neurogranin	Injury markers	Intracellular signal transduction	Neuronal	No direct biological pathway enrichment	NA
Fatty acid–binding protein, heart	Injury markers	n.r.	Neuronal	03320 PPAR signaling pathway	0.00163
Visinin-like protein 1	Injury markers	Intracellular signal transduction	n.r.	No direct biological pathway enrichment	NA
Chitinase 3 like protein 1	Injury markers	n.r.	n.r.	GO:0004553 hydrolase activity, hydrolyzing O-glycosyl compounds	0.000444
Neurofilament light	Injury markers	Structural plasticity	Neuronal	No direct biological pathway enrichment	NA
Osteopontin	Extracellular matrix	n.r.	Microglia Oligodendrocyte	04512: ECM-receptor interaction	5.61e-10
Fibroblast Growth Factor 4	Cell adhesion	n.r.	Astrocyte	04015: Rap1 signaling pathway	1.27e-14
Hepatocyte Growth Factor	Cell adhesion	n.r.	n.r.	04015: Rap1 signaling pathway	6.47e-10
Gamma enolase. GNPTVEVDLYTAK	Glyconeogenesis	Cell metabolism	Neuronal Astrocyte Oligodendrocytes	00010: Glycolysis / Gluconeogenesis	1.5e-26
Fructose bisphosphate aldolase A	Glyconeogenesis	n.r.	Astrocyte Endothelial cell	00010 Glycolysis / Gluconeogenesis	6.73e-23
Pyruvate kinase isozymes M1 M2	Glyconeogenesis	n.r.	n.r.	00010: Glycolysis / Gluconeogenesis	1.35e-19
Aspartate aminotransferase, mitochondrial	Glyconeogenesis	n.r.	Oligodendrocyte	00270: Cysteine and methionine metabolism	2.65e-15
Aspartate aminotransferase, cytoplasmic	Glyconeogenesis	Cell metabolism	Oligodendrocyte	00270: Cysteine and methionine metabolism	2.65e-15
Agouti Related Protein	Signaling	n.r.	n.r.	04080: Neuroactive ligand-receptor interaction	1.84e-06

Protein	Category		Cell type	Pathway / GO term	p-value
S100 calcium binding protein B	Immune system	n.r.	Neuronal Astrocyte Oligodendrocyte	GO:0045087 Innate immune response	2.89e-07
Apolipoprotein B 100. IAELSATAQEIIK	Lipid transport	n.r.	n.r.	GO:0097006 Regulation of plasma lipoprotein particle levels GO:0006869 Lipid transport	6.43e-16; 1.49e-13
Apolipoprotein D.VLNQELR	Lipid transport	n.r.	Neuronal Astrocyte Oligodendrocyte	GO:0006869 Lipid transport	0.0245
Apolipoprotein aL	Lipid transport	n.r.	n.r.	GO:0006869 Lipid transport	9.33e-14
Endothelin 1	Cell adhesion	n.r.	Astrocyte	04668: TNF signaling pathway	2.2e-07
Glial fibrillary acidic protein	Cell adhesion	n.r.	Astrocyte	No direct biological pathway enrichment	NA
Sortilin	Cell adhesion	n.r.	n.r.	04722: Neurotrophin signaling pathway	8.71e-05
Resistin	Glyconeogenesis	n.r.	Astrocyte	04152: AMPK signaling pathway	3.95e-07
N-terminal prohormone of brain natriuretic	Signaling	n.r.	Oligodendrocyte	04022: cGMP-PKG signaling pathway	0.000303
Macrophage Migration Inhibitory Factor	Metabolic pathways	Peptide neurotrophin signaling	n.r.	00360: Phenylalanine metabolism	1.61e-14
Leptin	Signaling	n.r.	n.r.	04920: Adipocytokine signaling pathway	2.74e-13
Thyroxine Binding Globulin	Signaling	n.r.	n.r.	GO:0010817 Regulation of hormone levels	0.0289
Inter alpha trypsin inhibitor heavy chain H1	Proteolysis	n.r.	n.r.	GO:0030162 Regulation of proteolysis	0.00744
Protein AMBP	Proteolysis	n.r.	n.r.	GO:0045861 Negative regulation of proteolysis	1.15e-06
Cystatin C	Extracellular matrix	n.r.	Microglia Neuronal Astrocyte	GO:0030198 Extracellular matrix organization	6.2e-05
Metalloproteinase inhibitor 1	Extracellular matrix	n.r.	n.r.	GO:0030198 Extracellular matrix organization	6.13e-09
Leucine rich alpha 2 glycoprotein	Cell adhesion	n.r.	Astrocyte	GO:0048871 Multicellular organismal homeostasis	2.14e-05
Serum Amyloid P Component	Immune system	n.r.	n.r.	GO:0006953 Acute-phase response	5.14e-05
Apolipoprotein H	Immune system	n.r.	n.r.	GO:0030195 Negative regulation of blood coagulation	3.19e-13

Supplementary Table 2. Continuation

Protein	Figure annotation	Gene functional annotation	Cell production type	Top KEGG/GO pathway	p FDR
N acetylmuramoyl L alanine amidase	Immune system	n.r.	Microglia	No direct biological pathway enrichment	NA
Myoglobin	Immune system	n.r.	-	No direct biological pathway enrichment	NA
Complement C3.TGLQEVEVK	Immune system	n.r.	Microglia Neuronal	04610: Complement and coagulation cascade	4.48e-19
Factor H	Immune system	n.r.	-	04610: Complement and coagulation cascade	5.19e-06
C reactive protein	Immune system	n.r.	Oligodendrocyte	GO:0006953 acute-phase response	1.79e-05
Interferon gamma Induced Protein 10	Immune system	n.r.	n.r.	04062: Chemokine signaling pathway	4.54e-21
Apolipoprotein E.CLAVYQAGAR	Alzheimer's disease	Cell metabolism	Astrocyte	05010: Alzheimer's disease	0.00762
Interleukin 3	Immune system	n.r.	n.r.	04630: Jak-STAT signaling pathway	8.79e-22
Apolipoprotein AI	Lipid transport	n.r.	n.r.	03320: PPAR signaling pathway; GO:0097006 Regulation of plasma lipoprotein particle levels	5.19e-06; 1.29e-19
Alpha 2 HS glycoprotein	Immune system	n.r.	Astrocyte Endothelial cell	04610: Complement and coagulation cascade	0.00163
Ceruloplasmin	Immune system	n.r.	n.r.	GO:0055076 Transition metal ion homeostasis	1.13e-09
Alpha 1B glycoprotein	Immune system	n.r.	n.r.	04610: Complement and coagulation cascade	1.04e-05
Afamin	Immune system	n.r.	n.r.	No direct biological pathway enrichment	NA
Complement C2	Immune system	n.r.	Neuronal	04610: Complement and coagulation cascade	4.48e-19
Complement C3	Immune system	n.r.	Microglia Neuronal	04610: Complement and coagulation cascade	4.48e-19
Complement C5	Immune system	n.r.	n.r.	04610: Complement and coagulation cascade	2.59e-22

Protein	Category		Cell type	Pathway	p-value
Complement component C6	Immune system	n.r.	n.r.	04610: Complement and coagulation cascade	2.59e-22
Complement factor B	Immune system	n.r.	n.r.	04610: Complement and coagulation cascade	4.48e-19
Prothrombin	Immune system	n.r.	n.r.	04610: Complement and coagulation cascade	2.59e-22
Plasminogen	Immune system	n.r.	Astrocyte	04610: Complement and coagulation cascade	4.57e-16
Hemopexin	Immune system	n.r.	n.r.	GO:0006898 Receptor-mediated endocytosis	3.3e-06
Kininogen 1	Immune system	n.r.	n.r.	04610: Complement and coagulation cascade	3.06e-13
Vitamin D binding protein	Metabolic pathways	n.r.	n.r.	GO:0042359 vitamin D metabolic process	2.05e-07
Mimecan	Metabolic pathways	n.r.	n.r.	00533: Glycosaminoglycan biosynthesis - keratan sulfate	1.51e-05
Kallistatin	Proteolysis	n.r.	n.r.	04610: Complement and coagulation cascade	0.000853
Monocyte differentiation antigen CD14	Immune system	n.r.	n.r.	04620: Toll-like receptor signaling pathway	1.24e-14
Clusterin	Immune system	n.r.	Microglia Astrocyte	GO:0002576 Platelet degranulation	7.46e-11
Ferritin	Immune system	n.r.	Microglia Neuronal Astrocyte Oligodendrocyte Endothelial cell	GO:0006892 Post-Golgi vesicle mediated transport	2.43e-05
Biotinidase	Metabolic pathways	n.r.	Astrocyte	GO:0006768 Biotin metabolic process	5.05e-18
EGF containing fibulin like extracellular matrix protein 1	Extracellular matrix	n.r.	Astrocyte	GO:0030198 Extracellular matrix organisation	6.2e-05
Cochlin	Extracellular matrix	n.r.	n.r.	No direct biological pathway enrichment	NA

Supplementary Table 2. Continuation

Protein	Figure annotation	Gene functional annotation	Cell production type	Top KEGG/GO pathway	p FDR
Neuronal pentraxin 1	Cell adhesion	Intracellular signal transduction	n.r.	No direct biological pathway enrichment	NA
Neurexin 1	Cell adhesion	Cell adhesion and transsynaptic signaling	Neuronal Astrocyte	04514: Cell adhesion molecules	1.55e-06
Neurexin 2	Cell adhesion	Cell adhesion and transsynaptic signaling	Neuronal	04514: Cell adhesion molecules	1.55e-06
Contactin 1	Cell adhesion	Cell adhesion and transsynaptic signaling	Neuronal	04514: Cell adhesion molecules	8.54e-05
Contactin associated protein like 2.VDNAPDQQNSHPDLAQEIR	Cell adhesion	Cell adhesion and transsynaptic signaling	Oligodendrocyte	04514: Cell adhesion molecules	0.000171
Neuronal pentraxin receptor	Cell adhesion	Intracellular signal transduction	n.r.	No direct biological pathway enrichment	NA
Neuronal pentraxin 2	Cell adhesion	n.r.	n.r.	GO:0006091 Generation of precursor metabolites and energy	0.00333
Vascular Endothelial Growth Factor	Cell adhesion	n.r.	n.r.	04510 Focal adhesion	6.34e-15
Proprotein convertase 1 inhibitor	Signaling	Peptide neurotrophin signaling	n.r.	GO:0016486 Peptide hormone processing	7.99e-08
VPS10 domain containing receptor SorCS1	NA	n.r.	n.r.	No direct biological pathway enrichment	NA
Monokine Induced by Gamma Interferon	Immune system	n.r.	Oligodendrocyte	04062: Chemokine signaling pathway	4.54e-21
Trefoil Factor 3	Immune system	n.r.	Astrocyte	GO:0002682 regulation of immune system process	0.000875
Cell surface glycoprotein MUC18	Cell adhesion	n.r.	Neuronal	GO:0048646 Anatomical structure formation involved in morphogenesis	0.00135

Protein	Category		Cell type	Pathway	p-value
Exostosin like 2	Metabolic pathways	n.r.	Astrocyte	GO:0030166 Protoglycan biosynthetic process	3.62e-15
Fibromodulin	Extracellular matrix	n.r.	Neuronal	GO:0018146 keratan sulfate biosynthetic process	6.06e-18
Dystroglycan	Extracellular matrix	n.r.	Microglia	04512: ECM-receptor interaction	1.43e-07
Cell adhesion molecule 3	Cell adhesion	n.r.	Neuronal	04514: Cell adhesion molecules	0.000171
Receptor type tyrosine protein phosphatase like N	Cell adhesion	n.r.	Microglia	No direct biological pathway enrichment	NA
Pigment epithelium derived factor	Cell adhesion	n.r.	n.r.	GO:0051130 Positive regulation of cellular component organization	0.0364
Neurosecretory protein VGF	Cell adhesion	n.r.	n.r.	GO:0010647 positive regulation of cell communication	0.000185
Peptidyl glycine alpha amidating monooxygenase	NA	n.r.	Neuronal	No direct biological pathway enrichment	NA
Thrombomodulin	Immune system	n.r.	n.r.	04610: Complement and coagulation cascade	4.57e-16
Alpha 1 antitrypsin. AVLTIDEK	Immune system	n.r.	n.r.	04610: Complement and coagulation cascade	1.04e-05
CD59 glycoprotein	Immune system	n.r.	Neuronal	04610: Complement and coagulation cascade	1.41e-10
N acetyllactosaminide beta 1,3 N acetylglucosaminyl-transferase	Immune system	n.r.	Neuronal Astrocyte	00601: Glycosphingolipid biosynthesis -lacto and neofacto series	9.72e-20
CD40 antigen	Immune system	n.r.	n.r.	04064: NF-kappa B signaling pathway	5.19e-18
Complement C1q subcomponent subunit	Immune system	n.r.	Neuronal	04610: Complement and coagulation cascade	2.59e-16
Golgi membrane protein 1.QQLQALSEPQPR	Immune system	n.r.	Neuronal Astrocyte	No direct biological pathway enrichment	NA
Amyloid β A4 protein. LVFFAEDVGSNK	Alzheimer's disease	n.r.	Oligodendrocyte	05010: Alzheimer's disease	3.11e-08
Amyloid β-38	Alzheimer's disease	n.r.	Oligodendrocyte	05010: Alzheimer's disease	3.11e-08
Amyloid β-40	Alzheimer's disease	n.r.	Oligodendrocyte	05010: Alzheimer's disease	3.11e-08

Supplementary Table 2. Continuation

Protein	Figure annotation	Gene functional annotation	Cell production type	Top KEGG/GO pathway	p FDR
Prostaglandin H2 D isomerase	Metabolic pathways	n.r.	Astrocyte Oligodendrocyte Endothelial cell	00590: Arachidonic acid metabolism	1.83e-26
Tumor necrosis factor receptor superfamily member 21	Metabolic pathways	n.r.	Astrocyte Microglia	GO:0044255 Cellular lipid metabolic process	2.04e-12
SPARC like protein 1	Extracellular matrix	n.r.	Microglia Neuronal Astrocyte Oligodendrocyte	GO:0018149 peptide cross-linking	1.29e-05
Fibulin 1	Extracellular matrix	n.r.	Oligodendrocyte	GO:0030198 Extracellular matrix organisation	7.38e-07
Neurexin 3	Cell adhesion	n.r.	Neuronal	GO:0007158 neuron cell-cell adhesion	7.73e-13
Protein FAM3C	Cell adhesion	n.r.	Neuronal	No direct biological pathway enrichment	NA
Poliovirus receptor related protein 1	Cell adhesion	Cell adhesion and transsynaptic signaling	Astrocyte	04514: Cell adhesion molecules	4.98e-09
Neurocan core protein	Cell adhesion	Cell adhesion and transsynaptic signaling	Astrocyte	04514: Cell adhesion molecules	0.0131
Neuronal cell adhesion molecule	Cell adhesion	Cell adhesion and transsynaptic signaling	n.r.	04514: Cell adhesion molecules	0.0131
Neogenin	Cell adhesion	Cell adhesion and transsynaptic signaling	n.r.	GO:0007411 Axon guidance	0.00381
Neural cell adhesion molecule 1	Cell adhesion	n.r.	Neuronal Astrocyte Oligodendrocyte	GO:0007411 Axon guidance	1.35e-06
Cadherin 13	Cell adhesion	Cell adhesion and transsynaptic signaling	Astrocyte	GO:0034332 Adherens junction organization	1.7e-20
Latrophilin 1.LVVSQLNPYTLR	Cell adhesion	GPCR signaling	n.r.	GO:0051965 Positive regulation of synapse assembly	0.00028

Protein	Category	Function	Cell type	Pathway	p-value
Calsyntenin 1	Cell adhesion	n.r.	Neuronal	No direct biological pathway enrichment	NA
Voltage dependent calcium channel subunit alpha 2 delta 1	Cell adhesion	Excitability	n.r.	GO:0070588 Calcium ion transmembrane transport	8.24e-18
Neuronal growth regulator 1	Cell adhesion	n.r.	Neuronal	No direct biological pathway enrichment	NA
Beta nerve growth factor	Cell adhesion	n.r.	n.r.	04722: Neurotrophin signaling pathway	3.64e-14
Seizure 6 like protein	Cell adhesion	n.r.	-	No direct biological pathway enrichment	NA
Glutamate receptor 4	Cell adhesion	GPCR signaling	Astrocyte	04080: Neuroactive ligand-receptor interaction	1.59e-13
Protein kinase C binding protein NELL2	Cell adhesion	n.r.	n.r.	GO:1902476 Chloride transmembrane transport	0.0109
Cholecystokinin	Signaling	Peptide neurotrophin signaling	Neuronal	GO:0007186 G-protein coupled receptor signaling pathway	1.26e-06
Secretogranin 1	Signaling	n.r.	n.r.	GO:0016486 Peptide hormone processing	7.99e-08
Secretogranin 2	Signaling	Peptide neurotrophin signaling	Neuronal Oligodendrocyte	GO:0016486 Peptide hormone processing	7.99e-08
Secretogranin 3	Signaling	n.r.	n.r.	GO:0016486 Peptide hormone processing	7.99e-08
Proenkephalin B	Signaling	Peptide neurotrophin signaling	n.r.	GO:0007218 Neuropeptide signaling pathway	2.3e-13
Chromogranin A.EDSLEAGLPLQVR	Signaling	Peptide neurotrophin signaling	Microglia	No direct biological pathway enrichment	NA
Inter alpha trypsin inhibitor heavy chain H5	NA	n.r.	n.r.	No direct biological pathway enrichment	NA
Plexin domain containing protein 1	NA	n.r.	n.r.	No direct biological pathway enrichment	NA
Protein CutA	NA	n.r.	n.r.	Neuronal Oligodendrocyte	No direct biological pathway enrichment	NA
Protein L isoaspartate(D aspartate) O methyltransferase	NA	n.r.	Microglia Neuronal Astrocyte Oligodendrocyte	No direct biological pathway enrichment	NA
Neuroblastoma suppressor of tumorigenicity 1	NA	n.r.	n.r.	GO:0007584 response to nutrient	7.55e-05

All values are mean (SD). All comparisons are made against the reference group (APOE ε4 non-carriers with normal amyloid and MMSE > 27) and were adjusted for gender and age. [a] is $p < .05$, [b] is $p < .01$, [c] is $p_{FDR} < .05$.

CHAPTER

6

Association of amyloid pathology with memory performance and cognitive complaints in cognitively normal older adults: a monozygotic twin study

Konijnenberg E, Den Braber A, Ten Kate M, Tomassen J, Mulder SD, Yaqub MM, Teunissen CE, Lammertsma AA, Van Berckel BNM, Scheltens P, Boomsma DI, Visser PJ

ABSTRACT

Amyloid pathology in cognitively normal older adults has been associated with low memory performance and cognitive complaints, but findings are conflicting. Using a monozygotic twin design we further explored this relation. We investigated 199 cognitively normal older adults (96 twin-pairs) and assessed cognitive performance, cognitive complaints and amyloid pathology on positron emission tomography (PET) and in cerebrospinal fluid (CSF). Participants were on average 70.5(SD=7.6) years and 114(57%) were female. Amyloid-PET abnormality on visual read and lower CSF $A\beta_{42/40}$-ratio were associated with lower Rey visuospatial memory performance (respectively β=-0.39(SE=0.17), p=0.02 and β=0.15(SE=0.07), p=0.04). Twin analyses showed that CSF $A\beta_{42/40}$ ratio in one twin of a pair could predict visuospatial memory performance in the co-twin (r=0.20(SE=0.10), p=0.04). Monozygotic twin discordance analyses further showed a probable effect of disease staging on face-name associative memory performance. Our results suggest amyloid aggregation to be associated with lower visuospatial and face-name associated memory performance in cognitively normal older adults, supporting the view that amyloid pathology leads to memory dysfunction in very early stages of the disease.

INTRODUCTION

Alzheimer's disease (AD) is characterized by aggregation of amyloid-beta in the brain, which may start up to 20 years before dementia onset [1, 2]. Identification of cognitively normal individuals at risk for amyloid aggregation is important as this will help to select participants for treatment studies in a stage when neurodegeneration is still limited. Previous studies showed that amyloid pathology in cognitively normal individuals may be associated with low-normal memory performance and cognitive complaints but findings have been conflicting [3-5]. This may be due to variability in memory tests and amyloid measures used. In particular in cognitively normal older adults, cerebrospinal fluid (CSF) amyloid markers may be more sensitive for amyloid pathology than positron emission tomography (PET) amyloid markers [6]. Furthermore, it is not clear whether the relation between amyloid pathology and cognitive performance has a common underlying biology.

Aim of this study is to investigate the relation of amyloid pathology, assessed by dynamic [18F]flutemetamol amyloid PET scan and amyloid-β 1-42/1-40 ratio ($A\beta_{42/40}$) in CSF, with memory performance, assessed with four memory tests, and degree of cognitive complaints in cognitively normal older adults using a monozygotic twin-pair approach. Monozygotic twins provide an unparalleled opportunity to explore the etiology of comorbidity among traits. Monozygotic twins share 100% of their genes. If two traits are influenced by the same genes, it follows that an across-participant association between traits will result in cross-trait association between twins from a pair. If amyloid pathology and memory dysfunction have a shared biology, we then expect that amyloid pathology in one twin will predict memory performance in the co-twin [7, 8]. In case within twin-pair differences in amyloid markers correlate with within twin-pair differences in memory function, this indicates that the relation between amyloid and memory is, at least partly, driven by non-shared environmental factors.

METHODS

Participants

We selected 199 cognitively normal monozygotic twins (96 complete pairs, and 7 twins of which the co-twin was not able to participate or did not have a measure for amyloid available) from the Netherlands Twin Register [9], who we enrolled in the European Information Framework for AD (EMIF-AD)-PreclinAD study [10]. Inclusion criteria were age ≥60 years and older, a delayed recall score >-1.5 SD of demographically adjusted normative data on the Consortium to Establish a Registry for Alzheimer's Disease 10 word list [11], a Telephone Interview for Cognitive Status modified score ≥23 [12], a 15-item Geriatric Depression Scale score of <11 [13], and a Clinical Dementia Rating score of 0 [14]. Exclusion

criteria were any significant neurologic, systemic, or psychiatric disorder that could cause cognitive impairment. Twin zygosity was confirmed by buccal cell DNA analysis. Participants gave written informed consent. The Medical Ethics Review Committee of the VU University Medical Center approved the study. Research was performed according the principles of the Declaration of Helsinki and in accordance with the Medical Research Involving Human Participants Act and codes on 'good use' of clinical data and biological samples as developed by the Dutch Federation of Medical Scientific Societies.

Assessment of memory performance and cognitive complaints

Cognitive complaints were assessed using the Cognitive Complaints Index (CCI), consisting of 20 questions on memory performance compared to five years ago [15]. We used this self-reported score since in cognitively normal adults self-reported complaints are supposed to best reflect actual disease [16]. We selected four memory tests that differed in type of material presented (verbal versus visual) and learning paradigm (unrelated items versus association between items), which were previously associated with amyloid pathology: the Rey complex figure three minute recall (visuospatial memory) [17, 18], total score from the FNAME-names delayed recall (face-name associative memory) [19, 20], CANTAB Paired Associate Learning total errors adjusted (visual associative memory) [21, 22], and the Rey auditory verbal learning task delayed recall (verbal memory) [23, 24]. Face-name associative memory data was missing in 22 out of 199 participants mainly because of refusal or lack of time as this test was performed at the end of the neuropsychological test battery. Participants with missing face-name scores were older, more often had a positive amyloid PET scan (32% vs 14%, p=0.01) and showed worse performance on Mini-Mental State Examination (MMSE), Rey visuospatial memory and paired associative learning compared to participants who completed the test.

Amyloid markers

Cerebrospinal fluid collection

Up to 20 mL CSF was obtained by lumbar puncture in 126 (62%) participants, between 10am and 2pm, after at least two hours of fasting. CSF was collected in Sarstedt polypropylene syringes using a Spinocan 25 Gauge needle in intervertebral spaces between L3 and S1. Samples were centrifuged at 1300-2000g at 4°C for 10 minutes and supernatants were stored in aliquots of 0.5 mL at -80°C until analysis. A maximum of 2 hours was allowed between lumbar puncture and freezing [25]. Levels of amyloid-β 1-42 and 1-40 were analyzed using kits from the same batch according to manufacturer instructions (ADx Neurosciences/ Euroimmun) [26].

Positron emission tomography scanning

Dynamic [^{18}F]flutemetamol amyloid PET scans were performed on a Philips Ingenuity PET-MRI scanner at VU University Medical Center. PET scans were acquired for 30 minutes under standard resting conditions (eyes closed, dimmed ambient light), immediately following a manual injection of 185 MBq (±10%) [^{18}F]flutemetamol [27]. After an interval of 60 minutes, in which the patient was taken from the scanner bed, a second scan of 20 minutes was acquired, starting 90 minutes after injection. Prior to each part of the PET scan a dedicated MR sequence was obtained for attenuation correction. PET scans were reconstructed using the LOR-RAMLA dedicated Philips reconstruction algorithm for the brain into 18 frames of increasing length (6x5, 3x10, 4x60, 2x150, 2x300, 1x600 s) and into 4 frames of 300s each. Data from two scans were combined into a single image data set after co-registration using Vinci Software 2.56 and in-house built software for decay correction of the second part. Regions of interest were automatically delineated based on the T1-MRI images using the Hammers atlas as implemented in PVElab [28, 29]. Parametric non-displaceable binding potential (BP$_{ND}$) images were generated from the entire image set using the receptor parametric mapping and cerebellar grey matter as reference tissue [30, 31]. Global cortical BP$_{ND}$ was calculated as the average BP$_{ND}$ of 22 regions located within frontal, parietal, temporal, posterior cingulate and medial temporal lobes [24]. Visual read on the dynamic BP$_{ND}$ [^{18}F]flutemetamol images as negative or positive was applied by the consensus of three readers, blinded to the clinical and demographic data.

APOE genotype

Apolipoprotein E (APOE) genotype was assessed based on two SNPs (rs429358, rs7412), genotyped on the Affymetrix Axiom array [32]; for two participants APOE data was missing.

Statistical analysis

Statistical analyses were performed in SPSS version 23 for Windows and RStudio version 3.3.1 (http://www.r-project.org/). Amyloid PET BP$_{ND}$ values were skewed, therefore log-transformation was used to normalize the data. Z-scores were used for all markers, obtained as standardized variables with a mean of 0 and a standard deviation of 1 (using the sample mean and standard deviation). Across-participant associations were assessed using Generalized Estimating Equations (GEE) with PET (dichotomous and continuous) or the CSF Aβ$_{42/40}$ ratio (continuous) as predictors and memory performance or CCI as outcome variables adjusted for clustering of twins within pairs (model 1) and for clustering of twins within pairs, age, gender, and education (model 2)[33]. When observing a significant effect for a covariate we subsequently tested for a interaction.

When a significant (Bonferroni-corrected p = 0.05/(5tasks*2amyloid measures) =0.005) across-participant association was found, we further examined whether amyloid in one twin could predict memory or CCI in its co-twin, by estimating the cross-twin cross-trait

correlations in OpenMx in R (Figure 1b) [34]. We used the monozygotic within twin-pair difference model [7] to test whether our data supports a direct relation between amyloid, memory and CCI. In monozygotic twin-pairs, the variances and covariances of difference scores are a function of unique environmental factors that influence the two traits and the correlation between these environmental factors. A significant relation between difference scores implies a correlation between unique environmental factors, that also is compatible with a direct influence of one trait on the other trait [35]. For this analysis we regressed within twin-pair differences in memory performance or CCI on within twin-pair differences in amyloid load (Figure 1c). We used a monozygotic twin discordance model based on amyloid-aggregation as measured by visual read of the PET scan and tested whether twin-pairs concordant for having an amyloid-negative PET scan (referred to as concordant negative/control group) differ from, discordant twin-pairs where one twin has an amyloid-negative PET scan (discordant negative group) and the co-twin has an amyloid-positive PET scan (discordant positive group) and twin-pairs concordant for having an amyloid-positive PET scan (concordant positive group). This model can function as a disease stage model, where twins discordant for amyloid pathology might be in an earlier amyloid stage compared to twins with both amyloid pathology. We tested whether group status (concordant negative, discordant negative, discordant positive and concordant positive) was associated with memory performance or CCI, adjusted for clustering of twins within pairs, age, gender and education using GEE.

RESULTS

Sample characteristics

We included 199 participants of which 196 had a PET visual read, 188 had dynamic PET BP_{ND} data, and 126 had CSF available. Participants were on average 70.5 years, 57% was female, and 33% carried at least one APOE-ε4 allele. The subgroup of 118 participants with both dynamic PET and CSF data was younger compared to participants with PET only (Table 1).

### Across-participant association between amyloid aggregation and memory performance

Participants with a positive amyloid PET scan on visual read (n=24) had lower scores on the Rey visuospatial memory test (Supplementary Table 1). A lower CSF $A\beta_{42/40}$ ratio was also associated with lower Rey visuospatial memory scores (β=0.15, p=0.04, Figure 2a, Table 2). Age showed a significant negative association with Rey visuospatial memory scores but the interaction of age with the CSF $A\beta_{42/40}$ ratio or amyloid PET visual read on Rey visuospatial memory was not statistically significant (p>0.44). We found no association between the CSF $A\beta_{42/40}$ ratio and other memory test scores nor between amyloid PET BP_{ND}/visual read and

Table 1. Sample characteristics

	Whole sample	Subgroup with CSF and PET data
N	199	118
Complete MZ pairs[a]	96	49
Concordant pairs with positive visual amyloid PET BP_{ND} read	6	5
Concordant pairs with negative visual amyloid PET BP_{ND} read	74	36
Discordant pairs for visual amyloid PET BP_{ND} read	14	8
Twins with missing amyloid data for co-twin	7	20[b]
Age, mean (SD)	70.5 (7.6)	68.9 (6.7)[*]
Years of education, mean (SD)	11.5 (2.6)	11.3 (2.7)
Female, n (%)	114 (57)	64 (54)
APOE ε4 carrier, n (%)[c]	65 (33)	40 (34)
Family history with dementia, n (%)	92 (45)	59 (50)
MMSE, mean (SD)	29.0 (1.0)	28.9 (1.1)
RCF recall 3 minutes, mean (SD)	18.4 (5.4)	18.9 (5.5)
FNAME delayed recall subscore names, mean (SD)	19.8 (10.0)	20.2 (10.3)
PAL total errors adjusted, mean (SD)	28 (16)	28 (16)
RAVLT delayed recall, mean (SD)	8.4 (2.9)	8.3 (2.9)
CCI, median (IQR)	21 (20-24)	21 (20-24)
Positive amyloid PET (visual read BP_{ND} images), n (%)[d]	28 (14)	16 (14)
PET global cortical BP_{ND}, mean (SD)	0.16 (0.12)	0.17 (0.14)
CSF available, n (%)	126 (63)	118 (100)
CSF ratio amyloid-β 1-42/1-40, mean (SD)	-	0.10 (0.03)

[a] In 2 twin-pairs PET was not performed in both twins, [b] twins with co-twin with either missing CSF or PET data [c] 2 participants missing, [d] 3 participants missing, [*] p<0.0001 difference between subgroup with CSF and PET versus subgroup with PET only. MZ: monozygotic; PET: positron emission tomography; BP_{ND}: non-displaceable binding potential; IQR: interquartile range; SD: standard deviation; APOE: apolipoprotein E; MMSE: mini mental state examination; RCF: Rey complex figure; FNAME: face-name associated memory exam; PAL: paired associate learning; RAVLT: Rey auditory verbal learning task; CCI: cognitive change index self-reported; CSF: cerebrospinal fluid

memory performance. None of the amyloid measures or memory tests were associated with the CCI. When analyses were repeated without participants with missing face-name associative memory scores (n=22), findings remained the same.
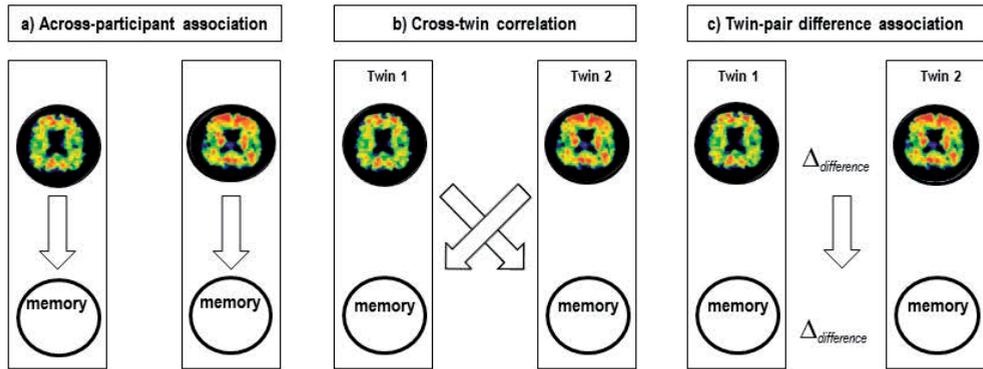
**Figure 1. Twin analyses on relation between amyloid markers and memory**
Illustration of analyses performed. a) association between amyloid measures and memory in total group; b) cross-twin cross-trait analysis: amyloid measure in one twin is correlated with memory score in the co-twin, a significant cross-twin correlation indicates that the relation is in part driven by common genetic and/or environmental factors; c) within twin-pair difference analysis: within twin-pair difference in amyloid measures is associated with within twin-pair difference in memory score, a significant within twin-pair difference association indicates that the relation is partly driven by unique environmental factors.

Table 2. Associations between memory performance, cognitive complaints, and amyloid pathology

Predictor	Dependent	Model 1 B (SE)	p-value	Model 2 B (SE)	p-value
PET global cortical BP_{ND}	FNAME delayed recall subscore names	-0.06 (0.06)	0.29	-0.02 (0.05)	0.69
PET global cortical BP_{ND}	RCF recall 3 minutes	-0.12 (0.08)	0.13	-0.05 (0.07)	0.49
PET global cortical BP_{ND}	PAL total errors adjusted	0.10 (0.07)	0.11	0.04 (0.06)	0.51
PET global cortical BP_{ND}	RAVLT delayed recall	-0.10 (0.07)	0.12	-0.02 (0.06)	0.74
PET global cortical BP_{ND}	CCI	-0.0 (0.08)	0.49	-0.10 (0.07)	0.16
Ratio CSF amyloid-β 1-42/1-40	FNAME delayed recall subscore names	0.11 (0.08)	0.17	0.06 (0.08)	0.51
Ratio CSF amyloid-β 1-42/1-40	RCF recall 3 minutes	0.26 (0.08)	0.001*	0.15 (0.07)	0.04
Ratio CSF amyloid-β 1-42/1-40	PAL total errors adjusted	-0.11 (0.09)	0.24	-0.04 (0.09)	0.65
Ratio CSF amyloid-β 1-42/1-40	RAVLT delayed recall	0.10 (0.09)	0.27	0.06 (0.09)	0.52
Ratio CSF amyloid-β 1-42/1-40	CCI	0.0 (0.10)	0.54	0.12 (0.10)	0.22
FNAME delayed recall subscore names	CCI	-0.09 (0.07)	0.19	0.01 (0.08)	0.93
RCF recall 3 minutes	CCI	-0.11 (0.07)	0.14	-0.05 (0.08)	0.50
PAL total errors adjusted	CCI	-0.01 (0.07)	0.85	-0.06 (0.07)	0.38
RAVLT delayed recall	CCI	-0.15 (0.09)	0.08	-0.10 (0.11)	0.36

PET: positron emission tomography; BP_{ND}: non-displaceable binding potential; FNAME: face-name associative memory exam; RCF: Rey complex figure; PAL: paired associate learning; RAVLT: Rey auditory verbal learning task; CCI: cognitive change index self-reported; CSF: cerebrospinal fluid;
Generalized estimating equations are shown unadjusted (model 1) and covariate unadjusted (age, gender, and education (model 2)). *significant after correction for multiple testing (Bonferroni corrected p<0.05 = 0.05/10 = 0.005). All models included random effect for twin status. Beta is z-scores of standardized residuals. A higher PET BP_{ND} and a lower CSF amyloid β 1-42/1-40 ratio indicate higher amyloid load.
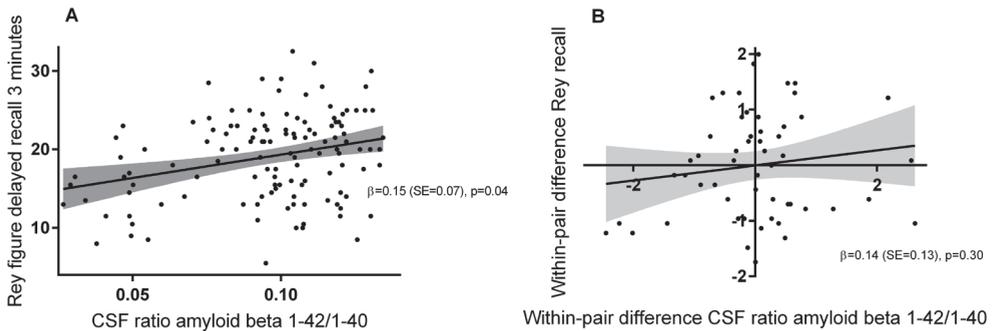
Figure 2. Association between CSF Aβ42/40 ratio and Rey visuospatial memory
a) Across-participant association: Generalized estimating equations are shown adjusted for age, APOE ε4 and gender. Analysis include random effect for twin status. A standardized beta is shown, calculated with z-scores. Each dot represents one participant. Amyloid aggregation is reflected by lower CSF amyloid-β 1-42/1-40 ratio.
b) Within twin-pair difference association: Linear regression result is shown for the relation between the standardized difference scores (z-scores) within a twin-pair for CSF Aβ$_{42/40}$ ratio with the Rey figure recall score. Each dot represents one twin-pair.

Cross-twin pair correlation between amyloid aggregation and memory performance

Since we observed a significant relation between amyloid aggregation with Rey visuospatial memory performance, we further tested the influence of shared genetic/environmental factors. We found that CSF Aβ$_{42/40}$ ratio in one twin could predict Rey visuospatial memory score in the co-twin (r=0.20, p=0.04) but this association was not statistically significant after correction for age (r=0.08, p=0.41). This suggests that the relation between amyloid aggregation and visual memory performance is partly driven by factors that are shared within identical twin-pairs (genes/environment)

Within twin-pair difference association between amyloid aggregation and memory performance

We also tested the influence of non-shared environmental factors on the relation between amyloid aggregation and Rey visuospatial memory performance by twin-pair difference analysis but did not observe a significant association between twin-pair difference in amyloid aggregation and twin-pair difference Rey visuospatial memory performance, suggesting non-shared environmental factors do not contribute to the observed association (Figure 2b).
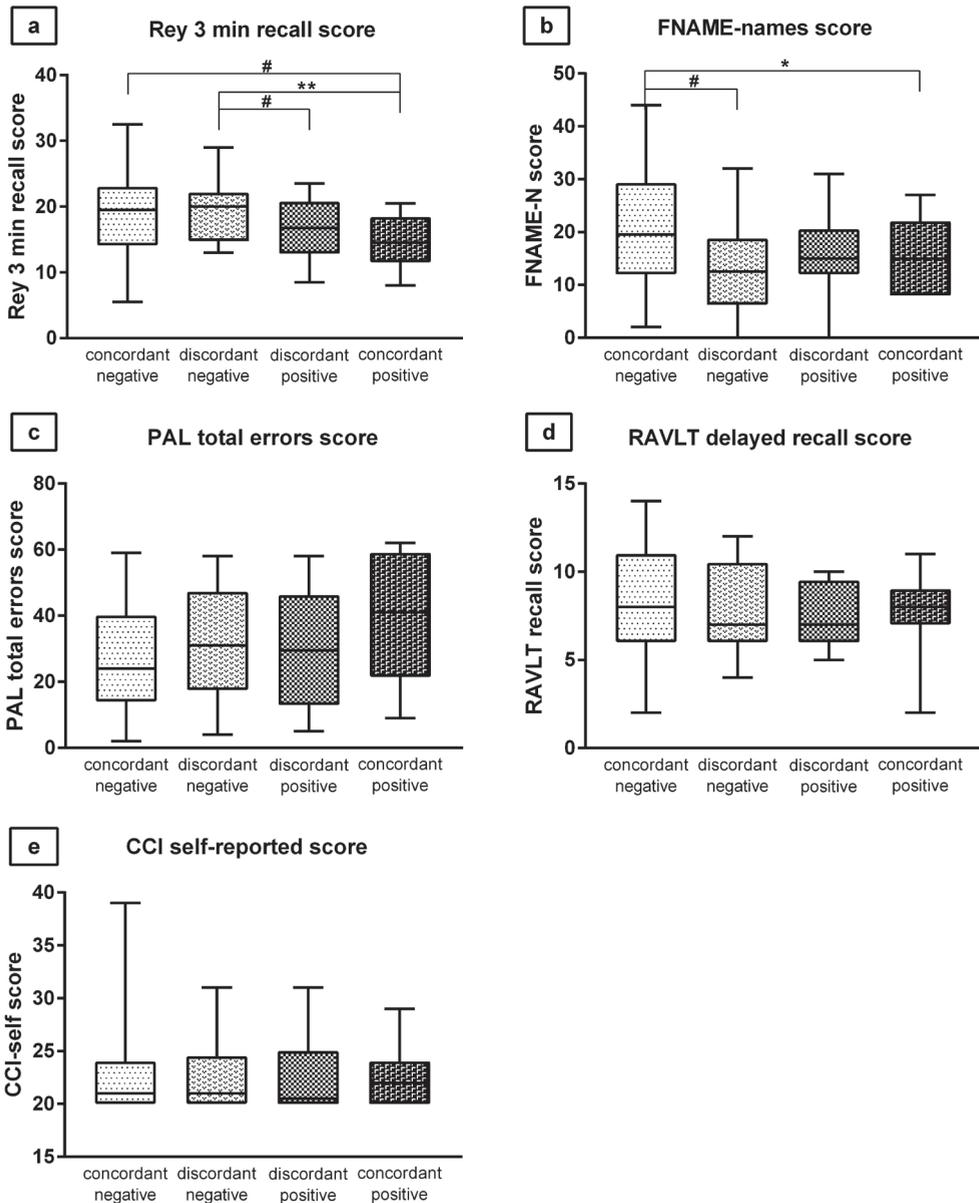
Figure 3. Memory and complaints score according to amyloid PET discordance status.
Boxplots show Rey 3 minute recall scores (A), FNAME-name subscore (B), PAL total errors score (C), RAVLT delayed recall score (D), and CCI self-reported score (E) for twins from pairs that have both a normal amyloid PET scan (concordant normal, N_{pairs}=74), twins from a discordant pair with normal amyloid-PET scan (discordant normal, n=14), twins from a discordant pair with abnormal amyloid-PET scan (discordant abnormal, n=14), and twins from pairs that have both an abnormal PET scan (concordant abnormal N_{pairs}=6).
** $p<0.01$, *$p<0.05$, #$p<0.10$ after correction for age, gender, and education. FNAME: face-name associated memory exam; PAL: paired associate learning; RAVLT: Rey auditory verbal learning task; CCI: cognitive change index self-reported.

Monozygotic twin discordance analysis - disease stage model

Finally, we tested possible effects of disease staging using the twin discordance model. This model can be used as a staging model for amyloid pathology, with concordant negative twin-pairs being the control group, discordant twins with a negative amyloid PET scan in a pre-amyloid stage, followed by discordant co-twins with a positive amyloid PET scan, and twin-pairs concordant for having a positive amyloid PET scan reflecting a more advanced stage of the disease. Fourteen twin-pairs were discordant (one twin had a negative amyloid PET scan and its co-twin had an positive amyloid PET scan), in 74 twin-pairs both twins had negative amyloid PET scans (concordant negative) and in six pairs both twins had positive amyloid PET scans (concordant positive) (Figure 3, Supplementary Table 2). Discordant amyloid negative twins had a higher PET BP_{ND} than concordant amyloid negative twins (Supplementary Table 2). Discordant twins with positive amyloid PET scan tended to show lower Rey visuospatial memory scores compared to their co-twins with a negative amyloid PET scan (p=0.08). Concordant positive twins performed worse on the Rey visuospatial memory task compared to discordant negative twins (p=0.009), and compared to concordant negative twins at trend level (p=0.08). Compared to concordant amyloid negative twins, the face-name associative memory score was lower in concordant positive twins (p=0.02) and tended to be lower in twins with negative amyloid PET scan from a discordant pair (p=0.07). Concordant and discordant twins did not differ from each other on paired associative memory, Rey verbal memory performance and CCI scores.

DISCUSSION

We found amyloid pathology to be associated with lower visual memory performance in cognitively normal older adults. Participants with higher levels of amyloid aggregation, measured with both PET and in CSF, showed worse visuospatial memory performance (Rey complex figure). We found no association between verbal memory performance and amyloid pathology, cognitive complaints and amyloid pathology nor between cognitive complaints and memory performance.

Amyloid aggregation and memory performance

Visuospatial memory

The Rey complex figure (visuospatial memory) task was found to be associated with amyloid pathology both on PET (visual read) and in CSF ($A\beta_{42/40}$ ratio). These results are in line with a previous study showing decline in Rey visuospatial memory performance to be associated with amyloid pathology at follow-up [18]. Our monozygotic twin-pair analysis showed that CSF $A\beta_{42/40}$ ratio in one twin could predict Rey visuospatial memory scores in the genetically

identical co-twin, suggesting this relation to be driven by factors that are shared within these twin-pairs (genes/environment). However, as the association was no longer present after correction for age, it is possible that the association resulted from the fact that both amyloid aggregation and memory dysfunction increase with age in a parallel way [4]. Using amyloid PET status of monozygotic amyloid discordant and concordant twins as a disease staging model for amyloid pathology, we found that Rey visuospatial memory scores in concordant amyloid positive twins were worse relative to concordant and discordant amyloid negative twins, which may suggest that Rey visuospatial memory is impaired in a relatively late stage of amyloid aggregation.

The fact that the relation between Rey visuospatial memory performance and amyloid abnormality on PET imaging was only found for a visual read of the PET scan, but not with the continuous amyloid PET BP_{ND}, may be explained by the low variability in PET BP_{ND} values, as the large majority of the sample showed low BP_{ND} levels.

Visual associative memory

While visual associative memory was not associated with amyloid aggregation in the total group, monozygotic twin amyloid discordance analysis showed a possible effect of disease staging on visual associative memory with a trend for lower face-name associative memory scores in amyloid PET discordant negative twins and lower scores for amyloid PET concordant positive twin-pairs compared to concordant negative twin-pairs. Contrary to Rentz and colleagues, we did not find that amyloid aggregation was associated with face-name associative memory in the total group. This may be explained by differences in amyloid quantification (global binding in our study versus regional binding in the other study). The absence of the association may also be due to selective drop-out as participants who did not complete the face-name associative memory task were older and had lower cognitive scores.

Cognitive complaints and amyloid aggregation

Amyloid measures did not correlate with cognitive complaints. One other study in community dwelling cognitively normal older adults showed that cognitive complaints were associated with higher amyloid load [36] which may be due to differences in definition of cognitive complaints and exclusion criteria used. Cognitive complaints may be more strongly associated with amyloid aggregation in a memory clinic setting [37]. We found no relation between CCI and memory performance, in line with previous studies [38, 39].

Strengths and limitations

A strength of this study is the large sample size of cognitively normal older monozygotic twins with amyloid biomarker data on PET, and in a substantial subsample in CSF as well. Possible limitations are the inclusion and exclusion criteria applied in our study, as these

reduced the range of memory performance and CCI scores, which may have limited the ability to detect associations. Our population was relatively healthy with a low prevalence of positive amyloid PET scans (14%), which may have also limited power to detect differences in the continuous PET analyses in relation to memory performance. The number of concordant amyloid positive twin-pairs was relatively small, which limited statistical power. By design we only included monozygotic twin-pairs and we could therefore not discriminate between the contribution of shared genetics and shared environment to the association between memory and amyloid pathology. However, shared environment is most often not involved, in twin correlations for brain aging markers in older adults [40, 41].

CONCLUSIONS

Visuospatial and face-name associative memory are among the types of memory sensitive for early AD. Our monozygotic twin study provides a useful approach to clarify mechanisms behind early amyloid pathology and memory loss in AD.

Disclosure statement

EK, MK, AB, JT, MY, SM, AL, DB, PS, PJV report no competing interests. CT has functioned in advisory boards of Fujirebio and Roche, received non-financial in the form of research consumables from ADxNeurosciences and Euroimmun, performed contract research or received grants from Janssen prevention center, Boehringer, Brainsonline, AxonNeurosciences, EIP farma, Roche. BB is a trainer for the visual interpretation of [^{18}F]flutemetamol PET scans. He does not receive personal compensation for this.

REFERENCES

1. Villemagne, V.L., et al., *Amyloid beta deposition, neurodegeneration, and cognitive decline in sporadic Alzheimer's disease: a prospective cohort study*, in *Lancet neurology*. 2013. p. 357-367.
2. Jansen, W.J., et al., *Prevalence of cerebral amyloid pathology in persons without dementia: a meta-analysis*, in *JAMA : the journal of the American Medical Association*. 2015. p. 1924-1938.
3. Chetelat, G., et al., *Relationship between atrophy and beta-amyloid deposition in Alzheimer disease.* Ann Neurol, 2010. **67**(3): p. 317-24.
4. Jansen, W.J., et al., *Association of Cerebral Amyloid-beta Aggregation With Cognitive Functioning in Persons Without Dementia.* JAMA Psychiatry, 2018. **75**(1): p. 84-95.
5. Perrotin, A., et al., *Subjective cognition and amyloid deposition imaging: a Pittsburgh Compound B positron emission tomography study in normal elderly individuals.* Arch Neurol, 2012. **69**(2): p. 223-9.
6. Palmqvist, S., et al., *Cerebrospinal fluid analysis detects cerebral amyloid-beta accumulation earlier than positron emission tomography.* Brain, 2016. **139**(Pt 4): p. 1226-36.
7. De Moor, M.H., et al., *Testing causality in the association between regular exercise and symptoms of anxiety and depression.* Arch Gen Psychiatry, 2008. **65**(8): p. 897-905.
8. F, V., B. M, and A. L, *The discordant MZ-twin method: One step closer to the holy grail of causality.* International Journal of Behavioral Development, 2009. **33**(4): p. 376-382.
9. Willemsen, G., et al., *The Adult Netherlands Twin Register: twenty-five years of survey and biological data collection.* Twin Res Hum Genet, 2013. **16**(1): p. 271-81.
10. Konijnenberg, E., et al., *The EMIF-AD PreclinAD study: study design and baseline cohort overview.* Alzheimers Res Ther, 2018. **10**(1): p. 75.
11. Morris, J.C., et al., *The Consortium to Establish a Registry for Alzheimer's Disease (CERAD). Part I. Clinical and neuropsychological assessment of Alzheimer's disease*, in *Neurology*. 1989. p. 1159-1165.
12. de Jager, C.A., M.M. Budge, and R. Clarke, *Utility of TICS-M for the assessment of cognitive function in older adults*, in *International journal of geriatric psychiatry*. 2003. p. 318-324.
13. Yesavage, J.A., et al., *Development and validation of a geriatric depression screening scale: a preliminary report*, in *Journal of psychiatric research*. 1982. p. 37-49.
14. Morris, J.C., *The Clinical Dementia Rating (CDR): current version and scoring rules*, in *Neurology*. 1993. p. 2412-2414.
15. Rattanabannakit, C., et al., *The Cognitive Change Index as a Measure of Self and Informant Perception of Cognitive Decline: Relation to Neuropsychological Tests.* J Alzheimers Dis, 2016. **51**(4): p. 1145-55.
16. Buckley, R., et al., *Self and informant memory concerns align in healthy memory complainers and in early stages of mild cognitive impairment but separate with increasing cognitive impairment.* Age Ageing, 2015. **44**(6): p. 1012-9.
17. Meyers, J.E., J.D. Bayless, and K.R. Meyers, *Rey complex figure: memory error patterns and functional abilities*, in *Applied neuropsychology*. 1996. p. 89-92.
18. Snitz, B.E., et al., *Cognitive trajectories associated with beta-amyloid deposition in the oldest-old without dementia.* Neurology, 2013. **80**(15): p. 1378-84.
19. Papp, K.V., et al., *Development of a Psychometrically Equivalent Short Form of the Face-Name Associative Memory Exam for use Along the Early Alzheimer's Disease Trajectory.* Clinical Neuropsychologist, 2014. **28**(5): p. 771-785.
20. Rentz, D.M., et al., *Face-name associative memory performance is related to amyloid burden in normal elderly*, in *Neuropsychologia*. 2011. p. 2776-2783.
21. Reijs, B.L.R., et al., *Memory Correlates of Alzheimer's Disease Cerebrospinal Fluid Markers: A Longitudinal Cohort Study.* Journal of Alzheimers Disease, 2017. **60**(3): p. 1119-1128.

22. Robbins, T.W., et al., *Cambridge Neuropsychological Test Automated Battery (CANTAB): a factor analytic study of a large sample of normal elderly volunteers*, in *Dementia*. 1994. p. 266-281.
23. Rey, A., *L'examen clinique en psychologie.*, in *Presses Universitaires de France*. 1964.
24. Tolboom, N., et al., *Relationship of cerebrospinal fluid markers to 11C-PiB and 18F-FDDNP binding.* J Nucl Med, 2009. **50**(9): p. 1464-70.
25. del Campo, M., et al., *Recommendations to standardize preanalytical confounding factors in Alzheimer's and Parkinson's disease cerebrospinal fluid biomarkers: an update.* Biomark Med, 2012. **6**(4): p. 419-30.
26. De Vos, A., et al., *C-terminal neurogranin is increased in cerebrospinal fluid but unchanged in plasma in Alzheimer's disease.* Alzheimers Dement, 2015. **11**(12): p. 1461-9.
27. Nelissen, N., et al., *Phase 1 study of the Pittsburgh compound B derivative 18F-flutemetamol in healthy volunteers and patients with probable Alzheimer disease.*, in *Journal of nuclear medicine : official publication, Society of Nuclear Medicine*. 2009, Society of Nuclear Medicine. p. 1251-1259.
28. Hammers, A., et al., *Three-dimensional maximum probability atlas of the human brain, with particular reference to the temporal lobe.* Hum Brain Mapp, 2003. **19**(4): p. 224-47.
29. Svarer, C., et al., *MR-based automatic delineation of volumes of interest in human brain PET images using probability maps*, in *NeuroImage*. 2005. p. 969-979.
30. Gunn, R.N., et al., *Parametric imaging of ligand-receptor binding in PET using a simplified reference region model*, in *NeuroImage*. 1997. p. 279-287.
31. Wu, Y. and R.E. Carson, *Noise reduction in the simplified reference tissue model for neuroreceptor functional imaging*, in *Journal of cerebral blood flow and metabolism : official journal of the International Society of Cerebral Blood Flow and Metabolism*. 2002. p. 1440-1452.
32. Ehli, E.A., et al., *A method to customize population-specific arrays for genome-wide association testing.* Eur J Hum Genet, 2017. **25**(2): p. 267-270.
33. Minica, C.C., et al., *Sandwich corrected standard errors in family-based genome-wide association studies*, in *European journal of human genetics : EJHG*. 2014.
34. Boker, S., et al., *OpenMx: An Open Source Extended Structural Equation Modeling Framework.* Psychometrika, 2011. **76**(2): p. 306-317.
35. Boomsma, D.I., *Twins and the fetal origins hypothesis: An application to growth data, in Hormones and the Brain,.* Springer-Verlag: Berlin Heidelberg, 2005.
36. Perrotin, A., et al., *Subjective cognitive decline in cognitively normal elders from the community or from a memory clinic: Differential affective and imaging correlates.* Alzheimers Dement, 2017. **13**(5): p. 550-560.
37. Molinuevo, J.L., et al., *Implementation of subjective cognitive decline criteria in research studies.* Alzheimers Dement, 2017. **13**(3): p. 296-311.
38. Alegret, M., et al., *Concordance between Subjective and Objective Memory Impairment in Volunteer Subjects.* J Alzheimers Dis, 2015. **48**(4): p. 1109-17.
39. Snitz, B.E., et al., *Do Subjective Memory Complaints Lead or Follow Objective Cognitive Change? A Five-Year Population Study of Temporal Influence.*, in *J Int Neuropsychol Soc*. 2015, Cambridge University Press. p. 732-742.
40. Blokland, G.A., et al., *Genetic and environmental influences on neuroimaging phenotypes: a meta-analytical perspective on twin imaging studies.* Twin Res Hum Genet, 2012. **15**(3): p. 351-71.
41. Lee, T., et al., *Genetic influences on cognitive functions in the elderly: a selective review of twin studies.* Brain Res Rev, 2010. **64**(1): p. 1-13.

SUPPLEMENTARY DATA

Supplementary Table 1. Baseline characteristics according to amyloid status

	PET amyloid negative^ n=168	PET amyloid positive^ n=28	P-value model 1	P-value model 2
Age, mean (SD)	69.8 (7.3)	75.4 (7.6)	0.01	-
Years of education, mean (SD)	11.5 (2.6)	11.3 (3.0)	0.34	-
Female, n (%)	97 (58)	17 (61)	0.98	-
APOE ε4 carrier, n (%)	50 (30)	14 (50)	0.17	-
Family history with dementia, n (%)	78 (46)	12 (43)	0.75	-
MMSE, median (IQR)	29 (29-30)	29 (28-30)	0.26	0.36
RCF recall 3 minutes, mean (SD)	18.8 (5.5)	15.5 (4.3)	0.001	0.02
FNAME delayed recall subscore names, mean (SD)	20.1 (10.3)	16.2 (7.3)	0.98	0.70
PAL total errors adjusted, mean (SD)	28 (15)	34 (19)	0.36	0.67
RAVLT delayed recall, mean (SD)	8.5 (3.0)	7.7 (2.1)	0.17	0.71
CCI, median (IQR)	21 (20-24)	21 (20-25)	0.89	0.36

^ Based on visual read BP_{ND} image
SD: standard deviation; APOE: apolipoprotein E; MMSE: mini mental state examination; RCF: Rey complex figure; FNAME: face-name associated memory exam; PAL: paired associate learning; RAVLT: Rey auditory verbal learning task; CCI: cognitive change index self-reported; IQR: interquartile range; PET: positron emission tomography.
Model 1: GEE with level for twin status, no covariates; Model 2: GEE with level for twin status corrected for age, gender, and education.

Supplementary Table 2. Baseline characteristics according to amyloid PET twin dis-/concordance status

	Concordant amyloid negative ^ (CN, n=148 (74 pairs))	Discordant amyloid negative (DN, n=14)	Discordant amyloid positive (DP, n=14)	Concordant amyloid positive (CP, n=12 (6 pairs))	Group difference
Age, mean (SD)	69.1 (6.9)	73.6 (7.6)	73.6 (7.6)	76.1 (6.9)	CN < DN*, DP*, CP*
Female, n (%)	84 (57)	8 (57)	8 (57)	8 (67)	-
Years of education, mean (SD)	11.6 (2.5)	10.9 (3.0)	11.6 (3.1)	10.9 (3.1)	-
APOE ε4 carrier (n,%)	40 (27)	8 (57)	8 (57)	6 (50)	CN < DN*, DP*
Family history dementia (n,%)	74 (50)	4 (29)	4 (29)	6 (50)	-
MMSE, mean (SD)	29.1 (1.0)	28.7 (1.4)	28.9 (1.3)	28.0 (1.6)	CN**, DP* > CP
RCF recall, mean (SD)	18.8 (5.6)	19.2 (4.5)	16.6 (4.5)	14.4 (4.2)	CN > CP#; DN > DP#, CP**
FNAME-names, mean (SD)	20.7 (10.3)	12.8 (9.5)	15.8 (7.6)	16.1 (7.4)	CN > DN#, CP*
PAL total errors, mean (SD)	27.0 (15)	31.9 (18)	30.5 (18)	38.7 (19)	-
RAVLT delayed recall, mean (SD)	8.5 (3.0)	8.2 (2.7)	7.5 (1.9)	7.7 (2.4)	-
CCI, mean (SD)	22.5 (3.7)	22.7 (3.5)	22.5 (3.8)	22.6 (2.8)	-
PET global cortical BP_{ND}, mean (SD)	0.12 (0.06)	0.15 (0.04)	0.43 (0.15)	0.43 (0.12)	CN < DN*, DP**, CP** DN < DP**, CP**

^ Based on visual read BP_{ND} image.
APOE: Apolipoprotein E; MMSE: Mini mental state examination; RCF: Rey complex figure 3 minutes recall; FNAME: face-name associated memory exam; PAL: paired associate learning; RAVLT: Rey auditory verbal learning task; CCI: cognitive change index, self-reported; PET: positron emission tomography; BP_{ND}: non-displaceable binding potential. CN: concordant normal; DN: discordant normal; DA: discordant abnormal; CA: concordant abnormal. GEE analysis with level for twin status, corrected for age, gender, and education, **p<0.01, *p <0.05, #p<0.10.

CHAPTER

7

Summary and Discussion

In this thesis we investigated the early pathophysiology of AD by comparing different markers for amyloid aggregation in cognitively normal individuals and investigating the association of amyloid aggregation with proteomic changes in cerebrospinal fluid (CSF) and cognitive function. The main findings of this thesis are (Figure 1):

I. Assessment of amyloid aggregation in cognitively normal individuals
  – Amyloid-PET visual assessment of amyloid aggregation on parametric [^{18}F] flutemetamol BP_{ND} images is more accurate than visual assessment of amyloid aggregation on SUV images.
  – CSF ratio amyloid-β 42/40 and [^{18}F]flutemetamol PET BP_{ND} seem to measure amyloid aggregation in a similar way.

II. Pathophysiology of amyloid aggregation
  – Increased amyloid production may be involved in AD pathophysiology in cognitively normal elderly.
  – The onset of amyloid aggregation in cognitively normal elderly is under substantial influence of unique environmental factors.
  – BACE1 may play a central role in *pre-amyloid stages* of AD.
  – CSF proteomic signatures associated with amyloid aggregation are dependent on APOE ε4 genotype. APOE ε4 carriers show changes in proteins associated with inflammation followed by changes in proteins associated with synapse function while this order was the other way around in individuals without the APOE ε4 allele.
  – Amyloid aggregation is associated with visual memory performance but not with cognitive complaints in community dwelling cognitively normal elderly.

Next, we will discuss these findings in more detail and comment on methodological issues regarding the studies in this thesis. We will conclude with implications of these results and future perspectives.
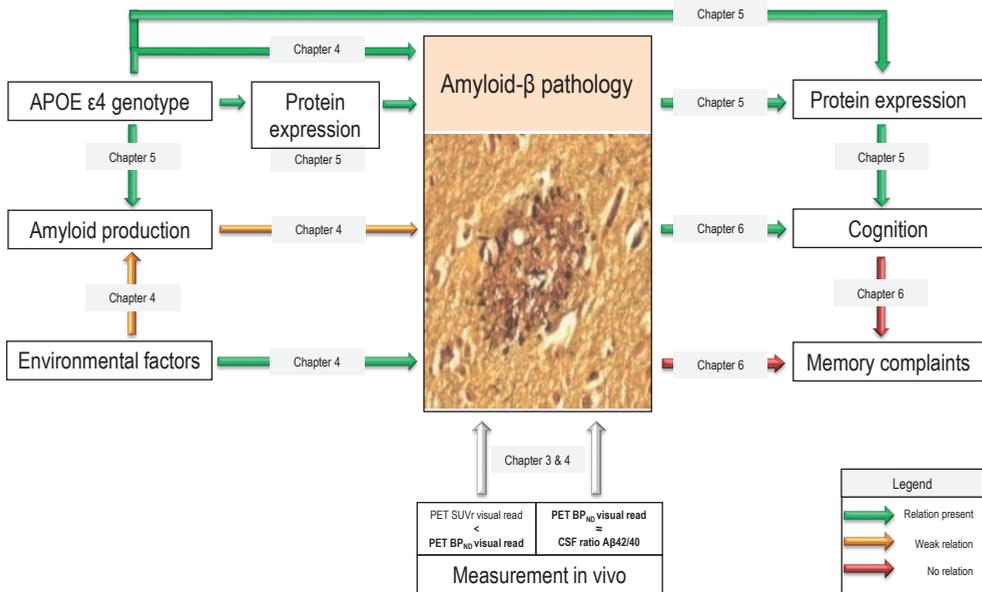
Figure 1. Summary of main findings

I. PRECLINAD COHORT

AD starts in cognitively normal individuals but there are relatively few cohorts that have tested amyloid pathology in these individuals. To study early pathophysiological mechanisms associated with amyloid pathology we initiated the EMIF-AD PreclinAD study in 2014.

In **chapter 2** we describe the PreclinAD study population, consisting of 285 cognitively normal elderly, recruited from two ongoing cohorts. At Manchester University 81 subjects were recruited from the Manchester and Newcastle Age and Cognitive Performance Research Cohort in the United Kingdom. At the VU University medical center in Amsterdam 204 subjects (including 99 monozygotic twin pairs) were selected from the Netherlands Twin Register (NTR). All subjects had data available for neuropsychological testing and questionnaires, medical history and medication use, physical measures, such as height, weight, waist measurement and resting blood pressure, ultrasound of the carotid artery, dynamic [18F]flutemetamol amyloid-PET scanning, and MRI. In the NTR sample CSF collection, Magneto-encephalography (MEG), and retinal imaging was performed as well (Figure 2). Participants were on average 74.8 (SD=9.7) years old, 64% female, and 30% APOE ε4 carrier. Manchester participants were older (85.7 vs 70.8, p<0.001), more often female (78 vs 58%, p<0.01), and had less often a positive family history for AD (19 vs 45%, p<0.001).

| Blood plasma & serum | Ultrasound carotid artery | MEG | Retinal imaging | Cerebrospinal fluid | PET & MRI |
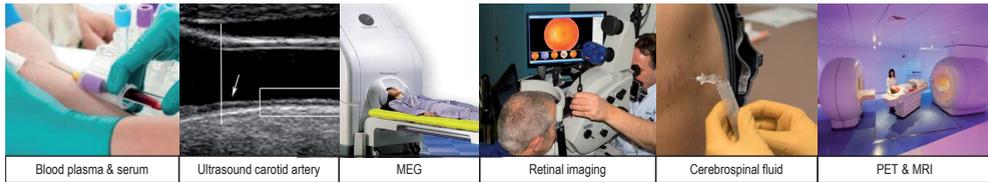
Figure 2. Biomarker data collected in PreclinAD sample.

Fifty-eight participants (22%) had an abnormal amyloid-PET scan, as visually read from static images. Participants from Manchester had more often an abnormal amyloid-PET scan (34 vs 16% p<0.01), probably because they were older. Amyloid abnormality increased with age, with 12% of subjects aged 60-70 years having an abnormal amyloid-PET scan, 16% of the subjects between 70-80 years and 36% of the subjects 80 years and older. These findings resemble earlier findings for amyloid pathology in the cognitively healthy elderly population [1].

II. ASSESSMENT OF AMYLOID PATHOLOGY

In **chapter 3** we investigated which of two methods to classify [^{18}F]flutemetamol PET images, SUVr or BP_{ND}, was best for visual assessment of amyloid pathology on PET in cognitively normal elderly. Visual rating is typically performed on summed late images or SUV images obtained from static PET acquisition [2-4], however SUVr might overestimate amyloid load compared to quantitative BP_{ND}, which is derived from dynamic PET acquisition [5]. As such, quantitative images may be more reliable, also for visual interpretation. We found a better inter-reader agreement for the visual assessment of the [^{18}F]flutemetamol dynamic images (BP_{ND}) compared to the static images (SUVr), and our analysis provided evidence that static images indeed overestimated actual amyloid load. When adding (semi) quantification to the visual assessment, the number of false-positive individuals decreased in the assessment of static images and decreased in the assessment of dynamic images to zero. A disadvantage of acquiring BP_{ND} images is that dynamic scanning is required from the moment of tracer injection (in our study 0-30 minutes after injection) in addition to the scanning in the plateau phase (90-110 minutes after injection). This may lead to a higher burden for participants, but for cognitively normal subjects this burden may be acceptable. The benefits of reducing false-positive diagnoses may outweigh the extra burden of an additional 30-minute scan, in particular if subjects are selected for an anti-amyloid trial.

In **chapter 4 and 6** we used CSF ratio $A\beta_{42/40}$ and PET BP_{ND} values to assess the relation between these amyloid aggregation markers and their relation with memory performance. In **chapter 4** we found a moderately strong association between CSF ratio $A\beta_{42/40}$ and PET BP_{ND}. In addition, the cross-twin cross-trait correlations between CSF ratio $A\beta_{42/40}$ and PET
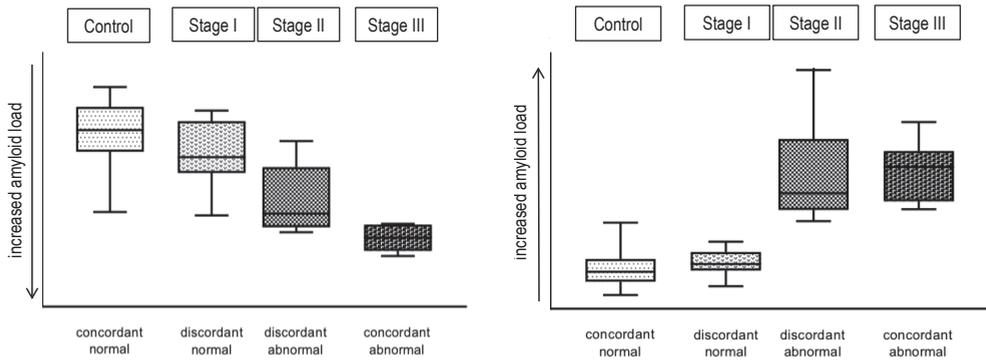
Figure 3. Twins discordance model as a hypothetical disease stage model
Boxplots for ratio Aβ42/40 (left) and [18F]flutemetamol BP_{ND} (right) showing amyloid load according to twin discordance status. Hypothetical model for amyloid aggregation severity: twins of a pair who have both a normal PET scan (concordant normal, Control), twins from a discordant pair with normal amyloid (discordant normal, Stage I), twins from a discordant pair with abnormal amyloid positive subjects (discordant abnormal, Stage II), and twin pairs who both have an abnormal PET scan (concordant abnormal, Stage III). From left to right with gradually increasing amyloid load from control group to stage I, II and III.

BP_{ND} was statistically significant, as well, supporting the notion that these markers measure largely, but not entirely, the same biological construct of amyloid aggregation. The moderate strength of the association is possibly due to a low variability in PET BP_{ND} values as 86% of the individuals had a normal amyloid-PET. It is also possible that CSF is an earlier marker for amyloid pathology, as suggested in previous studies using SUV PET images [6]. However, using the twin discordance design as an amyloid disease stage model, we found the same dose effect for CSF ratio $Aβ_{42/40}$ and PET BP_{ND} values (Figure 3). In **chapter 6** we found a relation between amyloid pathology and memory performance on the Rey Complex figure recall. We found a relation between Rey Figure recall and CSF ratio $Aβ_{42/40}$, and with amyloid-PET status as visually read on BP_{ND} images. Additionally, worse performance on the Rey complex figure recall was related to increased amyloid aggregation, measured with both CSF and PET. Nevertheless differences in amyloid aggregation marker performance between CSF and PET were found: PET BP_{ND} data were skewed with low variability and PET BP_{ND} as a continuous measure was not associated with Rey complex figure performance. This might suggest that PET BP_{ND} values are a bit less sensitive compared to CSF ratio $Aβ_{42/40}$. Overall, we found no strong evidence of CSF being an earlier marker for amyloid aggregation compared to PET in the earliest stage of AD.

III. PATHOPHYSIOLOGY OF AMYLOID AGGREGATION

Relation between amyloid production and aggregation

In **chapter 4** we investigated whether there is a relation between amyloid production and aggregation in the preclinical stage of AD. For this, we used three markers to assess amyloid production (CSF BACE1, Aβ40, Aβ38) and two measures to assess amyloid aggregation (CSF ratio $Aβ_{42/40}$ and [^{18}F]flutemetamol BP_{ND}). We found a negative association between BACE1 and the CSF ratio $Aβ_{42/40}$ in the total group and in addition a cross-twin cross-trait correlation between BACE1 and the CSF ratio $Aβ_{42/40}$ at trend level, possibly suggesting a shared biological background for this relation. Since CSF ratio $Aβ_{42/40}$ contains in part amyloid production (i.e. Aβ40), it could be suggested that amyloid production is driving the association between BACE1 and CSF ratio $Aβ_{42/40}$. However, using the twin discordance approach, based on visual amyloid-PET rating, we also found higher levels of BACE1 in both twins of discordant twin pairs (i.e. the twin with normal amyloid-PET *and* the co-twin twin abnormal PET), compared to concordant normal twins. The higher levels of BACE1 present in the non-affected twin of the discordant pairs suggest that BACE1 increases just before amyloid aggregation becomes detectable on visual read. Together these findings provide evidence for a role of increased amyloid production in very early sporadic AD. However, follow-up data are required to determine the temporal ordering of events, whether it is the case that BACE1 increases leading to amyloid aggregation, or the other way around. The relatively weak relation between amyloid production and aggregation suggests that there are other causes for amyloid aggregation, such as clearance problems or vascular damage causing amyloid to aggregate in sporadic AD [7].

Environmental influence on amyloid aggregation and production

In **chapter 4** we found that, of the 94 monozygotic twin pairs of which both twins had amyloid-PET data available, 14 (15%) were discordant for amyloid-PET, which indicates a substantial influence of unique environmental factors to amyloid pathology. This is supported by the lower twin-pair correlations (0.52-0.54) for amyloid aggregation markers compared to those for amyloid production markers (0.79-0.86). So unlike amyloid production, amyloid aggregation is considerably influenced by unique environmental, and therefore possibly modifiable, factors. Discovering these factors may lead to new prevention strategies for AD.

Effect of APOE ε4 on protein expression in CSF in AD subjects

In **chapter 5** we found that APOE ε4 carriers with amyloid aggregation showed altered concentrations of proteins involved in the complement pathway and glycolysis when cognition was normal and lower concentrations of proteins involved in synapse structure and function when cognitive impairment was moderately severe. APOE ε4 non-carriers with AD showed lower expression of proteins involved in synapse structure and function

when cognition was normal, and lower concentrations of proteins that were associated with complement and other inflammatory processes when cognitive impairment was mild. These results imply that AD pathophysiology depends on APOE genotype and that treatment for AD may need to be tailored according to APOE genotype and severity of the cognitive impairment. Cognitively normal subjects without amyloid but in possession of the APOE ε4 showed a subtle increase in BACE1 levels in CSF. The use of proteomics in CSF is a promising novel method for in vivo measurement of biological processes in the brain. Our findings are comparable to earlier studies, post-mortem and mice [8, 9], confirming our findings to be robust.

Memory performance in preclinical AD

In **chapter 6** we found amyloid aggregation is associated with visual memory performance in cognitively normal elderly. Twin discordance analysis, used as a disease stage model for amyloid pathology (Figure 3), showed visual memory and face-name associative memory to be among the types of memory sensitive to be influenced by early stage AD. This supports the notion that amyloid aggregation leads to subtle memory dysfunction in very early stages of AD. We found two different patterns of memory performance; for Rey complex figure subjects showed worse performance in the more advanced stage (concordant abnormal amyloid-PET, stage III), while for the FNAME subjects in the earliest stage (discordant with normal amyloid-PET, stage I) already tended to show lower scores. This might suggest that the FNAME can function as a screening tool for increased risk of amyloid pathology in the general population, however further studies in large samples are necessary to validate this hypothesis. There was no association between amyloid aggregation and SCD nor between SCD and memory. The inclusion and exclusion criteria applied in our study were very strict, resulting in a very healthy elderly cohort, reducing the range of amyloid aggregation, memory performance and complaint scores, which therefore limited the ability to detect associations. Hence, this might not be the right sample to investigate the effect of cognitive complaints in early AD.

IV. METHODOLOGICAL CONSIDERATIONS

Samples

In this thesis we analyzed data from two cohorts, one newly collected data set of cognitively normal elderly (PreclinAD study) and one existing dataset consisting of cognitively normal elderly and patients with AD across the disease spectrum (ADNI study). Both cohorts have a rich set of biomarkers available, facilitating us to thoroughly investigate AD pathophysiology, however some limitations must be acknowledged.

PreclinAD

The preclinAD cohort is a two-site study, with less than 30% of the subjects included in Manchester. Subjects from Manchester were older compared to Amsterdam subjects and showed amyloid pathology more often. One explanation for the younger age in Amsterdam is that we included complete monozygotic twin pairs. Older twin-pairs are relatively scarce, since when one of them is cognitively impaired or fulfilled other exclusion criteria, both twins of a pair were excluded from the study. Furthermore, Amsterdam subjects were all monozygotic twins. While this offers the possibility of exploring genetic and environmental influences on amyloid pathology, it decreases power in group-wise analysis as twins from a pair are not independent. Although scanning protocols were aligned at both sites, different PET scanners (HRRT in Manchester vs PET-MRI in Amsterdam) were used. While we did not perform analysis in the combined sample yet, the differences in design and data acquisition need to be taken into account in future analysis.

ADNI

The commonly used ADNI cohort consists of a selected population recruited mainly by advertisements. Together with the observation that ADNI participants are highly educated, this may limit the generalizability of the findings from this cohort to other settings.

Use of cross-sectional data

For all analysis performed in this thesis we used cross-sectional data. This has the disadvantage that we cannot be certain that observed findings are the result of different stage of disease or simply the natural variation of a trait. Furthermore, it is not possible to infer conclusions about causality in the observed associations. It will therefore be important to validate our findings in longitudinal studies with repeated biomarker and cognitive assessments.

Twin methodology

By design, we did not include dizygotic twin pairs in our twin sample. Although the classic twin design, to calculate heritability, requires besides monozygotic also dizygotic twins, for the aim of our study, assessing whether there is an actual biological background for a relation between two traits (using a monozygotic difference approach), and to assess the unique environmental influence on certain traits, a monozygotic twin design is the strongest approach [10]. However, studies applying a classic twin design with mono- and dizygotic twins, showed that for brain aging and cognition measures common environment does not play a role [11, 12], and that monozygotic twin-pair correlations may therefore be interpreted as the amount of variance within these traits explained by genetic variation (heritability).

An advantage of the monozygotic twin difference design is the possibility to support or reject causality of a relation between two traits, although for definite conclusions follow-up data is also needed [13]. We used the discordant twin design as a disease stage model for amyloid aggregation severity (Figure 2). However, AD-type dementia is 'only' 80% heritable, and with this amyloid disease stage model we assumed that both twins of a pair will get amyloid pathology even though they do not always both become demented. Our assumption was driven by earlier findings from Scheinin et al. who reported that twins that were discordant for a clinical diagnosis of AD-type dementia were concordant for amyloid aggregation on amyloid-PET imaging, while this was not the case for dizygotic twins [14]. However, AD pathology is also characterized by neuronal injury, therefore we must acquire follow-up data to establish to what extent preclinical AD in twins resembles AD-type dementia later on. This is underlined by twin-pair correlations for amyloid aggregation being substantially lower then twin concordance for AD-type dementia, however these dementia diagnoses were not biomarker confirmed.

CSF proteomics

The use of proteomics is approaching a data driven manner of investigating biological processes. However, our proteomic panels included up-to 300 pre-selected proteins based on earlier findings from other neurodegenerative diseases. Since in CSF thousands of proteins are present we may therefore have missed proteomic pathways. Another challenge of CSF proteomics, is interpretation of the data. Protein expression can be lower or higher, however, the consequences for different pathways are not straightforward. For example lower expression of a certain protein might indicate decreased activity, since there is less available of that protein in CSF (as with tau), or it may suggest increased activity of this protein, as it is used and therefore 'out of stock'. Pathway analysis used to interpret the findings of these proteomic expression profiles is a way to perform data-reduction, but these pathways are based on previous observations and may not cover novel pathophysiological mechanisms.

V. IMPLICATIONS

Early detection of amyloid pathology

Although it is common practice to use static amyloid-PET images for visual read [4], for the selection of subjects with preclinical AD, dynamic amyloid-PET images should be considered to avoid inclusion of false-positives in clinical trials. Both the twin and CSF analysis suggests CSF BACE1 upregulation to be the earliest sign of the start of amyloid aggregation, however this needs to be established further. When validated, BACE1 levels in CSF can be used as a selection criterion for inclusion in BACE1 inhibitor trials in the future. Since we show CSF ratio

$A\beta_{42/40}$ and PET BP_{ND} to measure the same biological construct, these measures both seem to be applicable as exchangeable continuous amyloid aggregation markers in preclinical AD [15].

Pathophysiology

CSF proteomic analysis is a useful tool to measure parallel processes in vivo in humans, it might therefore be applied in longitudinal studies to study evolvement of biological processes underlying AD. BACE1 may play a central role in in *pre-amyloid stages* of AD. We found that cognitively normal subjects without amyloid pathology but genetically at risk, either through a monozygotic co-twin already showing abnormal amyloid-PET or by possession of the APOE ε4 allele, to show a subtle increase in BACE1 levels in CSF, compared to controls, either twins with both a normal PET or subjects without an APOE ε4 allele.

Treatment

Since we only found a weak relation between amyloid production and aggregation, clinical trials might want to focus more strongly on clearance problems, instead of inhibition of amyloid production solely. The involvement of different proteins in amyloid pathology depending on APOE ε4 genotype, suggesting specific biological processes underlying AD pathology within these groups, suggests treatment might need to be tailored to APOE ε4 genotype. The substantial influence of environmental factors (around 50%), either directly or via epigenetic changes, on amyloid pathology in cognitively normal elderly shows that identification of these factors might lead to novel AD prevention targets.

Endpoints in trials

Our findings that specific biological processes underlie AD pathology dependent on APOE ε4 genotype and disease stage indicates that trials may need to select outcome measures for trial that differ for disease stage and/or APOE ε4 genotype.

VI. FUTURE PERSPECTIVES

For defining novel targets for anti-AD targets for lifestyle or medication, we next should try to identify the environmental factors, and/or epigenetic changes, that are influencing early AD pathophysiology. Therefore differences within twin-pairs discordant for amyloid-PET should be accurately investigated to identify factors for life style advice and/or medication targets. By studying epigenetic differences within twin-pairs discordant for amyloid aggregation novel targets for drug development might be identified. Furthermore, follow-up studies are needed to study the outcome of twin discordance in order to discover which twin-pairs become concordant abnormal (genetic influence) or stay discordant

(environmental influence). The collection of longitudinal data for twin analysis is also needed to assess possible relations between amyloid aggregation and actual cognitive decline in these healthy subjects. As injury markers in CSF are more strongly related to cognitive performance than markers of amyloid aggregation [16], these markers should be obtained and possible relations with cognitive decline investigated. Follow up data for proteomic CSF analysis will be essential, as for now it is not clear which proteins actually reflect disease cause or consequence. Finally, since monozygotic twins share 100% of their genes, CSF proteomics in this population might even shed light on gene expression difference in brain tissue. As a gold standard for amyloid pathology, and reflection of other biological processes in the brain, port-mortem pathological evaluation of brain tissue is important, therefore participating twins are currently asked to subscribe to the Netherlands Brain Bank, to enable studying their brain tissue after they are deceased.

REFERENCES

1. Jansen, W.J., et al., *Prevalence of cerebral amyloid pathology in persons without dementia: a meta-analysis*, in *JAMA : the journal of the American Medical Association*. 2015. p. 1924-1938.
2. Buckley, C.J., et al., *Validation of an electronic image reader training programme for interpretation of [18F]flutemetamol beta-amyloid PET brain images*. Nucl Med Commun, 2017. **38**(3): p. 234-241.
3. Thurfjell, L., et al., *Automated quantification of 18F-flutemetamol PET activity for categorizing scans as negative or positive for brain amyloid: concordance with visual image reads*. J Nucl Med, 2014. **55**(10): p. 1623-8.
4. Salloway, S., et al., *Performance of [(18)F]flutemetamol amyloid imaging against the neuritic plaque component of CERAD and the current (2012) NIA-AA recommendations for the neuropathologic diagnosis of Alzheimer's disease*. Alzheimers Dement (Amst), 2017. **9**: p. 25-34.
5. van Berckel, B.N., et al., *Longitudinal amyloid imaging using 11C-PiB: methodologic considerations*. J Nucl Med, 2013. **54**(9): p. 1570-6.
6. Palmqvist, S., et al., *Cerebrospinal fluid analysis detects cerebral amyloid-beta accumulation earlier than positron emission tomography*. Brain, 2016. **139**(Pt 4): p. 1226-36.
7. Zuroff, L., et al., *Clearance of cerebral Abeta in Alzheimer's disease: reassessing the role of microglia and monocytes*. Cell Mol Life Sci, 2017. **74**(12): p. 2167-2201.
8. Shi, Q., et al., *Complement C3 deficiency protects against neurodegeneration in aged plaque-rich APP/PS1 mice*. Sci Transl Med, 2017. **9**(392).
9. Rozemuller, A.J., et al., *Neuroinflammation and common mechanism in Alzheimer's disease and prion amyloidosis: amyloid-associated proteins, neuroinflammation and neurofibrillary degeneration*, in *Neuro-degenerative diseases*. 2012. p. 301-304.
10. Vitaro F, B.M., Arseneault L, *The discordant MZ-twin method: One step closer to the holy grail of causality*. International Journal of Behavioral Development, 2009. **33**(4): p. 376–382.
11. Lee, T., et al., *Genetic influences on cognitive functions in the elderly: a selective review of twin studies*. Brain Res Rev, 2010. **64**(1): p. 1-13.
12. Blokland, G.A., et al., *Genetic and environmental influences on neuroimaging phenotypes: a meta-analytical perspective on twin imaging studies*. Twin Res Hum Genet, 2012. **15**(3): p. 351-71.
13. De Moor, M.H., et al., *Testing causality in the association between regular exercise and symptoms of anxiety and depression*. Arch Gen Psychiatry, 2008. **65**(8): p. 897-905.
14. Scheinin, N.M., et al., *Early detection of Alzheimer disease: (1)(1)C-PiB PET in twins discordant for cognitive impairment*, in *Neurology*. 2011. p. 453-460.
15. Janelidze, S., et al., *Concordance Between Different Amyloid Immunoassays and Visual Amyloid Positron Emission Tomographic Assessment*. JAMA Neurol, 2017. **74**(12): p. 1492-1501.
16. Buckley, R.F., et al., *Region-Specific Association of Subjective Cognitive Decline With Tauopathy Independent of Global beta-Amyloid Burden*. JAMA Neurol, 2017. **74**(12): p. 1455-1463.

Appendix

Nederlandse samenvatting

INLEIDING

De ziekte van Alzheimer is de meest voorkomende oorzaak van dementie. In 2030 zullen naar verwachting 75 miljoen mensen lijden aan deze ziekte. Hoewel al veel over de ziekte van Alzheimer bekend is, weet men niet hoe de ziekte precies ontstaat.

De heersende veronderstelling is als volgt. Jaren voordat de ziekte zich als dementie manifesteert hoopt zich amyloid-β eiwit (of plaques) op in het hersenweefsel buiten de hersenencellen. Vervolgens vormen zich eiwitkluwens van gefosforyleerd tau in de hersencellen. Deze twee processen leiden tot zenuwschade en celdood, waarna in de regel geheugenproblemen volgen.

Tot op heden zijn medicijnonderzoeken met anti-amyloid middelen, bij patiënten met een milde tot matige vorm van de ziekte van Alzheimer, niet geslaagd. Dat is waarschijnlijk omdat deze patiënten al forse onherstelbare hersenschade hebben. Tegenwoordig richt onderzoek zich daarom vooral op secundaire preventie: het vroeg opsporen van de ziekte met een oogmerk om vroeg tot behandeling over te kunnen gaan en zo het ziekteproces te remmen. Het stoppen of afremmen van amyloid-β plaque-ophoping bij mensen zonder geheugenproblemen, zou ertoe kunnen leiden dat de tweede ziektefase, de vorming van gefosforyleerd tau, en daarmee de hersenschade, kan worden voorkomen.

Het primaire doel van dit proefschrift en het onderliggende onderzoek is het begin van het ziekteproces van de ziekte van Alzheimer inzichtelijk te maken. Wij hebben zowel amyloid-β stapeling in gezonde eeneiige tweelingen onderzocht, als eiwitprofielen in de hersenvloeistof van patiënten met de ziekte van Alzheimer geanalyseerd.

Preklinische ziekte van Alzheimer
Ongeveer 20% van de 60-jarigen en tot 40% van de 90-jarigen heeft amyloid-β stapeling in het hersenweefsel maar (nog) geen geheugenproblemen. Dit wordt beschouwd als het eerste ziektestadium, ook wel de 'preklinische' ziekte van Alzheimer genoemd. In dit proefschrift worden achtereenvolgens een aantal discussiepunten ten aanzien van de definitie van 'preklinische ziekte van Alzheimer', de diagnostische procedures en het ziekteproces achter vroege amyloid-β stapeling doorgenomen.

Het meten van amyloid stapeling
De meest precieze manier om amyloid-β stapeling te meten, is om na de dood het hersenweefsel te onderzoeken. Tegenwoordig kan amyloid-β stapeling ook in levende mensen gemeten worden, met behulp van biomarkers. Biomarkers zijn meetbare indicatoren van een stof, in dit geval van amyloid-β. Amyloid-β stapeling in de hersenen wordt

gezien als verhoogde amyloid binding op een PET scan en als verlaagde concentratie van amyloid-β 1-42 in het hersenvocht. Deze twee manieren van meten komen grotendeels overeen, echter bij 15% van de mensen is dit niet het geval. Om deelnemers met preklinische ziekte van Alzheimer voor anti-amyloid medicijnonderzoek te werven, is het van groot belang om een betrouwbare amyloid-β meting te kunnen doen.

Voor het bepalen van amyloid-β stapeling op PET beelden wordt meestal de visuele beoordeling van de opgetelde late semi-quantitative standardized uptake value ratio (SUVr) beelden gebruikt, gemaakt uit een 20 minuten durende scan. Eerdere studies laten een grote overeenkomst zien tussen visuele beoordelingen van SUVr beelden van verschillende raters en tussen de amyloid-β stapeling op PET beelden en post-mortem hersenonderzoek. Echter, het visueel (kwalitatief) scoren van SUVr beelden kan leiden tot overschatting van amyloid-β stapeling, in vergelijking met kwantitatieve 'non-displaceable binding potential' (BP$_{ND}$) waardes. BP$_{ND}$ PET beelden moeten worden gemaakt uit een 90 minuten durende scan, maar kunnen dan wel ook de klaring en bloedstroom door de hersenen meerekenen. Daarom zouden kwantitatieve BP$_{ND}$ beelden een hogere betrouwbaarheid kunnen hebben, zelfs voor visuele beoordeling. Dit geldt vooral voor mensen in een zeer vroeg ziektestadium, met relatief weinig amyloid-β plaques, aangezien de meeste ruis in PET scan gegevens zit in deze lage waardes. Voor [^{18}F]amyloid-radioliganden is nog niet onderzocht of visuele beoordeling, het beantwoorden van de vraag of er amyloid-β stapeling is, het best kan worden gedaan met SUVr of BP$_{ND}$ beelden.

Amyloid-β ontstaat door het knippen van het 'amyloid precursor protein' (APP) door BACE1 en daarna door gamma-secretase. Hierdoor ontstaan verschillende vormen van amyloid-β, waaronder amyloid-β 1-42, 1-40, en 1-38, alle drie meetbaar in het hersenvocht, waarvan amyloid-β 1-42 het meest gevoelig is om te gaan stapelen. Recente resultaten van onderzoek bij mensen zonder en met milde geheugenproblemen tonen zeer variabele waardes van amyloid-β 1-42 in het hersenvocht. Deze waardes verschillen per centrum en per gebruikte testkit. Eén van de redenen hiervoor zou kunnen zijn dat de waardes van amyloid-β 1-42 niet alleen stapeling maar ook deels (en per testkit en centrum verschillende hoeveelheden van) amyloid-β productie weergeven. Daarom is al vaker gesuggereerd dat het beter is om de ratio van amyloid-β 1-42/1-40 te gebruiken. Hierbij kan gecorrigeerd worden voor amyloid-β productie, waardoor de ratio waardes een betere weerspiegeling van daadwerkelijke amyloid-β stapeling zouden kunnen te zijn.

Amyloid-β biomarkers op PET en in hersenvocht komen het minst overeen bij mensen zonder geheugenproblemen, waarschijnlijk doordat deze mensen in een zeer vroeg ziektestadium zitten. In dit stadium is amyloid-β stapeling al wel gestart, maar nog niet zichtbaar als plaques op de PET beelden. Het is daarom nog onzeker welke van deze biomarkers de preklinische ziekte van Alzheimer het best weergeeft. Er is gesuggereerd dat amyloid-β veranderingen het eerst meetbaar zijn in hersenvocht, maar dit moet nog verder onderzocht worden.

Prestatie op geheugentesten in preklinische ziekte van Alzheimer

Eerdere onderzoeken hebben aangetoond dat amyloid-β stapeling bij mensen zonder geheugenproblemen een relatie zou kunnen hebben met minder goede prestaties op geheugentesten en met meer geheugenklachten. Maar tot nu toe zijn de resultaten niet eenduidig, mogelijk door een grote variatie in gebruikte geheugentesten, de definitie van geheugenklachten en de manier waarop amyloid-β is gemeten. We weten nog niet of de mogelijke relatie tussen amyloid-β stapeling en prestaties op geheugentesten ook een gedeeld onderliggend proces weergeeft.

Het proces van amyloid-β stapeling

Genen

Eerdere onderzoeken waarin dementie door de ziekte van Alzheimer genomen werd als uitkomst, hebben aangetoond dat de maximale bijdrage van genetische factoren ongeveer 80% is. Deze resultaten suggereren dat er een grote genetische bijdrage is aan het ontwikkelen van de ziekte van Alzheimer. Dat wordt verder onderbouwd door de oplopende tweelinggelijkenis voor Alzheimer dementie bij oplopende duur waarin de tweelingen gevolgd werden (d.w.z. beide helften van een identieke tweeling zullen de ziekte van Alzheimer krijgen, echter een van hen heeft een beschermende factor, niet-gedeeld binnen het paar, waardoor de ziekte zich bij diegene pas later openbaart). Er is echter ook bewijs voor een aanmerkelijk effect van omgevingsinvloeden. Dit blijkt uit de verschillen in leeftijd waarop de ziekte zich openbaart in eeneiige tweelingen die concordant zijn voor Alzheimer dementie (d.w.z. beide helften van de tweeling hebben de ziekte van Alzheimer). Verder is er nog weinig bekend over de genetische achtergrond van amyloid-β productie en stapeling in mensen zonder geheugenproblemen.

Het Apolipoprotein-E (APOE) ε4 allel is de grootste bekende genetische risicofactor voor de ziekte van Alzheimer. Hoewel het precieze onderliggende mechanisme niet bekend is, weten we wel dat mensen met een APOE ε4 allel eerder amyloid-β gaan stapelen. Ongeveer 25-40% van de patiënten met dementie op basis van de ziekte van Alzheimer hebben geen APOE ε4 allel en voor deze patiënten is het ontstaansmechanisme van de ziekte nog minder duidelijk. Eerder onderzoek laat zien dat de apoE4 eiwit vorm gelinkt wordt aan verminderde amyloid klaring en verwerking, synaptogenese, glucose en cholesterol metabolisme in de hersenen. De concentraties van twee met de ziekte van Alzheimer geassocieerde eiwitten, namelijk beta-secretase-1 (BACE1) en chitinase-3-like protein-1 (YKL40), lijken APOE ε4-afhankelijk te zijn. Daarom zou het goed kunnen dat APOE ε4 genotype ook andere eiwitten in het hersenvocht beïnvloedt. Het onderzoeken van eiwitexpressie in het hersenvocht kan mogelijk nieuwe inzichten geven in ontstaansmechanismes van de ziekte van Alzheimer en of deze APOE ε4 genotype afhankelijk zijn.

Uit Genome Wide Association Studies blijkt dat neuro-inflammatie een grote rol speelt in het ontstaan en de ernst van de ziekte van Alzheimer, hierbij is ook een aantal Alzheimer risicogenen geïdentificeerd. Inflammatie lijkt iets te maken te hebben met het ontstaansmechanisme van de ziekte van Alzheimer, waaronder met amyloid-β stapeling in de hersenen. Daarom zou het onderzoeken van inflammatie-eiwitten nieuwe inzichten kunnen geven in de rol van inflammatie in de ziekte van Alzheimer.

Tot slot wordt ongeveer 1% van de gevallen van de ziekte van Alzheimer veroorzaakt door een autosomaal dominante mutatie in amyloid-β productiegenen amyloid precursor protein (APP), presenilin1 (PSEN1), of presenilin2 (PSEN2). Deze mutaties leiden tot een overproductie van amyloid-β eiwitten, gevolgd door amyloid-β stapeling. We weten niet of, en zo ja in welke ziektefase, overproductie van amyloid-β ook een rol speelt bij amyloid-β stapeling in de niet-erfelijke ziekte van Alzheimer. Onderzoeken met BACE1 remmers, die de amyloid-β productie verminderen, waren eerder niet succesvol bij patiënten met gevorderde ziekte van Alzheimer en deze worden momenteel in de vroegste ziektefase getest. Om de beste interventiedoelen te vinden onderzoeken we de relatie tussen productie en stapeling van amyloid-β bij mensen zonder geheugenproblemen.

Omgeving

Uit eerder onderzoek is gebleken dat er verschillende omgevingsfactoren zijn, die mogelijk invloed hebben op het ontwikkelen van amyloid-β stapeling. Hieronder vallen bijvoorbeeld opleidingsniveau, medische voorgeschiedenis en leefstijlfactoren zoals roken, alcohol en voedingsgewoontes. Hoewel omgevingsfactoren mogelijk aangepast kunnen worden, ontbreekt tot op heden bewijs dat dit daadwerkelijk beschermt tegen het ontwikkelen van de ziekte van Alzheimer. Verder is nog niet goed bekend wat de invloed van omgevingsfactoren is op Alzheimer biomarkers.

Doel van dit proefschrift

Dit proefschrift heeft twee hoofddoelen:

I. Hoe kan de diagnose voor preklinische ziekte van Alzheimer het beste worden gesteld, wat is de meest accurate methode om [^{18}F]flutemetamol PET beelden visueel te beoordelen, met BP_{ND} of SUVr beelden, en zijn amyloid-β maten in hersenvocht en op PET beelden te vergelijken bij mensen zonder geheugenproblemen?

II. Hoe zit het ziekteproces achter de ziekte van Alzheimer in elkaar, heeft amyloid-β productie invloed op amyloid-β stapeling in de vroege fase van de ziekte van Alzheimer, zijn er APOE-afhankelijke moleculaire processen die te maken hebben met amyloid-β stapeling, en is amyloid-β stapeling gerelateerd aan geheugenfunctie in preklinische ziekte van Alzheimer?

RESULTATEN

Deel I. Preklinische ziekte van Alzheimer

In **hoofdstuk 3** hebben we onderzocht welke van de twee methoden (BP$_{ND}$ of SUVr beelden) om [^{18}F]flutemetamol PET beelden te scoren het meest accuraat is voor het visueel beoordelen van amyloid-β stapeling bij mensen zonder geheugenproblemen. Visuele beoordeling wordt meestal uitgevoerd op opgetelde late beelden of SUV-beelden verkregen van statische PET-acquisitie, maar SUVr kan, in vergelijking met kwantitatieve dynamische BP$_{ND}$ afbeeldingen, de amyloid-β stapeling overschatten. De beoordelingen van de PET-afbeeldingen op basis van BP$_{ND}$ kwamen beter overeen tussen de beoordelaars dan bij SUVr. Daarnaast lijkt het erop dat statische SUVr afbeeldingen inderdaad de werkelijke amyloid-β stapeling overschatten. Voor het rekruteren van gezonde mensen met amyloid-β stapeling voor medicatie onderzoek zou daarom, ondanks de langere scanduur voor het verkrijgen van BP$_{ND}$ afbeeldingen, overwogen kunnen worden om dynamische amyloid PET-scans te verrichten.

In **hoofdstuk 4 en 6** hebben we de hersenvocht ratio amyloid-β 1-42/1-40 en PET BP$_{ND}$-waarden gebruikt om de relatie tussen deze twee amyloid-β stapelingsmarkers te beoordelen. In **hoofdstuk 4** vonden we een redelijk sterke associatie tussen ratio amyloid-β 1-42/1-40 in het hersenvocht en PET-BP$_{ND}$. Bovendien waren de cross-twin cross-trait correlaties tussen ratio amyloid-β 1-42/1-40 in het hersenvocht en PET-BP$_{ND}$ ook statistisch significant. Dit zou er goed op kunnen wijzen dat deze twee markers hetzelfde biologische proces van amyloid-β stapeling meten. Daarnaast zagen we in **hoofdstuk 6** met het gebruik van het tweeling discordantie model (discordantie wil zeggen dat een helft van de tweeling geen amyloid-β stapeling heeft en de andere helft wel, zie Figuur 1) als een stadiëringsmodel voor amyloid-β pathologie zagen we eenzelfde dosis effect voor amyloid-β hoeveelheden gemeten in hersenvocht en op PET.

Deel II. Ziekteproces achter de ziekte van Alzheimer

In **hoofdstuk 4** hebben we onderzocht of er een verband bestaat tussen amyloid-β productie en stapeling in de preklinische fase van de ziekte van Alzheimer. We hebben hier-voor drie markers gebruikt als maat voor productie van amyloid-β (BACE1, amyloid-β 40, amyloid-β 38 in hersenvocht) en twee manieren om de hoeveelheid amyloid-β stapeling te meten (ratio amyloid-β 1-42/1-40 en [^{18}F] flutemetamol BP$_{ND}$). We vonden een zwakke, maar significante, relatie tussen hogere waardes van BACE1 (productie) en lagere waardes van de ratio amyloid-β 1-42/1-40 (stapeling), met een trend op cross-twin cross-trait analyse. Dit suggereert dat deze relatie een gedeelde biologische achtergrond heeft. Dit zagen we ook terug in het tweeling discordantie model: in beide tweelingen van een discordant paar zijn
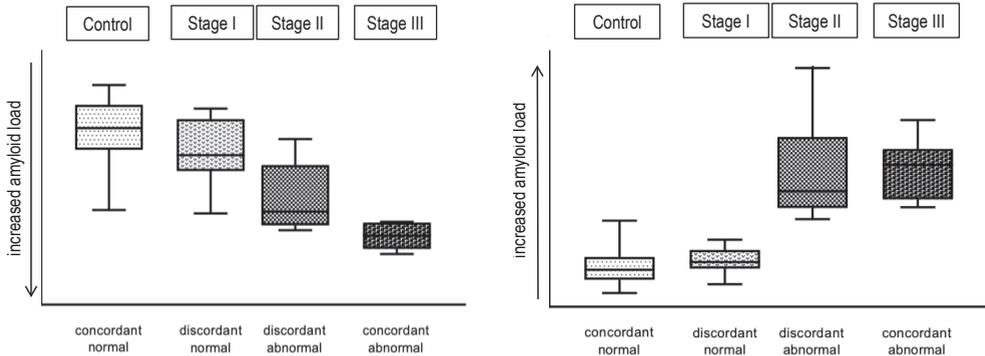
Figuur 1. Tweeling discordantiemodel als hypothetisch ziektestadiummodel
Boxplots voor de verhouding amyloid-β 1-42/1-40 (links) en [^{18}F] flutemetamol BP$_{ND}$ (rechts) die de amyloid-β stapeling tonen verdeeld over de status van tweeling discordantie. Hypothetisch model voor ernst van amyloid-β stapeling: tweelingen van een paar die beiden een normale PET-scan hebben (concordant normaal, controle), de helft van een tweeling van een discordant paar met normaal amyloid-β (discordant normaal, stadium I), de helft van een tweeling van een discordant paar met abnormaal amyloid-β (discordant abnormaal, stadium II) en tweelingparen die beiden een abnormale PET-scan hebben (concordant abnormaal, fase III). Van links naar rechts met geleidelijk toenemende amyloid-β stapeling van controlegroep tot stadium I, II en III.

de BACE1 waardes verhoogd ten opzichte van die van concordant normale tweelingen. Dit zou erop kunnen wijzen dat de BACE1 waardes omhoog gaan vlak voordat de amyloid-β stapeling op PET beelden zichtbaar is.

Daarnaast vonden we in **hoofdstuk 4** dat 15% van de tweelingen discordant was voor de aanwezigheid van amyloid-β pathologie, dit wijst op een substantiële bijdrage van omgevingsfactoren aan het ontwikkelen ervan. Dit werd verder onderbouwd door lagere tweeling correlaties (de overeenkomst voor een marker binnen een tweelingpaar) voor amyloid-β stapelings markers (0.52-0.54) dan voor productie markers (0.79-0.86). Dit wijst erop dat, in tegenstelling tot bij amyloid-β productie, amyloid-β stapeling beïnvloed wordt door omgevingsfactoren. En die factoren zijn mogelijk beïnvloedbaar.

In **hoofdstuk 5** hebben we onderzocht of het bezit van een APOE ε4 allel in patiënten met amyloid-β pathologie geassocieerd is met specifieke eiwitexpressiepatronen in het hersenvocht. De aanwezigheid van APOE ε4 afhankelijke eiwitexpressie zou meer duidelijkheid kunnen geven over de mogelijke verschillende onderliggende ziekteprocessen bij de ziekte van Alzheimer. In APOE ε4 dragers met amyloid-β pathologie vonden we bij deelnemers met een normaal geheugen veranderde concentraties van eiwitten die betrokken zijn bij de complementroute en glycolyse. Bij patiënten met een matige geheugenstoornis vonden we lagere concentraties van eiwitten die betrokken zijn bij synapsstructuur en -functie. De niet-dragers van een APOE ε4 allel met amyloid-β

pathologie en een normale geheugenfunctie vertoonden lagere concentraties van eiwitten die betrokken zijn bij synapsstructuur en –functie. En patiënten met een matig gestoord geheugen vertoonden lagere concentraties van eiwitten betrokken bij complement en andere ontstekingsprocessen. Dit wijst erop dat het ziekteproces van de ziekte van Alzheimer afhankelijk is van het APOE-genotype en dat behandeling voor de ziekte van Alzheimer mogelijk moet worden afgestemd op het APOE-genotype en de ernst van de geheugenstoornis. APOE ε4-dragers met een normale geheugenfunctie, maar (nog) zonder amyloid-β pathologie lieten subtiel verhoogde BACE1 waardes zien in hersenvocht, ten opzichte van deelnemers zonder APOE ε4 allel.

In **hoofdstuk 6** vonden we dat amyloid-β stapeling geassocieerd is met visuele geheugenprestaties bij mensen met een normaal geheugen. Met het tweeling discordantie model, wederom gebruikt als model voor de ernst van amyloid-β stapeling, zagen we dat het geheugen voor vormen en gezichts-naam combinaties in het begin van amyloid-β stapeling minder goed lijkt te worden. Dit ondersteunt het idee dat amyloid-β stapeling leidt tot subtiele geheugenstoornissen in zeer vroege stadia van de ziekte van Alzheimer. We vonden twee verschillende patronen van geheugenprestaties; voor de complexe Rey figuur zagen we dat mensen in het verder gevorderde stadium (concordant abnormaal, stadium III) slechter scoorden op deze taak, terwijl voor de gezichts-naam associatie taak mensen in de vroegste fase (discordant met normaal amyloid-β, stadium I) juist lager leken te scoren. Dit zou erop kunnen wijzen dat de laatstgenoemde taak kan fungeren als een instrument voor het screenen van mensen op een verhoogd risico op amyloid-β pathologie, maar dit moet nog verder worden onderzocht.

List of publications

Konijnenberg E, Fereshtehnejad SM, Kate MT, Eriksdotter M, Scheltens P, Johannsen P, Waldemar G, Visser PJ; **Early-Onset Dementia: Frequency, Diagnostic Procedures, and Quality Indicators in Three European Tertiary Referral Centers.** Alzheimer Dis Assoc Disord. 2017 Apr-Jun;31(2):146-151. doi: 10.1097/WAD.0000000000000152.

Zwan MD, Bouwman FH, **Konijnenberg E,** van der Flier WM, Lammertsma AA, Verhey FR, Aalten P, van Berckel BN, Scheltens P; **Diagnostic impact of [18F]flutemetamol PET in early-onset dementia.** Alzheimers Res Ther. 2017 Jan 17;9(1):2. doi: 10.1186/s13195-016-0228-4.

Demuru M, Gouw AA, Hillebrand A, Stam CJ, van Dijk BW, Scheltens P, Tijms BM, **Konijnenberg E,** Ten Kate M, den Braber A, Smit DJA, Boomsma DI, Visser PJ; **Functional and effective whole brain connectivity using magnetoencephalography to identify monozygotic twin pairs.** Sci Rep. 2017 Aug 29;7(1):9685. doi: 10.1038/s41598-017-10235-y.

Ten Kate M, Sudre CH, Den Braber A, **Konijnenberg E,** Cardoso MJ, Scheltens P, Ourselin S, Boomsma DI, Barkhof F, Visser PJ; **White matter hyperintensities and vascular risk factors in monozygotic twins**, Neurobiol Aging. 2018 Jun;66:40-48. doi: 10.1016/j.neurobiolaging.2018.02.002. Epub 2018 Feb 10.

Konijnenberg E, Carter SF, Ten Kate M, Den Braber A, Tomassen J, Nguyen HT, Maqsood M. Yaqub MM, Demuru M, Teunissen CE, Serne E, Stam C, Moll A, Barkhof F, Lammertsma AA, Hinz R, Pendleton N, Amadi C, Boomsma DI, Scheltens P, Van Berckel BNM, Herholz K, Visser PJ, **The EMIF-AD PreclinAD study: study design and baseline cohort overview**, Alzheimers Res Ther. 2018 Aug 4;10(1):75. doi: 10.1186/s13195-018-0406-7.

Collij LE*, **Konijnenberg E*,** Ingala S, Reimand J, Ten Kate M, Den Braber A, Lopes Alves I, Ossenkoppele R, Yaqub MM, Van Assema DME, Wink AM, Visser PJ, Barkhof F, Van Berckel BNM *shared first authors*; **Assessing Amyloid Pathology in Cognitively Normal Subjects using [18F]Flutemetamol PET: Comparing Visual Reads and Quantitative Methods,** J Nucl Med. 2018 Oct 12. pii: jnumed.118.211532. doi: 10.2967/jnumed.118.211532.

Van de Kreeke JA, Nguyen HT, **Konijnenberg E,** Tomassen J, den Braber A, Ten Kate M, Sudre CH, Barkhof F, Boomsma DI, Tan HS, Verbraak FD, Visser PJ; **Retinal and Cerebral Microvasculopathy: Relationships and Their Genetic Contributions,** Invest Ophthalmol Vis Sci. 2018 Oct 1;59(12):5025-5031. doi: 10.1167/iovs.18-25341.

Konijnenberg E, Den Braber A, Ten Kate M, Tomassen J, Mulder SD, Yaqub MM, Teunissen CE, Van Berckel BNM, Scheltens P, Boomsma DI, Visser PJ; **Association of amyloid pathology with memory performance and cognitive complaints in cognitively normal older adults: a monozygotic twin study,** Neurobiol Aging. 2019 Jan 21;77:58-65. doi: 10.1016/j.neurobiolaging.2019.01.006.

List of theses Alzheimer Center

1. L. Gootjes: Dichotic Listening, hemispheral connectivity and dementia (14-09-2004)
2. K. van Dijk: Peripheral Nerve Stimulation in Alzheimer's Disease (16-01-2005)
3. R. Goekoop: Functional MRI of cholinergic transmission (16-01-2006)
4. R. Lazeron: Cognitive aspects in Multiple Sclerosis (03-07- 2006)
5. N.S.M. Schoonenboom: CSF markers in Dementia (10-11-2006)
6. E.S.C. Korf: Medial Temporal Lobe atrophy on MRI: risk factors and predictive value (22-11-2006)
7. B. van Harten: Aspects of subcortical vascular ischemic disease (22-12-2006)
8. B. Jones: Cingular cortex networks: role in learning and memory and Alzheimer's disease related changes (23-03-2007)
9. L. van de Pol: Hippocampal atrophy from aging to dementia: a clinical and radiological perspective (11-05-2007)
10. Y.A.L. Pijnenburg: Frontotemporal dementia: towards an earlier diagnosis (05-07-2007)
11. A. Bastos Leite: Pathological ageing of the Brain (16-11-2007)
12. E.C.W. van Straaten: Vascular dementia (11-01-2008)
13. R.L.C. Vogels: Cognitive impairment in heart failure (11-04-2008)
14. J. Damoiseaux: The brain at rest (20-05-2008)
15. G.B. Karas: computational neuro-anatomy (19-06-2008)
16. F.H. Bouwman: Biomarkers in dementia: longitudinal aspects (20-06-2008)
17. A.A. Gouw: Cerebral small vessel disease on MRI: clinical impact and underlying pathology (20-03-2009)
18. H. van der Roest: Care needs in dementia and interactive digital information provisioning (12-10-2009)
19. C. Mulder: CSF Biomarkers in Alzheimer's disease (11-11-2009)
20. W. Henneman. Advances in hippocampal atrophy measurement in dementia: beyond diagnostics (27-11-2009)
21. S.S. Staekenborg: From normal aging to dementia: risk factors and clinical findings in relation to vascular changes on brain MRI (23-12-2009)
22. N. Tolboom: Imaging Alzheimer's disease pathology in vivo: towards an early diagnosis (12-02-2010)
23. E. Altena: Mapping insomnia: brain structure, function and sleep intervention (17-03-2010)
24. N.A. Verwey: Biochemical markers in dementia: from mice to men. A translational approach (15-04-2010)
25. M.I. Kester: Biomarkers for Alzheimer's pathology; Monitoring, predicting and understanding the disease (14-01-2011)
26. J.D. Sluimer: longitudinal changes in the brain (28-04-2011)
27. S.D Mulder: Amyloid associated proteins in Alzheimer's Disease (07-10-2011)
28. S.A.M. Sikkes: measuring IADL in dementia (14-10-2011)
29. A. Schuitemaker: Inflammation in Alzheimer's Disease: in vivo quantification (27-01-2012)
30. K. Joling: Depression and anxiety in family caregivers of persons with dementia (02-04-2012)
31. W. de Haan: In a network state of mind (02-11-2012) (Cum Laude)
32. D. van Assema: Blood-brain barrier P-glycoprotein function in ageing and Alzheimer's disease (07-12-2012)
33. J.D.C. Goos: Cerebral microbleeds: connecting the dots (06-02-2013)
34. R. Ossenkoppele: Alzheimer PEThology (08-05-2013)
35. H.M. Jochemsen: Brain under pressure: influences of blood pressure and angiotensin-converting enzyme on the brain (04-10-2013)
36. A.E. van der Vlies: Cognitive profiles in Alzheimer's disease: Recognizing its many faces (27-11-2013)

37. I. van Rossum: Diagnosis and prognosis of Alzheimer's disease in subjects with mild cognitive impairment (28-11-2013)
38. E.I.S. Møst: Circadian rhythm deterioration in early Alzheimer's disease and the preventative effect of light (03-12-2013)
39. M.A.A. Binnewijzend: Functional and perfusion MRI in dementia (21-03-2014)
40. H. de Waal: Understanding heterogeneity in Alzheimer's disease: A neurophysiological perspective (25-04-2014)
41. W. Jongbloed: Neurodegeneration: Biochemical signals from the brain (08-05-2014)
42. A.C. van Harten: The road less traveled: CSF biomarkers for Alzheimer's disease: Predicting earliest cognitive decline and exploring microRNA as a novel biomarker source (07-02-2014)
43. E.L.G.E. Poortvliet-Koedam: Early-onset dementia: Unraveling the clinical phenotypes (28-05-2014)
44. A.M. Hooghiemstra: Early-onset dementia: With exercise in mind (03-12-2014)
45. L.L. Sandberg-Smits: A cognitive perspective on clinical manifestations of Alzheimer's disease (20-03-2015)
46. F.H. Duits: Biomarkers for Alzheimer's disease, current practice and new perspectives (01-04-2015)
47. S.M. Adriaanse: Integrating functional and molecular imaging in Alzheimer's disease (07-04-2015)
48. C. Möller: Imaging patterns of tissue destruction – Towards a better discrimination of types of dementia (01-05-2015)
49. M. del Campo Milán: Novel biochemical signatures of early stages of Alzheimer's disease (19-06-2015)
50. M.R Benedictus: A vascular overview on cognitive decline and dementia: relevance of cerebrovascular MRI markers in a memory clinic (20-01-2016)
51. M.D. Zwan: Visualizing Alzheimer's disease pathology. Implementation of amyloid PET in clinical practice (03-03-2016)
52. E. Louwersheimer: Alzheimer's disease: from phenotype to genotype (21-06-2016)
53. W.A. Krudop: The frontal lobe syndrome: a neuropsychiatric challenge (23-09-2016)
54. E.G.B. Vijverberg: The neuropsychiatry of behavioural variant frontotemporal dementia and primary psychiatric disorders: similarities and dissimilarities (22-09-2017)
55. F. Gossink: Late onset behavioural changes differentiating between bvFTD and psychiatric disorders in clinical practice (20-04-2018)
56. M.A.A. Engels: Neurophysiology of dementia: the resting state of the art (18-05-2018)
57. S.C.J. Verfaillie: Neuroimaging in subjective cognitive decline: incipient Alzheimer's disease unmasked (12-09-2018)
58. M. ten Kate: Neuroimaging in predementia Alzheimer's disease (13-09-2018)
59. H.F.M. Rhodius-Meester: Optimizing use of diagnostic tests in memory clinics; the next step (24-09-2018)
60. E.A.J. Willemse: Optimising biomarkers in cerebrospinal fluid. How laboratory reproducibility improves the diagnosis of Alzheimer's disease (18-10-2018)
61. **E. Konijnenberg: Early amyloid pathology – Identical twins, two of a kind? (25-6-2019)**

Dankwoord

Zonder alle deelnemende tweelingen aan ons Twins 60++ cohort was dit onderzoek niet mogelijk geweest, deze wil ik daarom als állereerst heel hartelijk danken. Echter, zonder hulp van vele collega's was er uit al deze verzamelde data geen proefschrift ontstaan.

Philip Scheltens, wat is het Alzheimer Centrum een geweldige plek om onderzoek te mogen doen, groeiend, up to date en onder jouw bezielende leiding. Dank voor de positieve vibe, je humor, doortastendheid en scherpte, veel van geleerd!

Bart van Berckel, wat fijn dat je me de ins en outs van de ware nucleaire geneeskunde bijbracht, kritisch, maar ook stimulerend. Zonder jou hadden we de twins nooit zo precies kunnen fenotyperen qua amyloidload, veel dank!

Pieter Jelle Visser, veel dank voor het inkijkje in jouw academische wereld. Mijn cerebrale ontwikkeling heeft de afgelopen 5 jaar overuren gemaakt, zowel binnen het Alzheimer onderzoeksveld als daarbuiten, op het gebied van Bach, architectuur of tips voor in de moestuin.

Anouk den Braber, wat prachtig dat ik jou ook als copromotor mag bedanken, jij bent de drijvende kracht achter het twins-cohort geworden. Ik heb veel van je geleerd, op allerlei vlakken, en je hebt me volledig laten integreren op de afdeling biologische psychologie. Daarnaast ben je ook buiten werk een goede adviseur gebleken.

De leescommissie, voorzitter prof. dr. Robert de Jonge, prof. dr. Karl Herholz, dr. Gaël Chetelat, prof. dr. Guus Smit, dr. Dirk Smit, veel dank voor het lezen en beoordelen van dit proefschrift.

Veel dank ook aan alle coauteurs van dit proefschrift, many thanks to all collaborators and co-authors who contributed to the research described in this thesis.

Het Twins team: Anouk, Mara, Jori, Linda, en alle stagiairs en invallers die in de jaren hebben geholpen, wat ben ik trots dat we met elkaar zo'n prachtig cohort hebben verzameld.

Het NTR: Dorret, Michel, Dennis, Michel, Dirk, Natascha en allen die ik vergeet, dank voor alle hulp en gezellige kerstborrels natuurlijk.

Betty, dankzij jou versta ik de taal van R, waarvoor grote dank, gelukkig begrijpen we elkaar ook op het gebied van dresscodes.

Bunker 3, een voorrecht om hier de eerste 3 jaar van mijn promotie te vertoeven: dank Sofie, Welmoed, Sander, Anita, Nienke L, Roos, Linda, Mascha, en Charlotte.

Semioren-bunkergenoten, wat een rust, reinheid en regelmaat in het laatste jaar van mijn promotie, dankzij jullie is het af: Marissa (tevens goede kennismaking met Flute), Rosalinde, Annebet, Arno (fijn dat je mijn paranimf bent, mocht er nog iets geregeld moeten worden), Jessica, Nienke S en de flexers.

De Tau-twins, Tessa en Emma, wat heerlijk dat het Alzheimer Centrum zelfs het aannamebeleid 'vertwinst' heeft. Dank voor alle (nucleaire en niet-nucleaire) ondersteuning.

PJ's angels Lisa, Mara, Nienke L, Lianne. Thee en (PJ's) chocola op maandagmiddag, recept voor nieuwe wetenschappelijke inzichten, maar ook voor het opduikelen van verborgen talenten voor de revue act.

Alle collega's van het Alzheimer Centrum, teveel om op te noemen, ik heb enorm veel geleerd en ontzettend genoten in de afgelopen jaren. Wat een geweldige plek om promotieonderzoek te doen, van baanbrekende resultaten tot aan je conditie werken en wereldwijd voordrachten geven tot de vrijdagmiddagborrels met *jeux de mot* (Haan).

Alle andere afdelingen en collega's die het Twins onderzoek hebben mogelijk gemaakt: Nucleaire Geneeskunde, Klinische Neurofysiologie, Oogheelkunde, Vaatlab en Biobank, dank voor jullie flexibiliteit (x2).

Dan is er natuurlijk al (lang) voordat ik in het AC begon een belangrijke basis gelegd in Delft, Apeldoorn, Zutphen, Steenderen en Bronkhorst respectievelijk…

Lieve ClubPi's en 109 ladies, dankzij jullie heb ik naast studeren nog andere leuke dingen gedaan in Delft en nog steeds.

BC-matties, wat bijzonder dat we elkaar na al die tijd nog spreken, van Den Haag tripjes in de zomer, via kerstdiners, naar promotie nummer 3 alweer!

Esmee en Karien, vanaf de kleuterklas al een goed trio, laten we dat zo houden! PS stiekem denk ik dat jullie het allereerste begin zijn geweest van mijn interesse in tweelingen…

Huijonghs, aanhang en nakomelingen, dank voor alle wijze en onwijze woorden en momenten omringd door goed eten en drinken.

Lieve dad en mam, heel veel dank voor al jullie vertrouwen, het luisterend oor, en de mogelijkheid te ontsnappen naar kuuroord Bronkhorst. Jullie hebben me (binnen redelijke grenzen) de ruimte gegund om mijn eigen pad te kiezen en zonder jullie had ik hier niet gestaan. Marleen, liefste zus (en collega), veel met je gereisd en meegemaakt, heel blij dat jij als paranimf naast me op het podium zult staan.

Jan, samen met de hond-kind family, ben ik gelukkig met jou. ¡Olé!

About the author

Elles Konijnenberg was born on the 1st of June 1986 in Warnsveld. Together with her younger sister she grew up in Bronkhorst, the smallest town in the Netherlands (150 inhabitants). In 2004 she obtained her gymnasium diploma (cum laude) from the Baudartius College in Zutphen. She moved to Delft, where she started a bachelor in civil engineering at the TU Delft. However, after 1 year she decided to switch to Medicine at Erasmus University in Rotterdam. After successfully completing her doctoral exams, she worked at an orphanage in Kumasi, Ghana, for 6 weeks. She did her internships at the Elisabeth Hospital in Tilburg and Erasmus Medical Center in Rotterdam, and obtained her MD qualification in November 2012. During her internships, her interest in neurology became stronger, and so she performed a research internship at the department of neurology at the Erasmus MC and wrote a thesis on cognitive impairment and glucose metabolism in patients with a minor stroke. After this she received her MD degree and between November 2012 and January 2013 she worked as a research-assistant at the Alzheimer Center South West at the Erasmus MC.

Afterwards she moved to Amsterdam and in March 2013 she started working as a resident of neurology at the Onze Lieve Vrouwe Gasthuis in Amsterdam. At the end of 2013, she started her PhD project on the pathophysiology of amyloid pathology in elderly under the supervision of prof. Philip Scheltens, prof. Bart van Berckel, dr. Pieter Jelle Visser and dr. Anouk den Braber in the Alzheimer Center of the VU University Medical Center. She participated twice in the Dam tot Dam loop with the Alzheimer Center and once in the Head first rowing event. Besides that she set up a cohort with one hundred pairs of identical twins aged 60 years and older, for investigating genetic and environmental factors on amyloid pathology. After finishing her PhD time, she started a residency in neurology at the VU University Medical Center. She now lives in Nes aan de Amstel (985 inhabitants) with husband, child and dogs.